Novel anticancer silver(I) phosphines proven to target the mitochondrial-mediated cell death pathway in malignant cells

by

Zelinda Engelbrecht

THESIS

Submitted in fulfilment
of the requirements for the degree

PHILOSOPHIAE DOCTOR

in

BIOCHEMISTRY

in the

FACULTY OF SCIENCE

at the

UNIVERSITY OF JOHANNESBURG
Auckland Park
South Africa

SUPERVISOR: Prof. Marianne J. Cronjé
Department of Biochemistry

CO-SUPERVISOR: Prof. Reinout Meijboom
Department of Chemistry

January 2017


No bird soars too high if he
soars with his own wings.
William Blake
Hinkler Design Studio

I dedicate this Thesis to my late aunt,

Reinette Helene van der Linde

“Your life was a blessing, your memory a treasure. You are loved beyond words and missed beyond measure”

1952-2016

ACKNOWLEDGEMENTS

I would like to express my deepest gratitude to my supervisor Prof. Cronjé. Thanks for giving me the opportunity to fulfil my dreams and encouraging me along the way. You (Proffie ☺) are one awesome woman in science and if I can be half the women you are I will be able to take on the world.

My husband, Juan-Pierre, thanks for always believing in me and for your endless patience throughout my whole study career. You have been with me through the most exciting and tough times and supported me no matter what. You are my rock, my foundation and best friend. I love you so dearly.

My mother and father, Annelien and Ian, you are the two proudest people I know. You have always encouraged me and told me to follow my dreams. I know it wasn't always easy, but your words of wisdom pulled me through.

My co-supervisor, Prof. Reinout Meijboom, for your help and guidance when needed.

The contributors to science, the examiners, who's efforts are often ignored. Thanks for the time taken to read through this work. It is much appreciated.

My good friends in and out the lab, thanks for all the fun times, encouragement and support. You guys are awesome!

Dr. Heather-Ann Byth-Illing, for the continuous assistance in flow cytometry.

The University of Johannesburg, National Research Foundation (NRF) and the TTO office (especially Mrs Mandy-Lee Pietersen and Prof. Aart Boessenkool) for financial support throughout my study.

PREFACE

1. **Conferences:**

Engelbrecht, Z., Meijboom, R and Cronjé, M.J. (2016). Silver(I) phosphine complexes induce mitochondrial cell death in vitro. The University of Johannesburg Biochemistry Postgraduate Research day, Johannesburg, South Africa, July 2016, Received the award for being the most Meritorious student.

Engelbrecht, Z., Meijboom, R and Cronjé, M.J. (2016). Silver(I) phosphine complexes induce mitochondrial cell death in vitro and display low oral toxicity in vivo. 25th South African Society for Biochemistry and Molecular Biology (SASBMB) congress, East London, South Africa, 10 July-13 July 2016.

Human, Z., Meijboom, R and Cronjé, M.J. (2014). Cytotoxic and mechanistic studies of silver(I) phosphine complexes in human malignant cells. The University of Johannesburg Biochemistry Postgraduate Research day, Johannesburg, South Africa, November 2014.

2. **Patents:**

Meijboom, R. and Cronjé, M.J. (2016). The use of silver(I) mono-dentate and bi-dentate phosphine complexes as active pharmaceutical ingredients (API's) including anticancer agents. South African Patent Application - 2015/08527.

Meijboom, R. and Cronjé, M.J. (2013). Use of silver(I) complexes as anticancer agents. WO2013084185 A1, South Africa*.

*Patent applications were further filed in Cananda, Australia, USA, UK and India of which South Africa, Canada and Australia have been approved. We await the outcome of the other applications.

3. **Articles published, submitted and produced:**

Human-Engelbrecht, Z., Meijboom, R and Cronjé, M.J. (2017). Silver(I) cyanide-containing phosphine complex induces apoptotic cell death. Accepted by Cytotechnology.

Human, Z., Munyaneza, A., Omondi, B., Sanabria, N.M., Meijboom, R. and Cronjé, M.J. (2015). The induction of cell death by phosphine silver (I) thiocyanate complexes in SNO-esophageal cancer cells. *BioMetals*, *28*(1), pp.219-228.

Engelbrecht, Z., Potgieter, K., Mpela, Z., Malgas-Enus, R., Meijboom, R. and Cronjé, M.J. (2017). A comparison of the toxicity of mono, bis, tris and tetrakis phosphino silver complexes on SNO esophageal cancer cells. Submitted to Anti-Cancer Agents in Medicinal Chemistry.

Naganagowda, G., Engelbrecht, Z., Ncube, P., Cronjé, M.J. and Meijboom, R. (2017). Synthesis, crystal structure and spectral studies of silver(I)cyclohexyl diphenylphosphine complexes: towards the biological evaluation on malignant and non-malignant cells. Produced.

Engelbrecht, Z., Meijboom, R and Cronjé, M.J. (2017). Investigating the ability of a silver(I) thiocyanate 4-methoxyphenyl phosphine complex to induce mitochondrial cell death in esophageal cancer cells. Produced.

Engelbrecht, Z., Meijboom, R and Cronjé, M.J. (2017). Antibacterial properties of silver(I) phosphine complexes in *Enterococcus faecalis* and *Pseudomonas aeruginosa*. Produced.

TABLE OF CONTENTS

LIST OF FIGURES

LIST OF TABLES

LIST OF ABBREVIATIONS

Degrees of measurement

bp	base pair
°C	degrees Celsius
cm	centimetre
cm^3	cubic centimetre
g	acceleration due to gravity
kb	kilo base pair
kDa	kilo Dalton
µg	microgram
µl	microliter
mg	Milligram
ml	Millilitre
µm	Micrometer
µM	micromolar
mM	millimolar
MW	molecular weight
ng	nanogram
nm	nanometer
nM	nanomolar

A

AC	Adenocarcinoma
Ag	Silver
AIDS	Acquired immunodeficiency syndrome
AIF	Apoptosis inducing factor
Apaf-1	Apoptotic protease activating factor-1
Apo2L	Apo2 ligand
Apo3L	Apo3 ligand
ARTS	Apoptosis related protein in TGF-B signalling pathway
Ask-1	Apoptosis signal-regulating kinase 1
Asp	Aspartic acid

ATG	Autophagy-related genes
ATP	Adenosine triphosphate
ATPase	Adenosine triphosphatase
Au	Gold

B

Bad	Bcl-2 antagonist of cell death
Bag	Bcl-2 associated athanogene
Bak	Bcl-2 antagonist killer-1
Bax	Bcl-2 associated X protein
Bcl-2	B-cell lymphoma protein 2
Bcl-xL	Bcl-2 protein, long isoform
Bcl-sL	Bcl-2 protein, short isoform
Bcl-w	Bcl-2 like protein 2
Bfl-1	Bcl-2 related protein A1
BH	Bcl-2 homology domains
Bid	BH3 interacting domain death agonist
Bik	Bcl-2 interacting killer
Bim	Bcl-2 interacting mediator of cell death
BIR	Baculovirus IAP repeat
Blk	Bik-like killer protein
Bok	Bcl-2 related ovarian killer protein
Br	Bromide
BRCA1/2	Breast cancer-1 or -2 gene
BRIP1	BRCA1-interacting protein-1
Bruce	BIR repeat containing ubiquitin-conjugating protein
BSA	Bovine serum albumin

C

CAD	Caspase-activated DNase
CARD	Caspase-associated recruitment domain
Caspase	Cysteine-dependant aspartate-specific proteases
CCCP	Carbonyl cyanide 3-chlorophenylhydrazone
CDDP	Cisdichlorodiammineplatinum(II) (cisplatin)

cDNA	Complementary DNA
CDH1	Cadherin-1
c-FLIP	Cellular-FLICE inhibitory protein
CHEK2	Checkpoint kinase-2
cIAP1/2	Cellular IAP protein-1 or -2
C_T	Cycle threshold
Cu	Copper
CYLD	Cyclindromatosis
CYP450	Cytochrome P450

D

DAPK1	Death-associated protein kinase 1
dATP	Deoxyadenosine triphosphate
DD	Death domain
DED	Death effector domain
DIABLO	Direct IAP binding protein with low PI
$\Delta\psi_m$	Mitochondrial membrane potential
DISC	Death-inducing signalling complex
DMEM	Dulbecco's Modified Eagles media
DMSO	Dimethyl sulfoxide
DNA	Deoxyribonucleic acid
DNase	Deoxyribonucleic acid
DNTB	5,5'-Dithiobis (2-nitrobenzoic) acid
DPPE	1,2-Bis(diphenyl-phosphino) ethane
DPPP	1,3-Bis(diphenyl-phosphino) propane
D_2pypp	1.3-bis(di-2-pyridylphosphino) propane
DR	Death receptor

E

EDTA	Ethylene diaminetetraacetic acid
Endo G	Endonuclease G
ER	Estrogen receptor
ERBB2	V-erb-b2 erythroblastic leukemia viral oncogene homolog 2

F

FADD	Fas-associated death domain
FasL	Fas-ligand
FasR	Fas-receptor
FBS	Fetal Bovine Serum
FCS	Fetal Calf Serum
FGS	Fibroblast growth stimulant
FITC	Fluorescein isothiocyanate
FLIP	FADD-like ICE inhibitory protein
FM	Fibroblast media

G

GABA	Gamma aminobutyric acid
gDNA	Genomic DNA
GFP-LC3	Green fluorescent protein-microtubule associated protein light chain-3

H

HBSS	Hanks balanced salt solution
HCl	Hydrochloric acid
HDF-a	Human dermal fibroblasts (adult)
HEK293	Human embryonic kidney cells
HER-2	Human epidermal growth factor receptor-2
H_2O_2	Hydrogen peroxide
HRP	Horseradish peroxidase
Hsc	Constitutively expressed heat shock protein
HSE	Heat shock
HSF	Heat shock element
Hsp	Heat shock protein
HTATIP2	HIV-1 Tat interactive protein 2
HtrA2	High-temperature requirement protein 2

I

IAP	Inhibitor of apoptosis protein
IC_{50}	Inhibitory concentration 50
ICAD	Inhibitor of caspase activated DNase

ICE	Interleukin 1β converting enzyme
IGF1R	Insulin-like growth factor 1 receptor
IKK	I kappa kinase
ILP-2	IAP-like protein-2
IR	Infrared
ITGA	Integrin alpha
ITGB	Integrin beta

J

JNK	c-Jun N-terminal kinase

K

KCl	Potassium chloride
KH_2PO_4	Potassium dihydrogen phosphate

L

LC3	Microtubule-associated protein light chain-3
LDH	Lactate dehydrogenase
LMS	Leiomyosarcoma
log Kw	Lipophilicity profile
LOX	Lipoxygenase

M

MAPK	Mitogen activated protein kinase
MCF-7	Pleural effusion of breast adenocarcinoma
Mcl-1	Induced myeloid leukaemia cell differentiation protein-1
MDM2	MDM2 p53 binding protein homolog
m.p	Melting point
MPT	Mitochondrial-permeability transition
mRNA	Messenger RNA
MTA	Metastasis associated
mTOR	Mechanistic target of rapamycin

N

NaCl	Sodium chloride
$NaHCO_3$	Sodium bicarbonate
Na_2HPO_4	Sodium phosphate
NAIP	Neuronal apoptosis inhibitory protein
NaOH	Sodium hydroxide
NBS1	Nibrin-1
Nec-1	Necrostatin-1
NF-κB	Nuclear factor-kappa B
NIK	NF-κB inducing kinase
NMR	Nuclear magnetic resonance
NuRD	Nucleosome remodelling deacetylase

P

PALB2	Partner and localizer of BRCA2
PAGE	Polyacrylamide gel electrophoresis
PARP	Poly(ADP-ribose)polymerase
PBS	Phosphate buffered saline
PBMCs	Peripheral blood mononuclear cells
PCD	Programmed cell death
PCR	Polymerase chain reaction
Pd	Palladium
PI	Propidium iodide
PI3K	Phosphatidylinositol 3-kinases
PIKK	Phosphatidylinositol kinase-related kinase
PLAUR	Plasminogen activator urokinase receptor
PNN	Pinin, desmosome associated protein
$P(p\text{-}Cl_6H_4)_3$	Parachloro phosphine
PPh_3	Triphenylphosphine
PR_3	Tertiary phosphine
pRb	Retinoblastoma protein
Pro-IL-1b	Pro-interleukin-1b
PS	Phosphatidylserine
PSR	Phosphatidylserine receptor

Pt	Platinum
Puma	p53 up-regulated modulator of apoptosis
PVDF	Polyvinylidene difluoride

Q

qPCR	Quantitative real-time PCR

R

RHIM	RIP homotypic interaction motif
RING	Really interesting new gene
RIP	Receptor interacting protein
RIPK2	Receptor-interacting serine-threonine kinase 2
RNase	Ribonuclease
RNA	Ribonucleic acid
ROS	Reactive oxygen specie/s

S

SCC	Squamous cell carcinoma
SCN	Thiocyanate
SDS	Sodium Dodecyl Sulphate
SEM	Standard Error of the Mean
SD	Standard Deviation
Smac	Second mitochondria-derived activator of caspases

T

TAE	Tris-Acetic acid-EDTA
TBE	Tris-Boric acid-EDTA
TBS	Tris buffered saline
TBST	TBS-Tween 20
TEMED	N, N, N', N'-tetramethylethylenediamine
T_m	Melting temperature
tBid	Truncated Bid
TGFB	Transforming growth factor beta
TNB	5-Thio-2-nitrobenzoic acid

TNF	Tumour necrosis factor
TNFDD	TNFR receptor-associated death domain
TNFL	Tumour necrosis factor ligand
TNFR	Tumour necrosis factor receptor
TRADD	TNFR associated death domain
TRAF	TNF receptor-associated factor
TRAIL	TNF-related apoptosis inducing ligand
Tris	2-Amino-2-(hydroxymethyl)-1,3-propandiol
Trx	Thioredoxin
TrxR	Thioredoxin reductase
TWIST1	Twist homolog 1

U

UV	Ultraviolet

V

V	Volt

X

XAF1	XIAP-associated factor 1
XIAP	X-linked mammalian inhibitor of apoptosis protein

INTRODUCTION

Metal-based drugs have shown early promise as anticancer agents, suggesting the potential application of silver(I) complexes as apoptosis-inducing agents. This study forms part of a larger study investigating a group of serendipitously discovered novel synthetic silver(I) phosphine complexes, initially used for chemical catalysis, of their ability to induce cell death in cancer cells. Overall, the discovery led to the patenting of the genus species recently filed in 6 countries of which South Africa, Canada and Australia has been approved.

The main focus of this research project was to study the anticancer effect of a group of silver phosphine complexes and identify possible silver-based drugs that can be added to the arsenal of chemotherapeutic drugs already identified and in use. Furthermore, by focussing on various biochemical aspects and identifying possible drug targets, for individual cancers, will be beneficial in target-specific chemotherapy. The work reported in this thesis is structured into two parts of which the first part (Chapter 2) focusses on the anticancer mechanism of newly synthesized silver(I) phosphine complexes (complexes **1**-**6**), in an oesophageal and breast carcinoma cell lines, that have not been reported previously. The second part (Chapter 3) is a continuation of MSc. work focusing only on one complex (complex **7**) and the changes it caused on a genetic level in oesophageal cancer, which was not included due to time constraints (Human, 2013). Both Chapters 2 and 3 is further subdivided into a Preface, Materials and Methods, Results and Discussion section that only motivates the anticancer effect of the designated silver(I) complexes. Because both these chapters refer to the anticancer effect of silver(I) complexes, a combined Literature review and Conclusion will be given, located in Chapter 1 and Chapter 4 respectively. It is hoped that the research is conveyed in a clear report for the reader to follow.

SUMMARY

Cancer next to heart disease is the leading cause of death worldwide. It affects a large population of Africa and is regarded as a low public concern due to the prioritizing of other serious diseases (*e.g.* AIDS, malaria and tuberculosis) in the country. In 2008, over 680, 000 new cancer cases have been reported in Africa and over 500, 000 deaths of which these numbers could double by the year 2030. Apoptosis is an energy-dependant mechanism that is activated upon various stimuli that can either be external or internal of the cell. This form of cell death is the preferred route to induce malignant cell death because of the absence of an inflammatory response. Mutations in apoptotic genes, especially those from the *p53* gene sub-family, are the main contributors of therapeutic resistance in most cancers. Although a wide range of anticancer regimens has been explored to kill of malignancies, in most cases, their approach has not been successful. Platinum-based treatments like, cisplatin and other derivatives, have been studied extensively as anticancer agents and is currently used (or in combination with other chemotherapeutic drugs) to treat certain malignancies. The use of these platinum agents is limited by their low selectivity and cancer resistance that occur over time. Phosphine transition metals, like gold(I), copper(I) and ruthenium(III) phosphines have been studied as potential anticancer agents. In addition, first-generation silver(I) phosphine complexes gardened interest due to their ease of structural manipulation that can improve anticancer activity. Some studies suggest that silver(I) phosphine complexes that are lipophilic in nature cause malignant cell death through mitochondrial targeting. Overall, the specific targeting mechanism of the silver(I) complex family is not known and should be elucidated to further understand their role in cancer cell death.

Therefore, the objective of this project is to study the anticancer activity of six novel lipophilic silver(I) phosphine complexes and their potential mitochondrial targeting in two human malignant cell lines (SNO oesophageal and MCF-7 breast). Their cancer specificity was also tested by determining their cytotoxicity in two human non-malignant cell lines (HDF-a skin and HEK293 kidney) including a panel of malignant cell lines originating from various species. In addition, an alternative silver(I) complex, studied in the past, was used to identify the expression of cancer-related genes in SNO oesophageal cancer cells.

Dose-dependent studies were conducted with the silver(I) complexes and cisplatin to determine their IC_{50} concentrations in both malignant cell lines. Three different viability assays that include Trypan blue, alamarBlue® and CellTiterGlo™ were used to evaluate how these complexes alter specific cellular features. Furthermore, the complexes cytotoxic effects were compared to two non-

malignant cell lines. The mode of cell death was investigated using light microscopy, flow cytometry (Annexin-V and PI) and a caspase-3/7 assay. Mitochondrial targeting was further evaluated by a wide range of biochemical methods include: JC-1 assay (measures mitochondrial membrane potential ($\Delta_{\psi m}$)), fluorescent microscopy (determines mitochondrial integrity and cytochrome *c* release), an oxidative stress assay (measuring the amount of ROS), western blot analysis (determining cleavage of caspase-9, in addition, PARP cleavage and Hsp70 levels) and a thioredoxin reductase (TrxR) assay (to monitor the TrxR activity in the cells). Moreover, the involvement of a cytochrome P450 (drug metabolizing enzyme) isoform (CYP1B1) was monitored in the cells. A total of 16 malignant cell lines were used to test drug specificity. Lastly, in a separate study, a Human Cancer Pathway Finder RT^2 Profiler PCR array was used to determine the involvement of cancer-related genes.

The results reveal that all the complexes, including cisplatin, caused a dose-dependent decrease in both the SNO and MCF-7 cells. Although the MCF-7 cells were more resistant to the treatments than the SNO cells the complexes overall show an improved cytotoxicity at 10 µM when compared to cisplatin at 100 µM. Morphological and biochemical features associated with apoptosis were observed in both malignant cell lines along with cell cycle arrest. Most importantly, all the silver(I) complexes under study (except one) displayed a higher selectivity towards the non-malignant HDF-a and HEK293 cells. Selected complexes (based on low IC_{50} concentration, apoptosis induction and low non-malignant cytotoxicity) were further evaluated for their mitochondrial targeting. In the SNO cells a decrease in $\Delta_{\psi m}$, a decrease in mitochondrial integrity, cytochrome *c* translocation, increased ROS activity, caspase-9 and PARP cleavage, increased Hsp70 expression and decreased TrxR activity was observed. All the formerly mentioned changes were also observed in the MCF-7 cells, but at lower levels and in the absence of ROS activity. The selected complexes displayed a high cytotoxic potency in all cell lines ranging from human cervical and rat pancreatic malignancies. A formerly studied silver(I) complex targeted genes mostly associated with apoptosis, adhesion, invasion and metastasis in the SNO cells.

The lipophilic silver(I) phosphine complexes studied herein show promise as anticancer agents by inducing apoptotic cell death *via* the mitochondria. Even though this study gave more insight on the targeting mechanisms, further studies involving specific drug targets warrant further investigation.

CHAPTER 1: Literature Review

1.1 A general overview of cancer

1.1.1 Cancer statistics

Cancer is a global burden that is currently responsible for more deaths than a combination of three notorious diseases; malaria, human immunodeficiency virus (HIV) and tuberculosis (American Cancer Society; ACS, 2010). Furthermore, cancer is the second leading cause of death in the UK following heart disease (Kochanek *et al*., 2011). It is estimated, in 2008, that over 680, 000 new cancer cases and 512, 000 cancer-related deaths were reported for the African population. These numbers could rise to 1.27 million and 970, 000 respectively by the year 2030 (Ferlay *et al*., 2010). It is believed that in this time frame the number of cancers that are diagnosed in low and middle-income countries will increase from 59% to 65% (Bray *et al*., 2015). The drastic change in these numbers are mainly contributed by an increase in the population, ageing and risk factors associated with westernization (smoking, unhealthy diet, inactivity and cultural traditions) (Sylla and Wild, 2012; Gakunga and Parkin, 2015). Although cancer incidences are on the rise, it is considered as a low public concern in Africa owing to limited resources and other public health problems that are prioritized (ACS, 2011a). In addition, cancer management and treatment is expensive due to the high cost of therapies. Radiation is a treatment regime mostly used for cancer. Unfortunately, this type of therapy is scarce in the low developed regions of Africa (Abdel-Wahab *et al*., 2013). Africa has a total of 52 countries of which only 23 have radiation resources to treat cancer occurring mostly in the Southern and Northern regions. In less developed countries, cancer is diagnosed in the advanced stages contributing to a lower survival rate which is ascribed due to the lack of pathology laboratories in these regions (Vineis and Wild, 2014). Early detection, diagnosis, readily available and less expensive therapies are key in decreasing the overall mortality in African populations.

The most globally diagnosed cancers are lung, bronchial, colorectal, breast and prostate cancers. Breast and prostate cancer have been reported as the most common cancers in women and men respectively after lung cancer (Jemal *et al*., 2010; ACS, 2011a). In Africa, the most diagnosed cancers in women are that of the breast, cervix, liver and colorectal regions. In men, cancer of the prostate, liver, lung and oesophagus are more prevalent. The top four malignancies in men and women that are responsible for the highest death rates are prostate, liver, lung and oesophageal or cervical, breast, liver and colorectal respectively (ACS, 2016).

1.1.2 Summary of cancer causes, development and staging

Cancer is collectively known as a group of diseases that is associated with the abnormal and uncontrollable growth of normal cells. The abnormalities can develop based on exposure to a range of external (chemicals, infectious microbes, tobacco and radiation) and internal mediators (hormones, immune conditions, inherited and metabolic mutations) or a combination thereof (Siegel *et al*., 2016). A total of 5% of the cancers that exist develop based on hereditary causes (ACS, 2013). The remainder of cancer develops based on genetic damage from the external and internal mediators mentioned previously (Garcia *et al*., 2007; ACS, 2013). Hanahan and Weinberg (2011) suggested that the diverse range of cancers comprehend six different alterations that occur in their physiological processes (Figure 1.1).

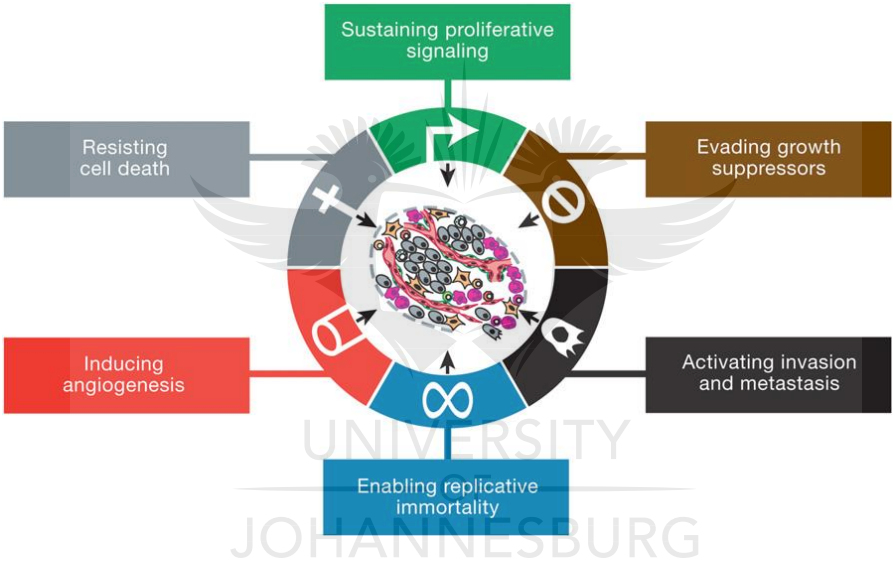

Figure 1.1: The six hallmarks of cancer (Adapted from Hanahan and Weinberg, 2011).

These include the ability to produce their own growth signals ensuring proliferation, they activate invasion and metastasis, undergo continuous replication which garners them immortal, induce angiogenesis and can evade cell death (specifically apoptosis) (Hanahan and Weinberg, 2000; Hanahan and Weinberg, 2011). In addition, two characteristic hallmarks have been further identified, which play a role in cancer pathogenesis (Hanahan and Weinberg, 2011). The first one involves the reprogramming of the cellular metabolism of normal cells at the tumour site, enabling the nonstop growth and proliferation. The second one involves the continuous evasion of malignant cells from innate immune cells that are designed to fight infection resulting in improved tumour development.

Cancer is staged by using the TNM-staging system. This system describes the size of the primary tumour (T), whether it has spread to the lymph nodes (N) or metastasized in a close or distant proximity of the original tumour site (M) (ACS, 2016). Upon diagnoses, the T, N and M groups are first determined followed by assigning a Greek number ranging from *0-IV* (zero to four) where *0* indicates that the malignancy is localized *in situ*, *I* being in the early stages till *IV* indicating the severe stages. The strategy for cancer treatment can only be determined once the malignancy is completely staged.

1.1.3 Cancer therapeutics

Cancer can either be treated by means of (a) surgery, (b) radiation, (c) hormone therapy, (d) immunotherapy, (e) targeted therapy or (f) chemotherapy. A short summary of these different treatments are indicated below;

(a) Surgery

Surgery is the most successful treatment for localized tumours. Of all the treatments available for cancer, surgery is the one with the highest success rate (Urruticoechea *et al*., 2010). It is usually done in the earlier stages, but can only be used in some patients depending on their health status (Tepper *et al*., 2008). It is important that during surgery, the entire tumour is removed to prevent the redevelopment or metastasis. Radiation is sometimes used post-surgery to destroy malignant cells that might have been missed during resection.

(b) Radiation

Radiation along with chemotherapy is only capable of destroying a portion of the malignant cells during each treatment. Radiation is the safer option where the radioactive material is placed near the site of the malignancy causing minimal damage to healthy surrounding tissue. It is used in patients that are unable to undergo surgery or to decrease the tumour size prior to surgery (Bold *et al*., 1997; ACS, 2016). It is believed that during radiation, the cellular DNA is damaged and cannot activate repair mechanisms resulting in malignant cell death (Bold *et al*., 1997).

(c) Hormone therapy

Hormonal therapy, also known as endocrine therapy (Zhao and Ramaswamy, 2014), uses selective estrogen receptor (ER) or progesterone receptor (PR) modulators that compete with the circulating hormone to bind to the targeted hormone receptor carrying cells. The modulator has a higher binding affinity for the receptor than the competing hormone resulting in the decreased levels or depletion of the targeted hormone in the tumour (Katzenellenbogen and

Katzenellenbogen, 2002; Jordan, 2003; Rau *et al*., 2005). Breast, prostate, testicular, ovarian and endometrial malignancies depend on hormonal activity (estrogen, progesterone and androgen) and mostly develop due to the dysregulation of hormone secretion, signalling and receptor action (Barrett-Connor, 1998; Weinberg *et al*., 2005; Urruticoechea *et al*., 2010; Abdulkareem and Zurmi, 2012; ACS, 2016). Multiple research platforms have studied the specific mechanism of action of steroid hormone receptors. These studies helped to identify potential molecular targets (*e.g.* Her2/neu and ER) that can be used to treat the formerly mentioned malignancies by using targeted therapy (Águas *et al*., 2005; Reviewed by Abdulkareem and Zurmi, 2012).

(d) Immunotherapy

The immune system is responsible for the removal of abnormal cells and to prevent cancer formation (Disis, 2014). Immune-editing is a term used to describe cancer that becomes resistant to cellular defence mechanisms (Dunn *et al*., 2006; Disis, 2014). The process of immune-editing in cancer occurs in three steps. The first step involves elimination whereby the malignant cells are identified and destroyed by the immune system of the host. During equilibration, the second step, the immune system fails to eliminate all the malignant cells but prevents further growth. During the escape phase, step three, the immune system can no longer remove the malignant cells because these cells have evolved by evading the immune response, continuing to grow and spread throughout the body (Dunn *et al*., 2006; Disis, 2014). Immunotherapy aims to initiate or amplify the immune system to detect and destroy cancer cells by preventing further metastasis. Immune stimulators like vaccines, lymphokines, *in vitro* stimulated effector cells of the immune system or antibodies are used to help boost the immune system (Dunn *et al*., 2006; Sharkey and Goldenberg, 2006; Wolchok *et al*., 2009; Disis, 2014; Drake *et al*., 2014). Cancers of the skin, kidney and lung are usually treated with immunotherapy (Reviewed by Drake *et al*., 2014; ACS, 2016).

(e) Targeted therapy

Targeted therapy is a novel approach that has been developed in recent years. Most of the traditional therapies cause severe side effects that are associated with low cell selectivity (ACS, 2012; Baudino, 2015). The combination of immunotherapy with that of targeted therapy has shown promise for the treatment of several malignancies (Vanneman and Dranoff, 2012). Targeted therapy is similar to chemotherapy, but the mechanism of action differs. Unlike chemotherapy, that can harm healthy surrounding tissue, targeted therapy specifically targets genes or gene products unique to the cancer cells (Baudino, 2015). This form of therapy can

make use of either a small molecule inhibitor (*e.g.* Avastin, Vectibix and Campath) or monoclonal antibodies (*e.g.* Gleevec, Iressa and Nolvadex) (Goldenberg, 2002; Sharkey and Goldenberg, 2006; Hamilton, 2008; Reviewed by Baudino, 2015). Small molecule inhibitors are primarily used when targeted proteins are significantly up- or down-regulated in cancer cells. They compete for the binding site of ATP in a tyrosine kinase and once bound, inactivate the enzymatic and downstream signalling processes (Gerber, 2008). Monoclonal antibodies also recognise targeted proteins and either disrupt protein function or downstream activities, causing antibody-dependant or complement-dependent cytotoxicity (Baudino, 2015).

(f) *Chemotherapy*

When cancer starts to metastasize, chemotherapy is rather used as a systemic treatment (Sbeity and Younes, 2015). During chemotherapy, a drug cocktail is administered into the bloodstream and spreads throughout the body (ACS, 2012). This type of treatment is effective in treating a wide range of malignancies. The malignant cells are targeted by the drug cocktail in a four-step process. Firstly, the cocktail disrupts the cellular homeostasis. Next, the cell senses the homeostatic change and recruits specific proteins which are predominately p53 proteins. This is followed by a cellular decision of whether the cell should be repaired or targeted for cell death. In the last step, cell death, in the form of apoptosis, is activated eliminating the malignant cell (Bold *et al*., 1997). Drug combinations that include pertuzumab, trastuzumab and docetaxel have shown improved anticancer activity in patients with metastatic breast cancer (Baselga *et al*., 2012). Furthermore, carboplatin and paclitaxel (Taxol®), cisdichlorodiammineplatinum(II) (cisplatin) and 5-fluorouracil (5FU), cisplatin in combination with capecitabine (Xeloda®), oxaliplatin and doxorubicin (Adriamycin®) have been used in chemotherapeutic cocktails for oesophageal cancer (Neuner *et al*., 2009; ACS, 2012). The major drawback of chemotherapy is that it tends to target healthy cells thus contributing to severe side effects (ACS, 2012; Baudino, 2015). Nevertheless, chemotherapy is still used to treat multiple malignancies regardless of its limitations which stress the need for alternative chemotherapeutic drugs.

1.2 Oesophageal cancer

Oesophageal cancer is the eighth most common malignancy worldwide and is responsible for a sixth of all cancer deaths (Pisani *et. al*., 1993). This form of cancer is extremely aggressive and has a poor survival rate. The latest data from 2012 GLOBOCAN illustrate that Southern Africa has the second highest incident and mortality rates for oesophageal cancer in the world next to Eastern Asia (Ferlay *et al*., 2012). In 2008, it was estimated that approximately 488, 000 new oesophageal cancer cases were reported with a predicted doubling by 2030 (Ferlay *et al*., 2010). The worldwide incident rate

of oesophageal cancer is more than double in men than women (Pickens and Orringer, 2003). In South Africa, oesophageal cancer is considered as a high risk in black males, especially in the Transkei and Sowetan regions (Jaskiewicz *et al*., 1987; Sumeruk *et al*., 1992; Dlamini and Bhoola, 2005, Somdyala *et al*., 2015). Oesophageal cancer is the second most frequently diagnosed malignancy in females next to cervical cancer in the rural regions of the Transkei (Somdyala *et al*., 2015). In the early stages, symptoms of oesophageal cancer are minimal, however, in the advanced stages they are more pronounced and include weight loss or painful and difficulty in swallowing (Garcia *et al*., 2007).

Oesophageal cancer exists in two histological forms, either as a squamous cell carcinoma or adenocarcinoma. The squamous cell carcinoma develops in the upper or middle region of the oesophagus, while the adenocarcinoma develops in the lower region (Kuwano *et al*., 2005; Garcia *et al*., 2007). During the development of squamous cell carcinoma, the squamous epithelium in the oesophagus is replaced with columnar epithelium resembling the stomach or the intestine. Gastric reflux is the main contributor for the epithelial transformation. This transformation causes Barrett's oesophagus that is a precursor for adenocarcinoma development (Enzinger and Mayer, 2003; Garcia *et al*., 2007). In the past, squamous cell carcinoma was reported in most oesophageal cancer cases, but adenocarcinoma is steadily rising (Blot *et al*., 1991). The former develops based on environmental factors such as smoking (includes hookah pipe), alcohol consumption and the contamination of food staples with carcinogens, particular by a fumonisin B1 mycotoxin (Rheeder *et al*., 1992; Vaughan *et al*., 1995; Dutton, 1996; Garcia *et al*., 2007; Nasrollahzadeh *et al*., 2008). The latter is mainly caused by the development of Barrett's oesophagus, lack of exercise and an unhealthy diet (Vaughan *et al*., 1995; Enzinger and Mayer, 2003; Garcia *et al*., 2007; Nasrollahzadeh *et al*., 2008). The consumption of hot beverages has shown to contribute to oesophageal cancer (Rolon *et al*., 1995). In Africa specifically, cultural traditions (*e.g.* traditional beer brewing) and lifestyle play a large role in the development of this malignancy (Rheeder *et al*., 1992; Dutton, 1996; Dlamini and Bhoola, 2005; Somdyala *et al*., 2015). A genetic link in oesophageal cancer also exists which explains the "oesophageal cancer Asian belt" in China (Hu, 1990).

Mutations associated with oesophageal cancer mainly involve that of the *p53* tumour suppressor gene family, whereby apoptotic cell death is prevented resulting in improved cancer cell survival. Other mutations associated are *p73*, *p21*, *p16*, *p15* and the retinoblastoma protein genes *(pRb)*, but are discussed elsewhere (Reviewed by Kuwano *et al*., 2005). Li *et al*. (2009) found that resistance in oesophageal cancer is also due to the activation of the nuclear factor-kappa B (NF-κB) pathway. The

malignant cells were treated with inhibitors (Bay11 and Sulfasalazine) of this pathway and have found to significantly increase apoptotic processes, confirming the role of NF-κB in the mechanistic survival of cancer. It is due to these mutations that make oesophageal cancer difficult to treat. Oesophageal cancer is generally treated with surgery, radiotherapy, chemotherapy or with a combination these treatments (Garcia *et al*., 2007). The major concern is that oesophageal cancer is only diagnosed in the late stages which give patients less than 10% chance of survival for 5 years despite the treatments regimes available (Pickens and Orringer, 2003). Therefore, it is of importance to identify molecular markers associated with oesophageal cancer and improved treatments that might increase the survival rate.

1.3 Breast cancer

Breast cancer is the most frequently diagnosed malignancy in women worldwide. It is estimated that in 2016, over 240, 000 new cases have been reported in the USA and over 40, 000 deaths (Siegel *et al*., 2016). In 2008, a total of 92, 600 cases have been reported for African women along with 50, 000 deaths. Of all the African countries, white South African women have the highest incident rates based on the higher prevalence for reproductive risks (Vorobiof *et al*., 2001; ACS, 2011b). In addition, a high proportion of breast cancer occurs in premenopausal women (Brinton *et al*., 2014). The most common symptom of breast cancer includes a painless lump or growth in the breast. The least common symptoms include the following: thickening or swelling of the breast, redness due to a skin irritation, scale formation and an abnormal shape or discharge from the nipple (ACS, 2016).

Various risk factors are associated with breast cancer development. They include that include increased weight or obesity over the age of 18, the use of menopausal therapy, smoking for long periods, and more recently it has been shown that irregular sleeping patterns could also contribute to the increased risk of breast cancer. Other factors that are associated with an increased risk for breast cancer are old age, history of the malignancy, the presence of inherited mutations, breast hyperplasia, history of ductal or lobular carcinoma *in situ*, exposure to a high-dose of radiation at a younger age, high breast and bone mineral density, type-2 diabetes (weight dependent), reproductive factors (*e.g.* abnormal menstrual cycles), the use of oral contraceptives, never having children or having the first child after the age of 30 and abnormal high levels of sex hormones (ACS, 2016).

Hereditary causes of breast cancer occur in 5-10% of women based on mutations in the autosomal dominant genes (Loman *et al*., 1998). The two most common gene mutations associated with hereditary breast carcinoma are *breast cancer-1 and -2* genes *(BRCA1* and *BRCA2*) that are

responsible for the repair of double-strand breaks. Mutations in these genes produce a truncated protein which yields a shortened BRCA protein that is not functional (van der Groep *et al*., 2011). A mutation responsible for a highly aggressive triple negative form of breast cancer is that of the tumour suppressor gene family *p53*. This is the most aggressive form of breast cancer and is very difficult to treat. Other genes that are frequently mutated in breast cancer and are major contributors to the development are *checkpoint kinase-2* (*CHEK2*), *cadherin-1* (*CDH1*), *nibrin-1* (*NBS1*), *RAD50*, *BRCA1-interacting protein-1* (*BRIP1*) and *partner and localizer of BRCA2* (*PALB2*) (Reviewed by Sheikh *et al*., 2015). Breast cancer can be divided into two groups, ER-positive and ER-negative. Malignancies that are ER-positive express ER, other ER-responsive genes, and genes encoding luminal proteins. ER-negative malignancies can be divided into three groups which include human epidermal growth factor receptor-2 (HER-2) positive, basal-like tumours and normal breast-like tumours.

Breast cancer is typically treated by surgery, where the tumour is either removed around the tissue or by mastectomy, where the whole breast is removed. Other treatments include radiation, chemotherapy, hormonal therapy or targeted therapy. If breast cancer in the early stages tests positive for hormone receptors, hormonal therapy for a minimum of 5 years is recommended. If the malignancy overexpresses a protein that promotes growth (*e.g.* HER-2 protein) then targeted therapy is rather considered. Breast cancer is mainly diagnosed in the stages when the tumour is localized without spreading where a 5-year survival rate of 99% is predicted. When cancer spreads to nearby or distant lymph nodes, the 5-year survival rate decreases sharply to 84 or 23% respectively (ACS, 2016).

1.4 Modes of programmed cell death

In 1964 programmed cell death (PCD) was identified for the first time and defined as a controlled sequence of events that continuously produce and remove cells maintaining normal homeostatic functions (Lockshin and Williams, 1964). Apoptosis is the most studied form of PCD and is highly regulated where the fate of the cell is determined upon exposure to stressors. Studies using three model organisms (*Caenorhabditis elegans, Drosophila melanogaster* and *Mus musculus*) helped to shape the understanding of how PCD plays a role in animals. In fact, the core apoptotic pathway and the role that caspases play in apoptosis were identified in studies using the nematode *C. elegans* (Ellis and Horvitz, 1986; Yuan *et al*., 1993). It was believed that apoptosis was the only form of PCD that existed, but other controlled cell death mechanisms have come to light. There are three forms of controlled cellular death pathways known as apoptosis (Type I), autophagy (Type II) and necrosis (Type III) (Schweichel and Merker, 1973; Clarke, 1990). These forms of cell death together decide the

fate of the cell in the organism. Apoptosis along with necrosis contribute to the death of the cell, whereas autophagy plays a role in both cell survival and death (Danial and Korsmeyer, 2004; Ouyang *et al*., 2012). These forms of cell death can be easily distinguished by their morphological appearance. Kerr *et al*. (1972) were the first to identify the two-step morphological manifestations of apoptosis with the aid of electron microscopy. The first stage involves the formation of vesicle filled structures known as apoptotic bodies. These apoptotic bodies are phagocytosed in the second stage and degraded by lysosomes (Kerr *et al*., 1972; Kerr *et al*., 1994). In the same study, some cells appeared to be ruptured upon cellular stress which rather serves as markers of necrotic cell death. The phagocytosed apoptotic bodies have been mistaken in the past for autophagic vacuoles which are structural components involved in autophagy (Kerr *et al*., 1972).

1.4.1 Type I form of cell death: Apoptosis

Apoptosis occurs naturally during development and ageing and further contributes to maintaining normal cellular homeostasis. Apoptosis is also involved in defence mechanisms such as immune reactions or when cells need repairing due to damage by a disease or agent (Norbury and Hickson, 2001; Elmore, 2007). Apoptotic induction is regulated by a family of cysteine-dependant aspartate-specific proteases (caspases) that are responsible for cleaving aspartic acid residues from their specific substrates (Alnemri *et al*., 1996). The caspases are subdivided either into the initiator caspases, like caspase-2, -8, -9 and -10, or effector caspases that include caspase-3, -6, -7 and -14 (Riedl and Shi, 2004). The former groups of caspases all play a role in cell death. In addition, other caspases that include caspase-1, -4 and -5, fall into another group of caspases that are involved in cytokine maturation and the inflammatory response. Unlike the initiator and effector caspases, the cytokine-based caspases tetrapeptide specificities do not correspond to the sites of most apoptotic proteins but match with sequences found on pro-cytokines like pro-interleukin-1b (pro-IL-1b) and pro-interleukin-18 (pro-IL-18) (Reed, 2000; Denault and Salvesen, 2002). In animal cells, caspases are present as inactive zymogens or proenzymes. These proenzymes are activated upon aspartic acid removal and generate a large 20 kDa and small 10 kDa subunit on the polypeptide chain. Overall, the active enzyme consists of two large and two small subunits along with two active sites for substrates to bind (Thornberry and Lazebnik, 1998). The proteolytic cleavage and activity of executioner caspases are dependent on the upstream initiator caspases. The cleavage site on the executioner caspases separates the large and small subunit of the proenzyme and contains a sequence that matches the tetrapeptide of the specific initiator caspases. In addition, other cellular proteins which act as substrates during apoptosis have the same corresponding sequence as the preferred caspases (Thornberry *et al*., 1997; Reed, 1999; Denault and Salvesen, 2002).

Apoptosis is an energy-dependent mechanism that is well coordinated and stringently controlled by either a ligand binding to a specific death receptor (extrinsic or ligand-mediated cell death pathway) or internal cytotoxic insults leading to the activation of proteases and other hydrolytic enzymes (intrinsic or mitochondrial-mediated cell death pathway) (Bayir and Kagan, 2008). Both these pathways cause characteristic biochemical and morphological features that result in cell death (Figure 1.2). The features include the following: cellular rounding, loss of adhesion, compact and segregated nuclear chromatin (pyknosis), internucleosomal cleavage of DNA, cytoplasmic condensation, plasma membrane blebbing, formation of apoptotic bodies (Kerr *et al*., 1972; Reed, 1999; Kerr *et al*., 1994; Elmore, 2007), phosphatidylserine (PS) externalization (Fadok *et al*., 2001) and the proteolytic cleavage of some intracellular substrates (Martin and Green, 1995). Apoptotic bodies are double-membraned structures that contain degraded cellular contents. The PS on the plasma membrane of the dying cell acts as a signal for phagocytes to engulf the apoptotic bodies (Fadok *et al*., 2000). The engulfed apoptotic bodies are then degraded by macrophages, parenchymal or neoplastic cells thus eliminating an immune response (Kerr *et al*., 1972; Kerr *et al*., 1994, Elmore, 2007). Various engulfment receptors have been identified and remain mostly evolutionary conserved from *C. elegans* to mammalian models (Figure 1.2). These receptors include a cluster of differentiation-91, -14, -36, (CD91, CD14 and CD36), $\alpha_v\beta_3$-integrin and the phosphatidylserine receptor (PSR) (Savill and Fadok, 2000).

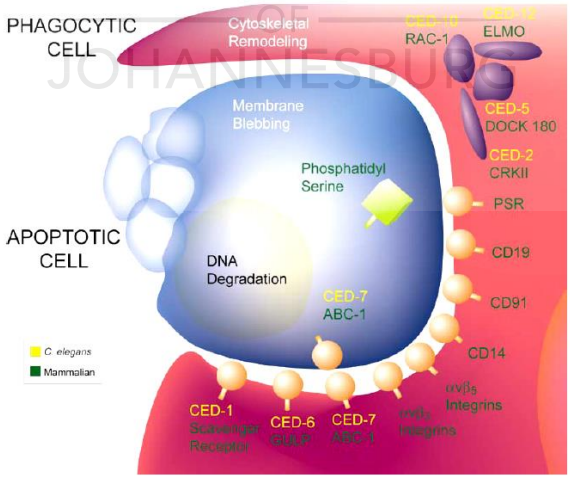

Figure 1.2: The engulfment of apoptotic cells by phagocytes, including the genes that encode the engulfment receptors in both mammalian (green) and *C. elegans* models (yellow). Some biochemical features that include DNA degradation, apoptotic body formation and membrane blebbing are also shown (Adapted from Danial and Korsmeyer, 2004).

1.4.1.1 Extrinsic or ligand-mediated cell death pathway

The extrinsic apoptotic pathway is activated by extracellular stimuli that result in the recruitment of death ligands to their respective death receptors on the cellular surface (Figure 1.3). The best-documented death receptors are those that form part of the tumour necrosis factor (TNF) gene subfamily (Locksley *et al*., 2001; Ashkenazi, 2002). These receptors have cysteine-rich domains that consist of two to five extracellular cysteine repeats. The receptors also have death domains (DD) that contain approximately 80 intracellular amino acid residues within the carboxy terminus. The DD is responsible for transmitting the extracellular death signal from the cellular surface to the intracellular region that in turn activates the downstream mechanisms (Ashkenazi and Dixit, 1998; Naismith and Sprang, 1998; Reed, 2000; Zimmermann *et al*., 2001). The best characterized death receptors and death ligands are: tumour necrosis factor receptor-1 and -2 (TNF-1 and TNF-2) with a tumour necrosis factor-α (TNF-α) ligand, CD95 (Fas or Apo1) receptor and CD95 related ligand (FasL or Apo1L), death receptor-3 (DR3 also known as Apo3, TRAMP or LARD) and Apo3 ligand (Apo3L or TWEAK), death receptor-4 (DR4) and Apo2 ligand (Apo2L or TRAIL), and lastly death receptor-5 (DR5 also known as Apo2, TRAIL-R2, TRICK or KILLER) of which its ligand is still unknown (Chicheportiche *et al*., 1997; Ashkenazi and Dixit, 1998; Peter and Krammer, 1998; Suliman *et al*., 2001; Zimmermann *et al*., 2001; Rubio-Moscardo *et al*., 2005; Elmore, 2007; Lavrik, 2011).

The extrinsic cell death pathway is best characterized by the Fas receptor/ligand (FasR/FasL) and the TNFR/TNFL model systems that involve a clustering of receptors after the binding of homologous trimeric ligand. When the ligand interacts with the receptor, specific adaptor proteins are recruited to the site which contains coinciding sequences on the DD followed by binding. When the FasL binds to the FasR, a Fas-associated death domain (FADD) adaptor protein is recruited to the site of the DD initiating the caspase cascade. In contrast, a TNFR receptor-associated death domain (TNFDD) adaptor protein is recruited and binds to the DD upon TNFL and TNF-α receptor interaction recruiting FADD and the receptor-interacting protein (RIP) (Hsu *et al*., 1995; Scaffidi *et al*., 1998; Wajant, 2002; Elmore, 2007). The FADD that contains the DD and death effector domain (DED) binds to the DD of Fas and further recruit's procaspase-8 to the DED domain forming the death-inducing signalling complex (DISC) (Kischkel *et al*., 1995). Procaspase-8 is automatically activated upon binding and the active caspase-8 is released, initiating the cleavage of downstream executioner caspase-3 and -7 (Scaffidi *et al*., 1998; Lavrik, 2011). The Fas pathway can follow another route that connects with the intrinsic apoptotic pathway which involves a B-cell lymphoma protein 2 (Bcl-2) family member, BH3 interacting domain death agonist (Bid). Bcl-2 blocks the Fas-mediated pathway and creates a mitochondrial-amplification loop where active caspase-8 cleaves Bid to the truncated

form (tBid). The tBid is translocated to the mitochondria and causes cytochrome *c* release followed by downstream caspase activation and finally apoptosis (Li *et al*., 1997; Luo *et al*., 1998; Zimmermann *et al*., 2001; Acehan *et al*., 2002).

Death receptors are not only involved in cell death but also play a role in cellular proliferation. The balance between cell death and survival is controlled by the presence of different complex DD or DED proteins (Danial and Korsmeyer, 2004). For example, the TNFR1 complex that either contains the TNFR associated death domain (TRADD), TNF receptor-associated factor-2 (TRAF2), cellular IAP protein-1 (cIAP1) DD-containing protein or receptor interacting protein-1 (RIP1) kinase promote survival by recruiting I kappa kinase (IKK) and activates NF-κB. The TRADD complex dissembles itself from the receptor and recruits FADD and procaspase-8. A protein inhibitor known as cellular-FLICE inhibitory protein (c-FLIP) is expressed and inhibits the activation of caspase-8 and in turn apoptosis (Chang *et al*., 2002; Micheau and Tschopp, 2003; Lavrik, 2011).

1.4.1.2 Intrinsic or mitochondrial-mediated cell death pathway

In contrast to the extrinsic pathway, the intrinsic pathway functions as a ligand-independent mechanism and is activated upon a series of internal stressors that act directly on targets within the cell (Figure 1.3). This pathway is mitochondrial-mediated and the stressors can either act as negative or positive initiators. In the negative setting, decreased levels of hormones, growth factors and cytokines prevent certain death programs in the cell, thus triggering apoptosis (Elmore, 2007). Other signals like chemotherapy, radiation, viral infections, hyperthermia, toxins and reactive oxygen species (ROS) are positive initiators resulting in the activation of the mitochondrial-mediated pathway (Kaufmann and Earnshaw, 2000; Wang, 2001; Elmore, 2007). These initiators target the mitochondria by disrupting the mitochondrial membrane potential ($\Delta_{\psi m}$), which results in the formation of a mitochondrial-permeability transition (MPT) pore and the release of two groups of Bcl-2 related proteins from the intermembrane space into the cytosol (Kroemer *et al*., 1997; Loeffler and Kroemer, 2000; Saelens *et al*., 2004; Elmore, 2007; Kroemer *et al*., 2007).

Cytochrome *c*, second mitochondria-derived activator direct Inhibitor of apoptosis protein (IAP), second mitochondria-derived activator of caspases (Smac/DIABLO) and the serine protease high- of caspase/temperature requirement protein 2 (HtrA2/Omi) form part of the first group of proteins released from the mitochondria (Cai *et al*., 1998; Du *et al*., 2000; van Loo *et al*., 2002; Garrido *et al*., 2006a). These proteins are responsible for activating the intrinsic pathway in a caspase-dependant manner (Chinnaiyan, 1999; Hill *et al*., 2004). The released cytochrome *c* then interacts with the apoptosis protease activating factor-1 (Apaf-1) that oligomerize in the cytosol. Inactive procaspase-9

is recruited to the oligomer and is activated upon binding. The assembly of the entire complex, in the presence of ATP/dATP, forms the apoptosome (Li *et al*., 1997; Chinnaiyan, 1999; Rodriguez and Lazebnik, 1999; Stennicke *et al*., 1999; Zou *et al*., 1999, Cain *et al*., 2002; Hill *et al*., 2004) or the so-called "death wheel" that ultimately activates downstream executioner caspase-3, -6 and -7 (Zimmermann *et al*., 2001).

Smac/DIABLO is responsible for improving the activation of caspases and in turn, inhibit IAPs (Ekert *et al*., 2001). The second group of proteins include the apoptosome inducing factor (AIF), endonuclease G (Endo G) and caspase activated DNase (CAD), which are released in the later stages of cell death. DNA is fragmented into 50-300 kb fragments and nuclear chromatin condenses after AIF translocates to the nucleus of the cell (Joza *et al*., 2001). The Endo G also translocates to the nucleus but is responsible for the formation of oligonucleosomal DNA fragments (Li *et al*., 2001). Both these proteins' activity is caspase-independent. The CAD protein functions in a similar manner to AIF and Endo G proteins, where it is transported to the nucleus after being cleaved by caspase-3 producing oligonucleosomal DNA fragmentation and more advanced chromatin condensation (Enari *et al*., 1998).

1.4.1.3 Bcl-2 family members and intrinsic cell death pathway

The Bcl-2 family proteins are critical components of apoptosis and act as central regulators in the mitochondrial-mediated or intrinsic cell death pathway (Soriano and Scorrano, 2010). Bcl-2 proteins are characterized by 1 to 4 conserved sequence motifs that are less than 20 amino acids long and are known as Bcl-2 homology domains (BH1 to BH4) (Borner, 2003). These proteins are mainly localized in the mitochondria, the smooth endoplasmic reticulum and in the perinuclear membranes in hematopoietic cells (Reed, 2008). A total of 30 families has been described that can either be classified as anti-apoptotic or pro-apoptotic proteins (Borner, 2003). The Bcl-2 family members can be subdivided into three groups based on their structural and functional characteristics.

The first group are the anti-apoptotic proteins that are made up of all four homology domains (BH1-BH4). These proteins are structurally similar and contain two hydrophobic α-helices located centrally. These helices are surrounded by six or seven α-helices that are amphipathic. In the central region, a hydrophobic pocket exists that serves as a binding site for BH3-only proteins which then terminates apoptosis (Soriano and Scorrano, 2010).

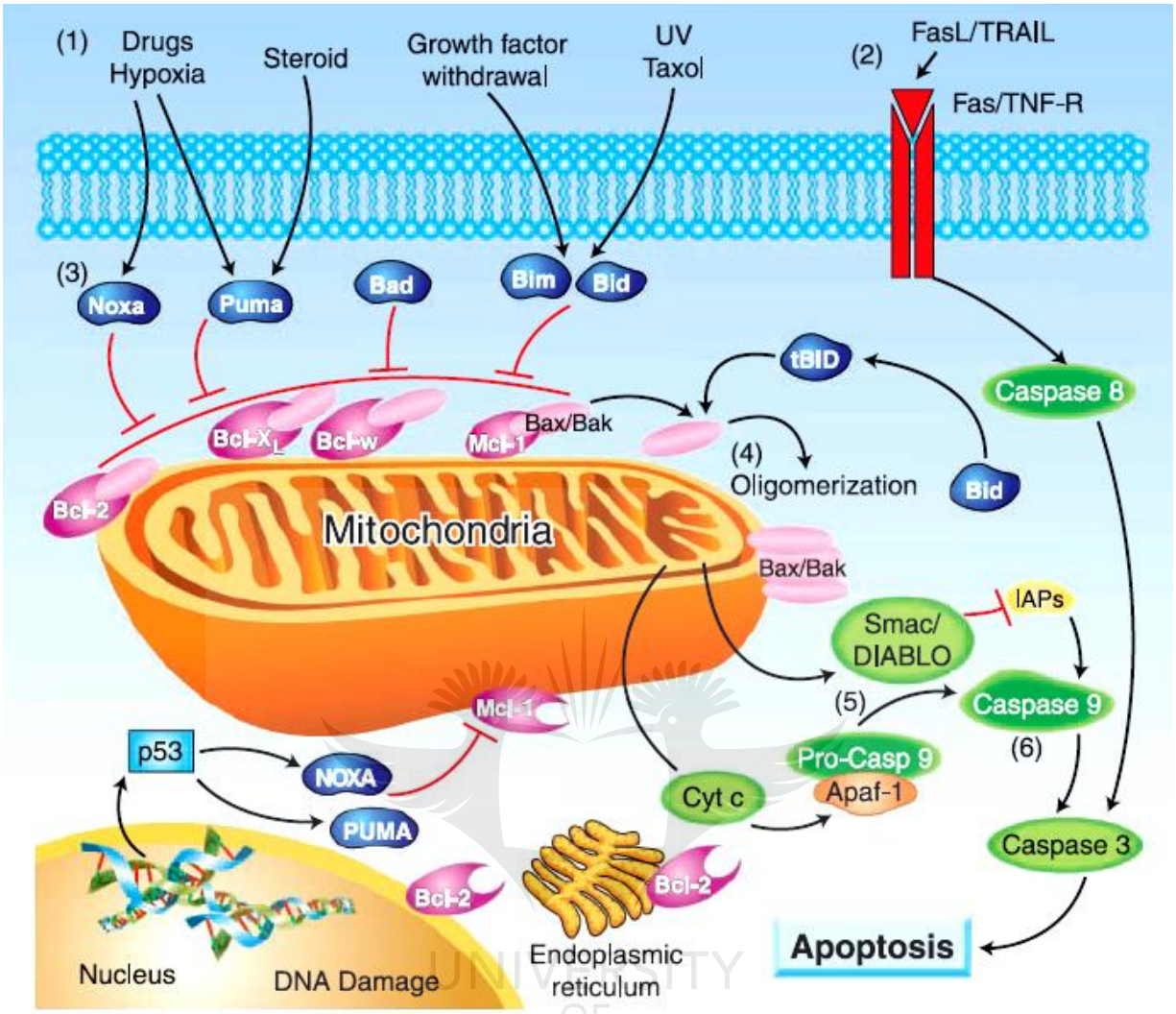

Figure 1.3: Summary of the apoptotic pathway that is divided into either the ligand-mediated or mitochondrial-mediated pathways. The mitochondrial-mediated pathway is activated by a range of intracellular stimuli (1) while the ligand-mediated pathway is activated by extracellular stimuli resulting in the activation of caspase-8 (2). Alternatively, caspase-8 cleaves Bid to form tBid resulting in mitochondrial activation and downstream caspase activities. The BH3-only proteins Bim, Bid, Bad, Puma and Noxa engage with the anti-apoptotic proteins relieving the inhibition of Bax and Bak (3). Bax and Bak oligomerize upon activation and makes holes in the mitochondrial membrane (4). Proteins released from the mitochondria into the cytosol include cytochrome *c* and Smac/DIABLO (5). Here they combine with an adaptor molecule, AIF-1, along with procaspase-9 and assemble to form the apoptosome complex (6). The active caspase-9 then cleaves downstream substrates, which lead to the activation of effector caspases (*e.g.* caspase-3) resulting in apoptosis. Some Bcl-2 proteins are also located in the endoplasmic reticulum and perinuclear membrane in hematopoietic cells (Adapted from Kang and Reynolds, 2009).

Examples of the anti-apoptotic proteins include Bcl-2, the long and short isoform of Bcl type protein 2 (Bcl-xL and Bcl-sL), Bcl-2 like protein 2 (Bcl-w), induced myeloid leukaemia cell differentiation protein 1 (Mcl-1) and Bcl-2 associated athanogene protein (Bag) (Zimmermann *et al*., 2001; Danial and Korsmeyer, 2004; Packham and Stevenson, 2005; Adams and Cory, 2007; Elmore, 2007; Soriano and Scorrano, 2010; Hanahan and Weinberg, 2011). Most of these proteins localize on the membranes of the mitochondria and inhibit the release of cytochrome *c*, thus preventing apoptosis (Soriano and Scorrano, 2010).

The second group are the pro-apoptotic proteins that only contain the three homology domains (BH1-BH3) termed multidomain proteins. Examples of these proteins include Bcl-2 antagonist killer-1 (Bak), Bcl-2 associated X protein (Bax) and Bcl-2 related ovarian cancer killer protein (Bok) (Zimmermann *et al*., 2001; Danial and Korsmeyer, 2004; Packham and Stevenson, 2005; Adams and Cory, 2007; Elmore, 2007; Soriano and Scorrano, 2010; Hanahan and Weinberg, 2011). The three domains in Bax form a hydrophobic pocket that resembles that of Bcl-2 and Bcl-xL. It contains a C-terminal tail that is folded back into the pocket and once this tail is released, the mitochondria are targeted, cytochrome *c* is released and downstream caspases are activated (Suzuki *et al*., 2001; Soriano and Scorrano, 2010).

The third group forms part of the pro-apoptotic family members, but only contain the homologous domain BH3 and is therefore termed the BH3-only proteins. They are inactive in healthy cells but are activated by apoptotic stimuli (Soriano and Scorrano, 2010). Examples of these proteins include BH3 interacting domain death agonist (Bid), Bcl-2 antagonist of cell death (Bad), Bcl-2 interacting mediator of cell death (Bim), Bcl-2 interacting killer protein (Bik), Bik-like killer protein (Blk), p53 up-regulated modulator of apoptosis (Puma) and Noxa (Zimmermann *et al*., 2001; Danial and Korsmeyer, 2004; Packham and Stevenson, 2005; Adams and Cory, 2007; Elmore, 2007; Hanahan and Weinberg, 2011). These proteins are activated upon transcription, phosphorylation and proteolysis (Soriano and Scorrano, 2010). Other BH3-only proteins that are released from the MPT pore are, of which some have already been mentioned, AIF (Susin *et al*., 1999; Cande *et al*., 2004), apoptosis-related protein in TGF-B signalling pathway (ARTS) (Larisch *et al*., 2000; Gottfried *et al*., 2004), cytochrome *c* (Budihardjo *et al*., 1999), Endo G (Li *et al*., 2001), HtrA2 (Suzuki *et al*., 2001) and Smac/DIABLO and IAP (Du *et al*., 2000; Verhagen *et al*., 2000), amongst others. These proteins can be further divided into sensitizer (Bad, Bik and Noxa) or activator proteins (Bim, Bid and Puma) (Letai *et al*., 2002).

The way the Bcl-2 proteins regulate apoptosis is not clear, nevertheless, two models have been proposed whereby they directly or indirectly activate cell death. The direct models explain the activity of BH3-only sensitizer or activator proteins (Letai *et al*., 2002). The activator proteins directly bind to Bax/Bak causing them to oligomerize resulting in the release of cytochrome *c*. In contrast, the sensitizer proteins cannot activate Bax/Bak directly but prevent anti-apoptotic proteins to interact with activator proteins or Bax/Bak rendering them inactive (Wang *et al*., 1996). In the second model, Bax/Bak activate apoptosis without the association with BH3-only activator proteins (Willis *et al*., 2007).

The Bcl-2 proteins are further regulated by the p53 tumour suppressor protein (Figure 1.3). The p53 protein plays a role in diverse cellular processes of which apoptotic regulation is the most important. It serves as a transcription factor that induces the expression of various pro-apoptotic genes (*Bax*, *Bid*, *Puma* and *Noxa*) activating both cell death pathways (Vousden and Lu, 2002; Kang and Reynolds, 2009). The p53 protein activates the expression of *Noxa* and *Puma* that is activated upon DNA damage (Wu and Deng, 2002). Furthermore, p53 can activate Bax either in a transcriptional-dependant or transcriptional-independent manner favouring cell death (Vousden and Lu, 2002; Chipuk *et al*., 2004).

1.4.1.4 Inhibitors of apoptosis (IAP)

In some pathological conditions (*e.g.* AIDS, ischemia and neurodegenerative diseases) apoptosis is overstimulated and consequently, inhibition of apoptosis is required (Elmore, 2007). Cells contain natural inhibitors known as IAPs that are the most important regulators of caspases in both the ligand- and mitochondrial-mediated pathways (Deveraux and Reed, 1999). Eight of these IAPs exist in mammalian cells and include the neuronal apoptosis inhibitory protein (NAIP), cellular IAP protein-1 and -2 (cIAP-1 and cIAP-2), X-linked mammalian IAP (XIAP), survivin, BIR repeat-containing ubiquitin-conjugating protein (Bruce), melanoma IAP (ML-IAP) and IAP-like protein-2 (ILP-2) (Vaux and Silke, 2003; Dubrez-Daloz *et al*., 2008; Gyrd-Hansen and Meier, 2010; de Almagro and Vucic, 2012). These IAPs contain a baculovirus IAP repeat (BIR) domain that is required to interact with the proteins to be inhibited (Takahashi *et al*., 1998). The IAPs like cIAP1, cIAP2, XIAP and ML-IAP are directly involved in apoptosis (Vaux and Silke, 2003; de Almagro and Vucic, 2012). These proteins are best described by having a really interesting new gene (RING) domain and is involved in the proteasome degradation *via* the ubiquitination pathway (Yang *et al*., 2000; Vucic *et al*., 2011). cIAP1 and cIAP2 also contain a CARD domain and is involved in caspase regulation (Lopez *et al*., 2011). These proteins are responsible for the regulation of the NF-κB pathway by stabilizing the NF-κB

inducing kinase (NIK) and stimulating the ubiquitination of RIP1 (Varfolomeev *et al*., 2007; Reviewed by de Almagro and Vucic, 2012).

In general, IAPs are responsible for protecting the cells against cell death, preventing apoptosis through caspase-3, -7 and -9 inhibition (Salvesen and Duckett, 2002). Mutations in these genes contribute to malignant resistance (Fulda and Vucic, 2012). Here proteins like Smac/DIABLO and HtrA2 help to maintain the balance. Smac/DIABLO acts as negative regulators of the intrinsic pathway, by interacting with XIAP and in turn prevent its caspase-9 association. This enables caspase-9 to activate caspase-3 followed by apoptosis (Du *et al*., 2000; Ekert *et al*., 2001). The serine protease HtrA2 protein acts in a similar manner (Martins *et al*., 2002).

1.4.1.5 Apoptotic dysregulation and disease

Under normal conditions, the body is responsible for producing thousands of cells every second. Apoptosis removes the same number of cells to maintain normal homeostatic functions (ACS, 2012). Apoptotic dysregulation causes numerous disease states. When apoptosis is enhanced neurodegenerative disorders (*e.g.* Alzheimer's, Parkinson's and Huntington's) could develop. Autoimmune diseases and myocardial infarction are also consequent effects. In contrast, when apoptosis activity is inhibited or fails, cancer is more prone to develop (Reed, 1999). As mentioned before, cancer develops due to the malfunctioning of genes responsible for regulating cellular growth and division (ACS, 2013; Siegel *et al*., 2016). These are usually genes associated with the tumour suppressor gene *p53* subfamily (Hollstein *et al*., 1991; Muller and Vousden, 2013). The protein, p53, encoded by this gene plays a central role in transcription, DNA repair, genomic stability, senescence, cell cycle regulation and apoptosis. Functional loss of *p53*, due to mutations occurring at this site, is prevalent in many cancers whereby their ability to survive and become resistant to chemotherapeutic agents are enhanced (Harris, 1996).

1.4.2 Type II form of cell death: Autophagy

Other than apoptosis, autophagy is a form of cell death that is activated upon the nutrient deprivation leading to cellular starvation (Mizushima, 2007). Autophagy can respond to either external or internal stressors that can lead to cellular survival, or in some cases, cell death if autophagy is overstimulated (Wang *et al*., 2011). Along with necrosis, autophagy is a caspase-independent mechanism that involves the formation of autophagosomes (Mizushima, 2007; Kroemer *et al*., 2009). The cytosolic content in the autophagosomes can be degraded by three forms of autophagy that include macroautophagy, chaperone-mediated autophagy and microautophagy (Dunn, 1994; Cuervo and Dice, 1998; Kim and Klionsky, 2000; Cuervo *et al*., 2005; Mizushima, 2007).

Microautophagy has not been well characterized in mammalian cells and chaperone-mediated autophagy is a secondary response that temporally follows macroautophagy (Klionsky and Emr, 2000). Macroautophagy is the major pathway for cytoplasmic degradation and is predominantly found in mammalian models (Klionsky and Emr, 2000). Thus, this section will only focus on macroautophagy that occurs in four steps: (1) induction, (2) autophagosome formation, (3) autophagosome docking and fusion and lastly (4) autophagic degradation (Figure 1.4) (Klionksy and Emr, 2000).

During autophagy, cytoplasmic content is sequestrated by phagophores, alternatively known as autophagic vacuoles (Klionsky and Emr, 2000; Mizushima, 2007; Kroemer *et al*., 2009). This step is controlled by GTPases (Petiot *et al*., 2000) and phosphatidylinositol 3-kinases (PI3K) (Ogier-Denis *et al*., 1996). Double membrane vesicles, known as autophagosomes, are formed and cellular degradation is absent at this point. Degradation only occurs once the autophagosomes fuse with lysosomes that are filled with multiple hydrolytic enzymes. The autophagosome membrane is degraded along with the cytoplasmic content (Klionsky and Emr, 2000; Mizushima, 2007; Kroemer *et al*., 2009). The degraded products are recycled in the cytosol and are of importance in gluconeogenesis, the tricarboxylic acid cycle and the synthesis of proteins which altogether contributes to increased energy resources for a limited time period (Reviewed by Mizushima, 2007). Morphological features associated with autophagy include vacuolization of the cytoplasm, degradation of cytoplasmic content (Arstila and Trump, 1968; Klionsky and Emr, 2000; Bursch, 2001) and minimal or no chromatin condensation (Arstila and Trump, 1968; Bursch, 2001; Kroemer *et al*., 2009).

It is difficult to distinguish features of autophagy from that of other forms of cell death using microscopy. Autophagic vacuoles have been mistaken for apoptotic bodies in the past (Kerr *et al*., 1972). Thus, other distinguishable markers are required to prevent confusion. A microtubule-associated light chain-3 (LC3) protein serves as such a marker. It takes on two distinctive forms known as LC3I and LC3II that either exists in nutrient-rich or nutrient-deprived cellular environments respectively (Mizushima, 2004; Tanida *et al.*, 2005). Most *autophagy-related genes* (*Atg*) products like Atg3, Atg5, Atg7, Atg10, Atg 12 an LC3 are involved in two ubiquitination-like modifications of target proteins, conjugation of Atg12 and LC3-modification which are essential in the autophagy pathway (Reviewed by Yoshimori *et al*., 2004).

LC3 is the essential regulator of autophagy that interacts with Atg or other autophagic effectors to initiate autophagosome formation (Figure 1.4) (Huang and Liu, 2015). The proLC3 form is processed to the cytosolic form, LC3I, and further processed by various effectors that include *Atg* products to produce the membrane-bound LC3II form (Figure 1.4) (Kabeya *et al*., 2000; Tanida *et al*., 2002; Mizushima, 2004).

When the fusion of autophagosomes with lysosomes are completed, the LC3II located in the fused structures are degraded (Kabeya *et al*., 2000). The LC3II is destined to bind to the membrane of the autophagosome and thus serves as a marker for autophagy. A green fluorescent protein-LC3 (GFP-LC3) fusion protein can be used to monitor autophagy. This GFP-LC3 protein interacts with the autophagosomes or autolysosomes producing a distinct green fluorescence (Kabeya *et al*., 2000). The conversion of LC3I to LC3II can also be monitored by SDS-PAGE and immunoblotting (Mizushima, 2004).

There are two key regulators of autophagy known as the mechanistic target of rapamycin (mTOR) complex and Beclin-1. mTOR, alternatively known as mTORC1, is a serine/threonine protein kinase that is a member of the phosphatidylinositol kinase-related kinase (PIKK) family. In addition, its activity is inhibited in times of starvation (Noda and Ohsumi, 1998). The mTOR complex is an inhibitor of autophagy and is activated upon interaction with the Atg1 kinase complex (Reviewed by Pattingre *et al*., 2008). In contrast to mTOR, Beclin-1 is a positive regulator of autophagy ensuring its activation. It is located upstream of the LC3 activity. Beclin-1 recruits the release of autophagy-regulating proteins, thus initiating the formation of the autophagosome. Beclin-1, which forms part of the tumour suppressor gene subfamily, interlinks autophagy and apoptosis. It functions through the NF-κB pathway where it promotes the inhibition of apoptotic processes (Reviewed by Pattingre *et al*., 2008; Kang *et al*., 2011). It interacts with Bcl-2, inhibits Bax activity and prevents the release of cytochrome *c* from the mitochondria. Low levels of Beclin-1 have been associated with tumour development and progression (Schwartz *et al*., 1993; Bursch *et al*., 2000). In cancer, autophagy is triggered in cells with malfunctioned apoptotic machinery serving as an alternative approach in cancer therapeutics (Crighton *et al*., 2006; Ghavami *et al*., 2011). In addition, p53 is an alternative regulator of autophagy either functioning as an inhibitor or an activator. This is mostly dependent on the status of the cells and the activation of their signalling pathways (Tasdemir *et al*., 2008).

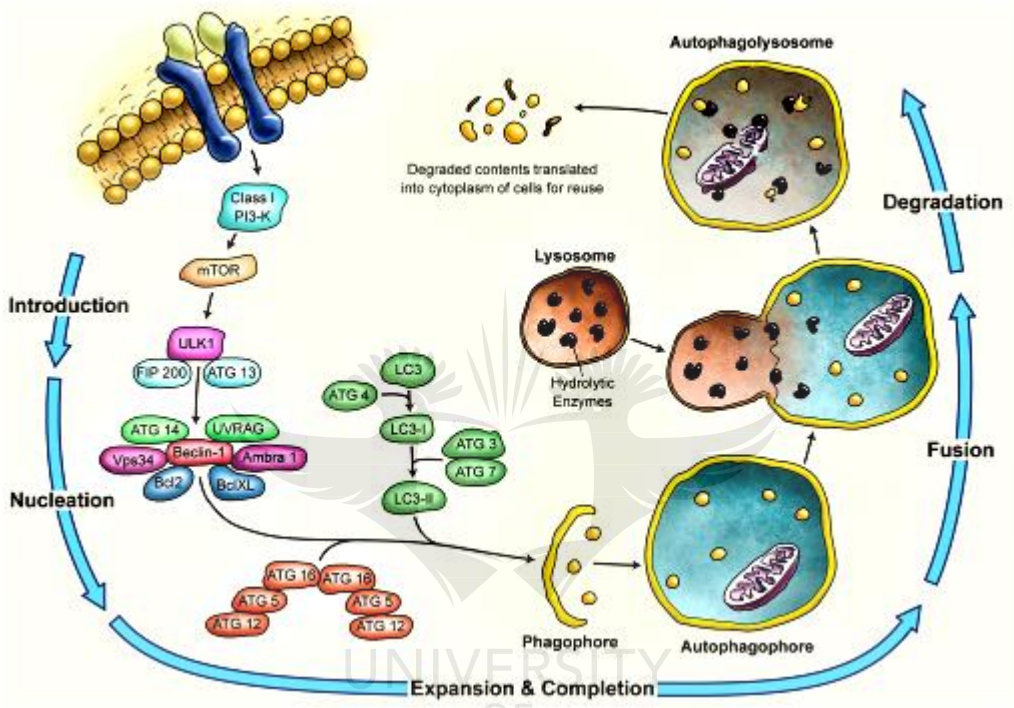

Figure 1.4: Summary of the macroautophagy pathway that is predominant in mammalian cells. Autophagy is triggered in states of starvation where it is responsible for removing or recycling of cellular contents. It is a five-step process that is a well-controlled mechanism, which is activated by Atg molecules. In the first step, the pathway is activated and is termed initiation or introduction. This is followed by phagosome nucleation, phagosome expansion and completion, phagosome and lysosome fusion leading to autophagosome formation, and finally degradation of the autophagosome (Adapted from Marzban *et al*., 2015).

1.4.3 Type III form of cell death: Necrosis

Unlike apoptosis, necrosis is an energy-independent process where cells passively fall victim to cell death in a caspase-independent manner (Los *et al*., 2002; Elmore, 2007). Necrosis has been considered over the years as a form of non-programmed cell death that is mainly caused by chemical or physical injury (Vandenabeele *et al*., 2010). However, accumulating evidence suggests, that necrosis is a controlled event and is regulated by signal transduction pathways (Festjens *et al*., 2006; Kroemer *et al*., 2009; Van Herreweghe *et al*., 2010; Galluzzi *et al*., 2012). Based on the regulatory role, necrosis can be referred to as necroptosis (Chaabane *et al*., 2013). Morphological features of necrosis differ from apoptosis and autophagy where the cellular volume increases, organelles start to swell, rupturing of the plasma membrane occurs, which is followed by the release of intracellular contents (Kerr *et al*., 1972; Proskuryakov *et al*., 2003; Kroemer *et al*., 2009). The released cellular debris triggers an inflammatory response in the surrounding tissue (Carswell *et al*., 1975; Proskuryakov *et al*., 2003; Festjens *et al*., 2006; Cho *et al*., 2009). It is due to this inflammatory response that apoptosis is the preferred method to target malignancies. A wide range of factors are involved in triggering necrotic cell death. These include ROS generation, irregularities in calcium homeostasis (specifically in the mitochondria), stimulation of ceramide and the release of certain protease (Reviewed by Festjens *et al.,* 2006).

As in the ligand-mediated cell death pathway of apoptosis, necrosis (or necroptosis) can be initiated when the TNF-α, FasL and TRAIL ligands are activated (Figure 1.5) (Christofferson and Yuan, 2010). The mechanism regarding these two pathways is still under intensive investigation, but it is known that a serine/threonine kinase, RIP1, is an important factor involved in necroptosis that is responsible for regulating the activities of TNF and NF-κB (Holler *et al*., 2000; Chan *et al*., 2003; Festjens *et al*., 2006). Under normal conditions, RIP1 activity is inhibited by necrostatin-1 (Nec-1) (Degterev *et al*., 2008). When TNF-α binds to the TNFR, the association along with RIP1 stimulates the production of two complexes known as the TNFR-1 signalling complex (complex I) and the cytoplasmic signalling complex (complex IIa) that activates the NF-κB and apoptosis respectively (Micheau and Tschopp, 2003; Chan *et al*., 2003; Cho *et al*., 2009). Complex I regulate the stabilization of NF-κB inducing kinase (NIK) and the ubiquitination of RIP1 through the NF-κB pathway with the help of cIAP1 (Varfolomeev *et al*., 2007; Reviewed by de Almagro and Vucic, 2012; Galluzzi *et al.,* 2012). Normally caspase-8, in complex I, inactivates RIP1 through cleaving. When caspase activity is inhibited, for example by the pancaspase inhibitor Z-VAK-fmk, complex IIb assembles with the help of cylindromatosis (CYLD) (Zhang *et al*., 2009; Galuzzi *et al*., 2012).

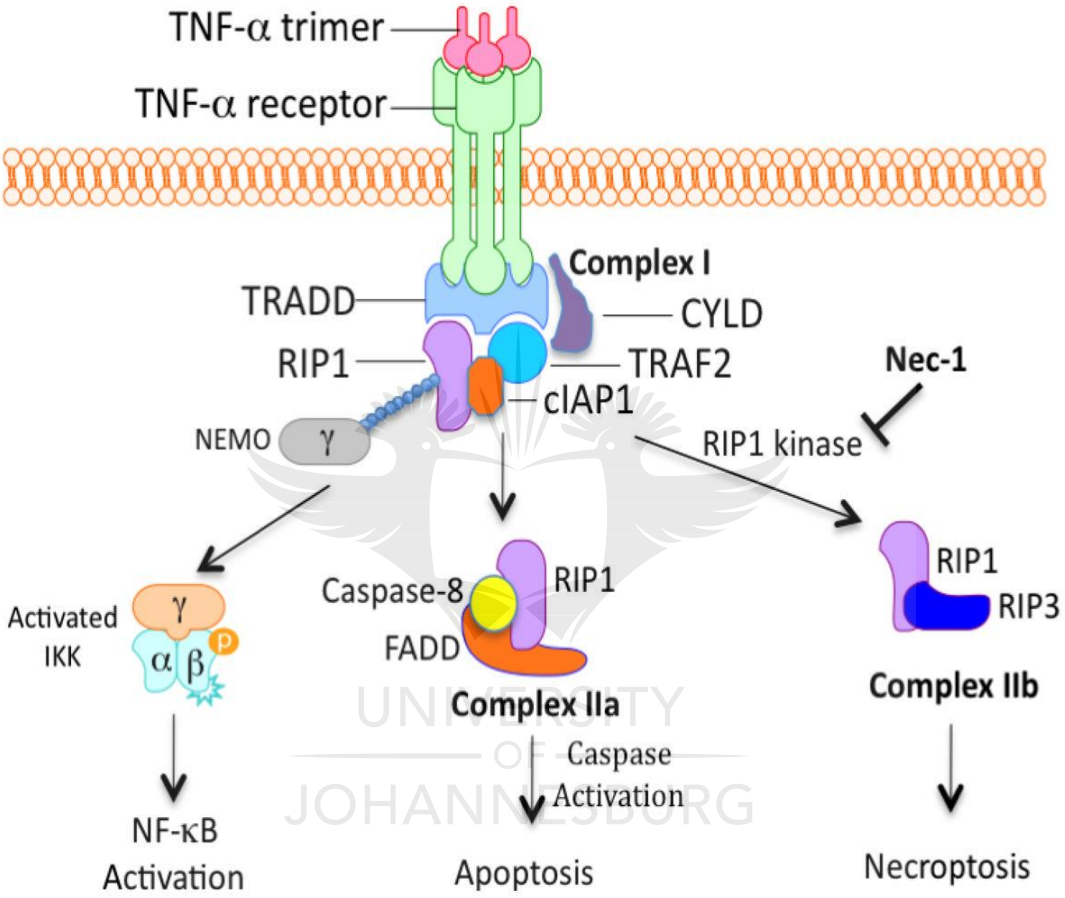

Figure 1.5: A summary of the signalling pathways of NF-κB, apoptosis and necroptosis activation (Adapted from Christofferson and Yuan, 2010). When the TNF-α ligand interacts with the TNF-α receptor, complex I is formed downstream containing TRADD, TRAF2 and RIP1. RIP1 is then deactivated and targeted for degradation by cIAP1, which further recruits Nemo, thus activating the NF-κB pathway. When caspase-8 activity is low or inhibited, CYLD ensures that RIP1 interacts with RIP3 to form complex IIb resulting in necroptosis. Complex II formation can also be inhibited by Nec-1 (Christofferson and Yuan, 2010; Galluzzi *et al*., 2012).

Complex IIb is formed when RIP1 and RIP3 proteins interact *via* the RIP homotypic interaction motif (RHIM) domain forming a pre-necrotic complex (Sun *et al*., 2002). The pre-necrotic complex's metabolic activity is enhanced by metabolic enzymes like glycogen phosphorylase, glutamate-ammonia ligase and glutamate dehydrogenase-1 in ROS production and ultimately leads to necrosis (Cho *et al*., 2009; Festjens *et al*., 2006; Zhang *et al*., 2009; Galluzzi *et al*., 2012).

This form of regulated necrosis could serve as an alternative triggering mechanism to fight pathogenic infections *via* host innate immunity (Chan *et al*., 2003; Cho *et al*., 2009). Poly(ADP-ribose) polymerase 1 (PARP1) is a modulator of necroptosis that is activated through RIP kinase (Moubarak *et al*., 2007; Galluzzi *et al*., 2012) or the synthesis of PAR polymers (Hassa, 2009). PARP1 is important for the activation of the c-Jun N-terminal kinase (JNK) that affect the integrity of the mitochondrial membrane leading to the release of mitochondrial proteins and necrosis (Xu *et al*., 2006).

1.5 Metal-based chemotherapeutic agents

The use of medicinal inorganic chemistry has been increasing in the last few years. This is based on the fact that metal-based complexes can be used and manipulated to design different therapeutic agents. A wide range of metal ions are important in some biological systems (*e.g.* zinc, iron, copper etc.) and in addition metal-based complexes are routinely administered to patients to act as a therapeutic (*e.g.* treatment of Wilson's disease, AIDS, antibacterial agent, cancer etc.) or as a diagnostic marker (Berners-Price and Sadler, 1988; Farrell, 1999; Orvig and Abrams, 1999; Farrell, 1992; Haas and Franz, 2009). It was realized in 1979, when cisplatin was discovered, that one of the most important functions of metal-based drugs is their ability to act as anticancer agents (Berners-Price and Sadler, 1988: Farrell, 1999; Frezza *et al*., 2010). Metal-based complexes can be divided into seven groups based on the functionality of the metal and ligand moieties. These groups contain metal complexes that are active in their inert form, metal complexes that are active in their reactive form, metal complexes acting as radiation enhancers, metal complexes containing a radioactive core, metals or their biotransformation products that are active, metals containing a biologically active ligand and lastly metals that only contain a fragment that is active (Hambley, 2007). For our study, metal-complexes falling into group six, metals containing a biologically active ligand, are of interest. The advantage of using these ligand metal-based complexes, in cancer therapeutics, is their ability to adapt various three-dimensional configurations with the ligand (Berners-Price and Sadler, 1988; Farrell, 1999; Meggers, 2009; Meijboom *et al*., 2009). This ensures that tailor-made metal drugs can be produced for specific molecular targets, therefore creating a targeted therapeutic approach.

A metal complex should fulfil the following requirements before being considered as a lead chemotherapeutic agent (Zaki *et al*., 2016):

(i) Should solubilize easily in a non-toxic solvent (*e.g.* saline) and reach the tumour site as an intact functional molecule.
(ii) Can be transported efficiently in blood and through cellular membranes.
(iii) DNA binding should be sufficient to ensure cell death with minimal reactivity with proteins.
(iv) Should be able to distinguish between malignant and non-malignant cells.
(v) Must be able to target cancerous cells that are or have become resistant to treatment.

With the above in mind, multiple studies have been reported by different research platforms to possibly identify a metal complex that could fit the mentioned criteria. Some of the metal-based complexes studied include platinum, ruthenium, gold, copper and silver.

1.5.1 Platinum complexes

The extensive study of metals in medicine is largely due to the approval of cisplatin as an anticancer drug (Orvig and Abrams, 1999). The geometrical configuration of cisplatin is square-planar where the platinum(II) centre is surrounded by two sets of ligands: two ammonias and two chlorides. These ligands orientate a *cis*-ligand configuration with respect to the metal centre (Hannon, 2007). Cisplatin on its own or in combination with other chemotherapeutic drugs, have been successful in treating oesophageal cancer (Walsh *et al*., 1996; Forastiere *et al*., 1997; Kelsen *et al*., 1998; Ilson *et al*., 1999; Tepper *et al*., 2008; Neuner *et al*., 2009), mice leukaemia, advanced sarcomas (Rosenberg and Vancamp, 1969), testicular, cervical, ovarian, breast, head and neck, small lung carcinomas (De Pas *et al*., 2001; Shah and Dizon, 2009; Zhang *et al*., 2010) and some cancers of the bladder (Vaughn and Malkowicz, 2001; Plimack *et al*., 2015).

Various anticancer mechanisms of cisplatin have been proposed, but the most defined one involves interaction with DNA (Lee *et al*., 2002; Rafique *et al*., 2010). The platinum-based complex enters the cell by passive diffusion and is transported intracellularly where it binds to the DNA (Gomez-Ruiz *et al*., 2012). This is then followed by adduct formation and intra-crosslinking of the DNA strands. Consequently, various signal transduction pathways involved in transcription and DNA replication are activated downstream and interfere with these cellular processes. For example, the crosslinking causes the sequestration of DNA repair mechanisms that involve RNA polymerase II. Failure to repair

the fault causes the activation of the ubiquitination pathway and targets the cell for apoptosis (Lee *et al*., 2002; Siddik, 2003; Rafique *et al*., 2010).

The problem with cisplatin as an anticancer agent is the fact that some malignancies (*e.g.* ovarian cancer) become resistant to the treatment because they are unable to accumulate the complex in the cell (Kelland *et al*., 1992; Borst *et al*., 2008). Cisplatin can also be trapped intracellularly at a higher extent preventing cancer cell death. It can provoke DNA repair mechanisms and prevent DNA damage and cell death from occurring (Borst *et al*., 2008). Treatment with cisplatin has also been known to be less selective by harming non-malignant cells (Segapelo *et al*., 2009; Rafique *et al*., 2010) including cells of the reproductive system (Ciftci *et al*., 2011). The low selectivity of cisplatin is associated with severe side effects that include toxicity of the kidneys (nephrotoxicity), neurons (neurotoxicity), inner ear (ototoxicity), gastrointestinal region and in addition nausea and vomiting, therefore, restricting it's use for cancer therapy (Reed *et al*., 1996; Fischer *et al*., 2008; Tsang *et al*., 2009).

Over 3000 platinum derivatives have been synthesized with the hope of having improved pharmacological characteristics. Less than 30 have been considered for clinical trials which include carboplatin and oxaliplatin. However, more than half of the considered platinum drugs have already been rejected in clinical studies (Desoize and Madoulet, 2002). Attention is given to several non-platinum metal complexes that have been studied extensively as anticancer agents with the hope of producing improved anticancer activities *in vitro* and *in vivo*. Other phosphine metal complexes, like ruthenium(II) triarylphosphine, have shown to be moderately active in ovarian cancer (Snelders *et al*., 2011). The well-known gold(I) complex, (2,3,4,6-tetra-O-acetyl-1-thio-β-D-glucopyranosato-S-triethylphosphine gold(I)) (auranofin) is one of the first synthesized phosphine containing metallo-drugs, including its silver(I) phosphine analogues that have shown to possess anticancer activities (Simon *et al*., 1981; Berners-Price and Sadler, 1988; McKeage *et al*., 1998; Zachariadis *et al*., 2004; Hadjikakou *et al*., 2008; Liu *et al*., 2008). Copper(I) phosphine derivatives tend to be potent in a range of *in vitro* cancer cell lines (Berners-Price *et al*., 1987; Berners-Price and Sadler, 1988; Marzano *et al*., 2008; Santini *et al*., 2011), although *in vivo* activity is less potent (Berners-Price *et al*., 1987; Berners-Price and Sadler, 1988).

1.5.2 Ruthenium complexes

To overcome the limitations of platinum complexes, ruthenium(II) and (III) complexes have been synthesized and tested for their anticancer activities especially in cisplatin-resistant cell lines. They have also been used to act as an immunosuppressant, antibiotics or antibacterial agents (Allardyce

and Dyson, 2001). To date, two ruthenium (III) complexes [ImH][trans-$RuCl_4$(DMSO)(Im)] (NAMI-A) and [InH][trans-RuCl4$(In)_2$] (KP1019) containing an imidazole (Im) or indazole (In) substitute respectively have been introduced in phase I clinical trials (Reviewed by Antonarakis and Emadi, 2010). NAMI-A is one of the first ruthenium drugs to reach clinical trials and has shown to act on tumours in an extracellular manner and inhibit metastasis. Studies reported that NAMI-A shows activity against colorectal, lung, melanoma, ovarian, pancreatic (Rademaker-Lakhai *et al*., 2004) and breast malignancies (Pacor *et al*., 2004). In contrast to NAMI-A, KP1019 is directly cytotoxic by promoting apoptosis in cancers like colorectal (Kapitza *et al*., 2005) and cervical carcinomas (Heffeter *et al*., 2010).

Ruthenium(II) and (III) are octahedral in structure, this means the central metal core is surrounded by six ligands, atoms or atom groups (Brabec and Nováková, 2006). The structure differs from cisplatin which orientates a square planar configuration (Hannon, 2007). Based on the structural differences, the mode of cell death should be different between these two complexes. DNA interaction has been reported (Cauci *et al*., 1987; Kelly *et al*., 1990; Snelders *et al*., 2011), albeit at a much lower level than cisplatin (Seelig *et al*., 1992; Pluim *et al*., 2004). Ruthenium complexes also induce apoptosis through the mitochondrial-mediated pathway (Reviewed by Antonarakis and Emadi, 2010).

NAMI-A in small doses can minimalize metastasis upon binding to proteins or RNA, causing the thickening of the protein layer of the tumour. The encapsulated tumour blood flow is reduced and metastatic cells cannot be released. The overall consequence is the suffocation of the tumour thereby decreasing its viability (Allardyce and Dyson, 2001). NAMI-A coordinates itself into the nucleic acids, therefore directly interacting with the DNA of the tumour (Pluim *et al*., 2004). Although NAMI-A and KP1019 share similar structures, their cancer targeting differs remarkably. KP1019 targeting is more direct, as mentioned before, by causing oxidative stress accompanied by features associated with the intrinsic cell death pathway that includes down-regulation of Bcl-2, increased mitochondrial membrane depolarization and caspase-3 activity (Kapitza *et al*., 2005; Brabec and Nováková, 2006; Reviewed by Antonarakis and Emadi, 2010).

Ruthenium appears to be a more selective chemotherapeutic agent than the platinum-based complexes with minimal toxicity in non-cancerous cells (Sava *et al*., 1984; Kapitza *et al*., 2005; Antonarakis and Emadi, 2010). Sava *et al*. (1984) described that the improved selectivity is based on the interaction of ruthenium with transferrin. Transferrin is found in abundance in tumour tissue

rather than healthy cells. Consequently, these complexes accumulate in the tumour and induce cell death. High doses of NAMI-A can cause skin blisters, but some side effects that include anaemia, fatigue, anorexia, stomatitis, peripheral oedema and diarrhoea are caused by this complex (Rademaker-Lakhai *et al*., 2004). The side effects of the mitochondrial targeting KP1019 complex is less severe and is in the process of entering phase II of clinical trials (Hartinger *et al*., 2006).

1.5.3 Gold complexes

Gold(I) complexes, specifically auranofin, have been studied for their therapeutic use to treat rheumatoid arthritis (Bombardier *et al*., 1986). In addition, auranofin and other gold(I) counterparts have shown to be beneficial in treating asthma (Szefler, 1992), malaria (Sannella *et al*., 2008) and HIV (Fonteh *et al*., 2010). Some studies have demonstrated that gold(I) display anticancer activities in melanoma (Berners-Price and Sadler, 1988; Caruso *et al*., 2007; Rackham *et al*. 2007), colon carcinoma (Rackham *et al*., 2007), breast adenocarcinoma (Humphreys *et al*., 2007; Rackham *et al*., 2007), lymphocytic leukaemia (Simon *et al*., 1981; Rigobello *et al*., 2008), cisplatin-resistant ovarian cancer (Marzano *et al*., 2007) and moderate activity in cervical adenocarcinoma (Segapelo *et al*., 2009).

Because of gold(III) structural similarity with cisplatin, one should expect that their mode of cell death should be comparable (Puddephatt, 1978). However, this is not the case, although the unique mechanism of gold analogues is not yet clear, some studies suggest they inhibit the activity of a mitochondrial enzyme, thioredoxin reductase (TrxR) (Rigobello *et al*., 2004; Rackham *et al*., 2007; Rigobello *et al*., 2008) thus differing from platinum. TrxR is an antioxidant enzyme dependent on thioredoxin (Trx) and NADPH that is responsible for catalysing the reduction of protein disulphides, removal of hydrogen peroxide (H_2O_2), formation of deoxynucleotides and the regulation of transcription factors (Arnér and Holmgren, 2000; Papp *et al*., 2007). Consequently, the mitochondria represent an important target for gold-based drugs downstream from the TrxR activity. For example, a gold(I) complex containing a 1,3-bis (di-2-pyridylphosphino) propane (d2pypp) ligand has shown to target the mitochondria of MDA-MB-468 breast cancer cells after treatment (Rackham *et al*., 2007). The complex studied therein inhibited the activity of Trx and TrxR, decreased the $\Delta_{\psi m}$ which led to the activation of caspases and finally apoptosis. Furthermore, the lipophilic character of the complex is believed to play a role in mitochondrial targeting and improved selectivity (Berners-Price *et al*., 1986; McKeage *et al*., 2000; Liu *et al*., 2008).

Even though gold complexes show to be promising anticancer agents their use is also limited. Gold complexes, especially auranofin and gold(III) complexes, are unstable in the presence of serum

proteins like albumin which could hinder their cytotoxic effect (Mirabelli *et al*., 1985; Segapelo *et al*. 2009). Some gold(I) complexes are less selective and tend to be cytotoxic to the liver (Berners-Price *et al*., 1987; Rush *et al*., 1987; Hoke *et al*., 1988) and non-malignant analogues (Humphreys *et al*., 2007; Segapelo *et al*., 2009). The side effects of gold, when it accumulates in the cells, occur mostly on the skin that includes rashes, dermatitis and stomatitis. In addition, the presence of proteins in urine (proteinuria), platelet deficiency (thrombocytopenia) and nephropathy (Ott, 2009) and brain damage at higher dosages have been reported in mice (Suwalsky *et al*., 2004).

1.5.4 Copper complexes

Among other metal species studied, copper, an essential metal, have been explored for its anticancer role (Berners-Price and Sadler, 1988). The concentration of copper should be strictly regulated in mammalian cells by means of homeostasis to prevent the cellular accumulation or deficiency (Puig and Thiele, 2002). Copper(I) complexes like $[Cu(dppey)_2]Cl$, $[Cu(dppp)_2]Cl$ and $(CuCl)_2(dppe)_3$ were shown to be cytotoxic to mice tumour models, but the degree of toxicity was comparable to that of a gold(I) complex, $[Au(dppe)_2]Cl$. Furthermore, the $[Cu(eppe)_2]Cl$ complex was inactive in mice bearing M5076 reticulum cell sarcoma and B16 melanoma (Berners-Price *et al*., 1987). In another study, a water-soluble Cu(I) phosphine complex displayed the highest anticancer activity in lung, breast, colon, cervical, ovarian and cisplatin-resistant ovarian cancer cell lines when compared to the other metal species studied therein (Santini *et al*., 2011). Three copper(II) complexes showed a marked degree of toxicity in an A549 lung, HCT-116 colon, MDA-MB-231 breast, HeLa cervical and in SH-SY5Y neuroblastoma cell lines (Acilan *et al*., 2016).

Regarding the mode of action, multiple studies suggest that copper complexes target the DNA of malignant cells (Huang *et al*., 2005; Sabolová *et al*., 2011; Acilan *et al*., 2016; Kathiresan *et al*., 2016). It is believed that the production of ROS causes oxidative DNA damage which is important for apoptosis-induced activities (Tan *et al*., 2009; Acilan *et al*., 2016; Zaki *et al*., 2016). Increased proteasome activity along with high levels of copper are predominant in tumour tissue and thus can be used as targets for therapy (Frezza *et al*., 2010). Some copper complexes have shown to decrease the activity of the proteasome in malignant cells that led to the activation of apoptosis (Chen *et al.,* 2007; Frezza *et al*., 2010).

Because copper is an endogenous element it could overcome some drawbacks that are presently found in other metal complexes, like cisplatin. This is especially important to improve the high cytotoxicity in normal cells and intrinsic and acquired resistance of malignant cells (Zhang *et al*.,

2003). Although copper complexes show to be less cytotoxic to aortic muscle cells (Acilan *et al*., 2016), cytotoxicity in kidney cells have been reported (Berners-Price *et al*., 1987).

1.5.5 Silver complexes

Silver(I) has long been known to possess potent antimicrobial properties and is one of the few drugs that can treat infections, burns and wounds and further preventing the spread of contagious diseases (Silver *et al*., 2006; Medici *et al*., 2016). Unfortunately, when antibiotics were introduced in the late 1940's the use of silver as a treatment decreased. Later it was realised that microbes can build up resistance to antibiotics, but not to the silver treatment (Pelgrift and Friedman, 2013). The use of silver(I) as an anticancer agent became very attractive because of its ability to take on various structural and nuclear configurations together with the occupancy of a diverse range of functional ligands (Zachariadis *et al*., 2004; Hadjikakou *et al*., 2008; Meijboom *et al*., 2009). The ease of structural manipulation could be beneficial when targeted chemotherapeutic drugs are synthesized. Silver(I) phosphine complexes have shown toxic activity in a wide range of malignant models (Berners-Price *et al*., 1987; Berners-Price and Sadler, 1988; McKeage *et al*., 1998; Liu *et al*., 2008; Zartilas *et al*., 2009; Kyros *et al*., 2010; Poyraz *et al*., 2011; Kriel and Coates, 2012; Banti *et al*., 2015). In fact, three studies in our research group showed that silver(I) thiocyanate complexes are ten times more active in oesophageal (Human *et al*., 2015; Potgieter *et al*., 2015; Potgieter *et al*., 2016) and breast malignancies (Ferreira *et al*., 2015) than cisplatin.

Most studies focus on the cytotoxicity of silver(I) phosphine complexes in malignant cells and not the specific cell death mechanism thereof. Some studies reveal that these complexes induce apoptosis (Kyros *et al*., 2010; Poyraz *et al*., 2011; Kriel and Coates, 2012; Human *et al*., 2015; Ferreira *et al*., 2015; Potgieter *et al*., 2016). It is believed that a lipophilic link exists between the silver(I) complexes (including that of the gold(I) complexes) and the mitochondria of the malignant cells (Berners-Price *et al*., 1986; McKeage *et al*., 2000; Liu *et al*., 2008). This is based on the concept that lipophilic cations are attracted to the anionic charged inner mitochondrial membrane space thus favouring the intrinsic cell death pathway (Chen, 1988; Ross *et al*., 2005). McKeage *et al*. (1998) suggested that lipophilic cations could suppress mitochondrial ATP synthase activity, even though this has not been confirmed yet. A decrease in the mitochondrial TrxR enzyme (Santini *et al*., 2011) and lipoxygenase (LOX) (Poyraz *et al*., 2011) activity have been reported in malignant cells after treatment with the studied silver(I) complexes. Although it seems that the mitochondria are the main targets for silver(I) complexes further studies are required to confirm this.

Silver(I) phosphine complexes are more biologically stable and less cytotoxic to liver cells than the gold(I) analogue, auranofin (Mirabelli *et al*., 1985; Liu *et al*., 2008). The silver complexes are also less toxic to normal kidney (Ferreira *et al*., 2015), peripheral blood mononuclear cells (PBMCs) (Kriel and Coates, 2012), skin (Ferreira *et al*., 2015) and lung fibroblast (Poyraz *et al*., 2011) cells.

1.6 Hypothesis and aims of study

In Africa, especially Southern Africa, both oesophageal and breast malignancies fall in the top 4 most diagnosed cancers. These cancers usually have a low prognosis largely due to the late diagnosis and lack of treatment resources available in the country. Furthermore, both oesophageal and breast carcinomas are mostly resistant to conventional chemotherapeutic drugs and are prone to metastasis. However, lipophilic metals-based drugs, like silver(I) phosphine, show promise as anticancer agents. A total of six novel silver(I) phosphine complexes (complexes **1**-**6**) were investigated for their cytotoxic effect, possible cell death mechanism and identification of possible drug target. An additional complex (complex **7**) was further studied to identify cancer-related changes on a genetic level. Based on the published research, it appears that these complexes target the "powerhouses", the mitochondria, of the malignant cells, consequently resulting in apoptosis. Thus, in this two-part study, it is hypothesised that the silver(I) phosphine complexes will selectively induce malignant cell death by means of the mitochondrial-mediated apoptotic pathway and will alter cellular features that are associated with metastasis thus improving patient response.

The aims of this study were therefore to:

- establish human derived cell cultures that include two malignant, SNO oesophageal and MCF-7 breast, and two non-malignant, HDF-a skin fibroblasts and HEK293 embryonic kidney cell lines (Part 1).

- estimate the IC_{50} concentrations of the silver(I) complexes in malignant cells by means of dose-response studies.

- study the cytotoxic effect of the complexes using four different viability assays.

- study the morphological changes, in the malignant cells, associated with the different treatments and in turn predict the mode of cell death.

- monitor if these complexes cause cell cycle arrest and PS externalization in the malignant cells.

- determine the role of executioner caspases-3/7 in the apoptotic pathway.

- test the cytotoxicity of the complexes in non-malignant HDF-a and HEK293 cells.

- determine if the specific uncoordinated phosphine ligands are cytotoxic to all four cell lines.
- establish if these complexes target the mitochondria-mediated pathway by studying different features associated with this pathway.
- identify possible drug targets by measuring the activity of two metabolically active enzymes after being exposed to the complexes.
- further screen the cytotoxicity of the complexes in a panel of 16 malignant cell lines.
- study the gene expression levels of various cancer-related genes, which include apoptosis, in the presence of a selected complex (Part 2).

CHAPTER 2: Cytotoxicity and cell death studies of complexes 1-6

2.1 Preamble

Silver(I) complexes, with the general formula $AgXL_n$ (X = non-coordinating or coordinating anion, L = tertiary phosphine, *n* = ligand ratio that could be 1-4) (Meijboom *et al*., 2009), form part of a group of patented complexes that were synthesized in-house. Complexes in this group have shown to be active in malignant cell models (Ferreira *et al*., 2015; Human *et al*., 2015; Potgieter *et al*., 2015; Potgieter *et al*., 2016). The complexes are synthesized by reacting adequate amounts of phosphine ligand with the silver(I) salts containing either silver-halides (Cl, Br or I), pseudo-halides (CN and SCN) or nitrate derivatives (NO_3). This is usually done under reflux (heated) in an acetonitrile solution followed by crystallization to obtain a powder of the silver(I) phosphine product (Meijboom *et al*., 2009). To further add complexes to the growing arsenal of silver(I) phosphines, the toxicity of a new set of silver(I) complexes were reported in this chapter and compared to a known chemotherapeutic drug, cisplatin. These complexes vary in metal to ligand ratio, silver salt and the species of the phosphine ligand coordinated to the complex. Their cytotoxicity is reported in an SNO oesophageal and MCF-7 breast cancer cell line and further compared to that of two HDF-a skin and HEK293 embryonic kidney non-cancerous cell lines to determine their selective properties. Furthermore, more insight is given in the mechanistic targeting of the silver(I) complexes that are beneficial in understanding their role in cancer and designing targeted anticancer agents.

2.2 Materials and methods

In Appendix 2, a list of the manufacturers of all reagents, materials, apparatus and software used are listed.

2.2.1 Synthesis of silver(I) phosphine complexes

2.2.1.1 Complex characterization

The silver(I) complexes in this chapter were synthesized in-house and characterized either by Dr. Gadada Naganagowda (complexes **1**, **3**-**6**) or Dr. Rehana Malgas-Enus (complex **2**) in the Department of Chemistry at the University of Johannesburg. The complexed silver salts were first characterized by various methods before being used for biological studies. Melting points were recorded on a Stuart Scientific Melting Point apparatus SMP10, and are uncorrected. FT-IR spectra were recorded on a Bruker Tensor 27 FT-IR spectrometer, using a PIKE miracle Gate ATR accessory. Nuclear magnetic resonance (NMR) spectra were measured and recorded on a Bruker Ultrashield Avance III 400 MHz spectrometer. The ^{1}H-NMR, ^{13}C-NMR and ^{31}P-NMR spectra were obtained in DMSO-d_6 at

400 MHz for ^{1}H nuclei, 75 MHz for ^{13}C nuclei and 161 MHz for ^{31}P nuclei. All chemical shifts were reported in ppm using residual H or C signals in deuterated chloroform ($CDCl_3$) as internal references. All ^{31}P NMR chemical shifts were referenced against H_3PO_4 as an external standard. Elemental analysis was performed at the Department of Chemistry at Rhodes University by Dr. Edith Antunes using a Thermo Flash 2000 series CHNS/O, Organic Elemental Analyser. The data output of the methods described above is indicated below.

2.2.1.2 Synthesis of 1:2 [Ag(p-OMeC$_6$H$_4$)$_3$P]SCN (Complex 1)

AgSCN salt (0.1014 g, 0.611 mmol) was added to a solution of tris(4-methoxyphenyl)phosphine (0.4255 g, 1.21 mmol) (**L1**) in acetonitrile (50 ml). The solution was heated under reflux for 6 hrs. The hot solution was filtered and evaporated to ±10 ml. Thereafter, the solution was left to crystalize at room temperature for 24 hrs forming small white crystals. **Yield:** 77%. **Melting point:** 180-183 °C. **IR (ν/cm^{-1}):** 3057.74, 3009.06, 2954.35 (asymm), 2834.14 (ν(=C-H),w); 2537.39 (ν(C-H), w); 2079.56 (ν(SCN), m); 1896.50 (w); 1590.47, 1567.55 (ν(C=C aromatic), asymm, s); 1496.23, 1457.73, 1439.61 (asymm) 1403.52 (ν(C=C aromatic), s, m); 1305.80, 1289.76, 1246.76, 1176.34 (ν(OCH_3), s); 1097.33 (s), 1024.01 (s); 820.92, 796.30 (ν(aromatic, δ C-H para),asymm, s); 757.55, 715.57 (ν(aromatic, δ C-H mono),asymm, s); 653.43, 635.53, 623.14 (ν(aromatic, δ C-H meta),asymm, m). **^{1}H NMR (400 MHz, $CDCl_3$) δ (ppm):** 3.72 (s, 18H, OCH_3), 6.74 (d, δ_1=6.733, δ_2=6.754, ^{1}J=8.4 Hz, 12H, C-H C3, C5), 7.18 (t, δ_1=7.156, δ_2=7.181, δ_3=7.202, ^{1}J=9.2 Hz, 12H, H-aromatic). **^{13}C{H} NMR (100 MHz, $CDCl_3$) δ (ppm):** 55.24 (s, OCH_3); 114.51 (d, δ_1=114.46, δ_2=114.56, ^{1}J(P-C)=7.5 Hz); 123.61 (d, δ_1=123.46, δ_2=123.76, ^{1}J(P-C)=22.0 Hz, para C); 126.54 (s); 135.19 (d, δ_1=135.10, δ_2=135.27, ^{1}J(P-C)=12.8 Hz, ipso C). **^{31}P{H} NMR (161 MHz, $CDCl_3$) δ (ppm):** 5.45. **Elemental Analysis:** $C_{86}H_{84}Ag_2N_2S_2P_4O_{12}$: Calculated: C, 59.32%; H, 4.86%; N, 1.61%; S, 3.68%. Found: C, 58.98%; H, 5.02%; N, 1.33%.

2.2.1.3 Synthesis of 1:2 AgCN(PPh$_3$)$_2$ (Complex 2)

AgCN salt (0.15 g, 1.12 mmol) was added to a solution of triphenylphosphine (0.6 g, 2.24 mmol) (**L2**) in acetonitrile (50 ml). The reaction mixture was heated under reflux overnight. The hot solution was filtered and evaporated to ±10 ml. Thereafter the solution was left to crystalize at room temperature for 24 hrs to form small needle like crystals. **Yield:** 75%. **Melting point:** 193 °C. **IR (ν/cm^{-1}):** 3056 (w), 2323 (w), 2119 (m), 1891 (w), 1823 (w), 1670 (w), 1585 (w), 1478 (s), 1433 (s), 1309 (m), 1182 (w), 1182 (w), 1156 (w), 1092 (s), 1069 (m), 1026 (w), 997 (w), 917 (m), 849 (w), 740 (s), 691 (s). **^{1}H NMR (400 MHz, $CDCl_3$) δ (ppm):** 7.19 (t, *J* =7.0 Hz), 7.18 (m, *J* =7.0 Hz), 3.33. **^{13}C{H} NMR (100 MHz, $CDCl_3$) δ (ppm):** 133.8 (d, *J*(C-P)=12.5 Hz), 133.4(d, *J*=12.0 Hz), 130.58, 129.3 (d, *J* =14.9 Hz). **^{31}P{H} NMR (161 MHz, $CDCl_3$) δ (ppm):** 25.53. **Elemental Analysis:** $C_{37}H_{30}AgNP_2$: Calculated: C, 67.49%; H, 4.59%; N, 2.13%. Found: C, 67.07%; H, 4.99%; N, 2.11%.

2.2.1.4 Synthesis of 1:3 Ag[(4-Cl-PPh$_3$)$_3$]NO$_3$ (Complex 3)

$AgNO_3$ salt (0.0527 g, 0.31 mmol) was added to a solution of tris(4-chlorophenyl)phosphine (0.3402 g, 0.93 mmol) (**L3**) in acetonitrile (50 ml). The solution was heated under reflux overnight. The hot solution was filtered and evaporated to ±10 ml. Thereafter, the solution was left to crystalize at room temperature for 24 hrs to form small needle like crystals. **Yield:** 73%. **Melting Point:** 169-171 °C. **IR (ν/cm-1):** 3060.73, 2360.76 (ν (=C-H),w), 1653.00, 1575.29, 1560.37 (m), 1477.95 (ν (C=C aromatic), m), 1381.55, 1313.90 (m), 1181.42 (w), 1080.31, 1011.54, 811.60 (s), 745.07 ((aromatic, C-H), s), 703.48 (ν (aromatic, C-H meta), s). **^{1}H-NMR (400 MHz, $CDCl_3$) δ ppm:** 7.118-7.257 (m, 36H, Ar-H). **^{13}C-NMR (100 MHz, $CDCl_3$) δ ppm:** 137.23 (s), 134.82 (d), 134.64 (d), 130.51 (d), 130.31 (d), 129.49 (d), 129.40 (d, Aromatic Carbons). **^{31}P NMR (161 MHz, $CDCl_3$) δ ppm:** 3.29 (Single Peak), **Elemental analysis:** $C_{54}H_{36}AgCl_9NO_3P_3$: Calculated: C, 51.20%; H, 2.86%; N, 1.11%. Found: C, 51.40%; H, 2.40%; N, 1.10%.

2.2.1.5 Synthesis of 1:3 Ag[(4-CH$_3$PPh$_3$)$_3$]NO$_3$ (Complex 4)

$AgNO_3$ salt (0.0527g, 0.31 mmol) was added to the solution of tri(*p*-tolyl)phosphine (0.2830 g, 0.93 mmol) (**L4**) in acetonitrile (50 ml). The solution was heated under reflux overnight. The hot solution was filtered and evaporated to ±10 ml. Thereafter, the solution was left to crystalize at room temperature for 24 hrs to form small needle like crystals. **Yield:** 74%. **Melting Point:** 171-173 °C. **IR (ν/cm^{-1}):** 3018.23 (ν (=C-H),w), 2920.23, 2360.64 (ν (alkane, C-H, stretch), asymm, w), 1700.48 (w), 1684.46, 1653.08, 1597.22, 1558.57, 1539.65 (ν (C=C aromatic), m), 1498.15 (ν (C=C aromatic), m), 1395.10 (ν (CH_3 bend), m), 1299.39 (s), 1188.86-801.21 (ν (aromatic, C-H bend, meta), s), 707.29 (ν (aromatic, C-H bend, ortho), m). **^{1}H-NMR (400 MHz, $CDCl_3$) δ ppm:** 2.31 (s, 27H, CH_3), 7.241-6.972 (m, 36H, Ar-H). ^{13}C-NMR (100 MHz, $CDCl_3$) δ ppm: 140.24 (s), 133.73 (d), 133.56 (d), 129.65 (d), 129.56 (d), 129.34 (d), 129.10 (d, Aramotic Carbon), 21.40 (s, CH_3). **^{31}P NMR (161 MHz, $CDCl_3$) δ ppm:** 5.86 (Single Peak). **Elemental analysis:** $C_{63}H_{63}AgNO_3P_3$: Calculated: C, 69.87%; H, 5.86%; N, 1.29%; Found: C, 69.49%; H, 5.81%; N, 1.20%.

2.2.1.6 Synthesis of 1:3 Ag[(4-CH$_3$PPh$_3$)$_3$]Br (Complex 5)

AgBr salt (0.1333 g, 0.71 mmol) was added to the solution of tri(*p*-tolyl)phosphine (0.6483 g, 2.31 mmol) (**L4**) in acetonitrile (50 ml). The solution was heated under reflux overnight. The hot solution was filtered and evaporated to ±10 ml. Thereafter, the solution was left to crystalize at room temperature for 24 hrs to form small needle like crystals. **Yield:** 91%. **Melting Point:** 224-226 °C. **IR (ν/cm^{-1}):** 3017.86, 2918.52, 2863.82 (ν (=C-H),w), 2140.60, 2024.24 (ν (alkane, C-H, stretch), asymm, w), 1908.55 (w), 1807.71 (s), 1647.99, 1597.43, 1560.32 (ν (C=C aromatic), m), 1497.66, 1446.44 (ν (C=C aromatic), m), 1396.08 (ν (CH_3 bend), m), 1379.59 (w), 1307.24 (s), 1271.94 (s), 1214.04 (w),

1188.05-805.00 (ν (aromatic, C-H bend, meta), s), 710.08, 641.95, 628.71, 609.33 (ν (aromatic, C-H bend, ortho), m). **^{1}H-NMR (400 MHz, $CDCl_3$) δ ppm:** 2.346 (s, 27H, CH_3), 7.265-7.055 (m, 36H, Ar-H). **^{13}C-NMR (100 MHz, $CDCl_3$) δ ppm:** 139.52 (s), 133.92 (d), 133.75 (d), 130.82 (d), 130.66 (d), 129.41 (d), 129.32 (s, Aromatic Carbon), 21.39 (s, CH_3). **^{31}P NMR (161 MHz, $CDCl_3$) δ ppm:** 0.70 (Single Peak). **Elemental analysis:** $C_{63}H_{63}AgBrP_3$: Calculated: C, 68.73%; H, 5.77%; Found: C, 68.70%; H, 5.55%.

2.2.1.7 Synthesis of 1:3 Ag[(4-$CH_3PPh_3)_3$]SCN (Complex 6)

AgSCN salt (0.0515 g, 0.31 mmol) was added to the solution of tri(*p*-tolyl)phosphine (0.2830 g, 0.93 mmol) (**L4**) in acetonitrile (50 ml). The solution was heated under reflux overnight. The hot solution was filtered and evaporated to ±10 ml. Thereafter, the solution was left to crystalize at room temperature for 24 hrs to form small needle like crystals. **Yield:** 78%. **Melting Point:** 190-192 °C. **IR (ν/cm^{-1}):** 3019.41 (ν (=C-H),w), 2916.25, 2359.84 (ν (alkane, C-H, stretch), asymm, w), 2076.35 (ν (SCN), m), 1675.47 (s), 1597.02, 1560.10 (ν (C=C aromatic), m), 1497.48, 1446.26 (ν (C=C aromatic), m), 1395.58 (ν (CH_3 bend), m), 1309.13-804.25 (ν (aromatic, C-H bend, meta), s), 708.24 (ν (aromatic, C-H bend, ortho), m). **^{1}H-NMR (400 MHz, $CDCl_3$) δ ppm:** 2.30 (s, 27H, CH_3), 7.240-6.984 (m, 36H, Ar-H). **^{13}C-NMR (100 MHz, $CDCl_3$) δ ppm:** 139.75 (s), 133.80 (d), 133.63 (d), 130.24 (d), 130.05 (d), 129.51 (d), 129.42 (d), 126.32 (s, Aromatic Carbon), 21.39 (s, CH_3). **^{31}P NMR (161 MHz, $CDCl_3$) δ ppm:** 3.59 (Single Peak**). Elemental analysis:** $C_{64}H_{63}AgNSP_3$: Calculated: C, 71.24%; H, 5.88% N, 1.30%; S, 2.97%; Found: C, 71.01%; H, 6.46%; N, 1.42%; S, 3.09%.

2.2.2 Complex preparation

Stock solutions of complexes **1-6** were prepared in cell culture graded dimethyl sulfoxide (DMSO: vehicle). Some complexes were not readily soluble in DMSO, but when heated (at 70 °C for 1 h) the crystals solubilized. Stock solutions of the ligands **L1**-**L4** were also prepared in DMSO. The ligands were exposed to the same conditions as the complexes even though they were readily soluble. All stocks were kept in the dark at 4 °C and heated at 70 °C for 30 min prior to treatment. The uncomplexed silver salts were excluded from the study due to their insoluble or less soluble nature in DMSO.

2.2.3 Cell lines

An adherent SNO oesophageal (ATCC, cat no. CCL-185) and MCF-7 breast (ATCC, cat no. HTB-22) cancer cell line were used in this study. Two adherent non-malignant cell lines were used as controls. These cell lines included the human dermal fibroblast adult (HDF-a: ATCC, cat no. PCS-201-010) and human embryonic kidney (HEK293: ATCC, cat no. CRL-1573) cells.

2.2.4 Cell culturing

It should be noted that all reagents used for culturing, sub-culturing and plating purposes were pre-warmed at 37 °C before use.

2.2.4.1 SNO and MCF-7 cell lines

Both malignant cells were cultured in Dulbecco's modified Eagles medium (DMEM-13.55 g/L) with additional sodium bicarbonate ($NaHCO_3$-3.7 g/L). The media was supplemented with 10% (v/v) fetal bovine serum (FBS), 1.6% (v/v) Penicillin/Streptomycin/Fungizone and 0.4% (v/v) gentamicin sulphate. The cells were incubated in 75 cm^2 culture flasks for 48 hrs at 37 °C in an HERAcell 150i incubator under a 5% CO_2 humidified atmosphere.

2.2.4.2 HDF-a cell line

The non-malignant HDF-a cells were cultured in Fibroblast Medium (FM) with additional fibroblast growth supplements (FGS), 2% (v/v) FBS along with 5% (v/v) Penicillin/Streptomycin/Fungizone and 1% (v/v) gentamicin sulphate. The cells were incubated in Corning® 75 cm^2 CellBIND® culture flasks for ±72 hrs at 37 °C in an HERAcell 150i incubator under a 5% CO_2 humidified atmosphere.

2.2.4.3 HEK293 cell line

The non-malignant HEK293 cells were cultured in DMEM (13.55 g/L) with additional $NaHCO_3$ (3.7 g/L). The media was supplemented with 10% (v/v) FBS, 1.6% (v/v) Penicillin/Streptomycin/Fungizone and 0.4% (v/v) gentamicin sulphate. The cells were incubated in Corning® 75 cm^2 CellBIND® culture flasks for ±72 hrs in an HERAcell 150i incubator under a 5% CO_2 humidified atmosphere.

2.2.5 Sub-culturing of cell lines

2.2.5.1 SNO and MCF-7 cell lines

The cells were washed once with 10 ml Hanks balanced salt solution (HBSS-9.5 g/L) with additional $NaHCO_3$ (0.35 g/L). Four millilitres of 1% (v/v) trypsin were added to the flasks and incubated for ±10 min. After incubation, the flasks were agitated to loosen the cells from the surface. This was followed by the addition of 6 ml supplemented DMEM to deactivate the trypsin. The cells were collected with a Heraeus Biofuge Promo R centrifuge at 779 x*g* for 4 min. The pellet was resuspended in 1 ml supplemented DMEM and split (volume dependent on stocks growth rate; if high, 250 µl was used or 500 µl, when low) into two 75 cm^2 culture flasks containing 20 ml supplemented DMEM. The cells were passaged every 48 hrs as described above. For experimental purposes, cells from passage number 2-7 were used.

2.2.5.2 HDF-a cell line

The cells were washed once with 10 ml HBSS (9.5 g/L) with additional $NaHCO_3$ (0.35 g/L). Four millilitres of 0.5% (v/v) trypsin was added to the flasks and incubated for ±2 min. After incubation, the flasks were agitated to loosen the cells from the surface. This was followed by the addition of 6 ml supplemented FM to deactivate the trypsin. The cells were collected with a Heraeus Biofuge Promo R centrifuge at 162 x*g* for 5 min. The pellet was resuspended in 1 ml supplemented FM and split into two Corning® 75 cm^2 CellBIND® culture flasks containing 40 ml supplemented FM. When the Corning® 150 cm^2 CellBIND® culture flasks were used, the volumes of all the reagents used were doubled. The cells were passaged every 72 hrs, the same way as described above. For experimental purposes, cells from passage number 2-7 were used.

2.2.5.3 HEK293 cell line

The cells were washed once with 10 ml HBSS (9.5 g/L) with additional $NaHCO_3$ (0.35 g/L). The HEK293 cells were removed from the culture flask without the addition of trypsin. A total of 10 ml DMEM was added followed by agitation until all the cells were detached. The cells were collected with a Heraeus Biofuge Promo R centrifuge at 779 x*g* for 4 min. The pellet was resuspended in 1 ml supplemented DMEM and split into two Corning® 75 cm^2 CellBIND® culture flasks containing 40 ml supplemented DMEM. The cells were passaged every 48 hrs, as described above. For experimental purposes, cells from passage number 2-7 were used.

2.2.6 Cell stocks

Cells were removed and collected as described in section 2.2.5. The pellet was resuspended in 90% (v/v) FBS including 10% (v/v) DMSO to a total volume of 1 ml. The cell stocks were stored in cryogenic vials at -80 °C until needed. When cells were taken out of stock, they were thawed in a preheated (37 °C) water bath. The thawed cells were added to respective 75 cm^2 culture flasks containing either 20 ml of DMEM or FM followed by incubation. After 24 hrs, the media was replaced with new supplemented media (20 ml) and the cells were further incubated until confluence.

2.2.7 Cell counting with Trypan blue dye exclusion assay

Cells were removed and collected as described in section 2.2.5. The pellet was resuspended in 4 ml supplemented DMEM/FM to improve counting efficiency. The cell suspension was vortexed and 10 µl added to 10 µl of Trypan blue dye (1:1). Ten microliters of the stained suspension were added to a TC10™ System-Counting slide. The cellular viability was determined using the TC10™ Automated Cell Counter. For experimental purposes, only cells at a viability of 94% or higher were used.

2.2.8 Plating

2.2.8.1 SNO and MCF-7 cell lines

Cells were removed, collected and counted as described in section 2.2.5 and 2.2.7. A concentration of 2 x 10^5 cells/ml to a final volume of 3 ml DMEM (6 x 10^5 cells) were seeded in 3.5 cm culture dishes. The cells were then incubated for 24 hrs prior to treatment.

2.2.8.2 HDF-a and HEK293 cell lines

Cells were removed, collected and counted as described in section 2.2.5 and 2.2.7. A concentration of 2 x 10^5 cells/ml in FM/DMEM were used of which 100 µl (6 x 10^4 cells) were seeded in a Corning® CellBIND® 96-well plate. The HDF-a cells and HEK293 cells were plated in triplicate and incubated for 24 or 48 hrs respectively before treatment.

2.2.9 Cell treatment

Treatment commenced over a 24 h period for all cell lines.

2.2.9.1 SNO and MCF-7 cell lines

Cells were plated as described in section 2.2.8.1. Used media was removed and a final volume of 1 ml DMEM containing the treatment was added to the 3.5 cm culture plates. The cells were either untreated (UC) or treated with the vehicle control (1% (v/v) DMSO) or 10 µM of complexes **1**-**6** as prepared in section 2.2.2. Cisplatin (CDDP), at a final concentration of 100 µM, was used as a positive apoptotic control. Cisplatin was prepared in 0.9% (w/v) sodium chloride (NaCl) followed by heating (20 °C) for 48 hrs. The cisplatin was stored in the dark at 4 °C and made fresh every 2 weeks. Where applicable a positive necrotic control, 25% (v/v) hydrogen peroxide (H_2O_2), was included and was prepared in DMEM before treatment. The cells were also treated with 10 µM of the phosphine ligands **L1**-**L4**. Dose-response studies (section 2.2.11) were completed in both cell lines to determine the IC_{50} concentration of complexes **1**-**6** and cisplatin. The DMSO concentration did not exceed 1% throughout the study.

2.2.9.2 HDF-a and HEK293 cell lines

Cells were plated as described in section 2.2.8.2. Used media was removed and a final volume of 100 µl of FM/DMEM containing the treatment was added in triplicate in a 96-well plate. The cells were either untreated (UC) or treated with the vehicle control (1% (v/v) DMSO) or 10 µM of complexes **1**-**6**. Cisplatin at a final concentration of 100 µM was used as a positive apoptotic control and prepared as described in section 2.2.9.1. A positive necrotic control, 25% H_2O_2, was included and was prepared

in DMEM prior to treatment. The cells were also treated with 10 µM of the phosphine ligands **L1**-**L4**. The DMSO concentration did not exceed 1% throughout the study.

2.2.10 Cell removal and collection

2.2.10.1 SNO and MCF-7 cell lines

Cells were plated and treated as described in section 2.2.8 and 2.2.9. Used media was removed and kept separately. The cells were washed once with 1 ml HBSS followed by the addition of 300 µl 1% (v/v) trypsin. Thereafter, the cells were incubated for ±5 min and removed from cell culture plates by gently squirting them of the surface. Once all the cells were removed, 1 ml supplemented DMEM was added for deactivation purposes. The cells were collected with an Eppendorf® 5415R bench top centrifuge at 400 x*g* for 4 min. The pellet was resuspended in the old media before experimental analysis.

2.2.10.2 HDF-a and HEK293 cell lines

Experimental analysis was done directly in the Corning® CellBIND® 96-well plates.

2.2.11 alamarBlue® proliferation assay

This assay was done to determine IC_{50} concentrations, for the malignant cells only, as well as cytotoxicity in both the malignant and non-malignant cell lines.

2.2.11.1 SNO and MCF-7 cell lines

Cells were prepared as described in sections 2.2.8-2.2.10. Ten microlitres of alamarBlue® dye was added to 100 µl trypsinized cells (triplicate) in a 96-well plate. Wells containing only media served as a blank. The plate was covered with aluminium foil and incubated for ±2 hrs at 37 °C under a 5% CO_2 humidified atmosphere. After incubation, the fluorescence was measured using a Synergy HT Multi-Detection Microplate reader at an excitation wavelength of 450 nm and an emission wavelength of 590 nm.

2.2.11.2 HDF-a and HEK293 cell lines

Cells were prepared as described in sections 2.2.8-2.2.10. Ten microlitres of alamarBlue® dye was added directly to each well containing 100 µl of the plated cells (see section 2.2.9). Wells containing only media served as a blank. The plate was covered in aluminium foil and incubated for ±2 hrs at 37 °C under a 5% CO_2 humidified atmosphere. After incubation, the fluorescence was measured using a Synergy HT Multi-Detection Microplate reader at an excitation wavelength of 450 nm and an emission wavelength of 590 nm.

2.2.12 CellTiter-Glo® luminescent cell viability assay

Malignant cells were prepared as described in sections 2.2.8-2.2.10. A CellTiter-Glo® kit was used to monitor the levels of ATP in the differentially treated cells. Manufacturer's instructions were followed. Briefly, the CellTiter-Glo® reagent was allowed to equilibrate at room temperature in the dark for 15 min until use. The cellular suspension (25 µl) was added in triplicate to a black 96-well plate together with 25 µl CellTiter-Glo® reagent in the dark. Wells containing only media served as a blank. The plate was gently agitated for 30 secs followed by a 30 min incubation at room temperature, stabilizing the luminescent signal. Total luminescence was quantified using a Synergy HT Multi-Detection Microplate reader.

2.2.13 Light microscopy

Both malignant and non-malignant cells were plated and treated as described in sections 2.2.8 and 2.2.9. Without removing the cells from the 3.5 cm culture or 96-well plates, the morphological features along with the changes were examined under an Axiovert 25 inverted microscope with Axio Version 3.1 software. Images were captured with a magnification of 200 x.

2.2.14 Cell cycle analysis

Malignant cells were prepared as described before. A total of 6 x 10^4 cells in 100 µl DMEM were transferred to a new tube. The cells were collected by means of centrifugation at 300 x*g* for 4 min followed by washing with 500 µl cold (4 °C) phosphate buffered saline (PBS). Thereafter, 100 µl of cold (4 °C) PBS along with 900 µl 70% (v/v) ethanol was added to the tubes and the cells were fixed for at least 2 hrs at 4 °C. The ethanol was removed by means of centrifugation for 5 min at 300 x*g*. Hundred microliters Propidium Iodide (PI) staining solution consisting of 0.1% (v/v) Triton X-100, 40 µg/ml PI and 0.1 mg/ml DNase-free RNase A in 1 x Binding Buffer ™, was added to the cellular pellets. The stained cells were then incubated in the dark at 37 °C for 20 min. After incubation, the cells were further diluted with 350 µl 1 x Binding Buffer™ followed by analysis using the FACSAria™ flow cytometer with FACSDiva™ software. An excitation wavelength of 488 nm and an emission wavelength of 617 nm was used. A total of 50 000 events were recorded. Data analysis and histograms were constructed using the FCS Express Plus 5 Software. The PI-W vs PI-A plots were constructed to exclude doublets. The final gate was used to construct the PI-A plot which discriminates between the different stages of the cell cycle.

2.2.15 Determining the mode of cell death with Annexin-V FITC and PI

Malignant cells were prepared as described before. In addition, the 100 µM cisplatin and 25% H_2O_2 treated cells were included as the apoptotic and necrotic controls respectively. To determine if either apoptosis or necrosis occurred, the cells were double-labelled with Annexin-V FITC and PI fluorochromes by means of an Annexin-V FITC Assay Kit. This was done according to manufacturer's instructions with a few adjustments. Briefly, the cells (± 3 x 10^5 cells) were washed twice with cold (4 °C) PBS, followed by the addition of 100 µl 1 x Binding Buffer™ supplied in the kit. Two and a half microliters of Annexin-V along with 5 µl PI were added in the dark and was incubated for 15 min at room temperature. After incubation, 400 µl 1 x Binding Buffer™ was added, followed by analysis using the FACSAria™ flow cytometer with FACSDiva™ software. An excitation wavelength of 492 nm and an emission wavelength of 520 nm was used for Annexin-V FITC. An excitation wavelength of 488 nm and an emission wavelength of 575 nm was used for PI. Compensation was used to construct the cell gates and a total of 10 000 events were recorded.

2.2.16 Caspase-3/7 activity luminescent assay

Malignant cells were prepared as described before. An Apo-ONE® Homogenous caspase-3/7 assay kit was used according to manufacturer's instructions. Briefly, Caspase®Glo reagent was allowed to equilibrate for 15 min in the dark at room temperature before use. The cell suspension (25 µl) was added in triplicate to a black 96-well plate together with 25 µl Caspase®Glo reagent in the dark. Wells containing only media served as a blank. The plate was lightly agitated for 30 secs and incubated at room temperature for 1 h. Total luminescence was quantified using a Synergy HT Multi-Detection Microplate reader.

2.2.17 Measuring the mitochondrial membrane potential ($\Delta\psi m$)

Malignant cells were prepared as described before. MitoProbe™ JC-1 Assay Kit was used to monitor the changes in the $\Delta_{\psi m}$. Manufacturer's instructions were followed with a few adjustments. A 200 µM (5',6,6'-tetrachloro-1,1',3,3'-tetraethylbenzimidazolylcarbocyanineiodide) (JC-1) dye was prepared by solubilizing the JC-1 powder with 230 µl DMSO and allowed to equilibrate at room temperature. A total of 6 x 10^4 cells (in 100 µl) were used for analysis. Untreated cells were incubated with 0.2 µl (50 µM) carbonyl cyanide 3-chlorophenylhydrazone (CCCP) in DMEM at 37 °C for 5 min which served as a positive mitochondrial membrane disrupter. One microliter of the 2 µM JC-1 dye was then added to both the CCCP and differentially treated cells (in DMEM) followed by incubation at 37 °C for 30 min. The labelled cells were washed twice after incubation with 2 ml pre-warmed (37 °C) PBS and collected at 400 x*g* for 4 min. The cells were resuspended in 300 µl PBS and

analysed using the FACSAria™ flow cytometer with FACSDiva™ software. An excitation wavelength of 488 nm with 530/30 nm and 585/42 nm bandpass emission filters were used. A total of 20 000 events were recorded. Data analysis and contour plots were constructed using FCS Express Plus 5 Software. Unstained cells along with the CCCP-treated cells were used for compensation and gating.

2.2.18 Nuclear, mitochondrial integrity and cytochrome *c* release using fluorescent microscopy

Malignant cells were plated as in section 2.2.8 onto coverslips, followed by treatment as described in section 2.2.9. After 24 hrs of treatment, the used media was removed from the 3.5 cm culture plates. Thereafter, 2 ml of 100 nM MitoTracker Orange CMTMRos probe in pre-warmed DMEM was added to each culture dish and incubated at 37 °C for 30 min. After incubation, the probe was discarded and culture plates washed three times with 2 ml pre-warmed (37 °C) PBS. The cells were then fixed with 4% (v/v) formaldehyde (2 ml) in PBS for 15 min at 37 °C followed by washing. The cells were permeabilzed with 2 ml 0.1% (v/v) Triton X-100 in PBS for 20 min at 4 °C followed by washing. Blocking buffer (1% (w/v) bovine serum albumin (BSA), 0.05% (v/v) Tween-20 in PBS, pH 7.4) was added to the cells and incubated for 30 min at room temperature. The blocking buffer was removed and the cells were incubated with 2 ml Alexa-Fluor® 488 labelled anti-cytochrome *c* antibody (0.5 µg/ml in PBS) for 1 h at room temperature followed by washing. Thereafter, 1 ml Hoechst-33258 (1 µg/ml in PBS) were added to the cells and incubated for 20 min at room temperature followed by washing. The coverslip was mounted on a glass slide containing a drop of mounting medium (9% (v/v) glycerol in PBS) and sealed with clear nail polish. The slides were kept in the dark at 4 °C until images could be captured. The slides were viewed under an Axioplan 2 inverted fluorescent microscope (with Axio Vision imaging software) using Axio Cam camera. Images were captured with a magnification of 1000 x.

2.2.19 Quantification of oxidative stress in cell populations

Malignant cells were prepared as described before. A Muse® Oxidative Stress Kit was used according to manufactures' instructions to measure the number of cells undergoing oxidative stress. A working solution of the Muse® Oxidative stress reagent was first prepared as follows: an intermediate reagent was prepared by diluting (1:100) 2 µl of the stock solution with 198 µl of the 1 x Assay Buffer supplied in the kit. The intermediate reagent was further diluted (1:80) with 1 x Assay Buffer to obtain the working solution. Before labelling, the cells were washed once in pre-warmed (37 °C) PBS and collected at 400 x*g* for 4 min. The pellet was resuspended in 100 µl 1 x Assay Buffer. Thereafter, 10 µl of the cell suspension (6 x 10^4 cells) was transferred to a new tube. To this, 190 µl of the

working solution was added and vortexed. This was followed by incubation for 30 min in the dark at 37 °C. After incubation, a total of 3000 events were recorded on a Muse® Cell Analyser.

2.2.20 Western blot analysis for detecting caspase-9 activity, PARP cleavage and induction of Hsp70

2.2.20.1 Protein extraction

Malignant cells were prepared as described before. The cells were centrifuged at 400 x*g* for 4 min. The pellet was resuspended in cold (4 °C) 100 µl 1 x Laemmli sample buffer (2 x Laemmli buffer: 65.8 mM Tris-HCl, pH 6.8, 2.1% (w/v) SDS, 26.3% (v/v) glycerol, 0.01% (w/v) bromophenol blue) with added 355 mM β-mercaptoethanol and protease inhibitor cocktail tablets. The cell solutions were kept on ice and sonified with an HD 2070 sonicator for 20 secs at 60% power. Thereafter, the lysed cells were heated at 100 °C in a dry bath for 10 min. This was followed by centrifugation at 16100 x*g* for 30 min to remove cell debris. The supernatant was removed and stored at -20 °C until further use.

2.2.20.2 Protein quantification

Protein samples were thawed and kept on ice. A standard stock of BSA was used to construct a standard curve (0.625, 5, 10, 20, 30 and 40 µg/µl). A total of 2 µl of each standard including each sample were loaded in duplicate on a cut 0.45 µM Supported Nitrocellulose membrane. The membrane was air dried and soaked in 50% (v/v) methanol for 5 min. The methanol was replaced by 1 x amido black solution and left for 5 min. The membrane was washed at least four times with 50% (v/v) methanol for 5 min and dried. Each spot was cut out and placed in a well of a 24-well plate to which 800 µl of 0.1 M NaOH was added to each well and allowed to elute on an orbital shaker for 1 h. The nitrocellulose paper was removed and absorbance was read using a Synergy HT Multi-Detection Microplate reader at 600 nm. A standard curve was constructed and the concentrations of the proteins were determined.

2.2.20.3 Protein separation using sodium dodecyl sulphate polyacrylamide gel electrophoresis (SDS-PAGE)

A Bio-Rad mini Protean gel system was assembled and cassettes were set up for casting. Firstly, a 10% separating gel was prepared with 30% (w/v) acrylamide/0.8% (w/v) bisacrylamide, 4 x Tris-HCl/Sodium dodecyl sulphate (SDS) at pH 8.8, 10% (w/v) ammonium persulphate (APS), N, N, N', N-N'-Tetramethylenediamine (TEMED) and dH_2O. The gel was left to polymerise for 45 min. The stacking gel solution was then prepared with 30% (w/v) acrylamide/0.8% (w/v) bisacrylamide, 4 x Tris-HCl/Sodium dodecyl sulphate (SDS) at pH 6.8, 10% (w/v) ammonium persulphate (APS), N, N, N',

N-N'-Tetramethylenediamine (TEMED) and dH_2O. After polymerization, the combs were removed and the gel plates assembled in the system. The tank was filled with 1 x electrophoresis buffer consisting of Tris, Glycine and SDS. An equal amount of protein (15 µg or 60 µg) along with 2 µl of Precision Plus Protein™ Standard was loaded. The gel was resolved for 45 min at 15 mA per gel. After separation, the gel was removed and marked, followed by soaking in Towbin buffer (25 mM Tris, 192 mM glycine and 20% (v/v) methanol) for 15 min.

2.2.20.4 Preparation of PVDF membrane and protein transfer

A Hybond-P™ polyvinylidene difluoride (PVDF) (0.2 µm pore size) was cut to size and activated by washing it in 100% (v/v) methanol for 5 min. The methanol was discarded and the membrane washed twice for 5 min with dH_2O. The membrane was incubated for 20 min in Towbin buffer. The transfer cassette was assembled with the sponges, pre-soaked filter paper, gel and PVDF membrane and placed in the Bio-Rad Mini-PROTEAN® Tetra electrophoresis transfer system with the gels at the negative electrode. The tank was filled with Towbin buffer and proteins transferred for 1.15 hrs (4 °C) at 70V.

2.2.20.5 Blotting and antibody labelling for protein detection

It should be noted that all blotting and labelling was done using light agitation on an orbital shaker. The transfer cassette was removed and the PVDF membrane was washed twice with 1 x TBS (50 mM Tris, 150 mM NaCl, pH 7.5) for 5 min. The membrane was blocked for 1 h in 5% (w/v) non-fat milk powder in TBS (nf-TBS) before primary antibody labelling. After 1 h nf-TBS was removed and the membrane incubated with the primary antibody, which was incubated overnight at 4 °C. The conditions for each antibody differed and are summarized in Table 2.1. The membrane was then washed three times with TBST (1% (v/v) Tween and TBS) for 5 min followed by two blocking steps using 2.5% (w/v) nf-TBS for 10 min each. Horseradish peroxidase-conjugated (HRP) secondary antibody (Table 2.1) was incubated with the membrane for either 1 h (β-actin, PARP and Hsp70) or 2 hrs (caspase-9) followed by three washing steps with TBST for 10 min. Finally, the membrane was incubated with 5 ml Clarity™ Western ECL substrate for 5 min to detect the HRP.

2.2.20.6 Detection using image analyser

A Bio-Rad Chemidoc™ Image analyser was used to visualize the protein bands. The membrane was placed on the Image analyser tray to detect the chemiluminescent signal and images were taken for 2-6 min using Image Lab™ v 4.1 software.

Table 2.1: Conditions for the primary and secondary antibodies to detect selected proteins of interest *via* western blotting for both SNO and MCF-7 cells.

Protein to detect	Primary ab used	[Primary ab]	Secondary ab used	[Secondary ab]
Full length and cleaved caspase-9	Rabbit-anti-human caspase-9 antibody	1:1000 in 2.5% nf-TBS	Anti-rabbit IgG HRP linked	1:2000 in 2.5% nf-TBS
Full length and cleaved PARP	Rabbit-anti-human monoclonal PARP antibody	1:1000 in 5% nf-TBS	Anti-rabbit IgG HRP linked	1:5000 in 2.5% nf-TBS
Inducible Hsp70	Mouse-anti-human monoclonal Hsp70 antibody	1:500 in 5% nf-TBS	Anti-mouse IgG HRP linked	1:5000 in 2.5% nf-TBS
β-actin (loading control)	Mouse-anti-human monoclonal β-actin antibody	1:1000 in 5% nf-TBS	Anti-mouse IgG HRP linked	1:2500 in 2.5% nf-TBS

2.2.21 Measuring the enzymatic activity of Thioredoxin Reductase (TrxR)

Malignant cells were prepared as described before. The activity of TrxR was determined with a TrxR Assay kit according to manufacturer's instructions. Briefly, cells were first centrifuged at 400 x*g* for 4 min. The pellet was resuspended in 100 µl Assay buffer containing Protease inhibitor and sonified for 20 secs at 60% power. The supernatant was collected by means of centrifugation at 10 000 x*g* for 15 min at 4 °C. Equal volumes (50 µl) of the supernatant was added in duplicate in a clear 96-well plate which represented either the DNTB or TrxR inhibited reaction respectively. In crude cell samples, TrxR including other enzymes such as glutathione peroxidase or glutathione reductase are able to reduce the activity of 5,5'-dithiobis (2-nitrobenzoic) acid (DNTB). Therefore, a TrxR specific inhibitor should be included in the assay to ensure that only TrxR reduction is measured. Ten microliters TrxR inhibitor was added to one set of the samples while the other set was adjusted to 60 µl by adding an additional 10 µl Assay buffer to measure the DNTB reduction. The plate was lightly agitated and 40 µl Reaction mixture (Assay buffer, DNTB solution and NADPH) was added to each well. The optical density was immediately measured at 412 nm using a Synergy HT Multi-Detection Microplate reader to obtain reading 1 (T_1). The plate was incubated at 25 °C in the dark for 40 min on an orbital shaker. After incubation, the optical density was measured again to obtain reading 2 (T_2). For both the DNTB and TrxR inhibited reactions, the T_2 was subtracted from T_1 to obtain the specific reduction by TrxR.

2.2.22 Measuring cytochrome P450 (CYP1B1) activity

Malignant cells were prepared as described before. The activity of CYP was measured with a Cytochrome P450-Glo™ Assay kit specific for the CYP1B1 isoform, according to manufacturer's instructions. The cell-based protocol was followed where the cells were washed twice with pre-warmed (37 °C) PBS. A 20 µM Luciferin-CEE substrate stock was diluted (1:50) to 100 µM in fresh DMEM without FBS. Fifty microliters of the diluted substrate were added to the cell samples and incubated for 3 hrs at 37 °C. After incubation, 25 µl of the DMEM cell suspension was transferred to a white 96-well plate and further incubated with 25 µl Luciferin detection reagent at room temperature for 20 min. Wells containing only media served as the blank. Total luminescence was quantified using a Synergy HT Multi-Detection Microplate reader.

2.2.23 Cellular cytotoxicity in a panel of malignant cell lines

Selected silver(I) complexes (complexes **1**, **3** and **5**) along with CDDP were sent to Bioassaix at the Nelson Mandela Metropolitan University (NMMU). These studies were done by Dr. Trevor Koekemoer under the supervision of Prof. Maryna van de Venter in the Department of Biochemistry and Microbiology. The cytotoxicity of the complexes and CDDP were screened in a panel of 16 malignant cell lines originating either from a human, mice or rat. All cell lines tested, culture media and conditions are summarized in Table 2.2. The complexes and CDDP were prepared as described in section 2.2.2. For the adherent cells, a total of 2 x 10^4 cells was seeded in a 96-well plate and left to adhere for 24 hrs. Used culture media was removed and replaced with fresh media containing the treatments where the final concentration was 10 µM for the silver(I) phosphine complexes and 100 µM for CDDP. For cells in suspension, a total 2 x 10^4 cells per 50 µl was seeded followed by a 50 µl of the test solution. Thereafter the cells were treated identically to the adherent cell lines. The cells were treated for a 24 h period followed by the alamarBlue® assay as described in section 2.2.11. The plate was covered in aluminium foil and incubated for ±2 hrs at 37 °C under a 5% CO_2 humidified atmosphere. After incubation, the fluorescence was measured using a Synergy HT Multi-Detection Microplate reader at an excitation wavelength of 450 nm and an emission wavelength of 590 nm.

2.2.24 Statistical analysis

The data was analysed using Microsoft™ Excel and the two-tailed Students *t*-Test. Where applicable, the data was represented as either the Standard Error of the Mean (±SEM), of which error bars were constructed, or the standard deviation (±Std dev). The *P*-values of $*P < 0.05$, $**P < 0.01$ and $***P < 0.001$ were deemed statistically significant with respect to the vehicle control where *n* represented the number of repeats (both technical and biological).

Table 2.2: Summary of cell lines and their culturing media used to determine the cytotoxicity of selected complexes

Malignancy	Cell line	ATCC cat #	Growth characteristics	Culture media
Human cervical adenocarcinoma	HeLa	CCL-2™	Adherent	RPMI with 10% FCS
Human colorectal adenocarcinoma	Caco2	HTB-37™	Adherent	DMEM with 10% FCS
Rat pheochromocytoma	PC12	CRL-1721™	Adherent	RPMI with 5% FCS, 10% HS
Human malignant melanoma	MeWo	HTB-65™	Adherent	DMEM with 10% FCS
Human colorectal adenocarcinoma	HT-29	HTB-38™	Adherent	DMEM with 10% FCS
Human histiocytic lymphoma	U937	CRL-1593.2™	Suspension	RPMI with 10% FCS
Mouse melanoma	B16F10	CRL-6475™	Adherent	DMEM with 10% FCS
Rat pancreatic insulinoma	Ins-1		Adherent	RPMI with 10% FCS
Human lung adenocarcinoma	A549	CCL-185™	Adherent	DMEM with 10% FCS
Human acute T cell leukaemia	Jurkat-T	TIB-152™	Suspension	RPMI with 10% FCS
Human prostate adenocarcinoma	PC3	CRL-1435™	Adherent	F12 Kaighns Mod with 10% FCS
Human neuroblastoma	SH-SY5Y	CRL-2266™	Adherent	F12 Ham/DMEM with 20% FCS
Human hepatocellular carcinoma	HepG2	HB-8065™	Adherent	EMEM with 10% FCS
Derivative of HepG2	HepG2-C3A	CRL-10741™	Adherent	EMEM with 10% FCS
Human pancreatic carcinoma	MiaPaCa	CRL-1420™	Adherent	EMEM
Human breast adenocarcinoma	MCF-7	HTB-22	Adherent	DMEM with 10% FCS

2.3 Results

2.3.1 Structure of silver(I) phosphine complexes

A novel group of silver(I) phosphine complexes have been synthesized and characterized by using a variety of techniques in the Department of Chemistry (section 2.2.1). The techniques included melting point analysis, IR, ^{1}H NMR, ^{13}C NMR, ^{31}P NMR and elemental analysis. The characterization was routinely done for each batch to ensure that a pure complex was used for biochemical studies. Complexes **1**-**6** were synthesized with varying silver salts and phosphine ligands. The silver salts included AgSCN, AgCN, $AgNO_3$ and AgBr and phosphine ligands included tris(4-methoxyphenyl)phosphine (**L1**), tris(4-chlorophenyl)phosphine (**L2**), triphenylphosphine (**L3**) and tri(*p*-tolyl)phosphine (**L4**) (Figure 2.1).

Both complex **1** and **2** are linear and have two phosphine ligands coordinated to one silver salt. Even though these complexes have the same metal: ligand ratio of 1:2, they are structurally different. Complex **1** can either exist in a dimeric or polymeric configuration, whereas complex **2** is only dimeric. The polymeric configuration suggests that monomers are present in solution (Ferreira *et al*., 2015). Complexes **3**-**6** orientate in a tetrahedral geometry, where the silver metal core is surrounded by three phosphine ligands thus are classified as 1:3 complexes. Inclusive, all complexes studied are considered lipophilic in nature due to their low solubility in hydrophilic solutions.

2.3.2 Dose-response studies and IC_{50} concentrations

In order to determine whether the silver(I) phosphine complexes have the ability to induce cancer cell death, an alamarBlue® assay was done after 24 hrs of treatment. Two different human malignant cell lines were used known as the squamous oesophageal carcinoma (SNO) and breast adenocarcinoma (MCF-7). The SNO cells were either untreated (UC, negative) or treated with 1% DMSO (vehicle) and varying concentrations of complex **1**-**6** (2 µM, 4 µM, 6 µM, 8 µM, 10 µM or 12 µM). The MCF-7 cells were either untreated (UC, negative) or treated with 1% DMSO (vehicle) and varying concentrations of complex **3**-**6** (4 µM, 6 µM, 8 µM, 10 µM or 12 µM). The anticancer activity of complexes **1**-**2** in the MCF-7 cells are reported elsewhere and is excluded in this study (Ferreira, 2015; Ferreira *et al*., 2015).

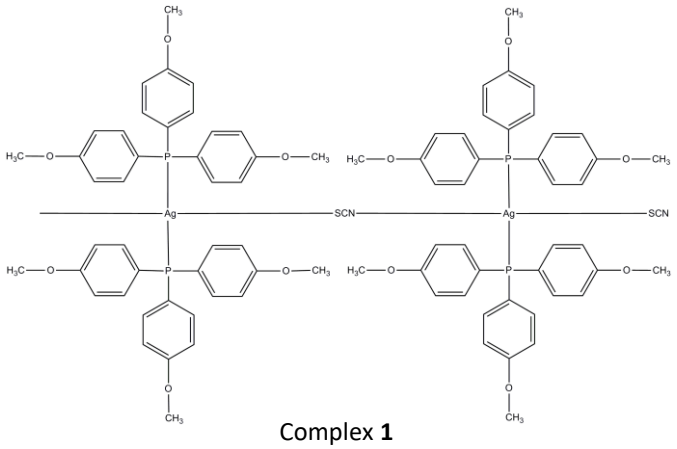

Complex **1**

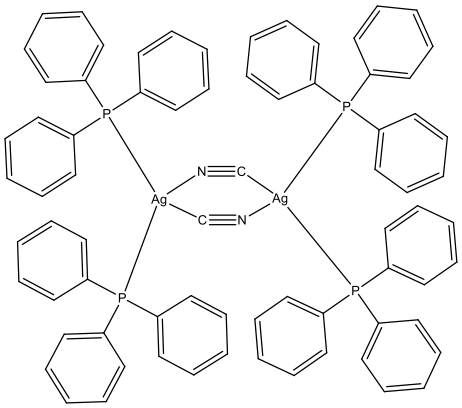

Complex **2**

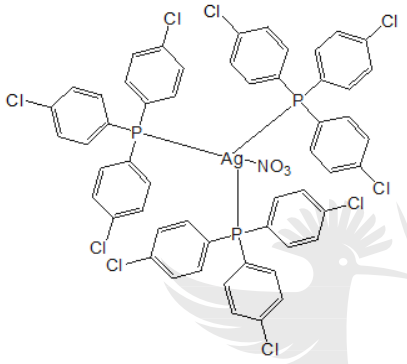

Complex **3**

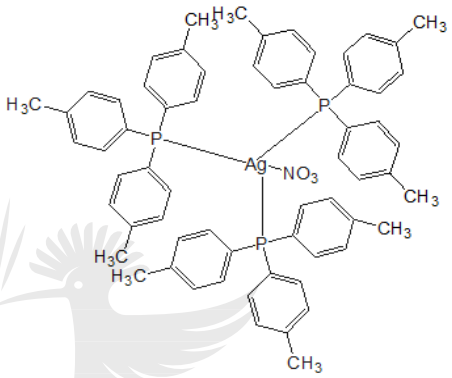

Complex **4**

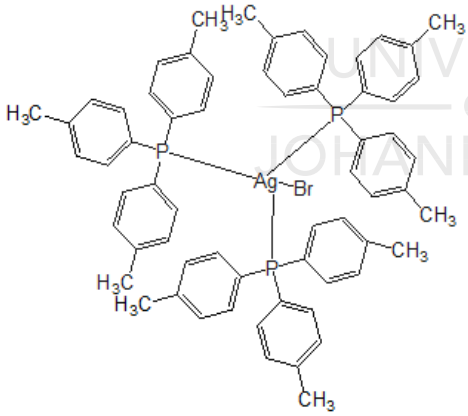

Complex **5**

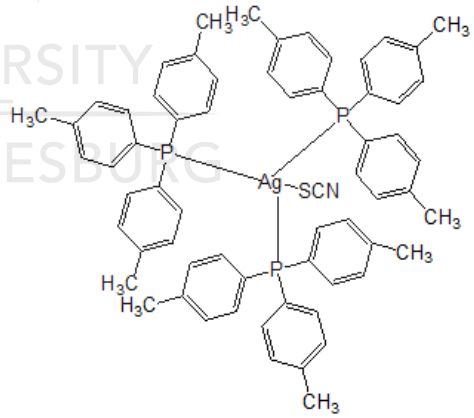

Complex **6**

Figure 2.1: Chemical structures of complexes **1**-**6**

Both cell lines were also treated with varying concentrations (10 µM, 30 µM, 50 µM, 70 µM and 100 µM) of cisplatin (CDDP) serving as the positive cell death and apoptotic control. The percentage viability for the dose-response studies was expressed with respect to DMSO (Figure 2.2 and 2.3).

The viability decreased significantly ($P < 0.05$, $P < 0.01$ or $P < 0.001$) in a dose-dependent manner in both the SNO and MCF-7 cells after being treated with increasing concentrations of the silver(I) complexes. When the cells were treated with the platinum-based complex, CDDP, a similar trend was observed. CDDP appeared to be less toxic to the SNO cells when compared to the MCF-7 cells. In general, the DMSO was minimally toxic to the cells when compared to the untreated control with the viability decreasing non-significantly with ±10%.

The IC_{50} concentration of complexes **1**-**6** and CDDP was calculated using the alamarBlue® assay. The IC_{50} value is the concentration of a drug that inhibits ±50% of the targeted biological process. These values indicate the antiproliferative potency of a drug under study. The IC_{50} concentrations were calculated using a polynomial function of nine subsequent repeats and are shown in Table 2.3.

Of the two 1:2 silver(I) complexes, complex **1** was found to be the most cytotoxic in the SNO cells with an IC_{50} value of 3.5 µM. The cyanide containing complex, complex **2,** was less cytotoxic than complex **1** with an IC_{50} value of 4.02 µM. The four 1:3 complexes were less active in the SNO cells when compared to the two 1:2 complexes. Complex **5** was the most cytotoxic (6.91 µM) in this group followed by complex **6** (7.61 µM), **4** (8.31 µM) and **3** (9.98 µM) respectively. For the MCF-7 cells, the IC_{50} values for complexes **3**-**6** were higher when compared to the SNO cells. Complex **3** was more cytotoxic in the MCF-7 cells with an IC_{50} of 9.84 µM. This was followed by complex **4** (10.75 µM), **6** (11.13 µM) and **5** (11.41 µM). In both the SNO and MCF-7 cells, CDDP was less cytotoxic compared to the silver(I) complexes under study with IC_{50} values of 47.39 µM and 20.72 µM respectively.

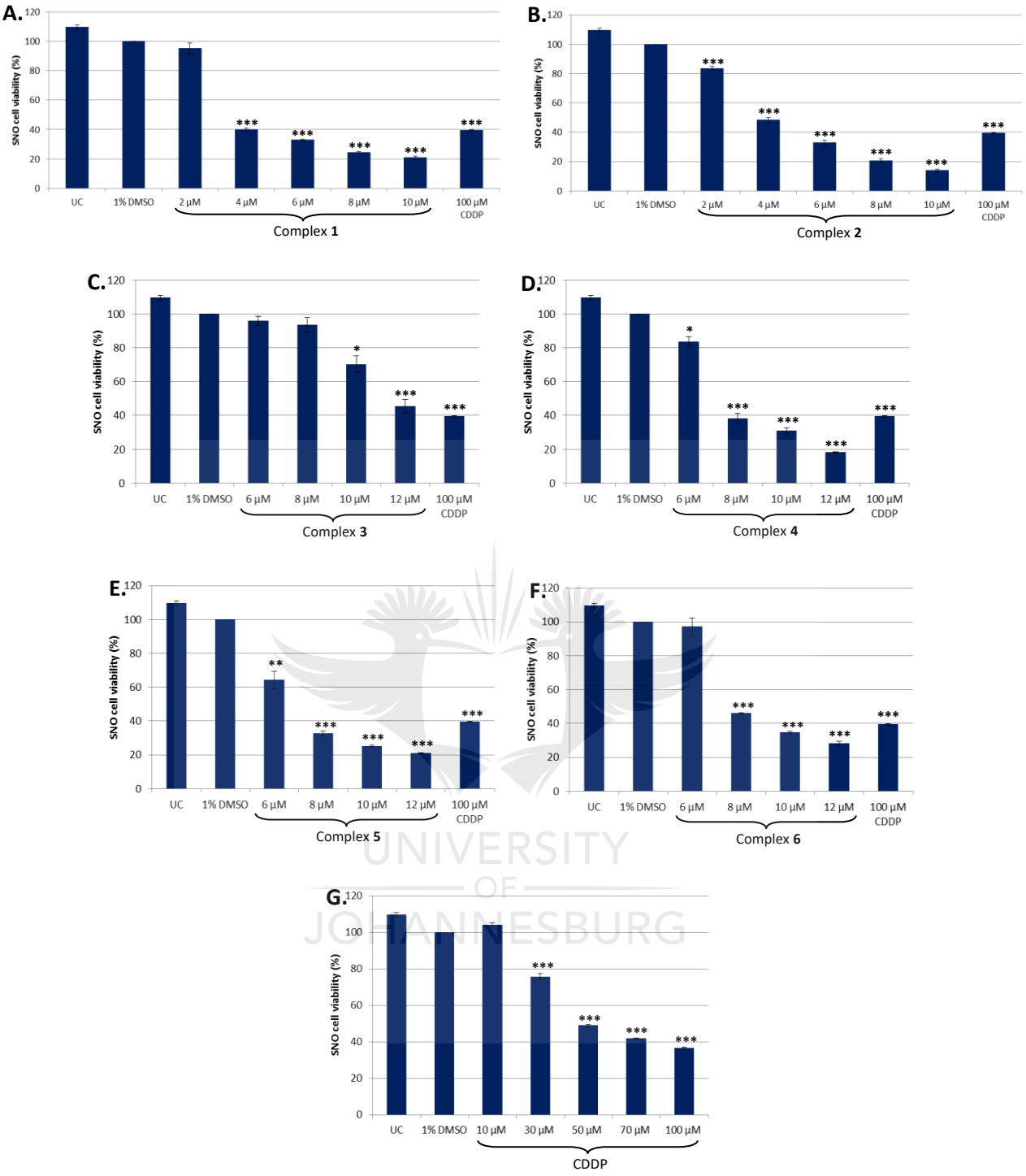

Figure 2.2: Dose-response studies of malignant **SNO** cells determined by the alamarBlue® assay. The cells were either untreated (negative) or treated with 1% DMSO (vehicle), varying concentrations of complexes **1**-**6** (A-F) or CDDP (positive) (G) for 24 hrs. The percentage viability was expressed with respect to 1% DMSO (100%). Error bars were constructed based on the ±SEM (n = 9). The P-value was calculated using the two-tailed Students t-Test. The treatments with P-values of $^{*}P < 0.05$, $^{**}P < 0.01$ and $^{***}P < 0.001$ were deemed significant with respect to DMSO.

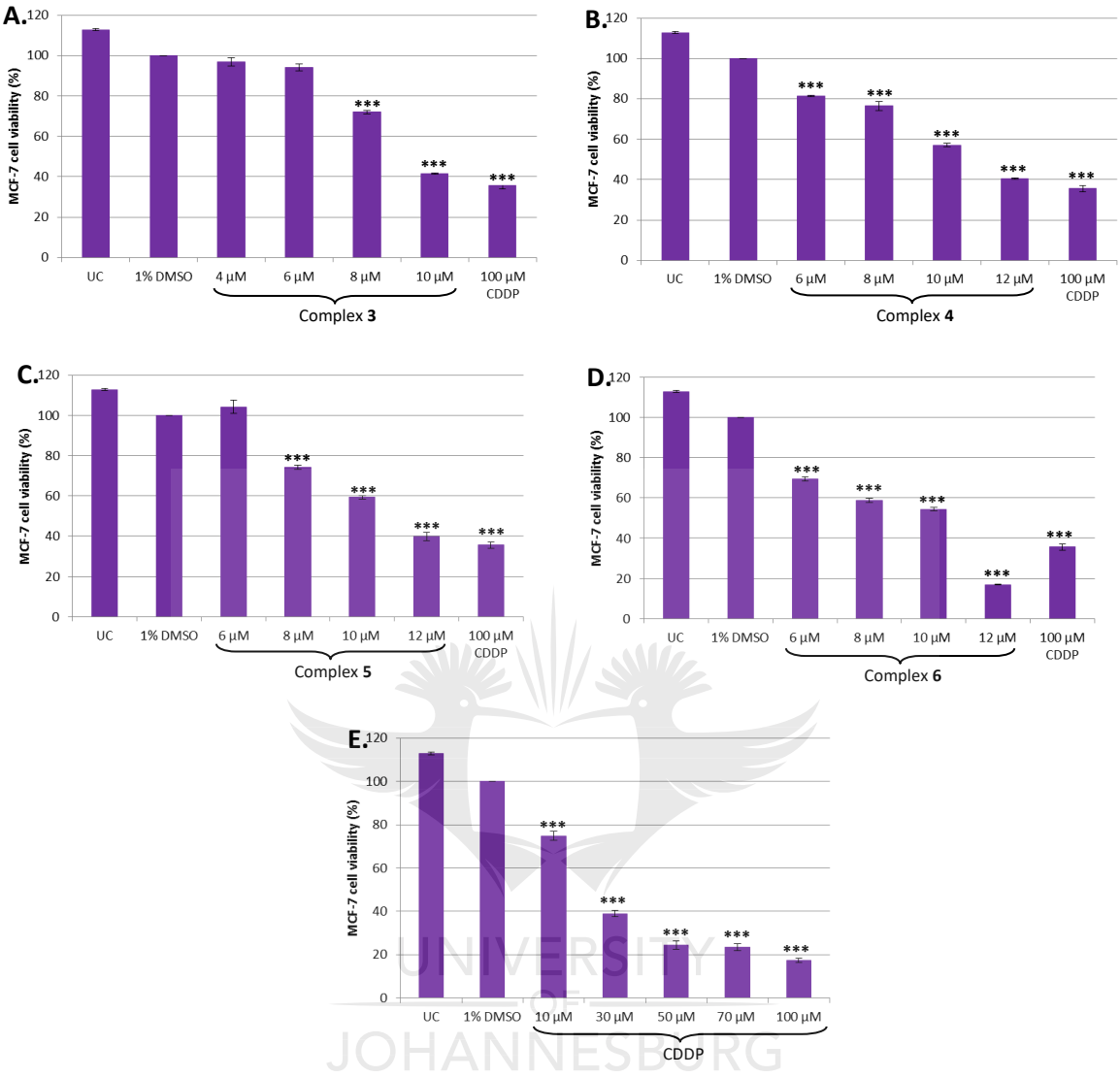

Figure 2.3: Dose-response studies of malignant **MCF-7** cells determined by the alamarBlue® assay. The cells were either untreated (negative) or treated with 1% DMSO (vehicle), varying concentrations of complexes **3**-**6** (A-D) or CDDP (positive) (E) for 24 hrs. The percentage viability was expressed with respect to 1% DMSO (100%). Error bars were constructed based on the ±SEM (n = 9). The P-value was calculated using the two-tailed Students t-Test. The treatments with a P-value of ***$P < 0.001$ were deemed significant with respect to DMSO.

Table 2.3: Calculated IC_{50} concentrations (µM) for complexes **1**-**6** (where applicable) and CDDP in malignant cells after 24 hrs of treatment. The polynomial function of nine subsequent repeats were used and the ±Std dev is indicated.

	Complexes (IC_{50}/±Std dev)						
Cell line	**1**	**2**	**3**	**4**	**5**	**6**	**CDDP**
SNO	3.50 µM/ ±0.91 µM	4.02 µM/ ±0.94 µM	9.98 µM/ ±1.30 µM	8.31 µM/ ±1.16 µM	6.91 µM/ ±0.38 µM	7.61 µM/ ±0.42 µM	47.39 µM/ ±7.05 µM
MCF-7	-	-	9.84 µM/ ±0.35 µM	10.75 µM/ ±0.30 µM	11.41 µM/ ±0.7 µM	11.13 µM/ ±0.65 µM	20.72 µM/ ±3.16 µM

2.3.3 Viability and cytotoxicity studies

The plasma membrane integrity, metabolic activity and ATP levels were monitored in both the SNO and MCF-7 cells using three different viability assays. These assays included the Trypan Blue dye exclusion assay, alamarBlue® cell proliferation assay and the CellTiter-Glo® luminescent assay. In addition, the Annexin-V FITC assay was also used to determine the cell viability. SNO and MCF-7 cells were either untreated or treated with 1% DMSO, 10 µM of complexes **1**-**6** (where applicable) or 100 µM CDDP for 24 hrs. For the Annexin-V FITC assay an additional treatment, 25% H_2O_2, was included serving as a necrotic control (Table 2.4, Figure 2.4 and 2.5).

With the Trypan Blue dye exclusion assay, healthy living cells have intact membranes and exclude the dye from the cytoplasm which makes them appear bright. When cells are dead their membranes are damaged and the dye enters the cell by staining the cytoplasm blue. The cell death of the SNO cells increased after being treated with the silver(I) complexes when compared to the UC and DMSO treated cells (Table 2.4). The percentage viability ranged from 43.83% to 65.5%. Complex **1** and **2** induced cell death in ±50% of the SNO cells while complexes **3**-**6** induced cell death in ±40% of the SNO cell. In contrast, complexes **3**-**6** were minimally toxic to the MCF-7 cells with viabilities ranging from 82% to 97%.

Table 2.4: The percentage viability of malignant cells determined by the Trypan Blue dye exclusion assay. The cells were either untreated or treated with 1% DMSO, 10 µM of complexes **1**-**6** (where applicable) or 100 µM CDDP for 24 hrs. The ±SEM is included where *n* = 6.

	Cell lines	
Complexes (10 µM):	**SNO**	**MCF-7**
1	50.33% (±5.11%)	-
2	43.83% (±2.47%)	-
3	65.5% (±4.55%)	82.83% (±2.30%)
4	61.67% (±4.86%)	95.83% (±0.86%)
5	65.5% (±7.2%)	95.83% (±0.3%)
6	59.0% (±3.06%)	97.0% (±0.39%)
Controls:		
UC (negative)	99.00% (±0.23%)	98.33% (±0.73%)
1% DMSO (vehicle)	98.67% (±0.19%)	98.83% (±0.44%)
100 µM CDDP (positive)	50.33% (±0.84%)	53.83% (±2.08%)

The alamarBlue® and CellTiter-Glo® assays are both mitochondrial-based assays and are complementary. The alamarBlue® dye was previously used to determine the IC_{50} values (Table 2.3). The non-toxic dye enters the cell *via* the cell membrane followed by metabolic oxidation-reduction reaction to reduce resazurin to a resorufin product. The formation of the product is directly proportional to the metabolic activity and by extension the viability of the cells. The CellTiter-Glo® assay works on a similar principle but quantifies the levels of ATP in the cell. This assay involves the use of luciferase that catalyses the production of a luminescent light from luciferin. The amount of light is proportional to the cellular levels of ATP and in turn metabolically active cells.

In both SNO and MCF-7 cells a significant ($P < 0.001$) decrease in cellular viability and ATP levels were observed after being treated with the different silver(I) complexes (Figure 2.4). The two 1:2 complexes, complex **1** and **2,** reduced the viability and ATP levels of the SNO cells to 20.92% (15.71% ATP) and 14.1% (8.02% ATP) respectively when compared to DMSO (Figure 2.4A). This was followed by the 1:3 complexes, complexes **3**-**6,** with viabilities ranging from 25.03% to 45.71% and ATP levels from 25.07% to 51.66%. Complexes **3**-**6** appeared to be less toxic to the MCF-7 cells when compared to the SNO cells (Figure 2.4B). Of the four complexes, complex **3** was the most cytotoxic with a viability of 41.47% and ATP levels of 37.53%. This was followed by complex **6**, **4** and **5** with viabilities and ATP levels of 54.33% (49.91% ATP), 57.13% (40.37% ATP) and 59.36% (56.27% ATP) respectively.

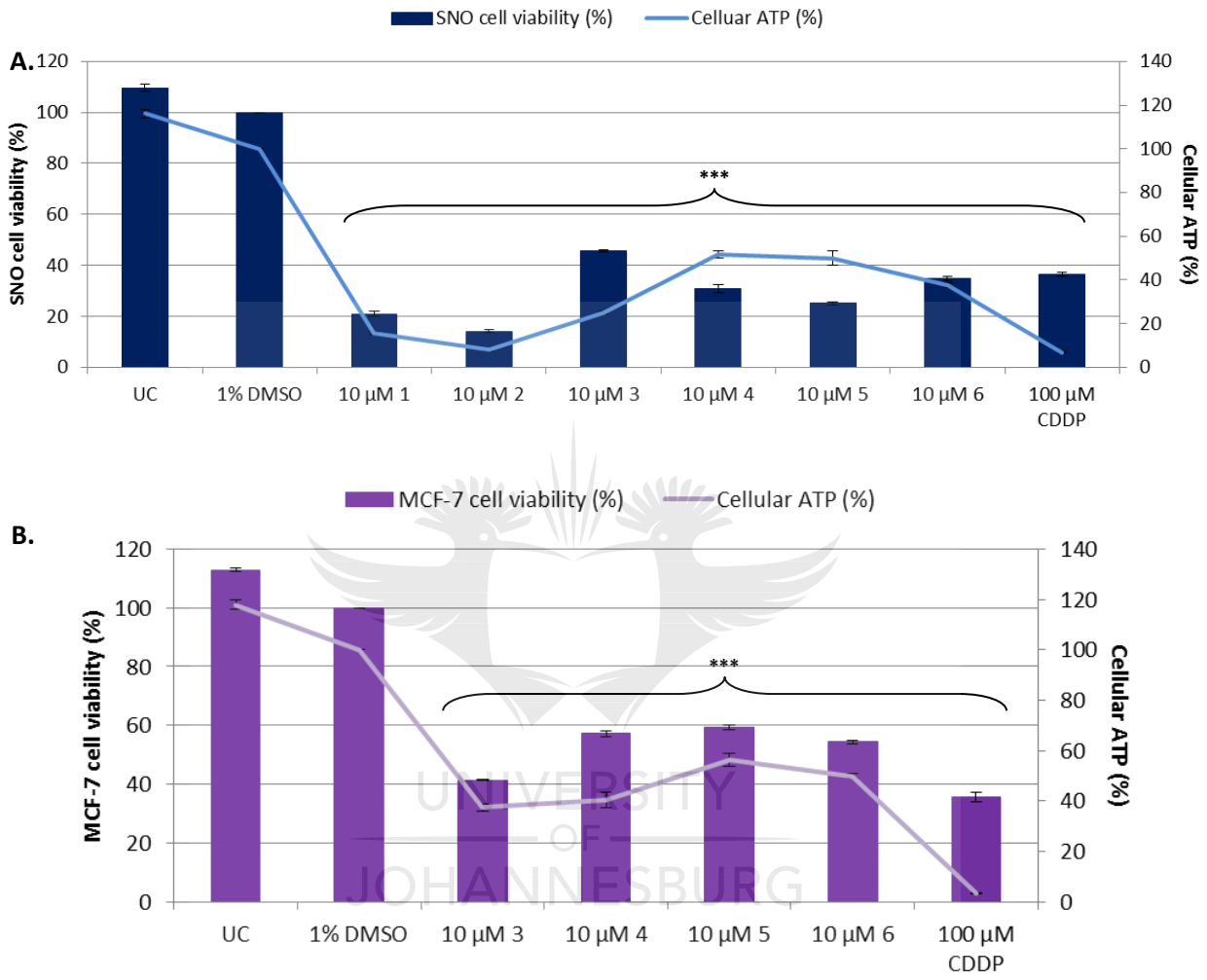

Figure 2.4: The percentage viability and cellular ATP in malignant **SNO** (A) and **MCF-7** (B) cells determined with the alamarBlue® and CellTiter-Glo® assays respectively. Both cell lines were either untreated (negative) or treated with 1% DMSO (vehicle), 10 µM of complexes **1**-**6** (where applicable) or CDDP (positive) for 24 hrs. The percentages were expressed with respect to 1% DMSO (100%). Error bars were constructed based on the ±SEM (n = 9). The P-value was calculated using the two-tailed Students t-Test. The treatments with P-value ***$P < 0.001$ were deemed significant with respect to DMSO.

The Annexin-V assay is a flow cytometry based assay that distinguishes cells that are alive from cells that are undergoing cell death (either apoptosis and/or necrosis) (Section 2.3.6). It is evident that the different treatment significantly ($P < 0.05$, $P < 0.01$ and $P < 0.001$) decreased the viability of both the SNO and MCF-7 cells (Figure 2.5).

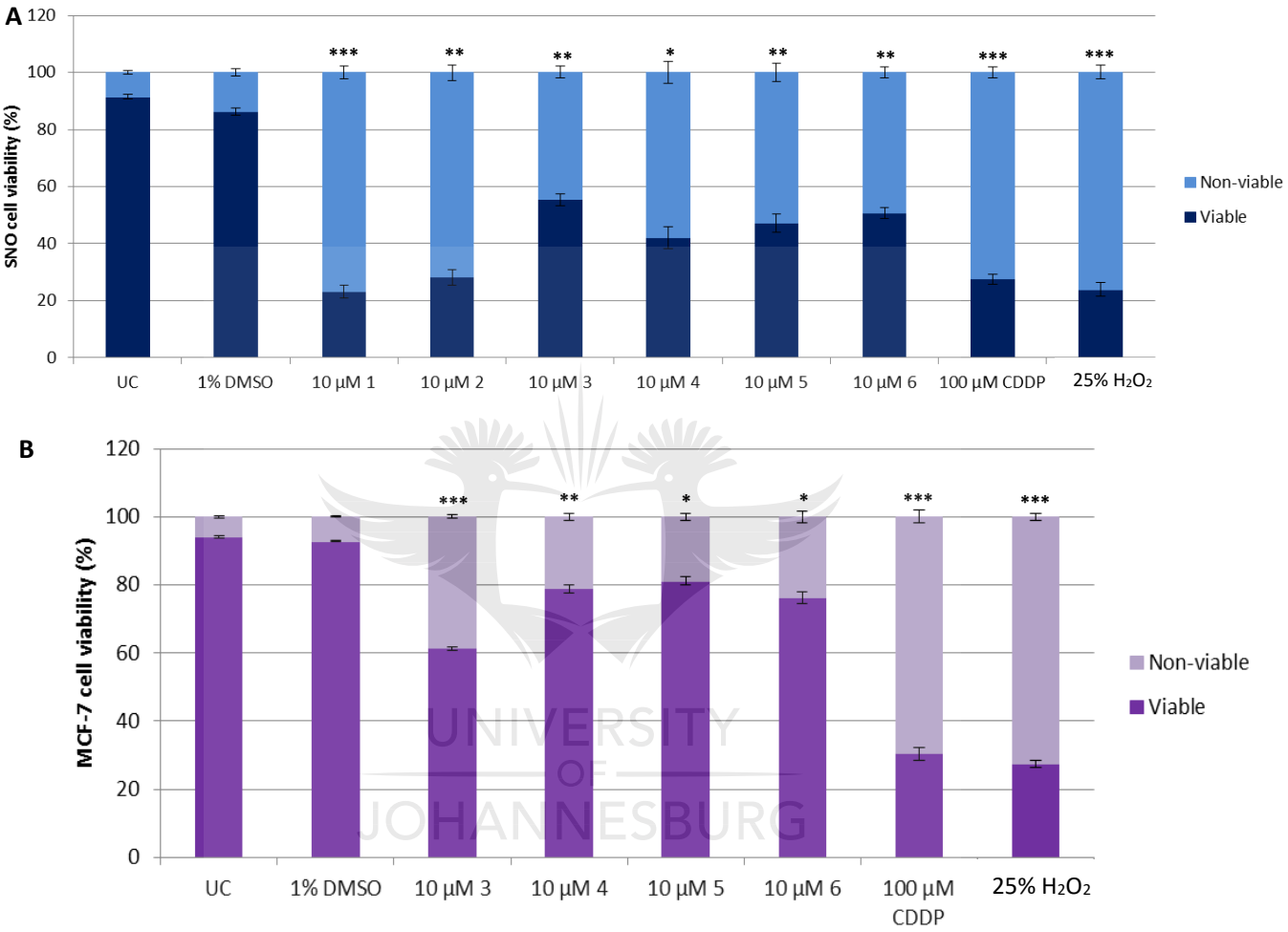

Figure 2.5: The percentage viability of malignant **SNO** (A) and **MCF-7** (B) cells determined with the Annexin-V FITC assay. Both cell lines were either untreated (negative) or treated with 1% DMSO (vehicle), 10 µM of complexes **1**-**6** (where applicable), CDDP (positive apoptotic) or 25% H_2O_2 (positive necrotic) for 24 hrs. It should be noted that the non-viable cells represent cells undergoing either apoptosis and/or necrosis. The percentages were calculated with respect to DMSO (100%). Error bars were constructed based on the ±SEM (n = 3). The P-value was calculated using the two-tailed Students t-Test. The treatments with P-values of $^*P < 0.05$, $^{**}P < 0.01$ and $^{***}P < 0.001$ were deemed significant with respect to DMSO.

Significant cell death (70%) was observed in the SNO cells when treated with complexes **1** ($P < 0.001$) and **2** ($P < 0.01$) (Figure 2.5A). A total of 44.67%, 58.03%, 52.8% and 49.93% SNO cells were dying when treated with complexes **3** ($P < 0.01$), **4** ($P < 0.05$), **5** ($P < 0.01$) and **6** ($P < 0.01$) respectively. Complex **3** ($P < 0.001$) only induced 38.6% cell death in the MCF-7 cells. Less toxic was complexes **6** ($P < 0.05$), **4** ($P < 0.01$) and **5** ($P < 0.05$) with cellular deaths ranging from to 18.86% to 23.67% (Figure 2.5B).

Although these assays rely on different principles, all assays (Trypan blue, alamarBlue®, CellTiter-Glo® and Annexin-V) mentioned in this section can be used to determine cell viability. When the viability and cytotoxicity studies are summarized, a similar trend in cell death can be observed in both the SNO and MCF-7 cells when comparing the different assays (Table 2.3, Figure 2.4 and 2.5). Overall, complex **1** and **2** (in the 1:2 group) and complex **5** (in the 1:3 group) were the more effective complexes in the SNO cells when compared to the activity of complexes **3**, **4** and **6**. For the MCF-7 cells, complex **3** was the most effective when compared to the activity of complexes **4**-**6**. In both cell lines, the untreated and vehicle controls caused a minimal change in viability. DMSO was minimally toxic to the malignant cells. Therefore, the biochemical changes will only be compared to DMSO and will exclude the untreated control in further studies. CDDP, in general, was toxic to both the malignant cells lines, but at different concentrations. The silver(I) complexes under study are 10-times more toxic than CDDP (10 µM vs 100 µM). The cytotoxicity of the phosphine ligands (**L1**-**L4**) on the malignant and non-malignant cells are reported in section 2.3.9.

2.3.4 Morphological and nuclear changes

Morphological studies were done after 24 hrs of treatment to determine if apoptosis or necrosis was responsible for the decrease in malignant cell viability previously observed (Table 2.3, Figure 2.4 and 2.5). Furthermore, a Hoechst-33258 nucleic acid stain was used to monitor the nuclear changes in the cells. SNO and MCF-7 cells were either treated with 1% DMSO or 10 µM of complexes **1**-**6** (where applicable). The morphology of the treated cells was compared to 100 µM CDDP (positive apoptotic control) and 25% H_2O_2 (positive necrotic control; only for light microscopy) (Figure 2.6-2.8).

Typical morphological features of apoptosis include cellular rounding, shrinkage of the cell and nucleus (pyknosis), nuclear breakdown (karyorrhexis), chromatin condensation, plasma membrane blebbing, and the presence of apoptotic bodies (Kerr *et al*., 1972; Kerr *et al*., 1994). Necrotic cell death is mostly associated with swelling of the cells and organelles, rupturing of the plasma membrane and the release of intracellular content (Kroemer *et al*., 2009). The morphology of the SNO and MCF-7 cells are represented in Figure 2.6. SNO cells treated with complexes **1**-**6** show

features similar to that of CDDP and indicate apoptotic cell death (white arrows). These features include cellular rounding, plasma membrane blebbing and apoptotic body formation (Figure 2.6A). Necrotic cell death (black arrows) was minimal in the SNO cells treated with complexes **1** and **2**. For the SNO cells treated with complexes **3**-**6**, necrotic cell death was, in fact, absent. A small number of SNO cells appear to be viable after treatment with complexes **3**-**6,** which contain intact cells, similar to that of the DMSO treated cells. Most the MCF-7 cells morphology resembled that of the vehicle whilst after being treated with the silver(I) complexes **3**-**6** (Figure 2.6B). The silver(I) treated MCF-7 cells appear to be alive based on the observed white nuclei present. Some MCF-7 cells were rounded and showed signs of plasma membrane blebbing (white arrows) after treatment with complexes **3**-**6**. Necrotic cell death was absent in the MCF-7 cells when compared to the 25% H_2O_2 treatment. In both malignant cell lines, cells treated with DMSO appear to be intact with no noticeable signs of cell stress or death.

Nuclear changes, like DNA fragmentation and chromatin condensation, were studied using Hoechst-33258 nuclear acid stain (Figure 2.7 and 2.8). The cell membrane is permeable to the stain which interacts with the minor groove of preferably double stranded DNA. The stain is sensitive to UV light and once excited, omits a blue fluorescence. Apoptotic cells have white nuclei with a bright fluorescence whereas those with intact nuclei have a weaker blue fluorescence. The nuclei of both SNO and MCF-7 cells, treated with DMSO, are uniformly stained appearing dark blue in colour (Figure 2.7A and Figure 2.8A). In contrast, when the SNO and MCF-7 cells were treated with the silver(I) phosphine complexes or CDDP, irregular staining of some nuclei (which was less in the MCF-7 cells) was evident (Figure 2.7B-H and Figure 2.8B-F) indicating DNA fragmentation and nuclear condensation. Uniformly stained nuclei were also visible in SNO cells treated with complexes **1**, **3**, **4** or **6** (Figure 2.7B, D, E and G) and in MCF-7 cells treated with complexes **3**-**6** (Figure 2.8B-E).

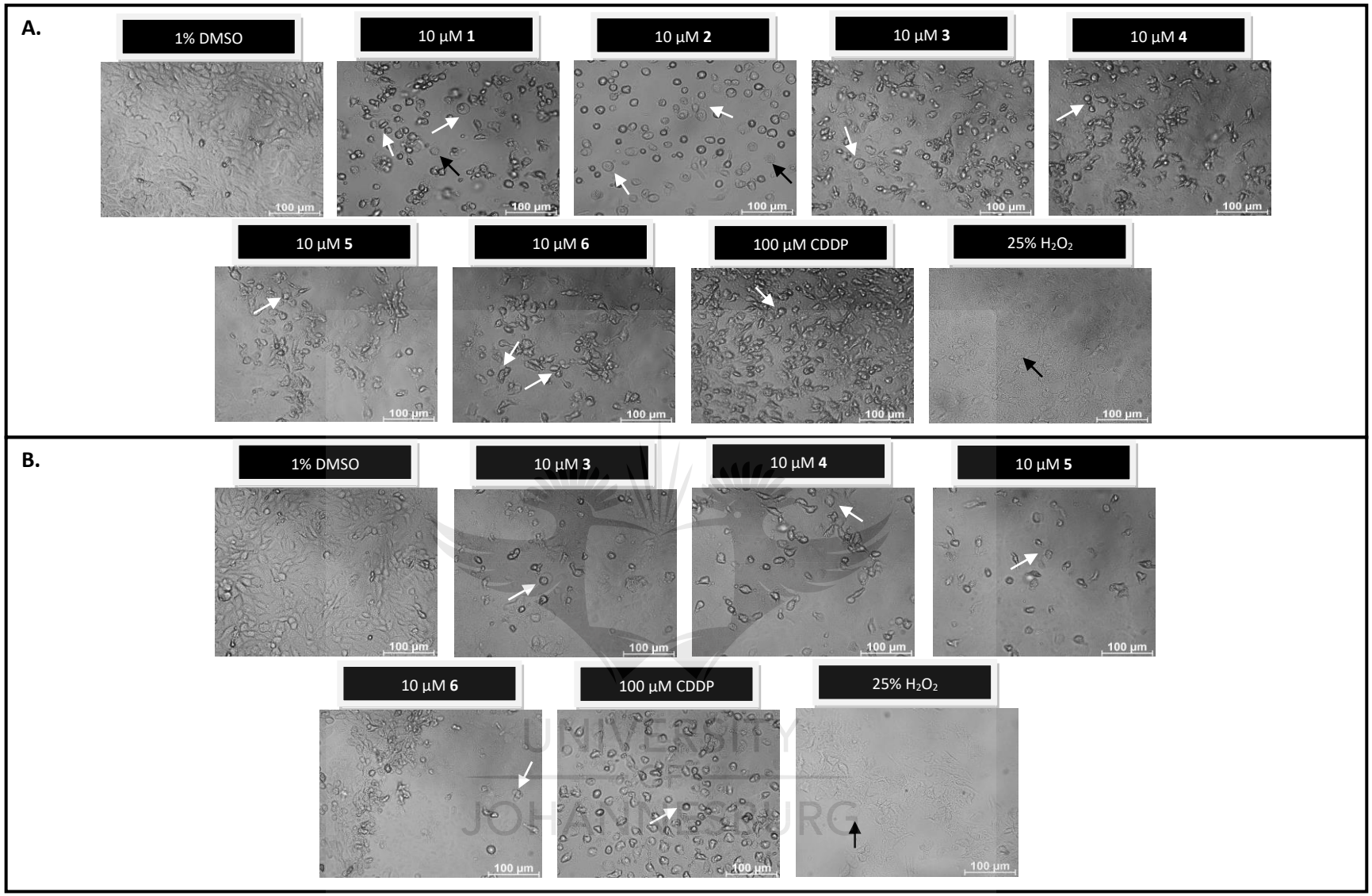

Figure 2.6: Light microscope images of malignant **SNO** (A) and **MCF-7** (B) cells taken 24 hrs after treatment. Both cell lines were treated with either 1% DMSO (vehicle), 10 µM of complexes **1**-**6** (where applicable), 100 µM CDDP (positive apoptotic) or 25% H_2O_2 (positive necrotic). Images were taken with a Zeiss Axiovert 25 inverted microscope using Axio Version 3.1 software at a magnification of 200 x. White arrows represent signs of apoptotic cell death which include cellular rounding, plasma membrane blebbing and apoptotic body formation. Black arrows indicate necrotic cell death due to swollen and burst cells visible.

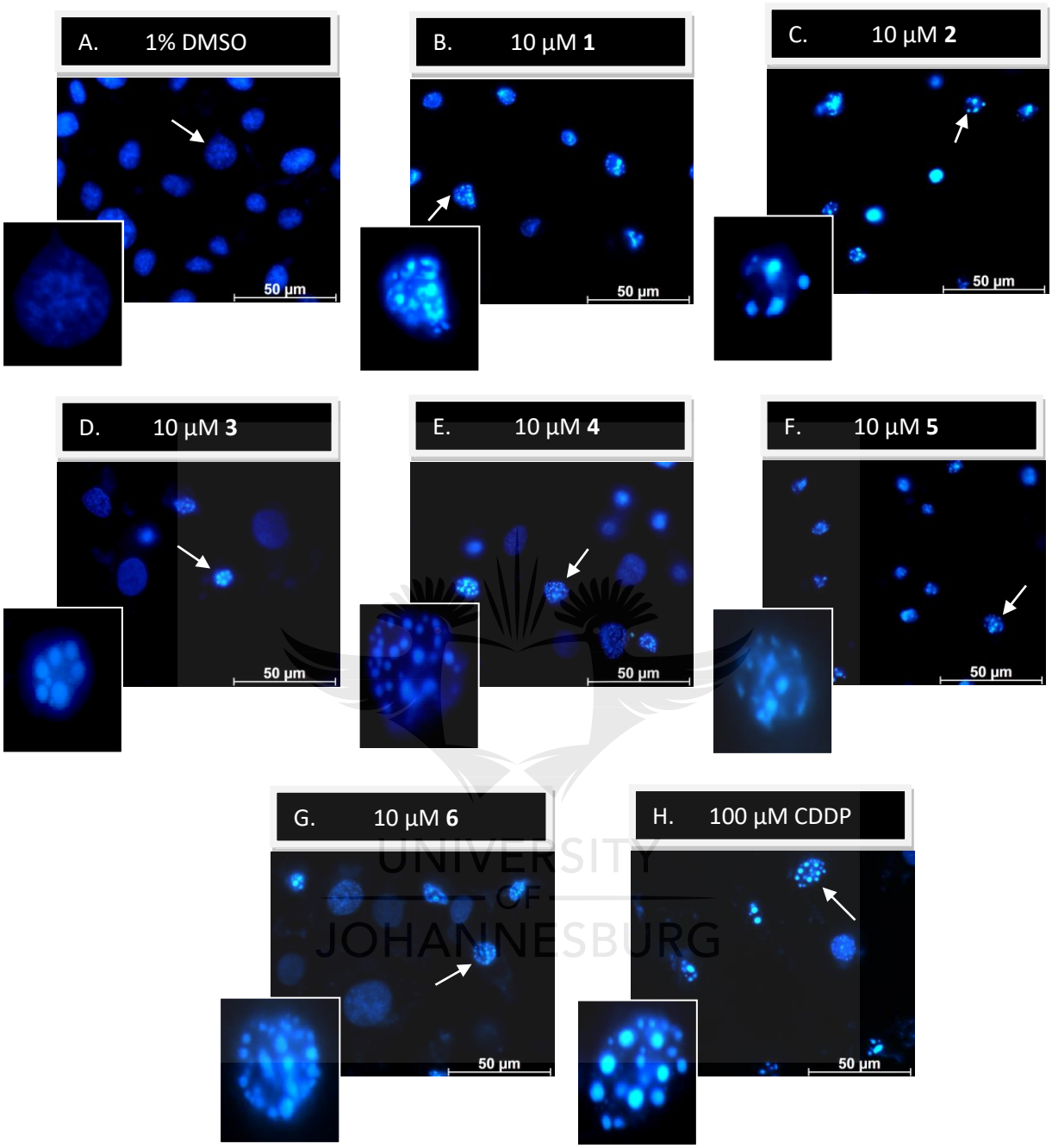

Figure 2.7: Changes in the nuclear morphology of malignant **SNO** cells stained with a Hoechst-33258 stain. The cells were treated with either 1% DMSO (vehicle) (A), 10 µM of complexes **1**-**6** (B-G) or 100 µM CDDP (positive) (H) for 24 hrs. Images were taken with a Zeiss Axioplan 2 inverted fluorescence microscope containing an Axio Cam camera at a magnification of 1000 x. White arrows either indicate healthy (uniformly stained) or damaged (irregular stained) nuclei.

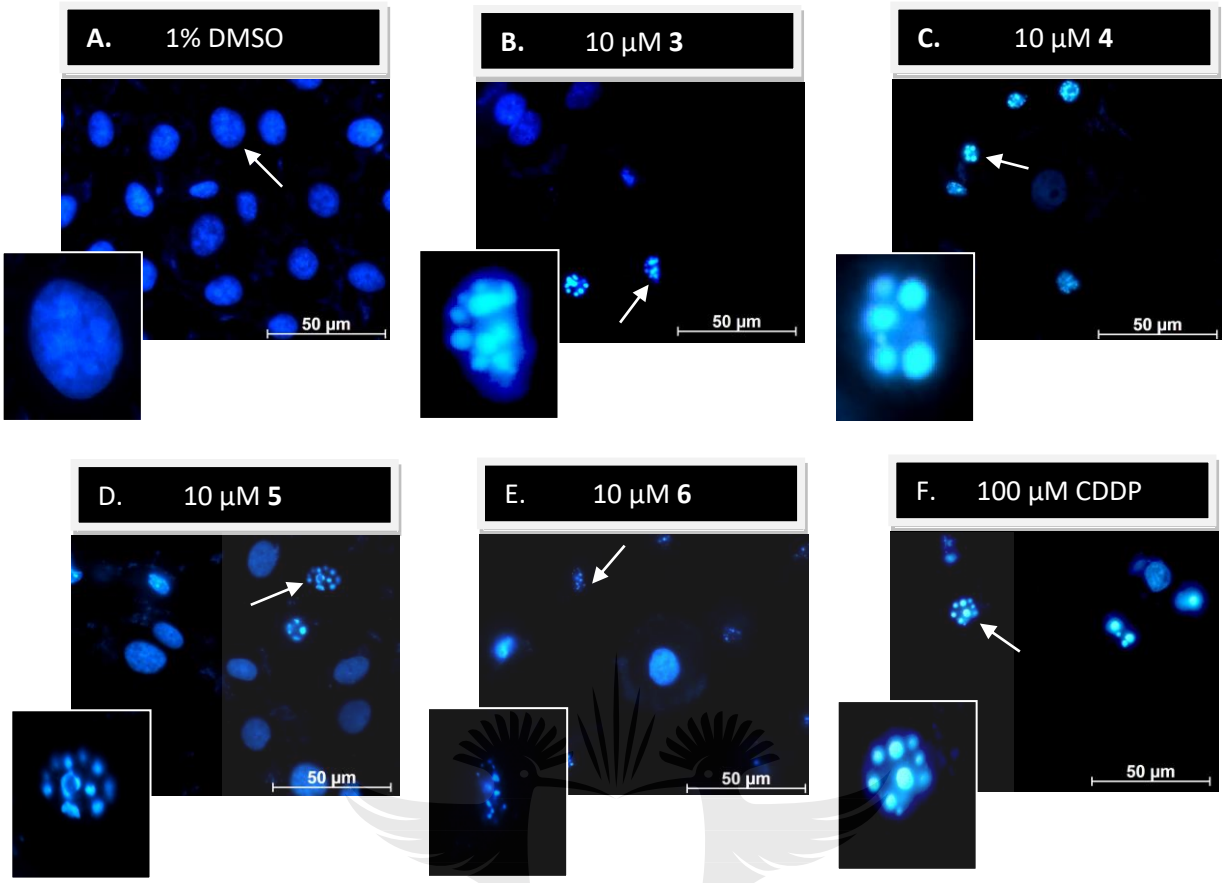

Figure 2.8: Changes in the nuclear morphology of malignant MCF-7 cells stained with a Hoechst-33258 stain. The cells were treated with either 1% DMSO (vehicle) (A), 10 µM of complexes **3**-**6** (B-E) or 100 µM CDDP (positive) (F) for 24 hrs. Images were taken with a Zeiss Axioplan 2 inverted fluorescence microscope containing a Axio Cam camera at a magnification of 1000 x. White arrows either indicate healthy (uniformly stained) or damaged (irregular stained) nuclei.

2.3.5 Cell cycle distribution

Cell cycle analysis was done to determine the variations in DNA content of the malignant cells by using a PI fluorochrome. The PI enters the permeabilized cells and binds to DNA. When cells start to divide, larger quantities of DNA are present and is proportional to the fluorescent intensity measured on the flow cytometer.

This enables one to study the distribution of the cells at different stages in the cell cycle that comprise of the G1-phase (growth and synthesis), S-phase (replication), G2-phase (before division) and the M-phase (mitotic). In addition, a Sub-G1 phase is also included that measures the number of cells undergoing cell death, particularly apoptosis. The data output is in a form of a histogram that calculates the percentages of the cells occupying the different stages in the cell cycle (Chan *et al.*,

2011). SNO and MCF-7 cells were either treated with 1% DMSO, 10 µM of complexes **1**-**6** (where applicable) or 100 µM CDDP for 24 hrs. The percentages of each phase in the treatment groups were compared to that of DMSO. Data analysis and histograms construction were done using FCS Express Plus 5 Software (Figure 2.9 and 2.10).

In both SNO and MCF-7 cells, a normal cell cycle distribution is seen after being treated with 1% DMSO (Figure 2.9A and Figure 2.10A). A drastic increase in the Sub-G1 population was observed in the SNO cells after being treated with complexes **1** and **2** with a shift of 97.86% or 88.45% respectively, when compared to that of the DMSO treated cells (Figure 2.9B and C). Treatment with complexes **3**-**6** also caused an increase in the Sub-G1 population of the SNO cells which ranged from 26.34% to 33.09% but was less significant when compared to the 1:2 complexes (Figure 2.9D-G). A similar trend was seen in the MCF-7 cells after being treated with complex **4**-**6** with ±25% cells located in the Sub-G1 population (Figure 2.10C-E). Complex **3** caused the highest Sub-G1 shift with more than 50% located in this region (Figure 2.10B). Overall, all the silver(I) complexes including CDDP caused a significant decrease in the G0/G1-population of both the SNO and MCF-7 cells ranging from 0.67% to 38.14% and 6.36% to 48.46% respectively. Complexes **1** and **2** decreased the amount of SNO cells found in the S-phase population to a minimal of 1.5% or 4.47% distinctly (Figure 2.9B and C). Furthermore, no cells were located in the G2/M-phase after being treated with these complexes, similar to that of CDDP. Complexes **3**-**6** caused an accumulation of SNO cells in the S- and G2/M-phases, indicating that complexes **3**-**6** can either result in cell cycle arrest during replication or division (Figure 2.9D-G). The majority of the SNO cells treated with complex **1**, **2** and CDDP were located in the Sub-G1 and it's, therefore, unclear if it causes cell cycle arrest. A decrease of the MCF-7 cells in the S-phase population was observed followed by an increase in the G2/M-phase population after being treated with complexes **3**-**6** (Figure 2.10B-E). This could indicate that these complexes cause the cell cycle to arrest during cellular division.

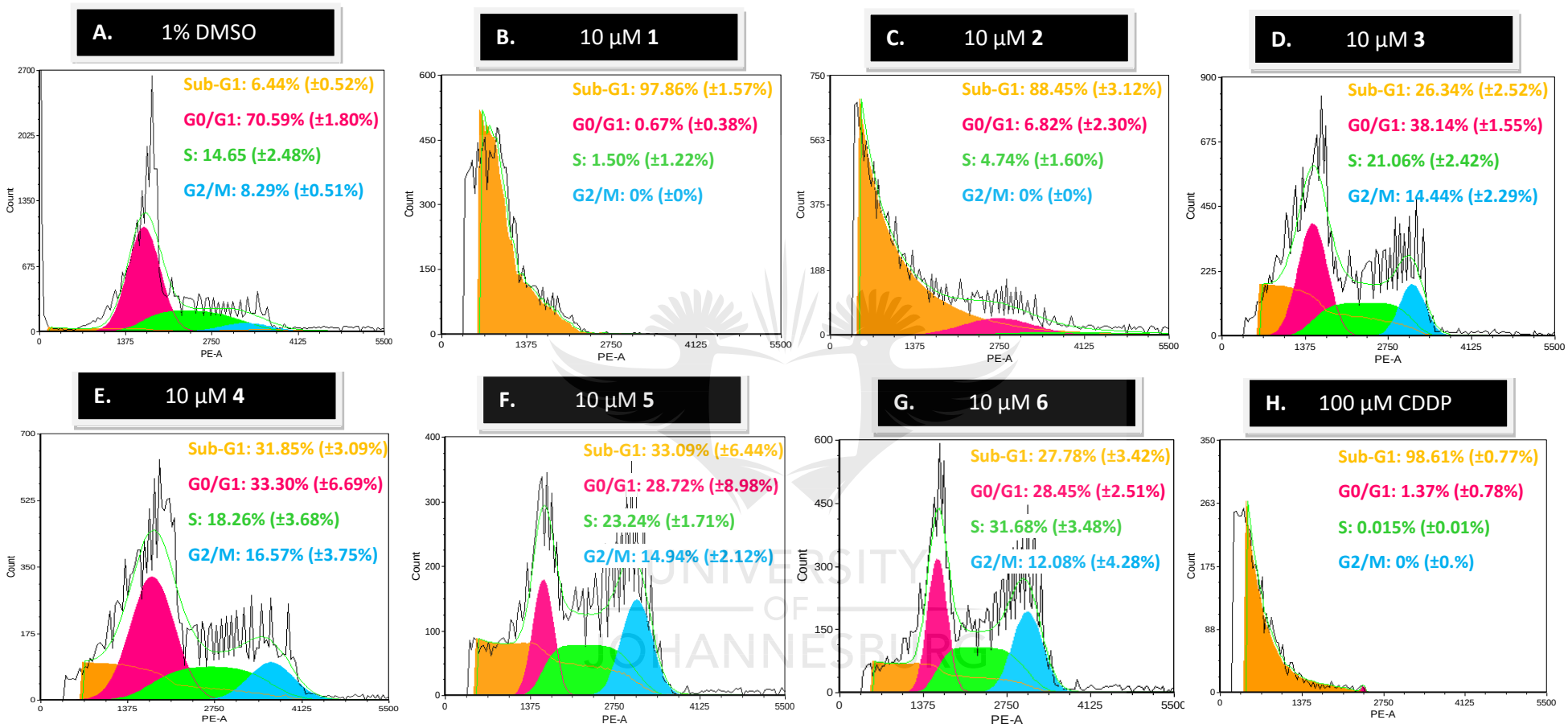

Figure 2.9: The DNA content and cell cycle analysis of malignant **SNO** cells determined by flow cytometry. The cells were treated with either 1% DMSO (vehicle) (A), 10 µM of complexes **1**-**6** (B-G), or 100 µM CDDP (positive) (H) for 24 hrs. The histograms are divided in different cell cycle phases which include apoptotic sub-G1 (orange), G0/G1 (pink), S (green) and G2/M (blue). The percentages of each phase are represented in each histogram followed by the ±SEM (*n* = 3).

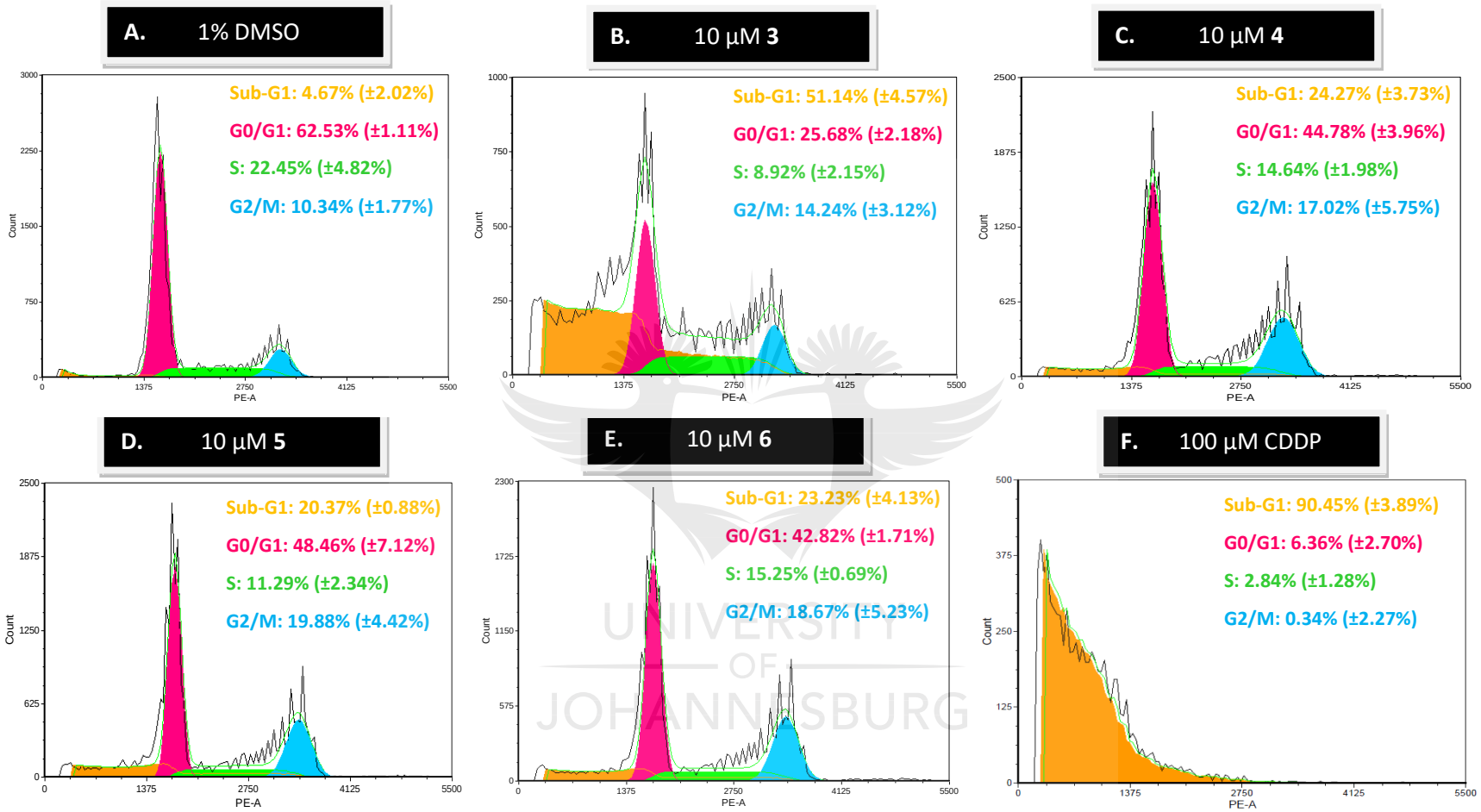

Figure 2.10: The DNA content and cell cycle analysis of malignant **MCF-7** cells determined by flow cytometry. The cells were treated with either 1% DMSO (vehicle) (A), 10 µM of complexes **3**-**6** (B-E) or 100 µM CDDP (positive) (F) for 24 hrs. The histograms are divided in different cell cycle phases which include apoptotic sub-G1 (orange), G0/G1 (pink), S (green) and G2/M (blue). The percentages of each phase are represented in each histogram followed by the ±SEM (*n* = 3).

2.3.6 Analysis of the mode of cell death

Taken together, silver(I) complexes appear to induce apoptotic cell death in both SNO and MCF-7 cells (Figure 2.6-2.10). To confirm if the assumed mode of cell death, apoptosis, was indeed induced an accepted method, Annexin-V/PI flow cytometry, was used. Cells contain a PS on the inner leaflet of the cell membrane. When apoptosis occurs, the inner PS is externalized and exposed to the surrounding environment. The Annexin-V fluorophore identifies these PS sites and binds to them that can be detected by a green fluorescence. As mentioned before, PI interacts with the DNA of dead or necrotic cells causing them to fluoresce red. Cells that are alive have intact cell membranes and do not contain any fluorescent properties. The data output is in the form of a dot blot that divides the cells into four different quadrants that either represent viable cells (Q3), early (Q4) or late (Q2) apoptotic cells and lastly necrotic cells (Q1). Therefore, SNO and MCF-7 cells were either treated with 1% DMSO and 10 µM of complexes **1**-**6** (where applicable) for 24 hrs. A positive apoptotic (100 µM CDDP) and necrotic (25% H_2O_2) control was included for comparison purposes. Dot blots of respective treatments were constructed using FACSDiva™ Software and are shown in Figure 2.11 and 2.12.

The DMSO treated cells showed minimal cell death with an average viability of 86.27% for the SNO cells and 92.87% for the MCF-7 cells in Q3 (Figure 2.11A and 2.12A). More than 60% of the SNO cells were located in the apoptotic quadrants Q4 and Q2 (early and late stages) after being treated with complexes **1** and **2** (Figure 2.11B-C and 2.12B-C). The remainder of the cells were either located in Q3 (23.13% for **1** and 28.17 for **2**) or minimally in Q1 (0.33% for **1** and 6.2% for **2**). The apoptotic effect of complexes **3**-**6** was minimal in the SNO cells when compared to that of complexes **1** and **2**, where more than 40% of the cells were located in either the apoptotic (±30% for complex **3**) or viable quadrants (Figure 2.11B-G). Even though complexes **3**-**6** were less toxic to the MCF-7 cells with viabilities of 61.43%, 78.83%, 81.13% or 76.3%, apoptotic cell death was induced in some cells (Figure 2.12B-E). A total of 35.06% cells were located in the apoptotic quadrant (late and early stages) after being treated with complex **3**. This was followed by complex **6** (21.9%), **4** (19.43%) and **5** (17.13%). Overall, necrotic cell death was minimal in the SNO and MCF-7 cells. The CDDP-treated SNO and MCF-7 cells were mostly apoptotic with a total of 72.4% and 67.3% respectively (Figure 2.11H and Figure 2.12F). The remainder of the cells were located in Q3 (27.5% for SNO and 30.43% for MCF-7). As expected, cells treated with 25% H_2O_2 were more than 60% necrotic and is located in Q1 (Figure 2.11I and Figure 2.12G).

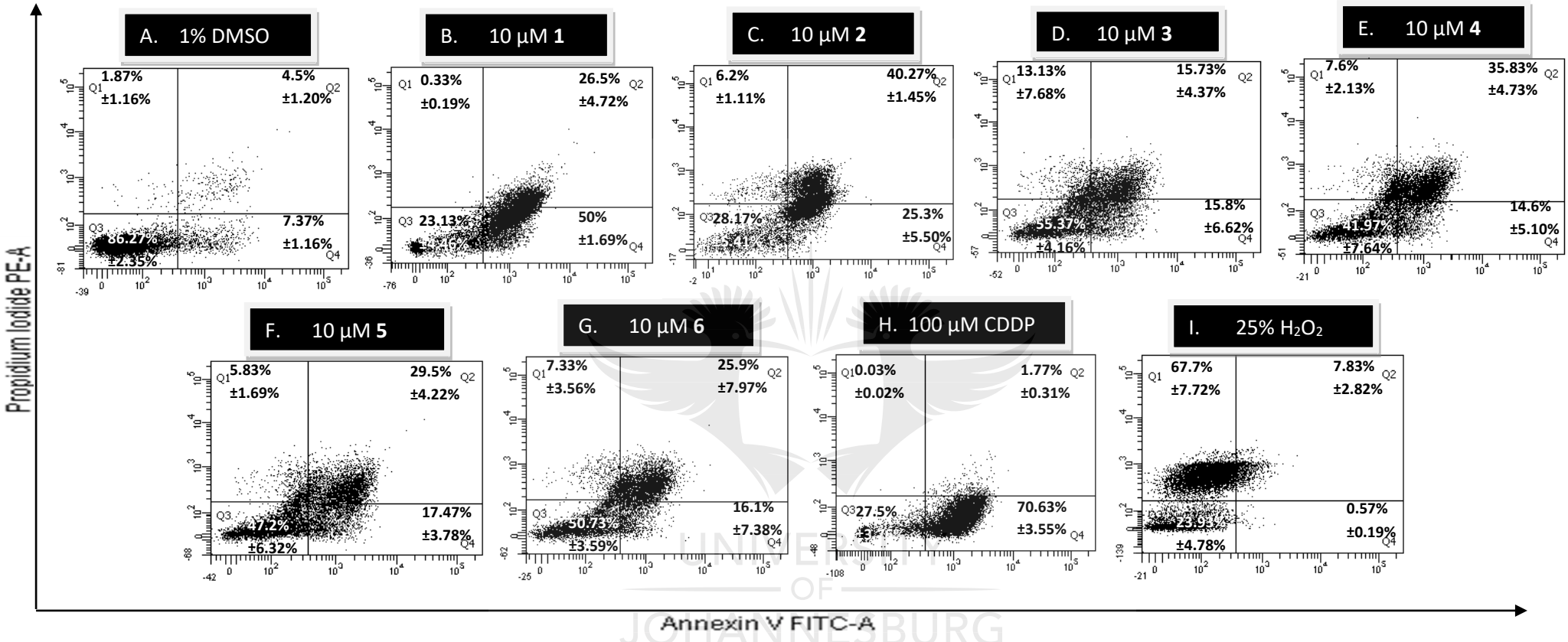

Figure 2.11: Dot blots representing the mode of cellular death induced in differentially treated malignant **SNO** cells. Analyses were performed using Annexin-V FITC and PI fluorochromes. Cells were treated with either 1% DMSO (vehicle) (A), 10 µM of complexes **1**-**6** (B-G), 100 µM CDDP (positive apoptotic) (H) or 25% H_2O_2 (positive necrotic) (I) for 24 hrs. The average percentage was calculated for all quadrants as represented in each quadrant, followed by the ±SEM (*n* = 3). The four quadrants represent Q3 that is negative for FITC and PI, Q4 that is positive for FITC but negative for PI, Q1 that is positive for PI, but negative for FITC and Q2 that is positive for both FITC and PI. Cells undergoing early apoptosis are more likely to be found in Q4 while those of late apoptosis will be found in Q2. Necrotic cells are found in Q1 while Q3 indicates intact viable cells.

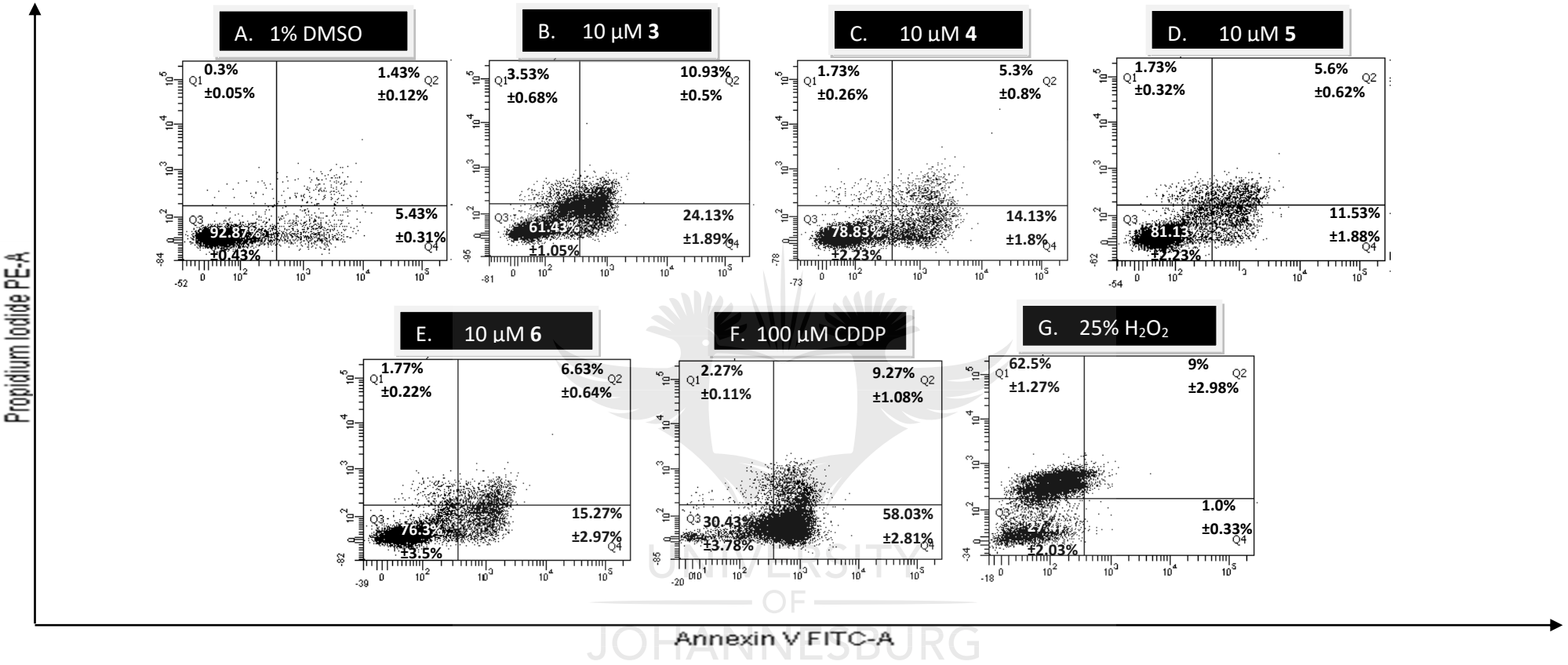

Figure 2.12: Dot blots representing the mode of cellular death induced in differentially treated malignant **MCF-7** cells. Analyses were performed using Annexin-V FITC and PI fluorochromes. Cells were treated with either 1% DMSO (vehicle) (A), 10 µM of complexes **3**-**6** (B-E), 100 µM CDDP (positive apoptotic) (F) or 25% H_2O_2 (positive necrotic) (G) for 24 hrs. The average percentage was calculated for all quadrants as represented in each quadrant, followed by the ±SEM (*n* = 3). The four quadrants represent Q3 that is negative for FITC and PI, Q4 that is positive for FITC but negative for PI, Q1 that is positive for PI, but negative for FITC and Q2 that is positive for both FITC and PI. Cells undergoing early apoptosis are more likely to be found in Q4 while those of late apoptosis will be found in Q2. Necrotic cells are found in Q1 while Q3 indicates intact viable cells.

2.3.7 Activity of executioner caspases-3 and/or -7

Caspases play an important role in regulating apoptotic cell death and can either act as initiator or executioner molecules. Caspase-3 and -7 specifically, are executioner caspases that are activated once the dimer (pro-form) is cleaved by initiator caspases. This then activates other downstream proteins favouring apoptosis (Riedl and Shi, 2004). The caspase-3/7 activity was monitored in the SNO and MCF-7 cells using an Apo-ONE® Homogenous caspase-3/7 assay that is principled similarly to the CellTiter-Glo®assay. The SNO and MCF-7 cells were either treated with 1% DMSO, 10 µM of complexes **1**-**6** (where applicable) or 100 µM CDDP for 24 hrs. The relative caspase-3/7 levels cells were calculated with respect to 1% DMSO (Figure 2.13A and B). MCF-7 cells do not express caspase-3 and therefore depend on caspase-7 for apoptotic activation, hence only the caspase-7 activity is reported (Jänicke *et al*., 1998). In addition, both cell lines were also treated with a cell permeable caspase inhibitor, Z-VAD-FMK, which interacts with the active site of the caspase enzyme and prevents apoptosis. This inhibitor allows one to determine if the apoptotic cell death pathway induced by the treatments is caspase-dependant or -independent.

Complex **1**, **5** and cisplatin significantly ($P < 0.001$) increased the caspase-3/7 activity more than 7-fold in the SNO cells when compared to the DMSO treated cells (Figure 2.13A). Complex **2**, **3**, **4** and **6** also significantly ($P < 0.05$, $P < 0.01$ or $P < 0.001$) increased the caspase-3/7 activity in the SNO cells, but less so when compared to the former with a fold change of 2.7, 1.99, 1.91 and 2.24 respectively. MCF-7 cells treated with complexes **3**-**6** led to a significant increase ($P < 0.01$ or $P < 0.001$) of caspase-7 levels with a fold change of 4.18, 4.83, 4.94 and 4.67 respectively (Figure 2.13B). In contrast, in MCF-7 cells treated with CDDP, caspase-7 activity was lower when compared to the silver(I) treatments with a fold change of 2.58. When both SNO and MCF-7 cells were treated with Z-VAD-FMK, the caspase-3/7 activity decreased significantly ($P < 0.01$ and $P < 0.001$) for all treatments when compared to the treatments where the inhibitor was absent. This signifies that the observed apoptotic cell death induced by the silver(I) complexes are in fact caspase-dependant.

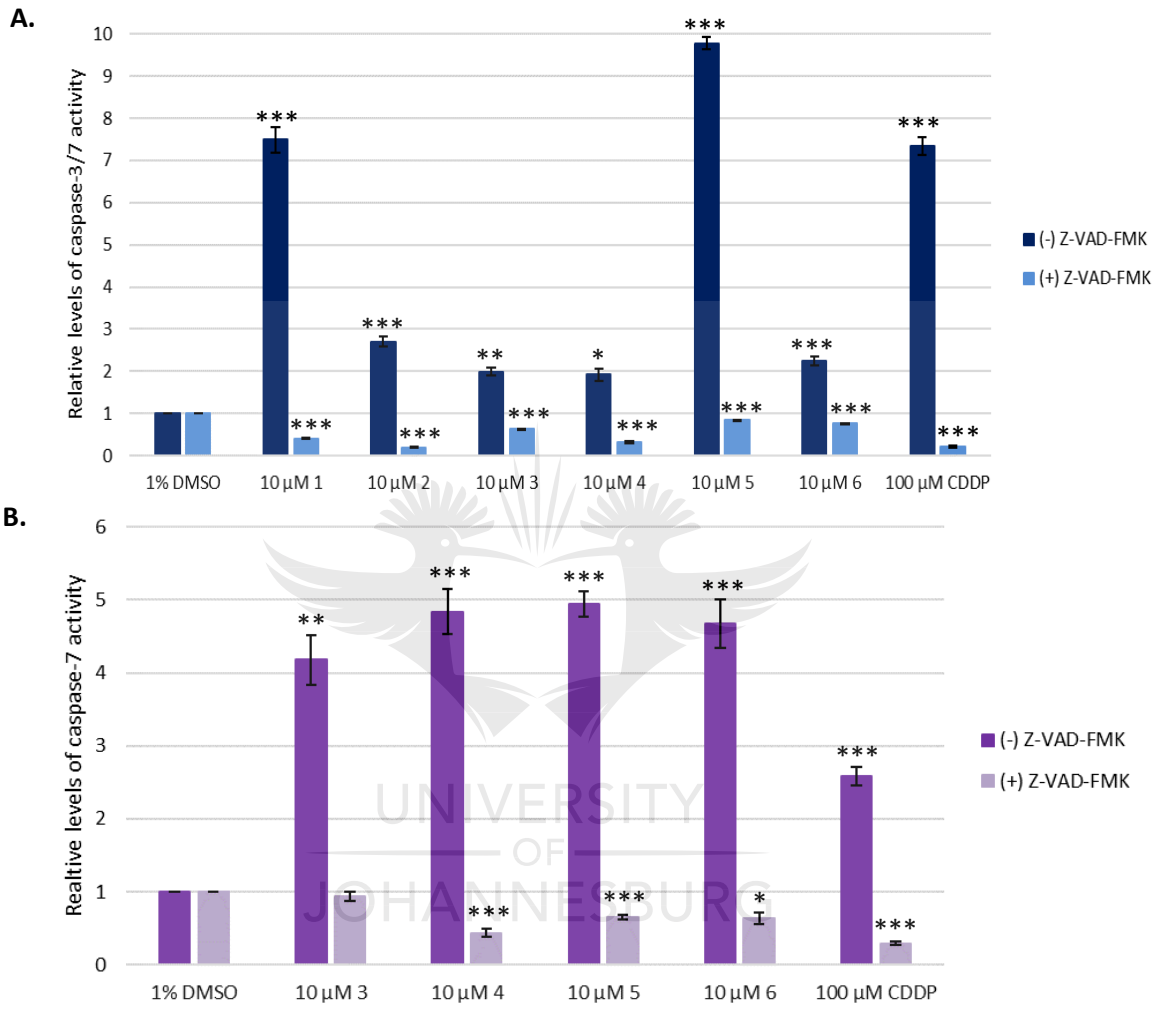

Figure 2.13: Caspase-3/7 activity detected in malignant **SNO** (A) and **MCF-7** (B) using a Caspase-GLO® assay. Both cell lines were either treated in the absence or presence of 20 µM Z-VAD-FMK (caspase inhibitor) for 24 hrs. The treatments were either 1% DMSO (vehicle), 10 µM of complexes **1**-**6** (where applicable) or 100 µM CDDP (positive). The relative caspase levels were expressed with respect to DMSO (1). Error bars were constructed based on the ±SEM (n = 6). The P-value was calculated using the two-tailed Students t-Test. The treatments with P-values of *P < 0.05, **P < 0.01 and ***P < 0.001 were deemed significant with respect to DMSO.

2.3.8 Effect of silver(I) complexes in non-malignant cells

During cancer treatment, it is important that the administered drug shows no or low cytotoxicity towards healthy cells at the site of the tumour and throughout the body. Therefore, non-malignant human fibroblast (HDF-a) and kidney (HEK293) cell lines were used to determine the activity and in turn the selectivity of the silver(I) complexes under study, using an alamarBlue® assay. Both cell lines were either untreated or treated with 1% DMSO, 10 µM of complexes **1**-**6** or 100 µM CDDP for 24 hrs. The percentage viability is expressed relative to DMSO (100 %) (Figure 2.14). The morphological changes were also observed using light microscopy where an additional treatment 25% H_2O_2 was included as a necrotic control (Figure 2.15).

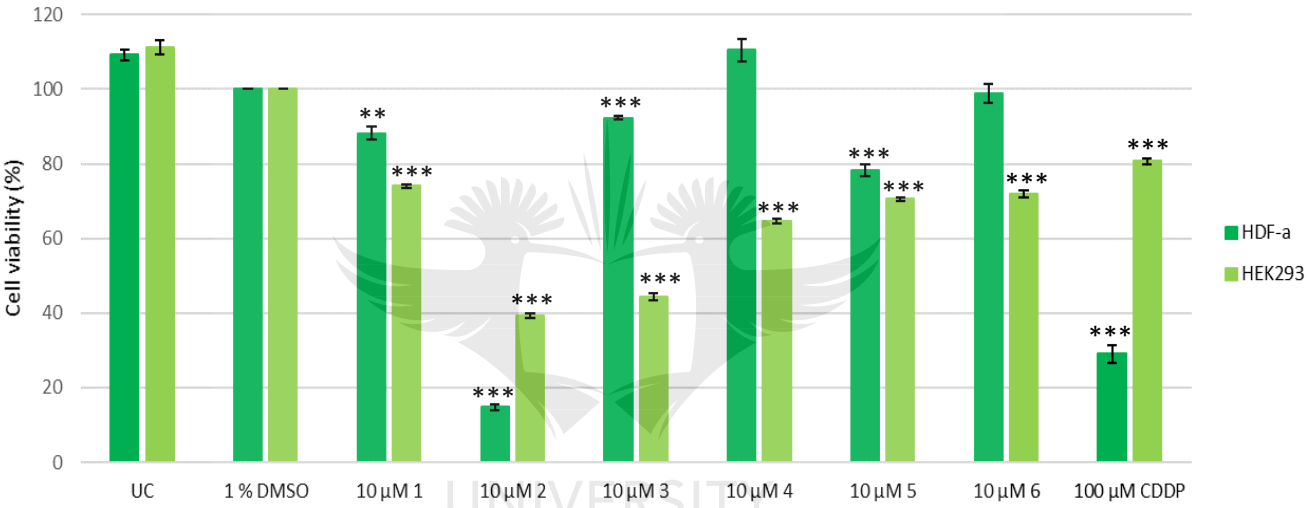

Figure 2.14: The percentage viability of non-malignant **HDF-a** and **HEK293** cells determined with the alamarBlue® assay. Both cell lines were either untreated or treated with 1% DMSO (vehicle), 10 µM of complexes **1**-**6** or 100 µM CDDP (positive) or 24 hrs. The percentages were expressed with respect to 1% DMSO (100%). Error bars were constructed based on the ±SEM (n = 9). The P-value was calculated using the two-tailed Students t-Test. The treatments with P-value $^{**}P < 0.01$ and $^{***}P < 0.001$ were deemed significant with respect to DMSO.

In general, the vehicle control was minimally toxic to both HDF-a and HEK293 cells when compared to the untreated control. Complex **4** was the least cytotoxic to the HDF-a cells with a viability of over 100%. This was followed by complexes **6**, **3**, **1** and **5**. Complex **1** was the least cytotoxic to the HEK293 cells followed by complexes **6**, **5**, **4** and **3**. Complex **2** was highly or equally cytotoxic to the HDF-a and HEK293 cells when compared to that of the malignant cell lines (Figure 2.4). Even though most of the silver(I) complexes significantly ($P < 0.01$ and $P < 0.001$) decreased the viability of the HDF-a and HEK293 cells, their cytotoxic effect was much greater in the SNO and MCF-7 cells (Figure

2.4). CDDP caused a significant decrease in viability of both the HDF-a and HEK293 cells but was less toxic to the HEK293 cells.

Morphological studies were performed for both HDF-a and HEK293 cells in a similar manner as for the malignant cells. Both cell lines were treated for 24 hrs with 10 µM of the silver(I) complexes **1**-**6** and their morphology compared to respective controls (untreated, vehicle, apoptotic and necrotic) (Figure 2.15). The HDF-a cells morphology appears spindlier than the HEK293 cells which are more rounded. Both the HDF-a and HEK293 cells treated with DMSO resemble that of the untreated control. These cells are intact with no signs of cell death. When compared to the DMSO treated cells, the majority of both the HDF-a and HEK293 cells treated with complexes **1** and **3**-**6** seem viable with minimal cellular rounding (white arrows). In contrast, cells treated with complex **2** resulted in morphological changes resembling that of the CDDP. These cells are rounded and apoptotic blebs are visible (white arrows). Necrotic cell death (black arrows) appears to be absent in both non-malignant cells after treatments with silver(I) phosphine complexes when compared to 25% H_2O_2. The cytotoxicity of the phosphine ligands (**L1**-**L4**) on HDF-a and HEK293 cells are reported in the next section (section 2.3.9).

2.3.9 Cytotoxicity of the phosphine ligands in both malignant and non-malignant cells

It has been shown that specific uncoordinated phosphine ligands are more or have similar cytotoxic profiles than the complexed silver(I) salt (Liu *et al*., 2008). In contrast, other studies show that the cytotoxicity of phosphine ligands is significantly lower than the functional complex (McKeage *et al*., 1998; Poyraz *et al*., 2011; Ferreira *et al*., 2015; Human *et al*., 2015; Banti *et al*., 2016). Therefore, in this study, the cytotoxic effect of the four phosphine ligands **L1**-**L4** in both the malignant and non-malignant cell lines was determined. An alamarBlue® assay was used to quantify the cell viability and light microscopy to identify structural changes or predict cell death if any. All the cell lines were either treated with 1% DMSO or 10 µM of the ligands **L1**-**L4** (Figure 2.16 and 2.17).

All four cell lines show varying degrees of cell viability after being treated with ligands **L1**-**L4** (Figure 2.16). When these treatments were compared to the DMSO treated cells, their viabilities were still above 80%. The uncomplexed ligands were overall less cytotoxic when compared to the complexed silver(I) phosphines studied herein (Figure 2.4 and 2.14). The morphology of all four cell lines treated with the ligands resembles that of DMSO which further confirms their low cytotoxicity (Figure 2.17).

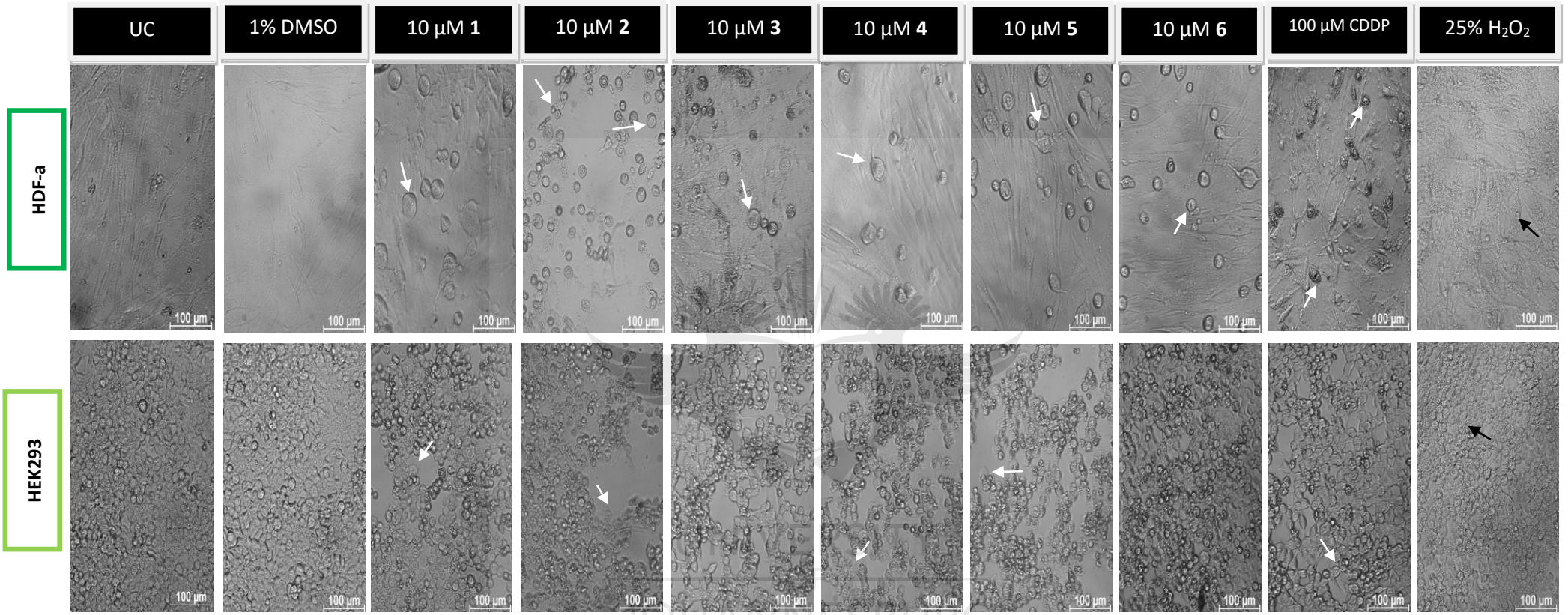

Figure 2.15: Light microscope images of non-malignant **HDF-a** and **HEK293** cells taken 24 hrs after treatment. Both cell lines were either untreated or treated with 1% DMSO (vehicle), 10 µM of complexes **1**-**6**, 100 µM CDDP (positive apoptotic) or 25% H_2O_2 (positive necrotic) for 24 hrs. Images were taken with a Zeiss Axiovert 25 inverted microscope using Axio Version 3.1 software at a magnification of 200 x. White arrows represent minimal signs of apoptotic cell death which include cellular rounding and plasma membrane blebbing. Black arrows indicate necrotic cell death due to swollen and burst cells.

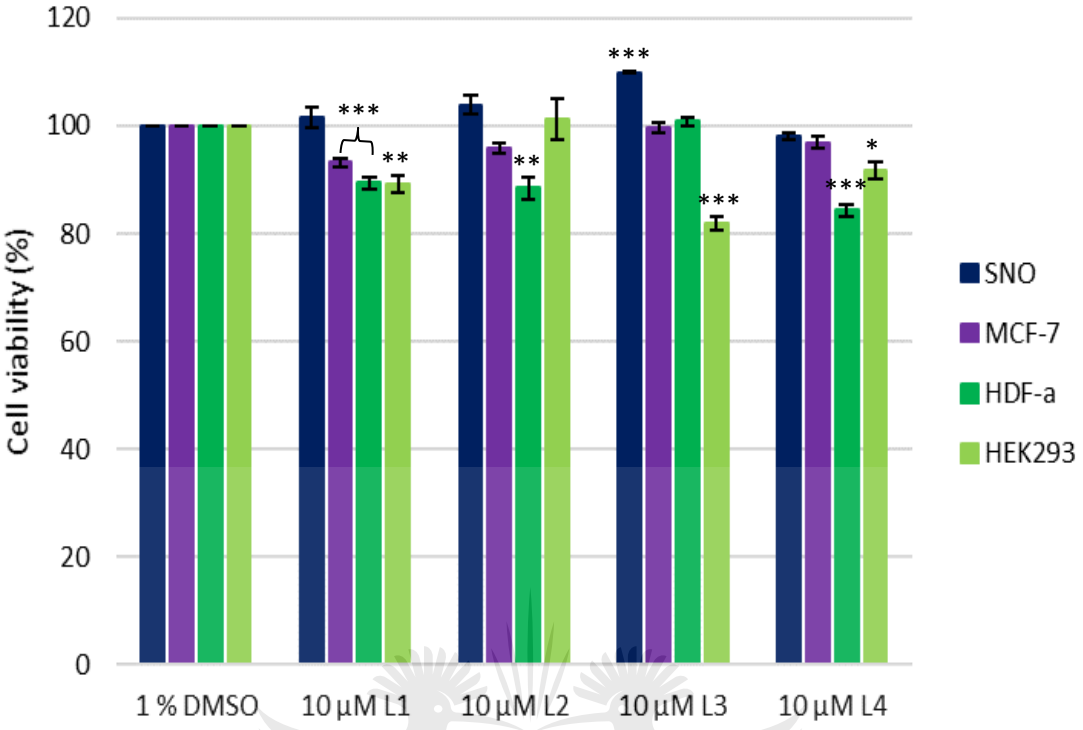

Figure 2.16: The percentage viability of **SNO**, **MCF-7**, **HDF-a** and **HEK293** cells determined with the alamarBlue® assay. All cell lines were treated with either 1% DMSO (vehicle) or 10 µM of ligands **L1**-**L4** for 24 hrs. The percentages were expressed with respect to 1% DMSO (100%). Error bars were constructed based on the ±SEM (n = 9). The P-value was calculated using the two-tailed Students t-Test. The treatments with P-values of $^{*}P < 0.05$, $^{**}P < 0.01$ and $^{***}P < 0.001$ were deemed significant with respect to DMSO.

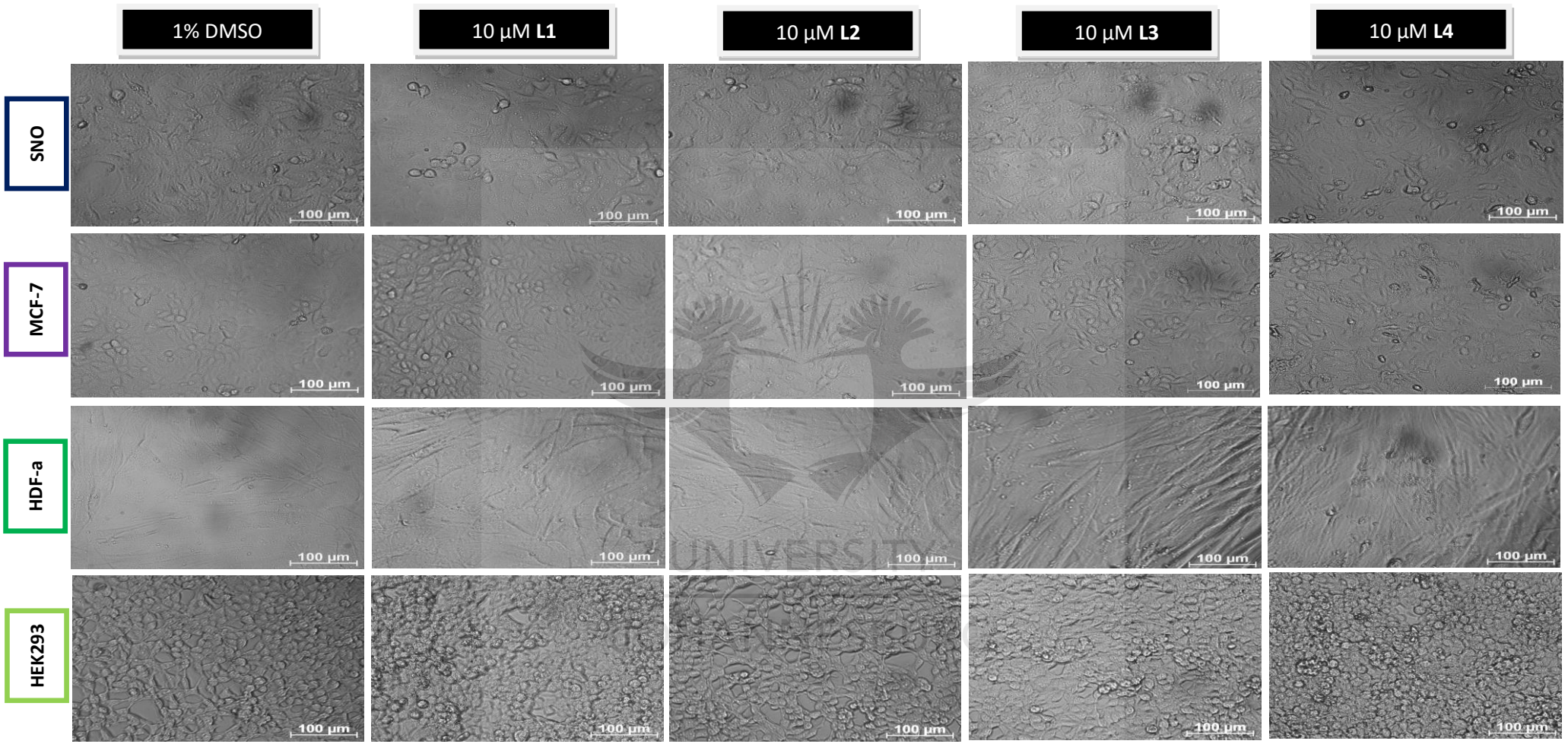

Figure 2.17: Light microscope images of **SNO**, **MCF-7**, **HDF-a** and **HEK293** cells taken 24 hrs after treatment. All cell lines were treated with either 1% DMSO (vehicle) or 10 µM of the ligands **L1**-**L4**. Images were taken with a Zeiss Axiovert 25 inverted microscope using Axio Version 3.1 software at a magnification of 200 x. All the cells appear to be intact with morphology resembling that of the DMSO treated cells.

2.3.10 Investigating aspects of mitochondrial-mediated apoptosis

It is believed that the mitochondria are targeted by lipophilic complexes (McKeage *et al*., 1998; Rackham *et al*., 2007; Kriel and Coates, 2012) which result in apoptosis *via* the intrinsic cell death pathway. Due to the lipophilic nature of our complexes, the involvement of various elements in the activation of the intrinsic cell death pathway was studied by flow cytometry, fluorescence microscopy and western blot analyses. It should be noted that these studies were only done with selected complexes. For the SNO cells, one complex from the 1:2 group (complex **1**) and one complex from the 1:3 group (complex **5**) were chosen. For the MCF-7 cells, only one complex from the 1:3 group (complex **3**) was chosen for further analysis. These complexes were chosen based on their low IC_{50} concentrations (Table 2.3), high malignant cytotoxicity (Table 2.4, Figure 2.4 and 2.5), apoptotic-inducing capabilities (Figure 2.6-2.13) and most importantly, low non-malignant cytotoxicity (Figure 2.14 and 2.15).

2.3.10.1 Alterations in mitochondrial membrane potential ($\Delta_{\psi m}$)

The changes in the $\Delta_{\psi m}$ was measured using a MitoProbe™ JC-1 flow cytometric kit. This kit detects the depolarization of the mitochondrial membrane coinciding with apoptosis. A cationic dye, JC-1, accumulates in the mitochondria as an aggregate and is detected as red fluorescence (at 590 nm). As the membrane starts to depolarize, the JC-1 is released from the mitochondria into the cytosol as a monomer causing a fluorescent shift from red to green (at 529 nm). The change in the $\Delta_{\psi m}$ is then measured by the decrease in red/green fluorescent intensity ratio. SNO and MCF-7 were either treated with 1% DMSO, 10 µM of the respective silver(I) complexes (SNO = complex **1** and **5**, MCF-7 = complex **3**) or 100 µM CDDP. In addition, a positive $\Delta_{\psi m}$ disrupter, 50 µM CCCP, as well as, an unstained control was included for gating purposes (Figure 2.18 and 2.19). Contour plots were constructed using FCS Express Plus 5 Software (Figure 2.18A and 2.19A). The fluorescent shift between red and green is also displayed in Figure 2.18B and 2.19B.

A significant shift in red to green fluorescence was observed in the SNO cells after being treated with complex **1** and **5**. Approximately 84% of the cells were located in the bottom left quadrant when compared to DMSO treated cells, where ±71% of the cells were located in the top left quadrant (Figure 2.18A). A significant ($P < 0.001$) decrease in the JC-1 red/JC-1 green ratio was also observed in cells after being treated with these complexes (Figure 2.18B). The same trend was observed in the MCF-7 cells after being treated with complex **3** where the cell population shifted from ±70% in the top quadrant (for DMSO) to ±83% in the bottom quadrant (Figure 2.19A).

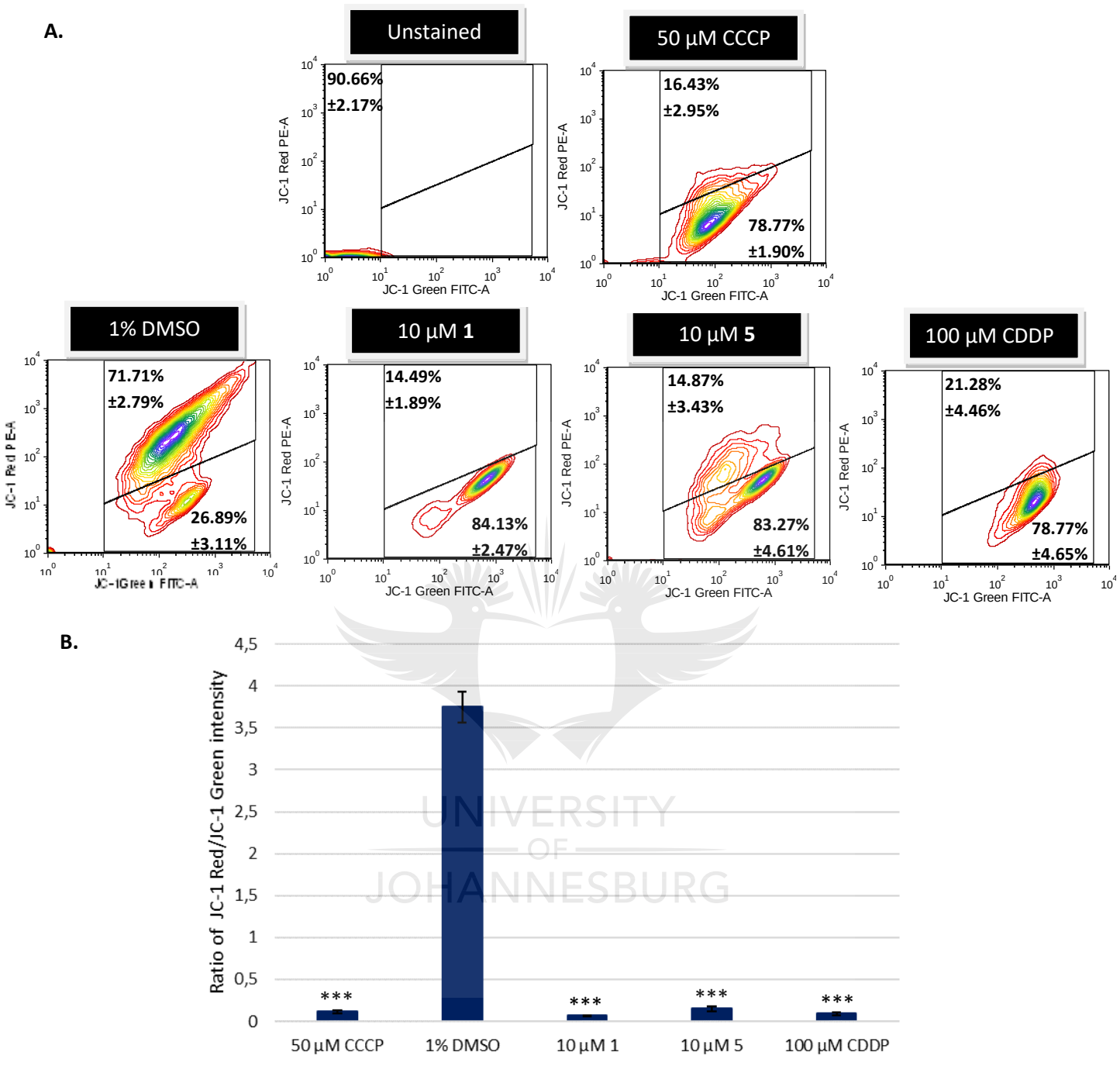

Figure 2.18: Contour plots indicating the distribution of JC-1 aggregates (red) and JC-1 monomer (green) in the mitochondrial membrane of malignant **SNO** cells (A). Cells were treated with either 1% DMSO (vehicle), 10 µM of complex **1** and **5** or 100 µM CDDP for 24 hrs. In addition, an unstained and a positive mitochondrial membrane depolarizer control, 50 µM CCCP, were included. The percentages followed by the ±SEM is represented in each quadrant (n = 4). The quantitative analysis of the mitochondrial shift from red fluorescence to green fluorescence was calculated (B). The error bars were constructed based on ±SEM (n = 4). The P-value was calculated using the two-tailed Students t-Test. The treatments with P-value of $^{***}P < 0.001$ were deemed significant with respect to DMSO.

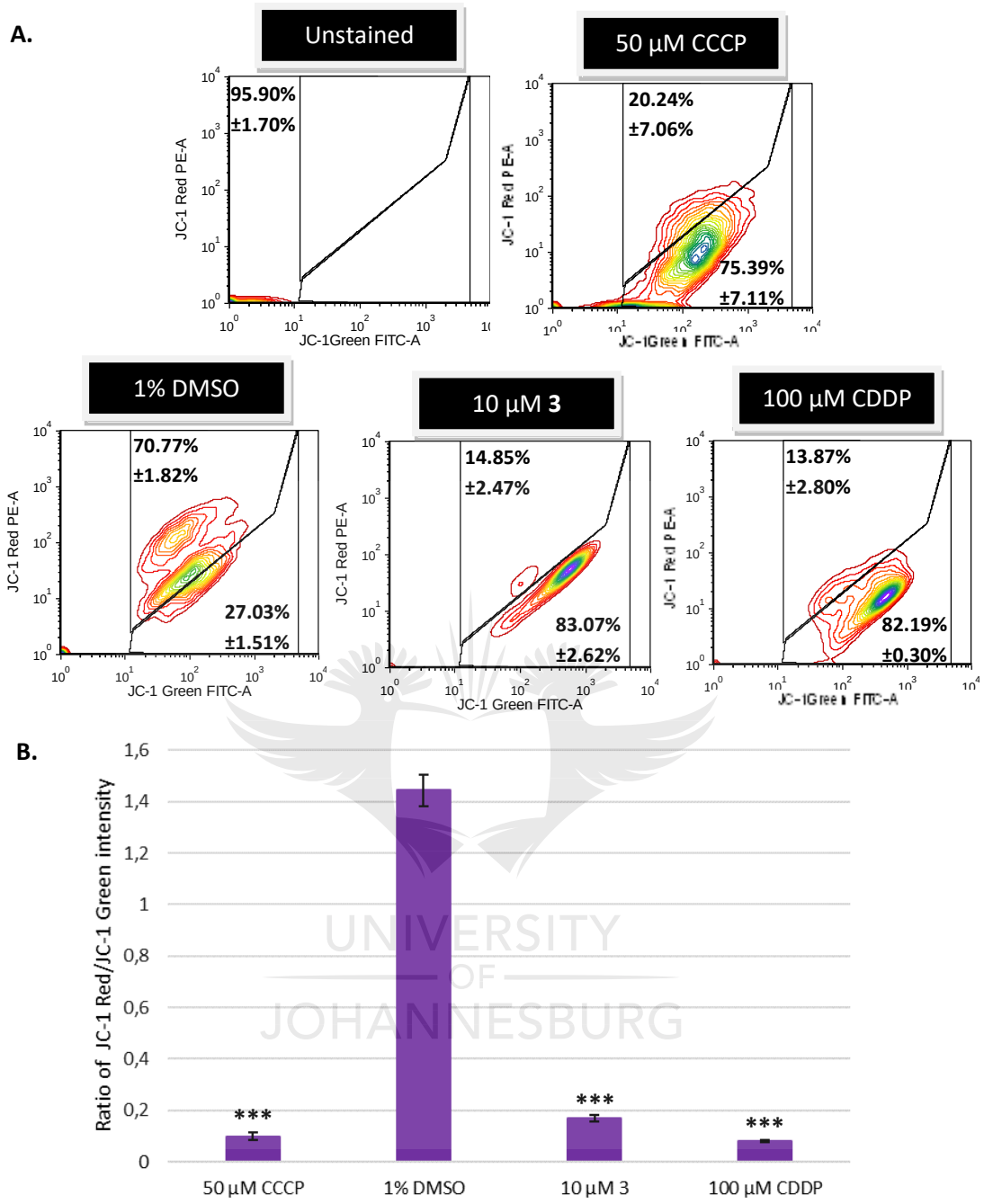

Figure 2.19: Contour plots indicating the distribution of JC-1 aggregates (red) and JC-1 monomer (green) in the mitochondrial membrane of malignant **MCF-7** cells (A). Cells were treated with either 1% DMSO (vehicle), 10 µM of complex **3** or 100 µM CDDP for 24 hrs. In addition, an unstained and a positive mitochondrial membrane depolarizer control, 50 µM CCCP, were included. The percentages followed by the ±SEM is represented in each quadrant (n = 4). The quantitative analysis of the mitochondrial shift from red fluorescence to green fluorescence was calculated (B). The error bars were constructed based on ±SEM (n = 4). The P-value was calculated using the two-tailed Students t-Test. The treatments with P-value of ***P < 0.001 were deemed significant with respect to DMSO.

A significant decrease ($P < 0.001$) in the JC-1 red/JC-1 green ratio was also observed in the MCF-7 cells (Figure 2.19B). The silver(I) complexes, including CDDP, contour plots resembled that of CCCP (being the positive mitochondrial membrane disrupter) which therefore confirms these treatments cause mitochondrial disruption.

2.3.10.2 Mitochondrial integrity and cytochrome c release

To further implicate mitochondrial targeting and intrinsic activation, mitochondrial integrity was analysed by fluorescent microscopy in conjunction with cytochrome *c* release after 24 hrs of treatment. SNO cells were either treated with 1% DMSO, the IC_{50} dosage and 10 µM concentrations of complex **1** and **5** or 100 µM CDDP. The MCF-7 cells were either treated with 1% DMSO, both the IC_{50} dosage and 10 µM concentration of complex **3** or 100 µM CDDP. By including the IC_{50} dosage as a treatment ensures that earlier cellular events are detected that could not be observed when the higher concentrations are used. The cells were probed with Hoecht-33258 (blue), Alexa-Fluor®488 labelled anti-cytochrome *c* specific antibody (green) and MitoTracker Orange (red). These probes stain the DNA, cytochrome *c* and mitochondria respectively. Fluorescent images are shown in Figure 2.20 and 2.21 for the SNO cells and Figure 2.22 and 2.23 for the MCF-7 cells (A digital copy of high-resolution images of Figures 2.20 and 2.22 are included).

All three probes appear to be localized in the intact organelles of the SNO and MCF-7 cells after treatment with DMSO (Figure 2.20-2.23). Changes in the Hoecht-33258 pattern after treatments have been discussed previously (Figure 2.7 and 2.8), but was included to discriminate between the cells. When the SNO cells were treated with the IC_{50} dosage of either complex **1** or **5**, the fluorescent pattern changed specifically for cytochrome *c,* but the mitochondrial stain was uniformly spread in the cells (Figure 2.20 and 2.21). It appears that cytochrome *c* is released from the mitochondria into the cytosol. The mitochondrial integrity is decreased after treatment with the 10 µM concentrations of complexes **1** and **5**, including CDDP. For the MCF-7 cells, both the IC_{50} dosage and 10 µM concentrations of complex **3** fluorescent pattern were similar (Figure 2.22 and 2.23). Although not as distinct as in the SNO cells, it appears that some cytochrome *c* is released from the mitochondria is specifically seen after treatment with both concentrations of complex **3** including CDDP. The decrease in mitochondrial integrity (Figure 2.20-2.23) of both the SNO and MCF-7 cells, along with a decrease in the $\Delta_{\psi m}$ (Figure 2.18 and 2.19) confirm that these complexes, in fact, target the mitochondria.

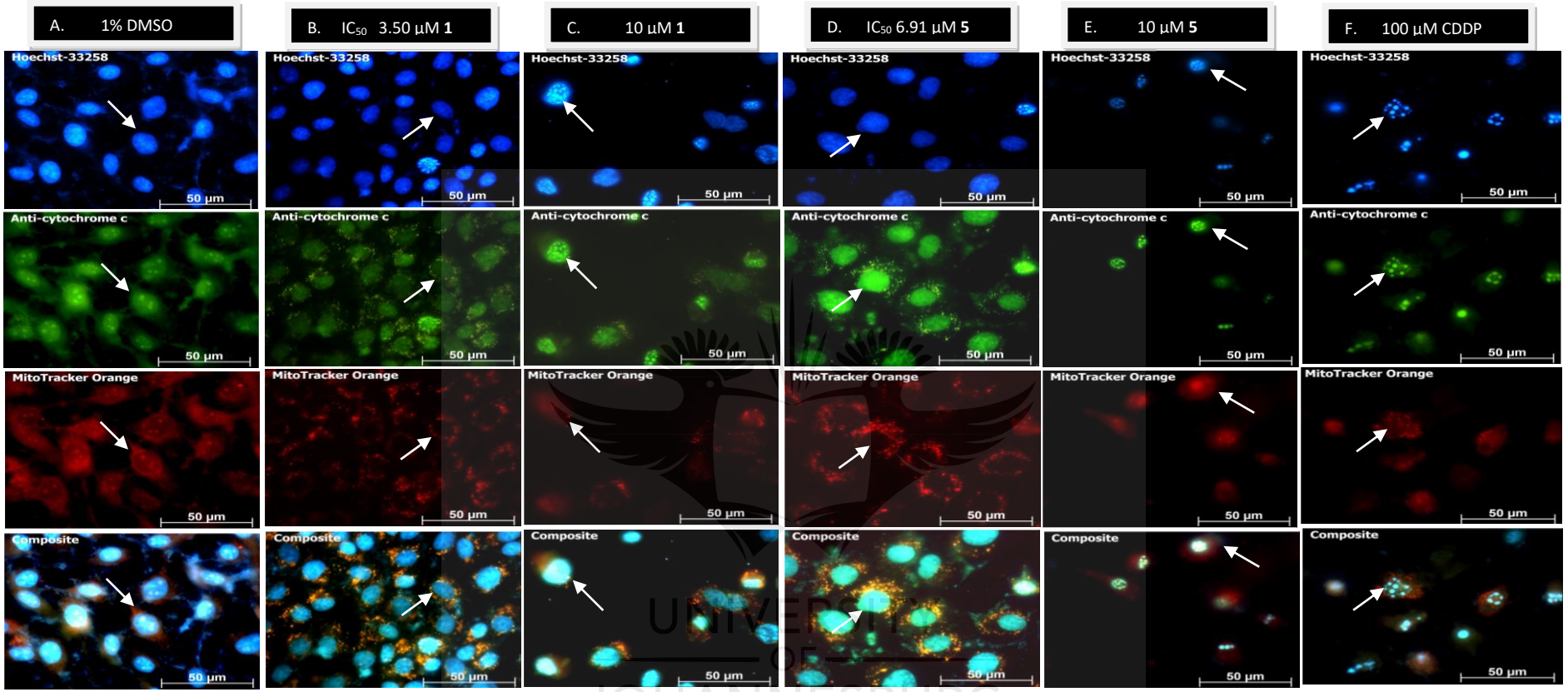

Figure 2.20: Fluorescent images of malignant **SNO** cells taken after 24 hrs of treatment. The cells were treated with either 1% DMSO (vehicle) (A), the IC_{50} value (3.50 µM and 6.91 µM) and 10 µM of complex **1** (B and C) and **5** (D and E) respectively or 100 µM CDDP (positive) (F). The cells were probed with Hoechst-33258 (blue), Alexa-Fluor®488 labelled anti-cytochrome *c* specific antibody (green) and MitoTracker Orange (red) which stains DNA, cytochrome *c* and mitochondria respectively. Images were taken with a Zeiss Axioplan 2 inverted fluorescence microscope using Axio Version software at a magnification of 1000 x. DNA appears to be condensed in most cells treated with the silver(I) treatments or CDDP. A decrease in mitochondrial integrity along with cytochrome *c* translocation can also be observed in treated cells. White arrows indicate the cells that have been enlarged and can be seen in Figure 2.21.

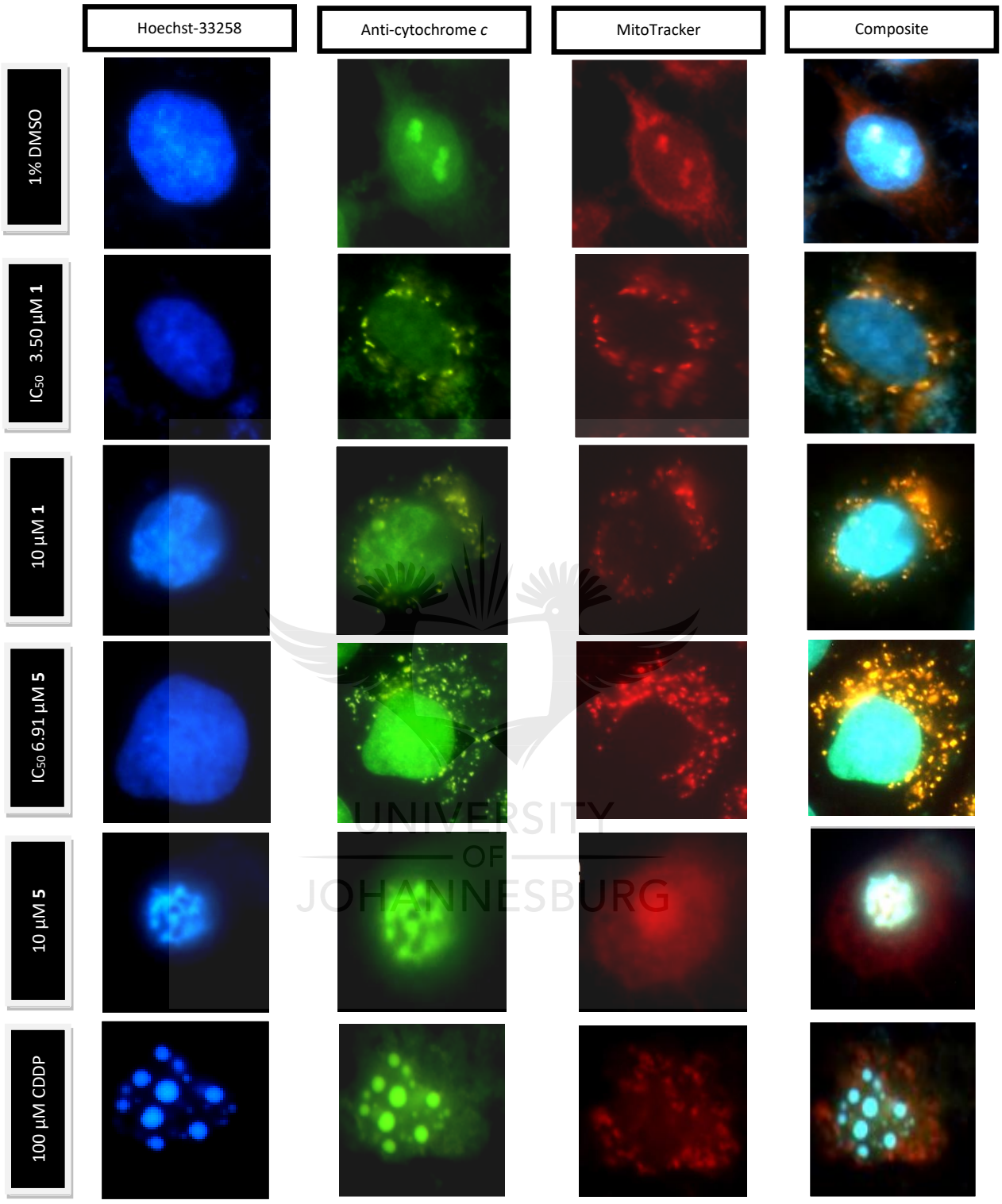

Figure 2.21: Enlarged fluorescent images of **SNO** cells taken from Figure 2.20.

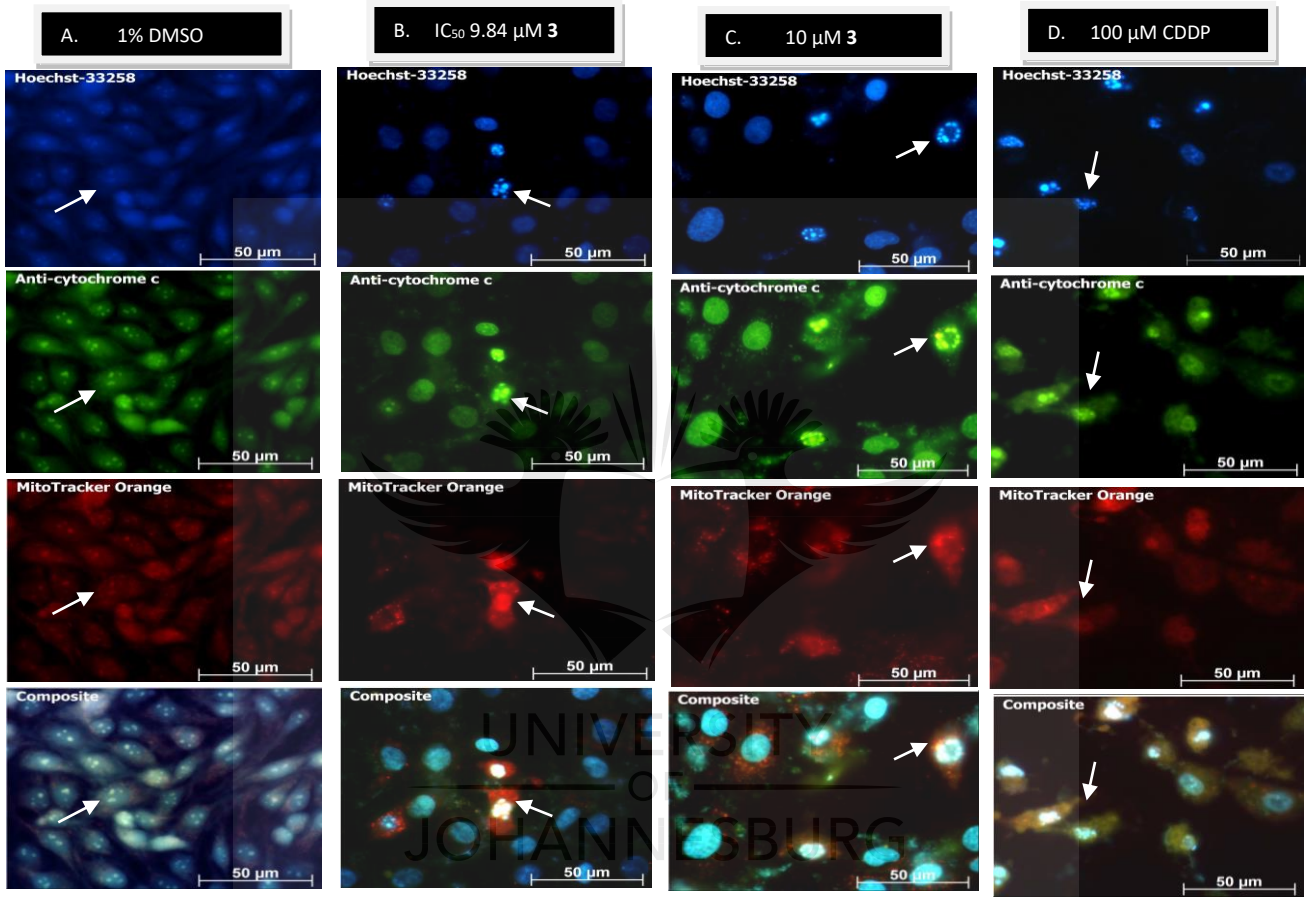

Figure 2.22: Fluorescent images of malignant **MCF-7** cells taken after 24 hrs of treatment. The cells were treated with either 1% DMSO (vehicle) (A), the IC_{50} value (9.84 µM) and 10 µM of complex **3** (B and C) or 100 µM CDDP (positive) (D). The cells were probed with Hoechst-33258 (blue), Alexa-Fluor®488 labelled anti-cytochrome *c* specific antibody (green) and MitoTracker Orange (red) which stains DNA, cytochrome *c* and mitochondria respectively. Images were taken with a Zeiss Axioplan 2 inverted fluorescence microscope using Axio Version software at a magnification of 1000 x. DNA appears to be condensed in some cells treated with complex **3** and CDDP. Mitochondrial integrity decreased including cytochrome *c* translocation is observed in the treated cells. White arrows indicate the cells that have been enlarged and can be seen in Figure 2.23.

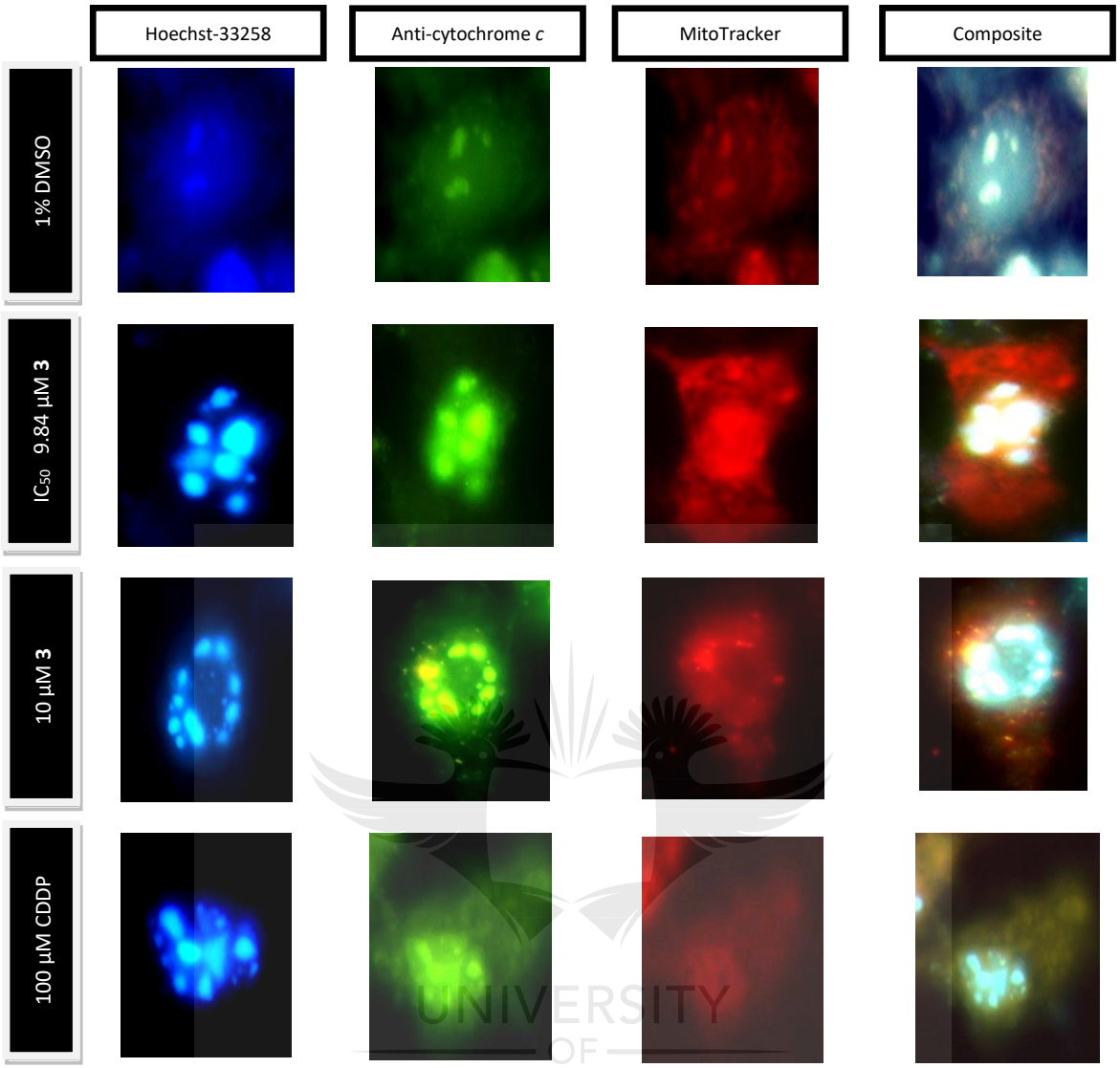

Figure 2.23: Enlarged fluorescent images of **MCF-7** cells taken from Figure 2.22.

2.3.10.3 The release of reactive oxygen specie/s (ROS)

Mitochondria produce ROS under times of cellular stress which plays a role in cell death pathways like apoptosis (Murphy, 2009). The ability of silver(I) complexes to induce ROS in the malignant cells, as a potential mechanism, leading to cell death were examined. The ROS levels were measured in the malignant cells by using a Muse® Oxidative Stress Kit. This kit quantifies the cellular populations undergoing oxidative stress by detecting superoxide. The data output is in a form of a histogram which either discriminates cells as ROS negative (-) (M1 on the histogram) or ROS positive (+) (M2 on the histogram). SNO and MCF-7 were treated with either 1% DMSO, 10 µM of the respective silver(I) complexes (SNO = complex **1** and **5**, MCF-7 = complex **3**) or 100 µM CDDP. The ROS activity was measured after 24 hrs of treatment and is presented in Figure 2.24.

Complexes **1** and **5** caused an increase in the number of ROS (+) SNO cells when compared to DMSO (Figure 2.24A). The same was seen in the SNO cells treated with CDDP where more than 40% of the cells were localised in the ROS (+) region. Interestingly, the ROS (+) activity was low in the MCF-7 cells treated with both complex **3** and CDDP resembling a similar pattern than DMSO (Figure 2.24B).

2.3.10.4 Analysis of downstream apoptotic events and stress proteins

Based on previous findings it is evident that the mitochondria are targeted by the silver(I) phosphine complexes resulting in the release of cytochrome *c* (Figures 2.18-2.24). Therefore, the involvement of caspase-9 and PARP cleavage was monitored on a protein level after 24 hrs of treatment. SNO and MCF-7 were either treated with 1% DMSO, 10 µM of the respective silver(I) complexes (SNO = complex **1** and **5**, MCF-7 = complex **3**) or 100 µM CDDP. Western blots of the respective treatments for SNO and MCF-7 cells are shown in Figure 2.25.

The protein levels of the full-length caspase-9 (47 kDa) significantly decreased in the SNO cells treated with complexes **1**, **5** and CDDP when compared to DMSO (Figure 2.25A). This was followed by a significant increase in the cleaved form of caspase-9 (37/35 kDa) for these treatments. This was accompanied by a significant decrease in the protein levels of full-length PARP (113 kDa) and a significant increase in the cleaved form (88/25 kDa) of which only the smaller 25 kDa fragment was detected (Figure 2.25A). The same was observed in the MCF-7 cells treated with complex **3** and CDDP with a significant decrease in the inactive form of PARP (when compared to DMSO) followed by an increase in the active form of PARP (Figure 2.25B). Moreover, a decrease in the inactive caspase-9 was observed followed by an increase in the active form but was less prominent when compared to the SNO cells (Figure 2.25A). Even though CDDP did not show any noticeable cleavage of caspase-9 in the MCF-7 cells, PARP cleavage was apparent.

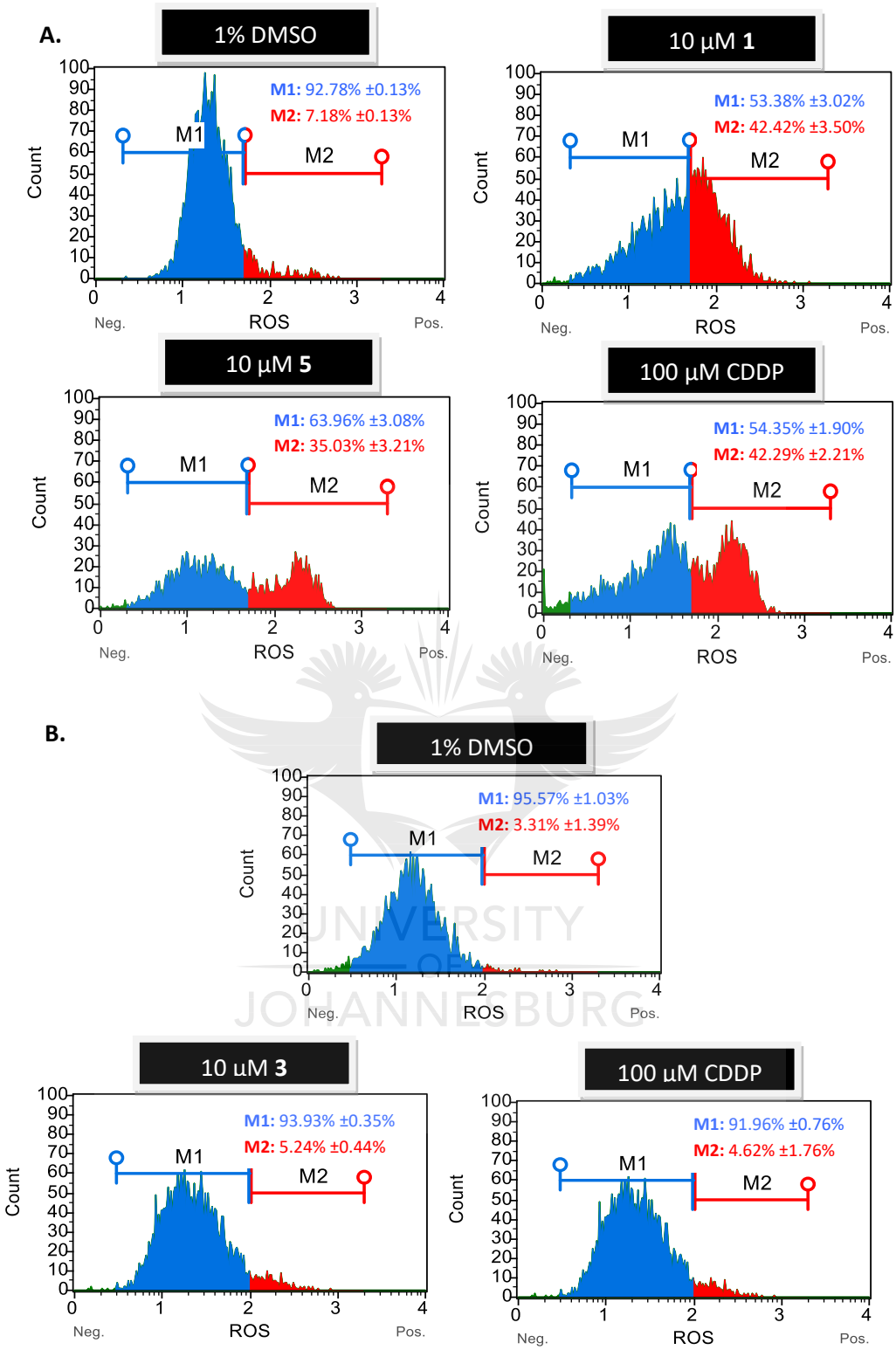

Figure 2.24: ROS production in malignant **SNO** (A) and **MCF-7** (B) cells measured using a Muse® Oxidative stress kit. Both cell lines were treated with either 1% DMSO (vehicle) or 100 µM CDDP (positive) for 24 hrs. SNO cells were treated with 10 µM of complex **1** or **5**, while MCF-7 cells were treated with 10 µM of complex **3**. The percentages indicate the cellular populations that are divided in ROS negative (M1, blue) or ROS positive (M2, red). The ±SEM is represented in each quadrant (*n* = 3).

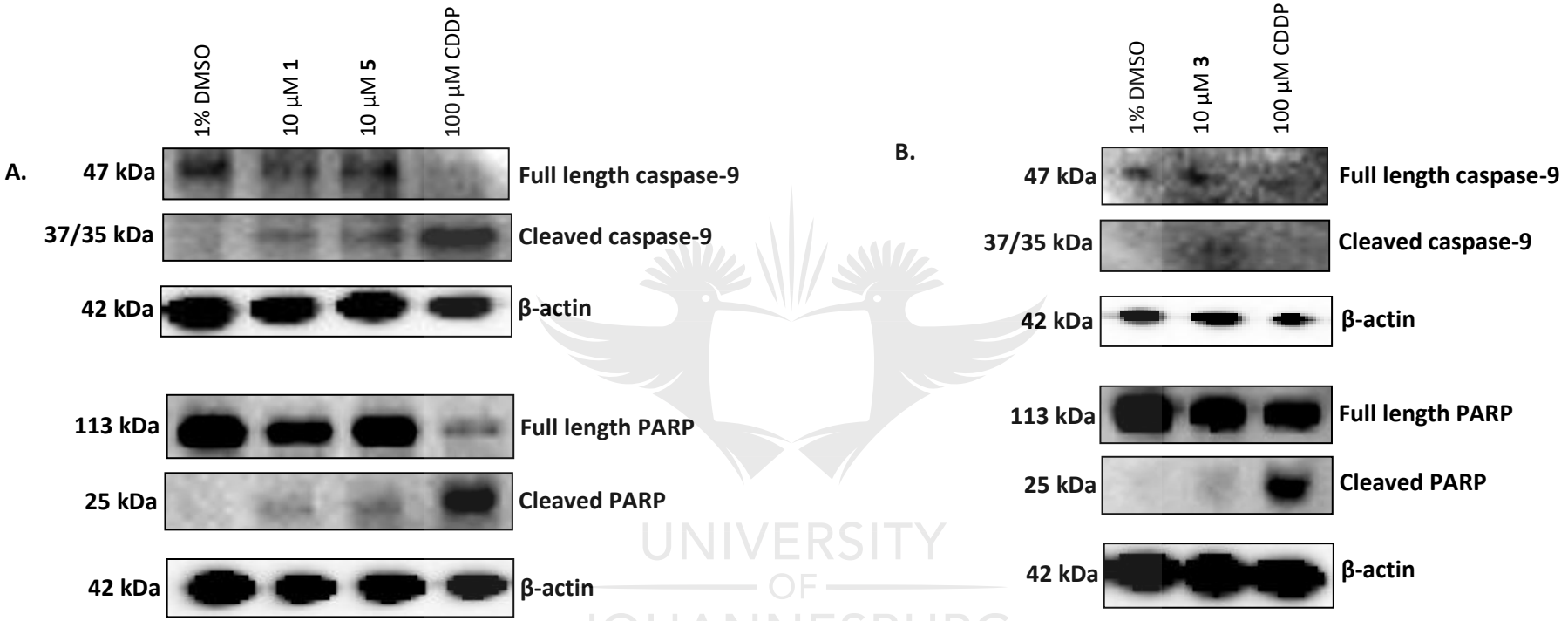

Figure 2.25: Western blot analysis of the activity of apoptotic proteins in the malignant **SNO** (A) and **MCF-7** (B) cells treated for 24 hrs. Both cell lines were treated with either 1% DMSO (vehicle) or 100 µM CDDP (positive). SNO cells were treated with 10 µM of complex **1** or **5**, while MCF-7 cells were treated with 10 µM of complex **3**. Protein bands were detected with rabbit-anti-human caspase-9 and rabbit-anti-human monoclonal PARP antibody. A mouse-anti-human monoclonal β-actin antibody was used to detect β-actin which served as the loading control.

Many anticancer agents, including the silver(I) complexes, may lead to cellular stress which results in the activation of chaperone proteins (*e.g.* Hsp70). Hsp70 is responsible for stabilizing other unfolded proteins following stress-induced damage (Hightower, 1991). The protein levels of the inducible Hsp70 was quantified in the SNO and MCF-7 cells after 24 hrs of treatment. Both cell lines were treated the same way as described before and western blots of respective treatments are shown in Figure 2.26.

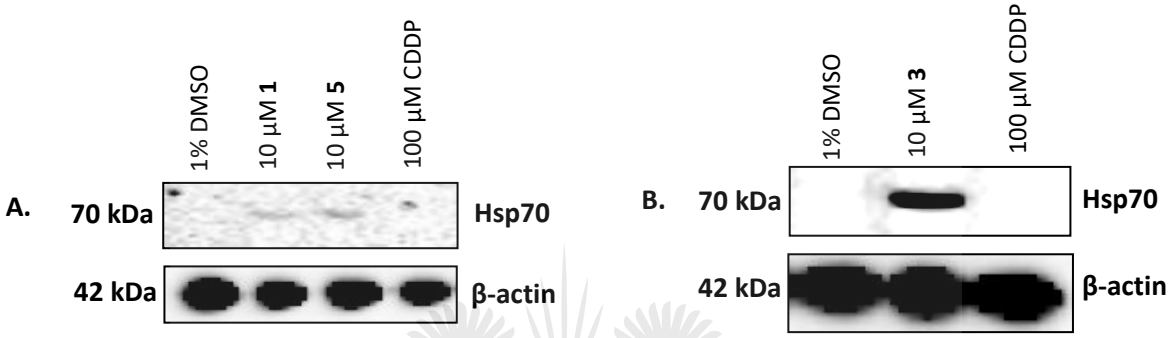

Figure 2.26: Western blot analysis of the activity of the inducible Hsp70 protein in the malignant **SNO** (A) and **MCF-7** (B) cells treated for 24 hrs. Cells were treated with either 1% DMSO (vehicle), 10 µM of complex **1** (SNO), **3** (MCF-7) and **5** (SNO), or 100 µM CDDP. Protein bands were detected with rabbit- mouse-anti-human monoclonal Hsp70 antibody. A Mouse-anti-human monoclonal β-actin antibody was used to detect β-actin which served as the loading control.

It appears that the silver(I) complexes induce cell stress at varying intensities as observed from the western blots. A slight increase in Hsp70 was observed in the SNO cells after treatment with complex **1** and **5** (Figure 2.26A). Hsp70 levels were more pronounced in the MCF-7 cells after being treated with complex **3** (Figure 2.26B). Hsp70 was not induced in either the SNO and MCF-7 cells after treatment with DMSO and CDDP.

2.3.11 Identifying possible drug targets

All the studies conducted thus far confirmed that apoptotic cell death was induced by the silver(I) complexes *via* the intrinsic cell death pathway. Collectively, the data shown here underscores the fact that silver(I) phosphines induce apoptosis *via* the mitochondrial-mediated pathway. However, what is not revealed here are the upstream targets that can result in the activation of apoptosis. Some studies allude to the fact that phosphine complexes target a mitochondrial-based enzyme, TrxR (Rackham *et al*., 2007; Rigobello *et al*., 2008; Gandin *et al*., 2010; Demir *et al*., 2014). TrxR is an NADPH-dependant enzyme that catalyses the reduction of Trx, including other free radical species,

to form reduced disulphide bonds which protects the cells against oxidative damage. To this end, the TrxR activity was determined in the SNO and MCF-7 cells by using an TrxR assay kit. In this kit, the reduction of 5, 5'- dithiobis (2-nitrobenzoic) acid (DTNB) to 5-thio-2-nitrobenzoic acid (TNB) is measured in the presence of NADPH. The reduction causes a yellow colour that can be measured at 412 nm. Since other enzymes (*e.g.* glutathione reductase or peroxidase) can also reduce DNTB, an TrxR specific inhibitor is included. SNO and MCF-7 were treated with 1% DMSO, 10 µM of the respective silver(I) complexes (SNO = complex **1** and **5**, MCF-7 = complex **3**) or 100 µM CDDP. The relative TrxR activity is expressed as a percentage either (with respect to the uninhibited DMSO) in the absence (-) or the presence (+) of the TrxR inhibitor (Figure 2.27).

Complex **1**, **5** and CDDP decreased the TrxR activity with high significance ($P < 0.001$) in the SNO cells (Figure 2.27A). The TrxR activity decreased in the MCF-7 cells after treatment with complex **3**, but was not significant as compared to CDDP (Figure 2.27B).

In addition, the effect that silver(I) complexes had on a drug metabolizing enzyme, cytochrome P450 (CYP450) was measured. The relative activity of this isoform was measured using a P450-Glo™ assay kit specific for the CYP1B1 isoform. Both cell lines were treated as mentioned previously in this section. The relative activity was measured with respect to DMSO (Figure 2.28).

Complex **1** and **5** caused a significant ($P < 0.05$) increase in CYP1B1 activity of the SNO cells when compared to DMSO treated cells (Figure 2.28A). No significant change of CYP1B1 activity was observed in the MCF-7 cells with either of the treatments (Figure 2.28B).

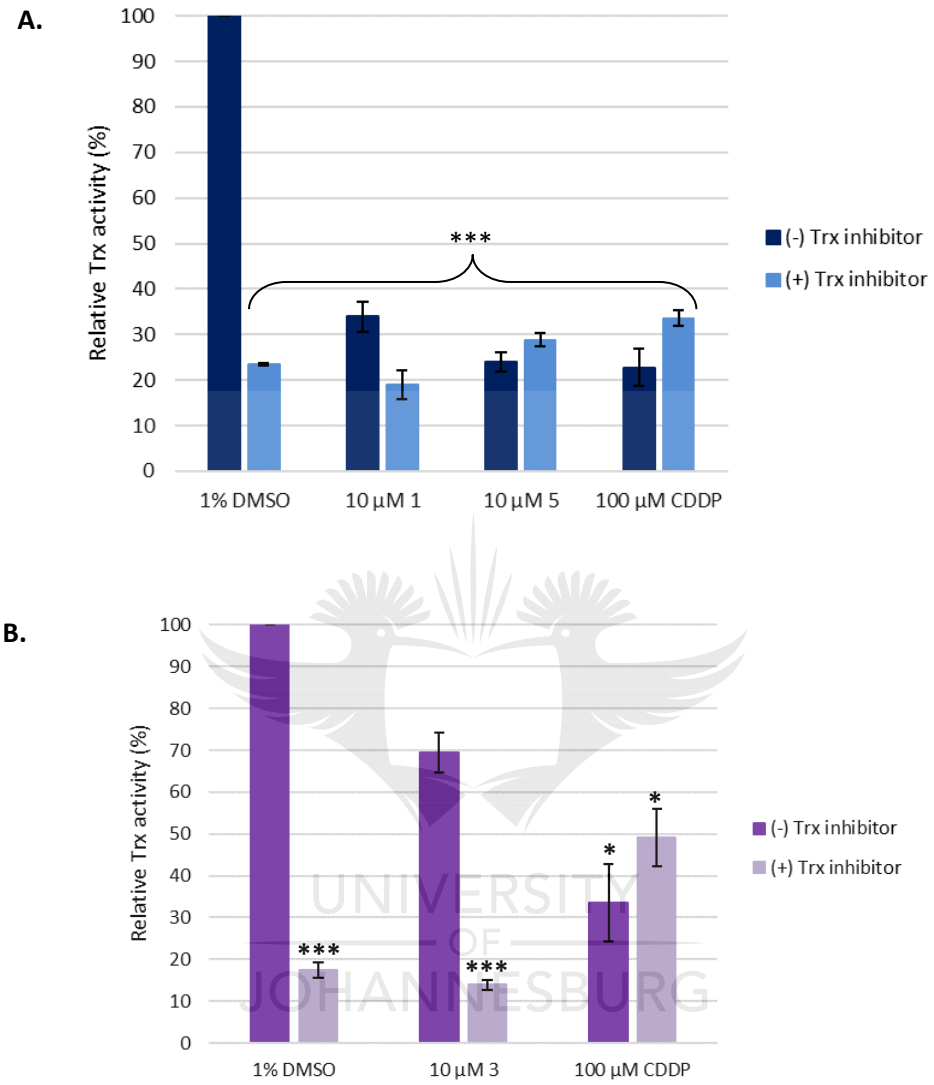

Figure 2.27: The relative TrxR activity in the malignant **SNO** (A) and **MCF-7** (B) cells. Both cell lines treated with either 1% DMSO (vehicle) or 100 µM CDDP (positive) for 24 hrs. SNO cells were treated with 10 µM of complex **1** or **5**, while MCF-7 cells were treated with 10 µM of complex **3**. The percentages were expressed with respect to 1% DMSO (100%). Error bars were constructed based on the ±SEM (n = 3). The P-value was calculated using the two-tailed Students t-Test. The treatments with P-values of $^{*}P < 0.05$ and $^{***}P < 0.001$ were deemed significant with respect to DMSO.

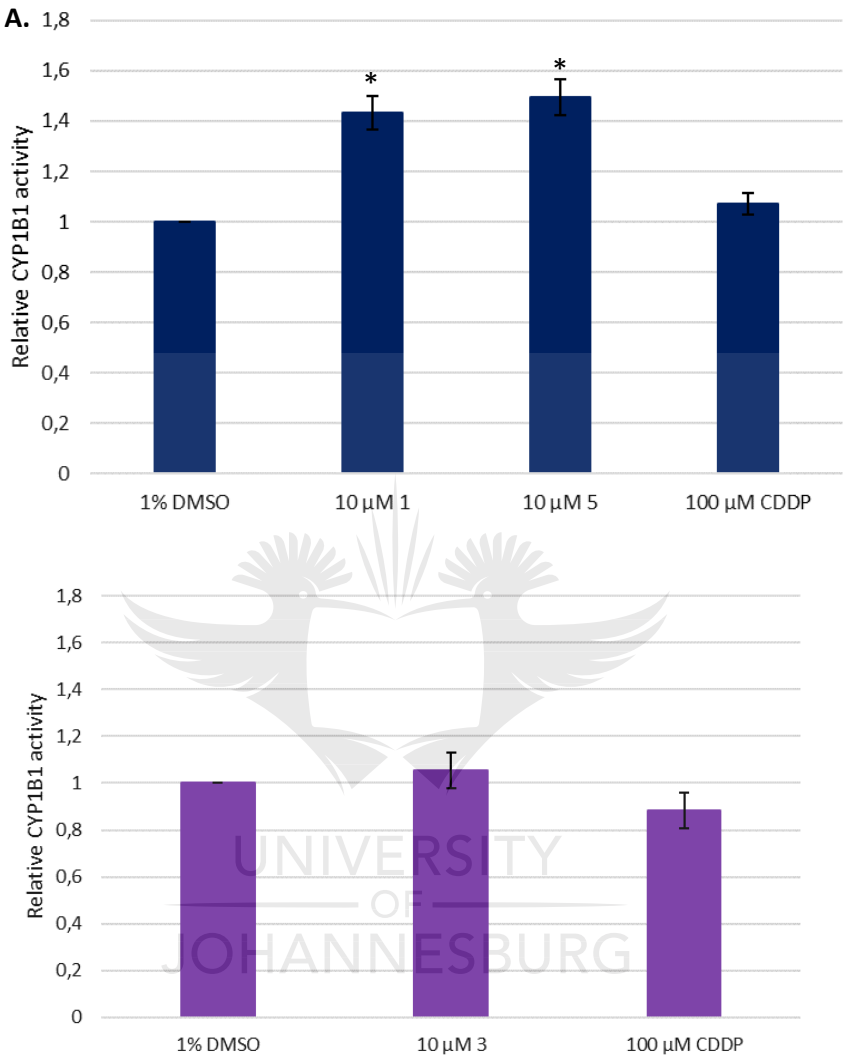

Figure 2.28: Relative CYP1B1 activity in malignant **SNO** (A) and **MCF-7** (B) cells. Both cell lines were treated with either 1% DMSO (vehicle) or 100 µM CDDP (positive) for 24 hrs. SNO cells were treated with 10 µM of complex **1** or **5**, while MCF-7 cells were treated with 10 µM of complex **3**. The percentages were expressed with respect to 1% DMSO (100%). Error bars were constructed based on the ±SEM (n = 3). The P-value was calculated using the two-tailed Students t-Test. The treatments with a P-value of $^*P < 0.05$ were deemed significant with respect to DMSO.

2.3.12 Cytotoxicity of selected complexes in a panel of malignant cells

Three silver(I) complexes (**1**, **3** and **5**) were outsourced and analysed *in vitro* by NMMU to determine if they have the ability to target a wide range of malignancies. These complexes were selected based on their low IC_{50} values (Table 2.3), high selectivity for malignant cells (Table 2.4, Figure 2.4 and 2.5), apoptotic inducing abilities (Figure 2.6-2.13, 2.18-2.25) and low cytotoxic potency to non-malignant cells (Figure 2.14 and 2.15). A total of 16 different malignant cell lines derived from either human, rat or mice were treated with either 1% DMSO or 10 µM of complexes **1**, **3** and **5** or 100 µM CDDP. The percentage viability was determined after 24 hrs of treatment using the alamarBlue® assay. The cell viabilities were calculated with respect to DMSO and are summarized in Table 2.5. The viabilities are arranged in ascending order of toxicity (from lowest to highest with the most cytotoxic drug being at the top and least cytotoxic drug at the bottom). It should be noted that an MCF-7 cell line was one of the 16 cell lines tested by NMMU. This was included for comparison purposes to monitor variations that might occur between different laboratories. Dose-response studies with MCF-7 cells were done by them and the IC_{50} values were in the same order of magnitude of those we found in our study (data not shown).

When looking at the top 7 ranked cell lines, HeLa cervical adenocarcinoma, PC12 rat pheochromocytoma and HT-29 colorectal adenocarcinoma fall in the top 3 cell lines with the lowest viabilities for complex **1** and **3** or top five of complex **5**. From Table 2.5 it is evident that all three complexes are very active in the HeLa and HT-29 cells (except complex **5** with a growth inhibition of 48.29%) with a growth inhibition of higher than 67%. Similar growth inhibition patterns were observed for Caco2 colorectal adenocarcinoma, MeWo malignant melanoma, U937 histiocytic lymphoma, Ins-1 pancreatic insulinoma, A549 lung adenocarcinoma and acute Jurkat-T leukaemia cells after treatment with the three silver(I) complexes which ranged from 30-59.35%. Complex **1** was the most toxic when compared to the other silver treatments in which the PC12 rat pheochromocytoma, MCF-7 breast adenocarcinoma, B16F10 mouse melanoma, PC3 prostate adenocarcinoma, C3A derivate of HepG2, HepG2 hepatocellular carcinoma and MiaPaCa pancreatic carcinoma growth was inhibited by 71.57%, 67.69%, 57.84%, 48.35%, 51.60%, 66.43% and 49.06% respectively. Complex **3** and **1** inhibited the growth of SH-SY5Y neuroblastoma cells with 49.91% and 42.29%. The MiPaCa and HepG2 cell lines were mostly resistant towards the treatment with complex **5** (along with complex **3** in the MiaPaCa cells). When comparing the cytotoxic activity of the silver(I) complexes with that of CDDP, the same phenomenon was observed as in Figures 2.2 and 2.3 where the complexes were 10-times more toxic. Overall, complex **1** was the most active complex with growth inhibition of 36-71.5% in all 16 tested cell lines when compared to the other silver treatments. This was followed by complex **3**, and lastly complex **5.**

Table 2.5: The percentage cell viability of 16 malignant cell lines determined by the alamarBlue® assay. All cell lines were treated with either 1% DMSO (vehicle), 10 µM of complexes **1**, **3** and **5** or 100 µM CDDP for 24 hrs. The percentages are expressed with respect to the control (100%) followed by the ±SEM (*n* = 4). The percentages are ranked in ascending order of toxicity of the complexes (from the lowest to the highest viability). The *P*-values was calculated using the two-tailed Students *t*-Test where the treatments with *P*-value**P* < 0.05, ***P* < 0.01 and ****P* < 0.001 were deemed significant with respect to DMSO.

Cell line	Complex	% Viability (±SEM%)	Cell line	Complex	% Viability (±SEM%)	Cell line	Complex	% Viability (±SEM%)	Cell line	Complex	% Viability (±SEM%)
HeLa	**1**	29.19 (±1.58)***	**HT-29**	**3**	27.56 (±1.06)***	**A549**	**1**	51.64 (±2.90)***	**HepG2**	**1**	33.70 (±1.60)***
	3	32.68 (±1.87)***		**1**	29.76 (±0.45)***		**3**	57.09 (±1.40)***		**3**	46.19 (±3.41)***
	5	32.96 (±1.31)***		**CDDP**	37.33 (±2.18)***		**CDDP**	57.40 (±3.81)***		**CDDP**	58.96 (±1.23)***
	CDDP	55.78 (±2.88)***		**5**	51.51 (±1.80)***		**5**	68.38 (±1.86)***		**5**	91.12 (±2.48)***
Caco2	**5**	40.67 (±1.00)***	**U937**	**1**	45.38 (±3.97)***	**Jurkat-T**	**3**	59.01 (±2.24)***	**HEPG2-C3A**	**1**	48.44 (±1.25)***
	1	42.50 (±0.82)***		**3**	45.78 (±4.26)***		**1**	64.00 (±3.14)***		**CDDP**	52.78 (±1.13)***
	3	51.70 (±1.73)***		**CDDP**	60.07 (±4.18)***		**5**	69.23 (±3.41)***		**3**	69.41 (±1.48)***
	CDDP	71.36 (±1.79)***		**5**	60.46 (±4.31)***		**CDDP**	72.86 (±3.31)***		**5**	75.97 (±1.74)*
PC12	**1**	28.55 (±1.23)***	**B16F10**	**1**	42.19 (±1.32)***	**PC3**	**1**	52.12 (±4.34)***	**MiaPaCa**	**1**	50.99 (±1.32)***
	3	42.19 (±3.44)***		**3**	50.89 (±2.70)***		**CDDP**	58.50 (±2.04)***		**3**	80.34 (±2.06)***
	5	42.56 (±0.62)***		**5**	60.93 (±1.42)***		**3**	64.52 (±5.52)**		**5**	93.40 (±1.53)**
	CDDP	65.24 (±2.82)***		**CDDP**	59.70 (±1.96)***		**5**	72.26 (±3.62)***		**CDDP**	60.10 (±1.49)***
MeWo	**5**	44.73 (±2.21)***	**Ins-1**	**3**	56.73 (±0.29)***	**SH-SY5Y**	**CDDP**	32.97 (±1.10)***	**MCF-7**	**1**	34.45 (±1.22)***
	1	45.23 (±1.82)***		**1**	57.66 (±0.30)***		**3**	50.29 (±2.56)***		**CDDP**	50.46 (±3.52)***
	3	46.03 (±3.14)***		**5**	62.14 (±0.66)***		**1**	57.51 (±2.07)***		**3**	50.74 (±5.14)***
	CDDP	65.99 (±4.88)***		**CDDP**	66.07 (±0.76)***		**5**	76.26 (±4.22)***		**5**	51.76 (±1.05)***

2.4 Discussion

Drugs containing metal centers are of importance in diagnostic imaging and in therapeutic applications that include anticancer approaches (Jackson *et al*., 2001). The serendipitous discovered drug, CDDP, is one of the most used metal-based drugs in cancer therapeutics. CDDP, including structural related platinum-based complexes, exerts is activity on malignant cells in four stages that include drug uptake, drug activation, DNA crosslinking and cellular processing resulting in apoptosis (Johnstone *et al*., 2015). The clinical success of cisplatin is limited by severe side effects (Reed *et al*., 1996; Fischer *et al*., 2008; Tsang *et al*., 2009) along with cancer resistance (Kelland *et al*., 1992; Borst *et al*., 2008). These limitations stimulated the search for alternative transition metal complexes that are more effective within the attempt to achieve greater selectivity. The use of silver(I) phosphine complexes has shown to be promising in the research of cancer. What makes the use of these complexes so attractive is their ability to be structurally diverse (Zachariadis *et al*., 2004; Hadjikakou *et al*., 2008) and stable in the presence of serum proteins (Berners-Price *et al*., 1995; Kriel and Coates, 2012) and most importantly they tend to be more selective than their gold(I) analogues (Kyros *et al*., 2010; Poyraz *et al*., 2011; Kriel and Coates, 2012).

Two cancer cell targeting models have been proposed for chemotherapeutic agents (Michels *et al*., 2014). Firstly, the anticancer agent should target the metabolic pathways that will do the most harm to the cancer cells. Secondly, the anticancer agent should impair the malignant signals involved in cancer metabolic rewiring. In order to do so, the role of biochemical markers in malignant cell death needs to be identified. Although the mechanism of platinum complexes, especially CDDP, have been well defined, little is known about the exact mechanism defining silver(I) complexes toxicity in cancer. With this in mind, the improved cytotoxic effect, mode of programmed cell death, mechanistic targeting thereof and possible drug targets were identified in two malignant cell lines.

2.4.1 Silver(I) complexes degree of cytotoxicity in malignant cells

Silver(I) saccharinate complexes with monophosphines (Yilmaz *et al*., 2014), salicylic acid with triphenylphosphines (Poyraz *et al*., 2011) and aryl phosphines (Banti *et al*., 2015) showed improved cytotoxicity in malignant cells when compared to CDDP. A similar trend was observed where it was reported in recent studies that silver(I) thiocyanate complexes showed to be more cytotoxic than CDDP in either oesophageal or breast malignancies (Ferreira *et al*., 2015; Human *et al*., 2015; Potgieter *et al*., 2015; Potgieter *et al*., 2016).

In order to evaluate the extent of cell toxicity of the complexes **1**-**6**, dose-response studies were performed using the alamarBlue® proliferation assay. This was done to determine the IC_{50}

concentration of the complexes including CDDP in malignant SNO and MCF-7 cell lines (Table 2.3). For the SNO cells, the order of decreasing toxicity, where the activity of complex **1** was the highest, were complex **1** (3.50 µM), **2** (4.02 µM), **5** (6.91 µM), **6** (7.61 µM), **4** (8.31 µM), **3** (9.98 µM) and CDDP (47.39 µM). For the MCF-7 cells, the order of decreasing cytotoxicity, where the activity of complex **3** was the highest, were complex **3** (9.84 µM), **4** (10.75 µM), **6** (11.13 µM), **5** (11.41 µM) and CDDP (20.72 µM). Overall, these complexes significantly induced malignant cell death to a higher extent than CDDP based on the high IC_{50} concentrations observed. The IC_{50} concentrations of the silver(I) complexes are in most instances either lower or comparable to those found in the literature. For example, lipophilic bidentate pyridyl phosphine silver(I) complexes showed to have varying IC_{50} concentrations ranging from a low 0.54 µM to high 100 µM in a range of CDDP-resistant and non-resistant ovarian cancer cell lines (Liu *et al*., 2008). In contrast, more soluble Cu(I), Ag(I) and Au(I) phosphine complexes were less toxic to HCT-15 colorectal adenocarcinoma cells with a majority of IC_{50} concentrations exceeding 9 µM (Santini *et al*., 2011). Silver(I) complexes with the formulae $[Ag(tptp)_2(salH)]$, $[Ag(tptp)_2(p\text{-}Hbza)]$ and $[Ag(tmtp)_2(salH)]$, IC_{50} concentrations in MCF-7 and HeLa cells ranged from 1.7 µM to 5.9 µM and 2.6 µM to 16.6 µM respectively (Banti *et al*., 2015). Similar silver(I) complexes were studied by Poyraz and co-workers (2011) and showed to be highly toxic to leiomyosarcoma cancer cells (LMS) and MCF-7 cells. Silver(I) tris(*p*-tolyl) phosphine complexes induced malignant cell death in LMS cells with IC_{50} concentrations ranging from 2.9 µM to 40.3 µM (Kyros *et al*., 2010). Ferreira *et al*. (2015) studied the effect of four silver(I) thiocyanate complexes with varying phosphine ligands at 1:2 ratios in MCF-7 cells. These complexes were highly toxic to these breast cancer cells with IC_{50} concentrations ranging from 3 µM to 3.59 µM.

The cytotoxicity of the complexes was further compared to identify which complex, taking into account the silver(I) salt, the phosphine ligand and the metal to ligand ratio, was more effective in inducing cell death in the malignant cells. When comparing the toxicities of the different silver(I) complexes, it seems that complexes **1** and **2**, with a metal to ligand ratio of 1:2, are more active in the SNO cells than the 1:3 complexes, with IC_{50} concentrations of ±3.5 µM (Figure 2.1, Table 2.3). Ferreira *et al*. (2015) studied the anticancer activity of complex **1** in MCF-7 breast cancer cells. The IC_{50} concentration was 3.0 µM, similar to the concentration found in our study, which could indicate that this complex has a broad range of cancer specificity. In addition, the silver salt, the phosphine ligand and cell subtype influenced the degree of toxicity in the malignant cells. Complexes **3** and **4** both contain an $AgNO_3$ as their salt, but they have different ligands. Interestingly, complex **3**, containing the tris(4-chlorophenyl)phosphine ligand, displayed similar toxicity profiles in each dependent cell line. Complex **4**, containing the tri(*p*-tolyl) phosphine ligand was more cytotoxic to

the SNO cells (IC_{50} = 8.31 µM) than the MCF-7 cells (IC_{50} = 10.75 µM). When comparing the effect of the silver salt (complexes **4**-**6**) different toxicity profiles were observed in both malignant cell lines. The AgBr complex was the most effective in the SNO cells (6.91 µM vs 7.61 µM vs 8.31 µM), followed by the AgSCN and the $AgNO_3$ complexes. In contrast, the $AgNO_3$ complex was the most effective in the MCF-7 cells (10.75 µM vs 11.13 µM vs 11.41 µM) followed by the AgSCN and the AgBr complexes. Overall, the MCF-7 cells seem to be more resistant to the silver(I) treatments than the SNO cells.

Complexes **1**-**6** were further tested for their *in vitro* anticancer activity by using assays that focus on different cellular aspects, but in turn, evaluate the viability of the cells. A similar trend in cancer cell viability was observed for these complexes for the various assays (Figure 2.2-2.5, Table 2.4). Of all these assays, the CellTiter-Glo® assay is of most interest. All the complexes significantly decreased the levels of ATP in the malignant cells (Figure 2.4). It is believed that silver(I) complexes target the mitochondria (Chen, 1988; Berners-Price *et al*., 1995; Ross *et al*., 2005) therefore lowering the production of ATP. Studies that were done in a yeast model, *Saccharomyces cerevisiae*, revealed that a silver(I) nitrate based phosphine complex targeted the mitochondria through the electron transport chain (Berners-Price *et al*., 1995). The alamarBlue® assay (Figure 2.4) is also a mitochondrial-based assay that measures the viability based on a functional electron transport chain. The lipophilicity including the charge of the complex might also be a major contributing factor for mitochondrial targeting, but will be addressed later in more detail (Section 2.4.5).

CDDP is currently used to treat oesophageal and breast cancer. In addition, previous studies found that CDDP in combination with other chemotherapeutic drugs, enhance the therapeutic effect (Ilson *et al*., 1999; Tepper *et al*., 2008; Eckstein, 2011), hence it's lower toxicity when used alone.

When comparing the results of the complexes **1**-**6** to that of CDDP, we can conclude that the silver(I) phosphine complexes under study are better candidates to target oesophageal and breast malignancies due to their high toxicities observed at lower concentrations.

2.4.2 Defining the mode of cell death induced in the malignant cells

Zeiss (2003) explained that the cell's ability to undergo apoptosis or necrosis depend on the cell death stimuli sensed, the type of tissue, the stage of development of the tissue and lastly the physiological milieu. Apoptosis is described as a controlled, energy-dependent process affecting individual or masses of cells (Zeiss, 2003; Bayir and Kagan, 2008). Apoptosis is characterised by nuclear and cytoplasmic condensation, DNA fragmentation, plasma membrane blebbing and

apoptotic body formation (Kerr *et al*., 1972; Kerr *et al*., 1994; Elmore, 2007). In contrast, necrosis is regarded as extensive swelling of cytoplasmic content (formation of vacuoles), DNA degradation, plasma membrane rupturing, organelle breakdown followed by the release of intracellular content (Kerr *et al*., 1994; Elmore, 2007; Kroemer *et al*., 2009). It was always believed that necrosis was an unregulated event, but the involvement of signal transduction pathways has been described, questioning this pathway (Festjens *et al*., 2006; Kroemer *et al*., 2009; Van Herreweghe *et al*., 2010; Galluzzi *et al*., 2012). Apoptosis is the preferred method for cancer cell targeting based on the absence of the inflammatory response which is present during necrosis (Festjens *et al*., 2006). Different studies can be performed to identify specific morphological and biochemical markers of apoptosis. In this study, we report the changes in the morphological features, the cell cycle distribution, PS externalization and the activity of apoptotic executioners. Apoptotic activation has been reported in other studies using related silver(I) thiocyanate (Ferreira *et al*., 2015; Human *et al*., 2015, Potgieter *et al*., 2015; Potgieter *et al*., 2016) or distant (Poyraz *et al*., 2011; Kriel and Coates, 2012; Kyros *et al*., 2014) silver(I) phosphine complexes.

Morphological features of apoptosis

Morphological features that include cellular rounding, plasma membrane blebbing and the presence of apoptotic bodies were observed in the SNO cells treated with the silver(I) complexes and CDDP (Figure 2.6A). These features are characteristic of apoptotic cell death as described previously (Kerr *et al*., 1972; Kerr *et al*., 1994). Although the MCF-7 cells appear to be more viable, comparable morphological features were observed as in the SNO cells (Figure 2.6B). Similar morphological features have been observed in SNO cells after being treated with a range of silver(I) thiocyanate complexes for 24 hrs (Human *et al*., 2015; Potgieter *et al*., 2015; Potgieter *et al*., 2016). MCF-7 cells treated for 48 hrs with a range of anti-inflammatory silver(I) phosphine complexes morphology resembled that of CDDP based on cellular rounding and shrinkage observed (Banti *et al*., 2016). Moreover, nuclear changes that involve DNA fragmentation and chromatin condensation were monitored using a Hoechst-33258 stain. Irregular staining of both the silver(I) and CDDP treated SNO (Figure 2.7) and MCF-7 (Figure 2.8) cells were observed. A gold(I) complex, [Au(xant)(PEt_3)], caused chromatin condensation and DNA fragmentation in human ovarian adenocarcinoma cells as visualized with a similar Hoechst and DAPI stain (Gandin *et al*., 2010). Auranofin and other gold(I) analogues cause an increase in apoptotic nuclei of human leukaemia Jurkat-T cells although some cells appeared to be necrotic (Rigobello *et al*., 2008). Even though silver(I) phosphine complexes were shown to interact with DNA (Kyros *et al*., 2014; Yilmaz *et al*., 2014), this study, to our knowledge is the first to report that nuclear condensation and DNA fragmentation occurs after

exposure to silver(I) phosphine complexes. CDDP is known to target the DNA of malignant cells, thereby inhibiting replication, followed by cell death (Lee *et al*., 2002; Rafique *et al*., 2010). Although it seems that the silver(I) complexes under study rather induce apoptosis than necrosis, it is difficult to distinguish morphological changes associated with these forms of cell death (Kerr *et al*., 1972). Thus, it is important to employ two or more biochemical assays to minimize uncertainty.

Cell cycle analysis

One of the hallmarks of cancer described by Hanahan and Weinberg (2011) is the ability to proliferate uncontrollably owing to the loss of the control in the cell cycle checkpoints. These checkpoints are responsible for evaluating the genetic quality of the cell and when the defect is detected, the cell cycle will arrest until it is resolved or if not, apoptosis is induced (Medema and Macůrek, 2012). The activation of these checkpoints forms part of an intricate network that involves the control of other checkpoints, DNA repair mechanisms, transcriptional regulation and apoptosis (Bartek and Lukas, 2007). The checkpoints can either be p53-dependent or -independent. The former is believed to be involved in *in vitro* systems where elevated levels of p53, because of DNA damage or stress signals, cause the cell cycle to arrest in the G1- or G2-phases and the latter in *in vivo* systems (Jackson *et al*., 2011). In most cancers, these checkpoints have defects mainly due to mutations occurring in the *p53* gene especially in the G1-phase (Harris, 1996; Muller and Vousden, 2013). The cancers are therefore more dependent on the S- and G2-phase checkpoints to prevent cell death. In contrast, non-cancerous cells depended more on the G1-phase checkpoint than the S- and G2-phases (Dai and Grant, 2010; Ma *et al*., 2011). The S- and G2-phases have therefore been considered as targets for cancer therapy. Cell cycle analysis can furthermore be used to detect DNA damage occurring in the late stages of apoptosis and is quantified in the histogram as the Sub-G1 phase.

Banti *et al*. (2016) studied the anticancer effect of nimesulide anti-inflammatory silver(I) complexes either containing a triphenylphosphine, tri(*p*-tolyl) phosphine, tripehylarsine or a triphenylantimony ligand on breast cancer cells. These complexes suppressed DNA replication and caused cell cycle arrest during the S-phase. In addition, another complex containing a tri(o-tolyl) phosphine moiety caused cell cycle arrest during the G2/M-phase. CDDP caused cell cycle arrest in both S- and G2/M-phases, which depends on the concentration of the drug used (Kroemer *et al*., 2007). In another study, the cellular population decreased in the S-phase and increased in the G2/M-phase of the MCF-7 cells after 24 hrs of treatment with the silver(I) thiocyanate complexes (Ferreira *et al*., 2015). In both these studies, a significant increase in the apoptotic Sub-G1 population was observed in the

breast cancer cells after treatment with the silver(I) complexes and CDDP (Ferreira *et al*., 2015; Banti *et al*., 2016). This coincides with the effect of the majority of silver(I) complexes studied herein. The cell population of the SNO and MCF-7 cells, after being treated with complexes **3**-**6**, caused cell cycle arrest in the G2/M-phase and an accumulation of cells in the Sub-G1 apoptotic phase (Figure 2.9 and 2.10). In addition, cell cycle arrest during the S-phase was also observed in the SNO cells. Complex **1** and **2** on the other hand, decreased the population of SNO cells in all three cellular phases, but cellular accumulation was seen in the Sub-G1 phase. A similar pattern was observed for CDDP in both cell lines (Figure 2.9H and 2.10F) and could be attributed to the high toxicity observed.

Phosphatidylserine (PS) externalization

To further investigate the involvement of apoptotic cell death, in the malignant cell lines, flow cytometry was performed to identify PS externalization. PS externalization is an early and prominent event that can be used as a marker for apoptosis (Martin *et al*., 1995a). Macrophages identify the exposed PS sites on the apoptotic cell followed by elimination *via* phagocytosis (Fadok *et al*., 1992; Fadok *et al*., 2000). PS externalization using related silver(I) complexes have been reported in MCF-7 breast cancer cells (Ferreira *et al*., 2015) and SNO oesophageal cancer cells (Human *et al*., 2015). Silver(I) phosphine complexes containing a mixture of triphenylphosphine and aspirin-based ligands has shown to increase PS externalization in LMS in a dose-dependent manner (Poyraz *et al*., 2011). PS externalization was also observed in a different study using LMS cells (Kyros *et al*., 2010). Gold(I) phosphine complexes have shown to induce apoptosis in leukaemia (Rigobello *et al*., 2008), melanoma (Caruso *et al*., 2007) and malignant breast cells (Rackham *et al*., 2007). Similar to the findings in the literature, complexes **1**-**6** (where applicable) caused PS externalization in both malignant cell lines (Figure 2.11 and 2.12).

Caspases-3/7

Both the ligand- and mitochondrial-mediated pathways are connected downstream by means of executioner caspases. When these caspases are activated further cleavage of proteins take place resulting in the biochemical markers of apoptosis (Riedl and Shi, 2004). Upon caspase-3 activation, caspase-3 activates ICAD forming CAD that results in chromosomal degradation and DNA fragmentation (Sakahira *et al*., 1998). Caspase-7 has similar substrate specificities than caspase-3 and is therefore regarded as a "backup" executioner molecule for downstream activities when caspase-3 is absent (Denault and Salvesen, 2002). Increased activity of caspase-3 or -7 has been reported in malignant cells treated with silver(I) (Li *et al*., 2014; Kaplan *et al*., 2015) and gold(I) complexes (Rackham *et al*., 2007; Rigobello *et al.,* 2008; Gandin *et al*., 2010).

Agreeing with these findings, all six complexes increased the activity of caspase-3/7 in the SNO cells with complex **1** and **5** causing the highest fold change (Figure 2.13A). MCF-7 cells have a functional 47 base-pair deletion within exon 3 of the *casp-3* gene and therefore lack caspase-3 activity. Thus, DNA fragmentation should be absent in this cell line (Jänicke *et al*., 1998). This was not the case in this study. Complexes **3**-**6** caused an increase in nuclear condensation and DNA fragmentation of the MCF-7 cells (Figure 2.8) and are accompanied by a more than a 3-fold increase in caspase-7 activity (Figure 2.13B). A study done by Mc Gee *et al*. (2002) showed that caspase-3 activity is not essential for DNA fragmentation in MCF-7 cells. In fact, caspase-7 activity could mediate the specific hallmark in response to other chemotherapeutic drugs. MCF-7 cells treated with an anticancer antibiotic, neocarzinostatin, caused an increase in caspase-7 activity and DNA fragmentation (Liang *et al*., 2001). The study of Ferreira *et al*. (2015) implied that caspase-7 activity increased in MCF-7 cells after being treated for 24 hrs with various silver(I) phosphine complexes. To determine whether these cell lines function in a caspase-dependent or -independent manner, the cells were exposed to a caspase inhibitor, Z-VAD-FMK, 1 h prior to treatment (Figure 2.13). Both these cell lines appear to function in a caspase-dependent manner based on the abrogated activity of caspase-3/7 in the presence of the inhibitor.

In general, the MCF-7 cell line was more resistant to the anticancer activity of the silver(I) phosphine complexes than the SNO cell line. This was particularly evident in the high IC_{50} concentrations observed (Table 2.3), minimal morphological alterations (Figure 2.6) and low levels of PS externalization (Figure 2.12). Nevertheless, significant levels of caspase-7 activity were detected (Figure 2.13B), but were less when compared to the SNO cells (Figure 2.13A). The more resistant nature of MCF-7 cells can be attributed to the absence of functional caspase-3 protein. It has been shown that MCF-7 cells reconstituted with caspase-3 are sensitized to chemotherapeutic drugs, doxorubicin and etoposide (Yang *et al*., 2001). Unusually high activity of caspase (specifically caspase-3, -7 and -6) activity, PARP cleavage and DNA fragmentation was detected in MCF-7 transfected cells compared to non-transfected cells. Malignant cells can become resistant to chemotherapeutic agents through drug inactivation, alteration of the drug targets, reduced drug accumulation, repair of damaged DNA in the cancer cell, inhibition of cell death, metastatic properties and lastly cancer cell heterogeneity (Reviewed by Housman *et al*., 2014).

2.4.3 Selectivity of complexes in non-malignant cells

Anticancer drugs, such as CDDP and oxaliplatin, have shown to significantly induce cytotoxicity in malignant cells. However, many of these drugs cause severe side effects mainly because of their inability to differentiate between malignant and non-malignant cells (Monti *et al*., 2005). The side

effects of CDDP include nausea, vomiting, nephrotoxicity and the loss of sensation in the extremities which rather is a consequence of non-specificity of the platinum complex (Lippert, 1999; Hannon, 2007). It is, therefore, important, albeit challenging to develop drugs with a high selectivity for malignant cells.

In order to study the selectivity of the lipophilic silver(I) complexes, two non-malignant human cell lines, HDF-a and HEK293, were exposed to the same conditions as to that of the malignant cells. When the alamarBlue® and morphological results are considered, all the complexes were more selectively toxic to either the malignant SNO or MCF-7 cells or both when compared to the HDF-a cells (Figure 2.4, 2.6, 2.14 and 2.15). Complexes **3**, **4** and **6** showed to be more toxic to the HEK293 cells than the HDF-a cells and might imply nephrotoxicity. Complex **2**, the cyanide containing complex, was less selective by being toxic to both malignant and non-malignant cell lines. Nevertheless, this complex can be used as a positive control for metal phosphine complexes, rather than CDDP, based on their similar apoptotic profiles observed (Figure 2.6, 2.7, 2.9 and 2.11). The reference complex, CDDP, was less selective than the complexes studied by causing a significant decrease in the viability of HDF-a cells. In contrast, CDDP was less toxic to the HEK293 cells. Featherstone *et al*. (1991) reported that CDDP, including carboplatin and another related platinum complex, JM9, were cytotoxic in human skin cells at 4 µM, 10 µM and 15 µM respectively.

The complex lipophilic character appears to be involved in the cancer cell selectivity of metal-based drugs. The heart and liver, contain large amounts of functional mitochondria to produce sufficient ATP. If these vital organs are damaged, cell death can be triggered and it could lead to unwanted side effects. This was the case for the anticancer gold(I) complex, $[Au(dppe)_2]^+$, that was discontinued after liver toxicity was observed (Berners-Price *et al*., 1986; Rush *et al*., 1987; Hoke *et al*., 1988). Other studies that included lipophilic silver(I) phosphine-based complexes were less potent to HDF-a (Ferreira *et al*., 2015) and MRC-5 (normal human fetal lung fibroblast) cells (Kyros *et al*., 2010; Poyraz *et al*., 2011; Banti *et al*., 2016). A hydrophilic/lipophilic balance should be maintained for the metal complex to ensure improved selectivity. For example, Kriel and Coates (2012) studied the effect of complexes containing a hydrazine-bridged diphosphine ligand in MCF-7 cells. The complex with altered lipophilicity was more potent to the malignant breast cells than non-malignant breast cells. Similarly, bidentate pyridyl phosphine gold(I) and silver(I) complexes showed the ability to selectively target a range of CDDP-resistant cancer cell lines, rather than non-malignant rat hepatocytes. Their targeting ability depended on the lipophilic character. Complexes that were predominantly lipophilic selectivity decreased and vice versa (Liu *et al*., 2008). In another study,

hydrophilic groups were incorporated into the ethane bridge of dppe to form a 2,3-bis(diphenylphosphino)maleic acid (dpmaa) (Berners-Price *et al*., 2005). When attached to Au(I) a more water soluble complex was formed than the dppe counterpart. This complex was evaluated in eight different cell lines revealing no cytotoxic activity in six of them (IC_{50} value of >200 µM). In the other two malignant MCF-7 (IC_{50} value = 91 µM) and HeLa (IC_{50} value = 160 µM) cell lines, little activity was observed. Even though ^{31}P NMR studies indicate that the 1:2 adduct was stable in the presence of 5% fetal calf serum, their lack of toxicity was attributed to the low cellular uptake of the hydrophilic complex.

2.4.4 Ligand toxicity on malignant and non-malignant cells

The choice of the ligand is of importance when a metal-based drug is designed. The thermodynamic stability, kinetic stability, solubility and lipophilic character should be considered during the design process (Porchia *et al*., 2013). The toxicity of the metal complex is regulated by the chemical properties, especially the phosphorous atom, found in the phosphine moiety (Nath *et al*., 2011).

The cytotoxicity of the uncoordinated ligands **L1**-**L4** were determined in both the malignant and non-malignant cell lines (Figure 2.16 and 2.17). All four ligands were less cytotoxic to the malignant SNO and MCF-7 cells including the non-malignant HDF-a and HEK293 cells when compared to the functional complexes (Figure 2.4, 2.6, 2.14 and 2.15). In accordance with Poyraz and co-workers (2011), the triphenylphosphine and o–hydroxy-benzoic acid (o-HbzaH) ligands used in their study were less toxic than the intact silver(I) phosphine complex. Furthermore, free tertiary phosphines have shown to be toxic to P815 mastocytoma tumour cells, although to a lesser extent than their gold(I), silver(I) and copper(I) phosphine counterparts (McKeage *et al*., 1998). In a study reported by Liu *et al*. (2008), the cytotoxicity of the uncomplexed 2- and 4-pyridyl phosphine ligands were similar to the functional silver(I) and gold(I) bidentate phosphine complexes in a range of ovarian malignancies. Phosphine ligands displayed a low potency *in vitro* when compared to their silver(I) thiocyanate complexes (Ferreira *et al*., 2015; Human *et al*., 2015). Moreover, triaryl phosphine ligands were less cytotoxic to malignant MCF-7, MDA-MB-231 and non-malignant MRC-5 cells based on higher IC_{50} concentrations observed in the ligands (Banti *et al*., 2016).

Due to the less soluble nature of the uncoordinated salts in non-toxic solvents, their cell toxicity could not be determined. Based on the above observations it is evident that the substituted silver(I) phosphine complex was required to induce significant cancer cell death. Therefore, this would imply that the structural change, produced by coordinating the salt to the respective ligand, was responsible for the inferred biological function and, therefore, the observed response.

2.4.5 Activation of the mitochondrial-mediated cell death pathway in treated malignant cells

It appears that mitochondrial targeting *via* the intrinsic cell death pathway is the predominant route of apoptosis induction for silver(I) complexes (Kriel and Coates, 2012; Ferreira *et al*., 2015), although activation of the extrinsic pathway has been reported (Ferreira *et al*., 2015). The mitochondria play a key role in the regulation of cell death pathways, like apoptosis, which make them an attractive target for cancer therapeutics. It was first predicted by Otto Warburg that cancerous cells can be killed by targeting their mitochondria without harming non-cancerous cells (Warburg, 1925; Warburg *et al*., 1927). Cancer cells are highly dependent (more than non-cancerous cells) on the glycolytic pathway where glucose uptake is increased to produce sufficient ATP for proliferation and survival (Warburg, 1925; Warburg *et al*., 1927; Liberti and Locasale, 2016). Furthermore, the lipophilicity and charge could also be a major contributing factor for mitochondrial targeting. It is believed that lipophilic cations are transported over the lipid bilayer of the mitochondria. Internally the mitochondrial inner membrane contains a large negative potential that attracts positively charged metal complexes. When the complexes bind, they are transported into the mitochondria, where they accumulate and favour cell death (Chen, 1988; Ross *et al*., 2005).

Mitochondrial membrane potential ($\Delta\psi_m$)

Au(I) (Caruso *et al*., 2007; Rackham *et al*., 2007) and Ag(I) phosphine complexes (Kriel and Coates, 2012) have shown to act on the mitochondria by decreasing the $\Delta\psi_m$. Bis(di(4-methoxyphenyl) phosphino)-1,2-diethylhydrazinedi(gold(I)chloride) and Bis(bis(di(4-methoxyphenyl) phosphino)dimethylhydrazine) silver(I) nitrate complexes decreased the $\Delta\psi_m$ in PBMCs after being treated for 1 h (Kriel and Coates, 2012). In another study, a lipophilic $[Au(d_2pypp)_2]Cl$ complex caused an increased uptake of JC-1 within the malignant MDA-MB-468 cells which resulted in a decreased $\Delta\psi_m$. Interestingly, the uptake of JC-1 by non-malignant HMEC cells was less (Rackham *et al*., 2007) thus confirming the fact that malignant cells are more metabolically active as suggested by Warburg. This was true from the findings in both the SNO and MCF-7 cells where the $\Delta\psi_m$ decreased significantly when treated with complex **1** and **5** (Figure 2.18) or **3** (Figure 2.19) respectively. Although complexes **1** and **5** are structurally different (1:2 vs 1:3) it seems that they follow the same route of cell death. It is not yet clear whether the silver(I) complexes under study become cationic in solution, but based on their lipophilic nature and decreased ATP activity (Figure 2.4) they could act as mitochondrial disrupters, hence activating the mitochondrial-mediated cell death pathway of apoptosis. According to Berners-Price *et al*. (1999) a hydrophilic 4-pyridyl analogue of $[Au(dppe)_2]^+$, has the ability to retain its cationic nature which under a physiological pH protonates at least one 4-pyridyl nitrogen thereby increasing the overall positive charge, resulting in improved malignant

toxicity. In contrast, the carboxyl group of another complex, gold(I) dpmaa, can be deprotonated causing the complex to become more anionic causing a decrease in malignant activity (Berners-Price *et al*., 2005).

Cytochrome c

When the mitochondria are targeted and the membrane potential is disrupted, MPT pores are formed which releases various pro-apoptotic proteins into the cytosol (Kroemer *et al*., 1998; Loeffler and Kroemer, 2000; Saelens *et al*., 2004; Elmore, 2007; Kroemer *et al*., 2007). Once such protein is cytochrome *c*, which is released in the earlier stages of cell death, initiating downstream caspase assembly and activation (Zimmermann *et al*., 2001). To further implicate the activation of the intrinsic pathway, the mitochondrial integrity and cytochrome *c* translocation was monitored with fluorescent microscopy (Figure 2.20-2.23). When the SNO and MCF-7 cells were treated with their respective silver(I) treatments, the mitochondrial integrity decreased and cytochrome *c* translocation was evident especially in the IC_{50} treated cells. This phenomenon was more distinct in the SNO cells than the MCF-7 cells. To the best of our knowledge, this is the first study to implicate cytochrome *c* in silver(I) phosphine induced apoptosis. They might function in a similar manner than their gold(I) counterparts. Marzano *et al*. (2007), observed that a gold(I) complex, auranofin, stimulated the release of cytochrome *c* in both CDDP-resistant and CDDP-sensitive ovarian cancer cells. CDDP was ineffective in the more resistant ovarian subtype, but the resistance was overcome when treated in the combination with auranofin. In another study, human leukaemia Jurkat-T cells exposed to auranofin induced the release of cytochrome *c* (Rigobello *et al*., 2008). A gold(I) chloro-triphenylphosphine based complex not only initiated the release of cytochrome *c* in melanoma cells, but also the release of pro-apoptotic factors like Smac/DIABLO and inhibited the anti-apoptotic factors c-IAP1, XIAP and survivin (Caruso *et al*., 2007). Regarding CDDP, cytochrome *c* translocation was observed in both cell lines (Figure 2.20-2.23) and is required for CDDP-induced apoptosis (Blanc *et al*., 2000; Zhu *et al*., 2015). In one study, CDDP was able to disrupt the mitochondria of a head and neck squamous cell carcinoma by forming adducts in the mitochondrial DNA, which led to cytochrome *c* release and ultimately apoptosis (Yang *et al*., 2006).

Reactive oxygen specie/s (ROS)

Under normal conditions, a balance exists between the level of antioxidants and ROS in healthy cells which is known as ROS homeostasis. Generally, the levels of these two components are low in healthy tissue when compared to malignant tumours and cellular changes won't cause a drastic effect. In malignant cells, however, the ROS homeostatic balance can be altered and changes in

these two components are more severe based on the presence of larger quantities of ROS. For example, when malignant cells are treated with antioxidants or when ROS activity is lowered, the cells will lose their ability to grow causing cytostasis and senescence. In contrast, when the levels of antioxidants are lowered and the ROS activity drastically increases, cancer-specific oxidative cell death could occur (Sulivan and Chandel, 2014). ROS activity has been linked to facilitate the critical MPT-dependent release of cytochrome *c* due to the upstream activity of Bax and Bak that facilitates the formation of the MPT pore (Ott *et al*., 2002). It is believed that metals cause DNA damage through the generation of free radicals (Florea and Büsselberg, 2011).

Rigibello *et al*. (2008) assessed the production of ROS in cells using a spectrofluorometric assay. The oxidizing species increased in the Jurkat-T cells after being treated with the gold(I) complexes. Auranofin was the most potent treatment by causing the highest accumulation of ROS in the cells. Auranofin, antimycin and a combination thereof caused an increase in the levels of ROS in human ovarian cancer cells (Marzano *et al*., 2007). In this study, CDDP (55 µM) was able to stimulate the formation of ROS, but to a lower extent to the other treatments. A ruthenium complex, KP1019, caused a dose-dependent increase of H_2O_2 in HT-29 colorectal cancer cells (Kapitza *et al*., 2005). This was accompanied by a decrease in the $\Delta\psi_m$. Although the authors found that DNA damage was not sufficient to kill the cells, they predicted that the H_2O_2 interacted with the unsaturated fatty acids in the mitochondrial membranes preferably, which then contributed to the mitochondrial membrane depolarization. In the current study, the basal ROS levels of both malignant cell lines were similar, but when treated with the silver(I) complexes and CDDP the levels differed significantly (Figure 2.24). High ROS activity was only detected in the SNO cells and was minimal in the MCF-7 cells. Increased ROS activity has been reported in MCF-7 cells after being treated with platinum-based complexes (Gęgotek *et al*., 2014). This is surprising because the mitochondrial damage is usually associated with ROS generation (Frantz and Wipf, 2010) and mitochondrial depolarization was observed in the MCF-7 cells treated with complex **3** (Figure 2.19). These findings might indicate that the toxicity of complex **3** in these cells might be independent of ROS. Low ROS levels have been reported in MCF-7 cells treated with 50 µM CDDP for 24 hrs (Osbild *et al*., 2006). These authors believed that the decreased cellular stress observed in the cells was mainly due to the increased activity of the antioxidant, glutathione, thus making these cells more resistant to treatment. Therefore, future studies will include the quantification of glutathione to determine if, the observed resistance, especially in the MCF-7 cells are due to high levels of is this antioxidant.

Caspase-9

In most cell lines, procaspase-9 is located in the mitochondria and is released into the cytosol once this organelle is permeabilized (Krajewski *et al*., 1999; Susin *et al*., 1999). The procaspase-9 is activated upon association with Apaf-1 and ATP to form the functional apoptosome complex that further activates apoptotic proteolytic activities (Li *et al*., 1997; Rodriguez and Lazebnik, 1999). The silver(I) complexes in this study induced the cleavage of caspase-9 into its active form (Figure 2.25). Taken together, the ATP levels (Figure 2.4), mitochondrial targeting (Figure 2.18 and 2.19) and cytochrome *c* release (Figure 2.20-2.23) seem to indicate that these complexes do in fact target the mitochondrial-mediated apoptotic pathway. Caruso *et al*. (2007) reported that a chlorotriphenylphosphine-1,3-bis(diphenylphosphino)propanegold(I) complex increased the catalytic activity of caspase-9 and caspase-3, as assessed by the hydrolysis of specific fluorogenic substrates in melanoma cells. The activity of caspase-9 was enhanced when the gold(I) complex was used at a concentration of 10 µM. Although most silver(I) complexes target the intrinsic cell death pathway, the involvement of the extrinsic cell death pathway should not be completely ignored. In breast cancer cells, the silver(I) complexes' toxic effect caused an increase of caspase-9 both on an enzymatic and protein level (Ferreira *et al*., 2015). These authors also observed a slight increase in caspase-8 activity, which plays a central role in the ligand-mediated cell death pathway. Increasing concentrations of CDDP resulted in increased caspase-9 activity in certain human head and neck squamous cell carcinoma cell lines (Kuwahara *et al*., 2000).

Although caspase-9 cleavage was observed in the MCF-7 cells treated with complex **3**, the same activation appeared to be absent in the MCF-7 cells treated with CDDP (Figure 2.25B). The same observation was made in the Ferreira *et al*. (2015) study where the same breast cell line was used. Blanc *et al*. (2000) explained that caspase-3 is a central regulator of caspase-9 and caspase-8 activities, especially in CDDP-dependent cell death. As mentioned previously, MCF-7 cells are deficient in caspase-3 activity and mostly depend on other caspases to activate apoptosis. It was further revealed that enriching MCF-7 cells with caspase-3 enhanced the release of cytochrome *c*, nuclear and DNA fragmentation in CDDP-induced cell death (Blanc *et al*., 2000). A non-platinum aquatin(IV) chloride benzyltin complex increased the activity of caspase-9 and caspase-7 in a dose- and time-dependent manner when MCF-7 cells were used (Fani *et al*., 2016). Their results also revealed that the mitochondria are targeted based on the up-regulation of Bax and Bad, down-regulation of Bcl-2 and the release of cytochrome *c*. This might explain that the caspase-9 activity observed in the MCF-7 cells are silver-dependent rather than CDDP-dependent.

Poly (ADP-ribose) polymerase (PARP)

PARP is another marker of apoptosis and is responsible for catalysing, in the presence of NAD, the poly(ADP-ribosylation) of numerous nuclear proteins contributing to DNA repair (Berger, 1985; Berger and Petzold, 1985; Boulares *et al*., 1999; Javle and Curtin, 2011). When PARP is cleaved, it cannot respond to DNA strand breaks due to the separation of the active site and the DNA-binding domain which is required for the completion of apoptosis (Kaufmann *et al*., 1993; Oliver *et al*., 1999). PARP cleavage was evident in both the cell lines treated with respective silver(I) complexes but was more distinct after exposure to CDDP (Figure 2.25). PARP cleavage has been reported in the CDDP-treated cervical (Saggioro *et al*., 2007), lung (Germain *et al*., 2010) and breast cancer cells (Yde and Issinger, 2006). Gold(III) dithiocarbamate, induced apoptotic cell death in breast cancer cells as confirmed by morphological features of apoptosis and PARP cleavage (Milacic and Dou, 2009). Moreover, PARP cleavage was observed in HepG2 liver cancer cells treated with silver(I) heterocyclic complexes when a concentration of 40 µM or higher was used (Thati *et al*., 2009). Although caspase-3 is described as the main regulator of PARP cleavage (Boulares *et al*., 1999), the involvement of caspase-7 has also been reported (Walsh *et al*., 2008).

2.4.6 The activity of stress-inducible Hsp70

Hsp70 family members act as molecular chaperones that help synthesize, refold and protect proteins from being degraded. These proteins have been implicated in the development of tolerance to heat and other drugs (Hightower, 1991). Under normal conditions, Hsp70 proteins are found in low abundance, but once protein damage signals, in the form of heat shock, oxidative stress, hypoxia or heavy metals are sensed, the levels are increased (Voellmy, 1996; Morimoto, 1998; Sherman and Gabai, 2015). The gene expression of Hsp70 is regulated by the heat shock transcription factor (HSF) that interacts with Hsp70 in the cytoplasm, once damage signals are sensed, forming HSF homotrimer complex. The complex then migrates to the nucleus where it interacts with the heat shock element (HSE) in the promoter region of the *Hsp* gene thus favouring transcription (Murata *et al*., 1999; Aït-Aïssa *et al*., 2000; Urani *et al*., 2001). Increased transcriptional and translational activation of Hsp70 and nuclear accumulation is a key characteristic of the heat shock or stress response (Knowlton and Salifity, 1996; Kiang and Tsoskos, 1998).

Because metals have shown to increase the levels of stress proteins, the effect of silver(I) complexes on the stress-inducible Hsp70 expression was monitored (Figure 2.26). Hsp70 was expressed in both the malignant SNO and MCF-7 cells treated with the silver(I) complexes but was more distinct in the latter than the former cell line. The overexpression of Hsp70 in most cancers is indicative of the phenotypic property that contributes to chemotherapeutic resistance and inhibition of programmed

cell death (Jäättelä, 1999; Garrido e*t al*., 2006b). According to Niu *et al*. (2006), high levels of Hsp70 appears to decrease DNA damage when malignant cells are exposed to DNA damaging agents. It is, therefore, possible that the silver(I) complexes could, in fact, target the DNA. A significant increase of Hsp70 activity has been reported in the tissue of breast cancer patients and various breast cancer cells that include the MCF-7 cell line (Jagadish *et al*., 2016). Similarly, the expression of inducible Hsp70 has shown to enhance MCF-7 cells proliferation and protect these cells against hypothermic conditions. It is, therefore, possible that Hsp70 protects the MCF-7 cells against the toxicity of the silver(I) phosphine complex. Heat shock proteins, *e.g.* Hsp70 and Hsp90, have been linked to the mediated regulation and transport of steroid receptors (DeFranco *et al*., 1998; Echeverria and Picard, 2010). Work done by Hurd *et al*. (2000) illustrated that when Hsp70 is transfected in MCF-7 cells, a significant increase in estrogen-stimulated activity is observed. Although high levels of Hsp70 have been reported in oesophageal cancer (Kawanishi *et al*., 1999) the significant expression of the inducible Hsp70 observed might play a more protective role in the MCF-7 than in the SNO cell line. It is a well-established fact that Hsp70 inhibits apoptosis, providing resistance to induced cell death (Mosser *et al*., 2000). This could also explain the increased resistance of the MCF-7 cells to the silver(I) complexes studied herein when compared to the SNO cells. CDDP's main cell death target involves DNA interaction, but surprisingly no Hsp70 was expressed in either CDDPn-treated cell lines.

2.4.7 Identifying possible drug targets for treatment

Although several silver(I) complexes showed improved cytotoxicity in different malignant cell lines compared to CDDP (Poyraz *et al*., 2011; Yilmaz *et al*., 2014; Banti *et al*., 2014; Human *et al*., 2015; Ferreira *et al*., 2015; Potgieter *et al*., 2015; Banti *et al*., 2016; Potgieter *et al*., 2016), the presence of specific biomarkers should be considered in developing an effective chemotherapeutic drug.

Thioredoxin reductase (TrxR)

Mammalian TrxR is a seleno-dependent homodimeric flavoprotein that forms part of the pyridine nucleotide-disulfide oxidoreductase family that also includes glutathione reductase, trypanothione reductase, alkyl hydroperoxide reductase, lipoamide dehydrogenase and mercuric reductase (Argyrou and Blanchard, 2004; Lu and Homgren, 2014). The mammalian TrxR exists in three forms either located in the cytosol (TrxR1), the mitochondria (TrxR2) and the testis, testis-specific thioredoxin glutathione reductase (TGR) (Lu and Holmgren, 2009; Lu and Holmgren, 2014). The thioredoxin reductase system comprises of thioredoxin (Trx), TrxR and an NADPH binding domain that together supplies electrons to most of the enzymes (Holmgren, 1985; Lu and Holmgren, 2014). This system is responsible for regulating critical biological processes that include DNA synthesis, cell

growth, ROS scavenging, cell signalling and p53 functioning in apoptosis (Yoo *et al*., 2006; Arnér, 2009; Gandin and Fernandes, 2015). Trx acts as an anti-apoptotic molecule by interacting with apoptosis signal-regulating kinase 1 (Ask-1), preventing its activation, and in turn downstream apoptotic activities (Saitoh *et al*., 1998). Overexpression of TrxR, and in some cases the Trx substrate, has been reported in a majority of cancers (Soini *et al*., 2001; Yoo *et al*., 2006; Cadenas *et al*., 2010; Shabani *et al*., 2014). It is believed that the reason for TrxR accumulation in malignant cells is owing to increased ROS and hypoxic environments of the malignancy (Shabani *et al*., 2014). The overexpression has also been linked to cancer prognosis and increased malignant proliferation (Yoo *et al*., 2006; Cadenas *et al*., 2010) which suggest that TrxR or Trx can be used as a target for cancer therapy.

Compelling evidence suggests that TrxR activity is especially vulnerable for inhibition by anticancer metal or semimetal species like auranofin, CDDP, silver(I) derivatives, NAMI-A, motexafin gadolinium and organotellurium *etc.* (Reviewed by Gandin and Fernandes, 2015). TrxR activity decreased in both malignant cells lines after being treated with the silver(I) complexes and CDDP (Figure 2.27). These results are in accordance with other studies in the literature that focus on Trx inhibition. For example, research by Zhang *et al*. (2016) focussed on the ability of carboplatin, CDDP and auranofin to inhibit Trx1 activity in mice with hepatocellular carcinoma containing increased serum levels of TrxR. Carboplatin was the least active causing no alteration in the TrxR activity. This was followed by CDDP that inhibited the activity between 1 to 2 hrs after the drug was injected. Auranofin was the most effective by rapidly inhibiting TrxR activity post-administration. In another study, auranofin was more effective than CDDP to inhibit the TrxR activity in CDDP-resistant and CDDP-sensitive ovarian cancer cell lines with minimal effect on the related selenoenzyme, glutathione reductase (Marzano *et al*., 2007). Gold(I) and gold(III) complexes have shown to be more effective TrxR inhibitors than CDDP and other metal species (Rigobello *et al*., 2004). In addition, gold(III) complexes were also able to inhibit the activity of glutathione peroxidase and glutathione reductase. Gold complexes are generally accepted as TrxR inhibitors but little evidence exists that silver(I) phosphine specifically target TrxR activity in a similar manner. However, antimitochondrial activity was observed for the silver(I) phosphine complexes (Figure 2.18 and 2.19) thus suggesting the interaction of redox enzymes that should aid in mitochondrial stability. In one study, Au(I) and Ag(I) $[M(PTA)_4]PF_6$ complexes inhibited TrxR activity at nanomolar concentrations (Santini *et al*., 2011). Inhibition of LOX, an anti-apoptotic enzyme, has also been reported for silver(I) complexes and was able to activate apoptosis (Poyraz *et al*., 2011; Banti *et al*., 2016). Even though presently, the mechanistic

role of TrxR inhibition is not clear, our studies validate that TrxR can be a potential target for cancer therapy.

Cytochrome P450 (CYP450)

The CYP450 enzymes play a major role in the biotransformation of drugs and xenobiotics. Their principal function is to aid in the detoxification of many drugs and the synthesis of steroids and bile acids (Martinez *et al*., 2008). *CYP450* forms part of an entire gene complex that encodes different isoforms which all contribute to the functional entity (Mishra *et al*., 2010). Of the gene family, the CYP1B1 isoform is of most interest and is has also been involved in metabolizing xenobiotics (Shimada *et al*., 1997). CYP1B1 is highly expressed in hormone-induced cancers like that of the breast, ovarian, prostate (McFayden *et al*., 2001; Gajjar *et al*., 2012) and endometrial (Saini *et al*., 2009), as well as oesophagus, skin, brain, colon, small intestine and uterine malignancies (Murray *et al*., 1997). CYP1B1 plays a role in the metabolism of estrogen where 17β-estradiol is converted to a carcinogenic 4-hydroxyestradiol which then forms adducts in the DNA. This is followed by metabolic redox reactions that produce ROS and damage cellular DNA other molecules (Liehr *et al*., 1986; Yager and Leihr, 1996; Zhu and Conney, 1998; Husbeck and Powis, 2002). Interestingly, Trx1 has shown to regulate the expression of CYP1B1 and is needed for the induction of CYP1B1 and CYP1A1 in breast cancer cells exposed to dioxin (Husbeck and Powis, 2002).

Limited amounts of CYP1B1 have been detected in non-malignant cells both at mRNA and protein level (Murray *et al*., 1997; Gajjar *et al*., 2012). In a study done by Saini *et al*. (2009), CYP1B1 activity was up-regulated in endometrial carcinoma leading to cell survival. When these cells were depleted of CYP1B1, the cell growth decreased and apoptosis was induced based on the expression of TRIAL. Therefore, targeting CYP1B1 might be beneficial during cancer therapy. CYP1B1 activity was minimally altered in this study (Figure 2.28) thus likely excluding it as a therapeutic target for silver(I) complexes. Although treatment with complex **5** caused a significant increase in CYP1B1 activity in the SNO cells, the activity was marginally similar than complex **1**.

2.4.8 Batch testing of silver(I) complex specificity in 16 malignant cell lines

The use of *in vitro* cancer models play a very important role in the early stages of drug screening and development before *in vivo* models or clinical trials can be considered. Three silver(I) complexes were selected and toxicity screened in 16 malignant cell lines that either originated from the same or different regions of the body. Overall, the cytotoxic profiles of these complexes including CDDP differed between the related and unrelated cell lines (Table 2.5).

Silver(I) phosphine complexes have shown to be active in oesophageal (Human *et al*., 2015; Potgieter *et al*., 2015; Potgieter *et al*., 2016), breast (Poyraz *et al*., 2011; Ferreira *et al*., 2015; Banti *et al*., 2014; Banti *et al*., 2015), cervical (Banti *et al*., 2014; Banti *et al*., 2015), ovarian (McKeage *et al*., 1998; Berners-Price *et al*., 2005; Liu *et al*., 2008; Banti *et al*., 2014), kidney (Banti *et al*., 2014), lung (Banti *et al*., 2014), skin (Pettinari *et al*., 2011) and blood malignancies (Zartilas *et al*., 2009). Aryl and anti-inflammatory silver(I) complexes were more cytotoxic to MCF-7 breast cancer cells than in HeLa cervical cancer cells after being exposed for 24 hrs (Banti *et al*., 2015). Pettinari *et al*. (2011) studied the toxicity of [Ag(Tpms)], [Ag(Tpms)(PPh_3)], [Ag(Tpms)(PCy_3)], [Ag(PTA)(MeOH)][BF_4] and [Ag(Tpms)(PTA)] complexes on a A375 melanoma cell line. The PCy_3 and PPh_3 containing complexes displayed the lowest IC_{50} values whereas the PTA methyl containing complex had the highest IC_{50} value of all the treatments. An iodine-containing complex, {[AgI(MBZT)($TPP)_2$]} displayed similar toxicity profiles in MCF-7 (breast, ER-positive), MDA-MB-231 (breast, ER-negative), A549 (lung), OAW-42 (ovarian) and Caki-1 (renal) cancer cell lines (Banti *et al*., 2014). Similarly, four silver(I) *p*-substituted diphenyl phosphine (Potgieter *et al*., 2016) and triphenyl phosphine complexes (Human *et al*., 2015) were equally toxic to an SNO oesophageal cancer cell line with viabilities of ±20%. In another study, a similar trend was observed in MCF-7 cells (Ferreira *et al*., 2015). Furthermore, tetrameric and monomeric tri(*p*-tolyl)-phosphine complexes were more cytotoxic to sarcoma cancer cells from rat than murine leukaemia and T lymphocyte cells (Zartilas *et al*., 2009). Lui *et al*. (2008) demonstrated that silver(I) complexes with bidentate pyridyl phosphines displayed different toxicity profiles in a range of CDDP-resistant ovarian cancer cells.

Based on the observations in literature and in this study, the cell line, silver(I) complex species, including the treatment conditions, should be considered which makes screening a very important step in identifying potential anticancer drugs. For the more resistant cell lines that include Ins-1, A549, Jurkat-T, PC3, HEPG2-C3A and MiaPaCa a longer treatment period or higher concentrations of the silver(I) complexes might be required to induce cell death if the non-malignant cells aren't significantly affected.

Cancer cell models are not only beneficial for drug screening but in some cases, they can help to identify possible drug targets. For example, both Caco2 and HT-29 cell lines are colorectal adenocarcinomas, but the toxicity profiles of complex **1**, **3**, **5** and CDDP differed between them (Table 2.5). The cytotoxic effect of complex **1**, **3** and CDDP is higher in the HT-29 cells when compared to the Caco2 cells. In contrast, complex **5** is more cytotoxic to the Caco2 cells than the HT-29 cells. Thus, these complexes could target different cellular moieties contributing to cell death.

Both HT-29 and Caco2 adenocarcinoma cell lines were established by Jorgen Fogh and originated from a female and male patient respectively (Fogh and Trempe, 1975; Rousset, 1986). In a study done by Peters and Roelofs (1992), Caco2 cells were more resistant to a chemotherapeutic drug Adriamycin, also known as Doxorubicin, than the HT-29 cells with IC_{50} concentrations being 525 µM and 19 µM respectively. Interestingly of all the enzymatic activities studied, glutathione S-transferase activity was significantly increased in the Caco2 rather than the HT-29 cells and could be the reason for its increased resistance observed. In a different study, higher levels of estrogen receptor-β (ER-β) was detected in Caco2, T84 and SW1116 colon cancer cells. The levels of ER-β was less in the HT-29 and SW48 colon cancer cells. Furthermore, four colon cancer cells (HT-29, Caco2, T-84 and SW1116) were negative for estrogen receptor-α (ER-α) which was abundantly found in MCF-7 cells (Campbell-Thompson, 2001). A similar observation was made by a different research group by using five human colon (HT-29, Colo320, Lovo, SW480 and HCT-116) and two breast (MCF-7 and T47D) cancer cell lines (Arai *et al*., 2000). RT-PCR analysis revealed that ER-α activity was only detected in the breast cancer cell lines and was absent in the colon cancer cell lines. In contrast, ER-β activity was detected in most of the colon derivatives with minimal or no activity in the HT-29 and breast cancer cells. Complex **5** was also the most effective treatment to induce cell death in the MeWo melanoma cell line of which the ER-β receptor is rather expressed than the ER-α receptor (Marzagalli *et al*., 2015). Based on these observations, complex **5** could act on cancer cells by targeting and inhibiting the activity of the ER-β receptor.

Estrogen is an important hormone that is required for the development of mammary glands and reproductive organs. It can also influence the pathological processes of hormone-dependent cancers (Pearce and Jordan, 2004). The activities of estrogen are regulated by the estrogen receptors, ER-α and ER-β. These receptors work together to regulate downstream transcriptional processes activating genes in different tissues (Chen *et al*., 2008; Lee *et al*., 2012a). According to Chen *et al*. (2008) estrogen, including its receptors, contribute to the development of different tumours and can be classified into four groups. The first group include cancers of the breast and reproductive system that include the ovaries, cervical and endometrial malignancies. The second group are endocrine gland cancers that include adrenocortical, ovarian, pancreatic, prostate and thyroid malignancies. The third and fourth group involve cancers of the digestive system (colorectal, oesophageal, liver and pancreatic cancers) and lungs respectively. Although most of these tumours express both ER ligands, high activity of the ER-α receptor enhances the proliferation of the cancers in the first two groups but prevents the growth of the cancers in the third and fourth group and vice versa.

It is interesting to note that complex **1** displayed the highest toxicity (±30% viability) in human HeLa cervical adenocarcinoma, PC3 prostate adenocarcinoma, MCF-7 breast adenocarcinoma, HEPG2 hepatocellular carcinoma and rat PC12 pheochromocytoma cell lines. These cell lines are scattered between the four groups as described by Chen *et al*. (2008). MCF-7 cells are ER-positive breast cancer cells that express high levels of ER-α (Martin *et al*., 2003). Tamoxifen is commonly used to treat ER-positive malignancies. Its effect is enhanced when used in combination with other drugs like Avemar (Marcsek *et al*., 2004). This combination causes a significant decrease of ER-α activity and an increased apoptotic effect in the MCF-7 cells. PC12 cells, that is produced from the adrenal medulla of the rat, is mostly used to study neurodegenerative diseases (Greene and Tischler, 1976). CDDP that was encapsulated by apoferritin displayed toxic activity to PC12 cells (Yang *et al*., 2007). The PC3, HeLa and HepG2 are estrogen-negative cells that are characterized as being more metastatic with a malignant phenotype leading to a poorer prognosis (Kelly *et al*., 2014; Cunningham and You, 2015). In addition, complex **1** decreased the viability of liver carcinoma cell line, HepG2, with ±70%, but for the HepG2 derivative, C3A, 20% more cells were viable. HepG2 is an ER-negative cell line that does not express these receptors (Kelly *et al*., 2014). This suggests that the anticancer effect of complex **1** could be regulated by multiple mechanisms which explain the broad cancer cell specificity. From the data obtained in this study, it is uncertain to predict the molecular target/s of complex **3**. Based on the toxicity of both complex **1** and **3** in the HT-29 cells it appears that complex **3** might target one of the alternative targets (except ER-α) of complex **1** due to similar viabilities observed.

Even though the studies regarding the mechanism or drug targets are limited, by characterizing malignant cell models one could elucidate the mechanism of both resistant and non-resistant subtypes of a drug and further develop drugs that are more targeted for the malignancy (Ferreira *et al*., 2013).

2.4.9 Possible cell death pathway

Based on the above-discussed results one can confirm that silver(I) complexes selectively target malignant cells. When focussing on the anticancer activity of complex **1**, **3** and **5** it is evident that these novel species activate the mitochondrial-mediated cell death pathway in the following manner (Figure 2.29). The DNA of the cells are targeted and mutations in *p53* could cause up-regulation of its activity, although not shown in this study, stimulating the activation of the pro-apoptotic Bax protein. The generation of ROS, mainly due to DNA damage, causes the disruption of the mitochondrial membrane and decreased levels of ATP. Although ROS activity was only observed for complex **1** and **5**, the mitochondrial disruption was still observed by complex **3**. Cytochrome *c* along

with inactive caspase-9 is released from the damaged mitochondria and upon formation of the apoptosome complex, caspase-3/7 (in the SNO oesophageal cancer cells) and caspase-7 (in the MCF-7 breast cancer cells) activate downstream processes like PARP cleavage, PS externalisation, plasma membrane blebbing and apoptotic body formation that are causative signs of apoptosis. Furthermore, TrxR activity is inhibited by all three treatments and Hsp70 expressed only in the cells treated with complex **1** and **5**. In the MCF-7, the increased resistance observed after being exposed to the silver(I) complexes might be attributed to the deficiency of caspase-3 and the induction of Hsp70.

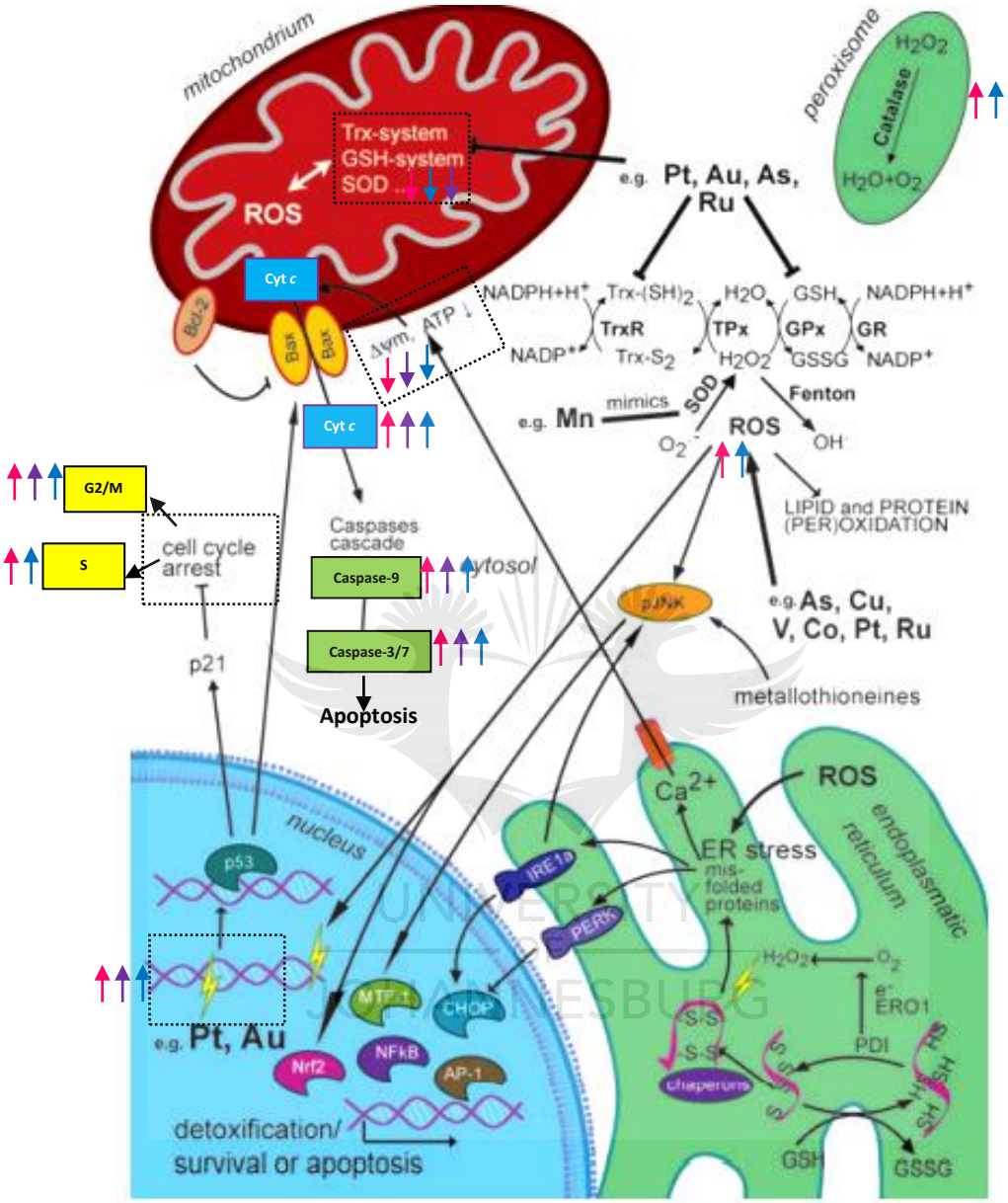

Figure 2.29: Modified illustration of the main interaction sites of metal-based drugs, including the possible apoptotic mechanism of the novel silver(I) phosphine complexes in the malignant cells. Biochemical changes identified are represented by arrows ↑ (increased activity) or ↓ (decreased activity) and is either colour coded pink (complex **1**), blue (complex **3**) or purple (complex **5**). The complexes caused cell cycle arrest and target the mitochondria followed by the activation of the downstream caspase cascade resulting in apoptosis (Adapted from Jungwirth *et al*., 2011).

CHAPTER 3: Changes in gene expression induced by complex 7

3.1 Preamble

Gene expression was monitored in SNO oesophageal cancer cells after being treated with an alternative silver(I) complex (complex **7**), which contains an AgCl salt coordinated with three tris(4-chlorophenyl)phosphine ligands. This complex was previously studied for its anticancer activity and was very effective in malignant SNO cells (Human, 2013; Appendix 1). Complex **7** was chosen for gene expression profiling based on its low cytotoxicity in non-malignant HDF-a fibroblast skin cells (Figure A1.1A) and apoptotic inducing capabilities in the malignant SNO cells (Figure A1.1B). Like the complexes studied in the previous chapter, complex **7** significantly ($P < 0.01$) increased the activity of caspase-9 rather than caspase-8 (Figure A1.1C) thus implying the activation of the mitochondrial-mediated cell death pathway. Furthermore, a significant ($P < 0.05$) increase in caspase-3/7 activity was also observed in the SNO cells (Figure A1.1C). In an attempt to identify the detailed mechanism and possible drug targets of complex **7** in the SNO cells, an RT^2 Profiler PCR array preloaded with 84 cancer-related genes and 12 controls (Table 3.1) were used. It should be noted that a concentration of 14 µM rather than 10 µM, as in the previous chapter, was used. The reason being, when complex **7** was synthesized it was assumed that two phosphine ligands were coordinated to the AgCl salt, therefore being a 1:2 complex. However, the elemental analysis revealed that complex **7** orientates three phosphine ligands, rather than two, thus the concentration was recalculated to 14 µM.

3.2 Materials and Methods

In Appendix 2, a list of the manufacturers of all reagents, materials, apparatus and software used are listed.

3.2.1 Synthesis of the silver(I) phosphine complex

3.2.1.1 Complex characterization

The silver(I) complex (complex **7**) in this chapter was synthesized in-house and characterized with assistance from Dr. Rehana Malgas-Enus in the Department of Chemistry at the University of Johannesburg. Melting points were recorded on a Stuart Scientific Melting Point apparatus SMP10, and are uncorrected. FT-IR spectra were recorded on a Bruker Tensor 27 FT-IR spectrometer, using a PIKE miracle Gate ATR accessory. NMR spectra were measured and recorded on a Bruker Ultrashield Avance III 400 MHz spectrometer. The ^{1}H NMR, ^{13}C NMR and ^{31}P NMR spectra were obtained in DMSO-d_6 at 400 MHz for ^{1}H nuclei, 75 MHz for ^{13}C nuclei and 161 MHz for ^{31}P nuclei. All chemical shifts were reported in ppm using residual H or C signals in $CDCl_3$ as internal references. All ^{31}P NMR

chemical shifts were referenced against H_3PO_4 as an external standard. Elemental analysis was performed at the Department of Chemistry at Rhodes University by Dr. Edith Antunes using a Thermo Flash 2000 series CHNS/O, Organic Elemental Analyser. The data output of the methods described above is indicated below.

3.2.1.2 Synthesis of [AgCl {($pClC_6H_4$)$_3$P}$_3$] (Complex 7)

AgCl salt (0.033 g, 0.2864 mmole) was added to a solution of tris(4-chlorophenyl)phosphine (0.25 g, 0.6859 mmole) (**L3**) in acetonitrile (50 ml). The solution was heated under reflux overnight. The hot solution was filtered and evaporated to ±10 ml. Thereafter, the solution was left to crystallize at room temperature for 24 hrs. The supernatant was discarded and the crystals washed twice with 2 ml acetonitrile followed by drying under a vacuum. **Yield:** 55%. **Melting Point:** 210-211 °C. **IR (v/cm^{-1}):** 3049w (C-Hs), 2531w, 2360.53w, 2169w,2038w, 1641w, 1572m, 1560m,1475s, 1385s, 1298w, 1177w, 1093s, 1078s, 1011s, 948w, 842w, 810s, 757w, 738s, 712w, 704m, 629, 589w, 553. **^{1}H-NMR (400 MHz, $CDCl_3$) δ ppm:** 7.57 - 7.52 (m, 10 H), 7.45 (d, J=7.8 Hz, 10 H), 7.23 - 7.30 (m, 31 H), 7.17 ppm (d, J=7.5 Hz, 30 H). **^{13}C-NMR (100 MHz, $CDCl_3$) δ ppm:** 136.59 (s, d4) 134.89 (d1, J=18 Hz) 131.78 (d2, J=11.0 Hz) 129.15 (d3, J=7 Hz). **^{31}P NMR (161 MHz, $CDCl_3$) δ ppm:** 1.71 (s). **Elemental analysis:** $C_{55}H_{36}AgCl_{10}P_3$: Calculated: C, 52.3%; H, 2.93%. Found: C, 52.32%; H, 2.91%.

3.2.2 Complex preparation

A stock solution of complex **7** was prepared in cell culture graded DMSO (vehicle). The complex was heated at 70 °C for 1 h to ensure complete solubilization. The stock was kept in the dark at 4 °C and heated at 70 °C for 30 min prior to treatment.

3.2.3 Cell line

An adherent SNO oesophageal cell line (ATCC, cat no. CCL-185) was used for array analysis.

3.2.4 Cell culturing

It should be noted that all reagents used for culturing, sub-culturing and plating purposes were pre-warmed at 37 °C before use. Cells were cultured in DMEM (13.55 g/L) with additional $NaHCO_3$ (3.7 g/L). The media was supplemented with 10% (v/v) FBS, 1.6% (v/v) Penicillin/Streptomycin/Fungizone and 0.4% (v/v) gentamicin sulphate. The cells were incubated in 75 cm^2 culture flasks for 48 hrs at 37 °C in an HERAcell 150i incubator under a 5% CO_2 humidified atmosphere.

3.2.5 Sub-culturing of SNO cells

The cells were washed once with 10 ml HBSS (9.5 g/L) with additional $NaHCO_3$ (0.35 g/L). Four millilitres of 1% (v/v) trypsin were added to the flasks and incubated for ±10 min. After incubation, the flasks were agitated to loosen the cells from the surface. This was followed by the addition of 6 ml supplemented DMEM to deactivate the trypsin. The cells were collected with a Heraeus Biofuge Promo R centrifuge at 779 x*g* for 4 min. The pellet was resuspended in 1 ml supplemented DMEM and split (volume dependent on stocks growth rate; if high, 250 µl was used or 500 µl, when low) into two 75 cm^2 culture flasks containing 20 ml supplemented DMEM. The cells were passaged every 48 hrs, as described above. For experimental purposes, cells at a passage number of 3 were used.

3.2.6 Cell counting with Trypan blue dye exclusion assay

Cells were removed and collected as described in section 3.2.5. The pellet was resuspended in 4 ml supplemented DMEM to improve counting efficiency. The cell suspension was vortexed and 10 µl added to 10 µl of Trypan blue dye (1:1). Ten microliters of the stained suspension were added to a TC10™ System-Counting slide. The cellular viability was determined using the TC10™ Automated Cell Counter. For experimental purposes, only cells at a viability of 94% or higher were used.

3.2.7 Cell plating and treatment

Cells were removed, collected and counted as described in section 3.2.5 and 3.2.6. A total of 6 x 10^5 cells (2 x 10^5 cells/ml) were seeded in 3.5 cm culture dishes to a final volume of 3 ml. The cells were then incubated for 24 hrs prior to treatment. Used media was removed and a final volume of 1 ml DMEM containing the treatment was added to the 3.5 cm culture plates. The cells were either treated with the vehicle control (1% (v/v) DMSO) or 14 µM of complex **7**. The DMSO concentration did not exceed 1% throughout the study and the treatment period commenced for 12 hrs.

3.2.8 Cell removal and collection

Cells were plated and treated as described in section 3.2.6 and 3.2.7. Used media was removed and kept separately. The cells were washed once with 1 ml HBSS followed by the addition of 300 µl 1% (v/v) trypsin. Thereafter, the cells were incubated for ±5 min and removed from cell culture plates by gently squirting them of the surface. Once all the cells were removed 1 ml supplemented DMEM was added for deactivation purposes. The cells were collected with an Eppendorf® 5415R bench top centrifuge at 400 x*g* for 4 min. The pellet was resuspended in the used media before experimental analysis. The cells were further pelleted by means of centrifugation at 400 x*g* for 4 min.

3.2.9 RNA isolation

Cells were collected as described in section 3.2.8. The total RNA was isolated from the cells using a Quick-RNA™ MiniPrep kit according to manufacturer's instructions. The pellet was resuspended in RNA Lysis buffer and vortexed to ensure complete lysis. The lysed solution was then centrifuged for 1 min at 10 000 x*g*. The supernatant was transferred into a Spin-Away™ filter in a Collection tube and centrifuged for 1 min at 10 000 x*g* to remove most of the genomic DNA (gDNA). Absolute (95-100%) ethanol (300 µl) was added to the eluent and vortexed. This mixture was then transferred to a Zymo-Spin™ IIICG Column in a Collection tube and centrifuged for 30 secs at 16 000 x*g*. The eluent was discarded and the samples washed with 400 µl RNA Wash Buffer by means of centrifugation for 30 secs at 16 000 x*g*. The remaining DNA was removed from the samples by adding a DNase I reaction mixture (1U/µl DNase, 10 x DNase I Reaction Buffer, DNase/RNase-free water and RNA Wash Buffer). The sample in the column was then incubated for 15 min at room temperature. After incubation 400 µl RNA Prep Buffer was added followed by centrifugation. The eluent was discarded and the samples were washed twice with RNA Wash Buffer for 2 min at 16 000 x*g*. The RNA was eluted from the column into clean tubes by adding 30 µl DNase/RNase-Free water (pre-warmed to 95 °C to increase RNA elution) and centrifuging for 30 secs at 16 000 x*g*.

3.2.10 RNA quantification and integrity

The total RNA was quantified using a NanoDrop ND-1000 Spectrophotometer. Only samples with an A_{260}: A_{230} ratio of greater than 1.7 and an A_{260}: A_{280} ratio of 1.8-2.0 were used. The concentration at A_{260} did exceed the recommended 40 µg/ml. The integrity of the total RNA was determined by means of agarose gel electrophoresis. On a 1% (w/v) agarose gel, 1 µg of total RNA along with 6 x Orange loading dye was loaded. The agarose gel contained Gelstar® Nucleic Acid Gel Stain (10 000 x) and was run using a 1 x TBE Buffer (Tris, boric acid and EDTA) for ±30 min at 100 V. A Fermentas Ultra-Low range DNA ladder was included as the molecular weight marker. The gel was visualized under UV light with an Image analyser with Quantity One® Software Version 4.6.1. This was done to identify the two distinctive 18S and 28S ribosomal bands which indicate intact non-degraded RNA. A total of four RNA samples each (1% DMSO and 14 µM complex **7**) were prepared and the best three (based on the above-mentioned criteria) were used for further analysis (see Appendix 1; Figure A1.2). The total RNA was used immediately for cDNA synthesis and not stored.

3.2.11 Synthesis of cDNA

The cDNA was synthesized using an RT^2 First Strand kit according to manufacturer's instructions. Briefly, 1 µg of the total RNA was incubated with a genomic DNA elimination mixture for 5 min at 42 °C and placed on ice immediately for 1 min. After all the genomic DNA was eliminated, 10 µl of the

reverse transcription mixture (5 x Buffer BC3, Control P2, RE3 Reverse Transcriptase mix and RNase-free water) were added to each sample and mixed gently. The samples were then incubated at 42 °C for 15 min, then stopped immediately by incubating for 5 min at 95 °C. A total of 91 µl RNase-free water was added to each sample and placed on ice. After the cDNA was synthesized, 1 µg was run on an 1% (w/v) agarose gel as described in section 3.2.10 (see Appendix 1; Figure A1.3).

3.2.12 Real-time PCR using RT^2 Profiler PCR array

To analyse the expression of various cancer-related genes a Human Cancer Pathway Finder RT^2 Profiler PCR array (PAHS-033A) along with RT^2 SYBR Green Mastermix was used. The arrays were preloaded with 96 primer sets that contain primer sets for 84 cancer-related genes, 5 housekeeping genes (HKG), 1 human genomic DNA control (HGDC), 3 reverse-transcription controls (RTC) and 3 positive PCR controls (PPC). The HKG included *beta-2-microglobulin* (*b2m*), *hypoxanthine phosphoribosyltransferase 1* (*hprt1*), *ribosomal protein L13a* (*rpl13a*), *glyceraldehyde-3-phosphate dehydrogenase* (*gapdh*) and *beta-actin* (*actb*) which was used for normalisation purposes. The HGDC detects the presence of any non-transcribed genomic DNA with high sensitivity. The RTC is a built-in reverse-transcriptase control that tests the efficacy of the RT^2 First Strand Kit responsible for synthesizing the cDNA. The PPC is an artificial DNA sequence that determines the efficacy of the polymerase chain reaction. All these controls determine the consistency between the replicate arrays. The 84 cancer-related genes can be divided into six groups that focus on different cellular functions. The groups include (1) cell cycle control and DNA damage repair, (2) apoptosis and cell senescence, (3) signal transduction molecules and transcription factors, (4) adhesion, (5) angiogenesis and (6) invasion and metastasis. All 96 genes that were analysed are represented in Table 3.1.

Table 3.1: Gene position, UniGene code, reference sequence, symbol, description and name of all 96 genes located on the Human Cancer Pathway Finder RT^2 PCR array.

Position	UniGene	RefSeq	Symbol	Description	Gene Name
A01	Hs.525622	NM_005163	**AKT1**	V-akt murine thymoma viral oncogene homolog 1	AKT, CWS6, PKB, PKB-ALPHA, PRKBA, RAC, RAC-ALPHA
A02	Hs.369675	NM_001146	**ANGPT1**	Angiopoietin 1	AGP1, AGPT, ANG1
A03	Hs.583870	NM_001147	**ANGPT2**	Angiopoietin 2	AGPT2, ANG2
A04	Hs.552567	NM_001160	**APAF1**	Apoptotic peptidase activating factor 1	APAF-1, CED4
A05	Hs.367437	NM_000051	**ATM**	Ataxia telangiectasia mutated	AT1, ATA, ATC, ATD, ATDC, ATE, TEL1, TELO1
A06	Hs.370254	NM_004322	**BAD**	BCL2-associated agonist of cell death	BBC2, BCL2L8
A07	Hs.624291	NM_004324	**BAX**	BCL2-associated X protein	BCL2L4
A08	Hs.150749	NM_000633	**BCL2**	B-cell CLL/lymphoma 2	Bcl-2, PPP1R50
A09	Hs.516966	NM_138578	**BCL2L1**	BCL2-like 1	BCL-XL, S, BCL2L, BCLX, BCLXL, BCLXS, Bcl-X, PPP1R52, bcl-xL, bcl-xS
A10	Hs.194143	NM_007294	**BRCA1**	Breast cancer 1, early onset	BRCAI, BRCC1, BROVCA1, IRIS, PNCA4, PPP1R53, PSCP, RNF53

A11	Hs.599762	NM_001228	**CASP8**	Caspase 8, apoptosis-related cysteine peptidase	ALPS2B, CAP4, Casp-8, FLICE, MACH, MCH5
A12	Hs.244723	NM_001238	**CCNE1**	Cyclin E1	CCNE
B01	Hs.437705	NM_001789	**CDC25A**	Cell division cycle 25 homolog A (S. pombe)	CDC25A2
B02	Hs.689624	NM_001798	**CDK2**	Cyclin-dependent kinase 2	p33(CDK2)
B03	Hs.95577	NM_000075	**CDK4**	Cyclin-dependent kinase 4	CMM3, PSK-J3
B04	Hs.732576	NM_000389	**CDKN1A**	Cyclin-dependent kinase inhibitor 1A (p21, Cip1)	CAP20, CDKN1, CIP1, MDA-6, P21, SDI1, WAF1, p21CIP1
B05	Hs.512599	NM_000077	**CDKN2A**	Cyclin-dependent kinase inhibitor 2A (melanoma, p16, inhibits CDK4)	ARF, CDK4I, CDKN2, CMM2, INK4, INK4A, MLM, MTS-1, MTS1, P14, P14ARF, P16, P16-INK4A, P16INK4, P16INK4A, P19, P19ARF, TP16
B06	Hs.731912	NM_003879	**CFLAR**	CASP8 and FADD-like apoptosis regulator	CASH, CASP8AP1, CLARP, Casper, FLAME, FLAME-1, FLAME1, FLIP, I-FLICE, MRIT, c-FLIP, c-FLIPL, c-FLIPR, c-FLIPS
B07	Hs.505297	NM_007194	**CHEK2**	CHK2 checkpoint homolog (S. pombe)	CDS1, CHK2, HuCds1, LFS2, PP1425, RAD53, hCds1
B08	Hs.517356	NM_030582	**COL18A1**	Collagen, type XVIII, alpha 1	KNO, KNO1, KS
B09	Hs.654393	NM_005225	**E2F1**	E2F transcription factor 1	E2F-1, RBAP1, RBBP3, RBP3
B10	Hs.446352	NM_004448	**ERBB2**	V-erb-b2 erythroblastic leukemia viral oncogene homolog 2, neuro/glioblastoma derived oncogene homolog (avian)	CD340, HER-2, HER-2, neu, HER2, MLN 19, NEU, NGL, TKR1
B11	Hs.644231	NM_005239	**ETS2**	V-Ets erythroblastosis virus E26 oncogene homolog 2 (avian)	ETS2IT1
B12	Hs.244139	NM_000043	**FAS**	Fas (TNF receptor superfamily, member 6)	ALPS1A, APO-1, APT1, CD95, FAS1, FASTM, TNFRSF6
C01	Hs.533683	NM_000141	**FGFR2**	Fibroblast growth factor receptor 2	BBDS, BEK, BFR-1, CD332, CEK3, CFD1, ECT1, JWS, K-SAM, KGFR, TK14, TK25
C02	Hs.25647	NM_005252	**FOS**	FBJ murine osteosarcoma viral oncogene homolog	AP-1, C-FOS, p55
C03	Hs.90708	NM_006144	**GZMA**	Granzyme A (granzyme 1, cytotoxic T-lymphocyte-associated serine esterase 3)	CTLA3, HFSP
C04	Hs.90753	NM_006410	**HTATIP2**	HIV-1 Tat interactive protein 2, 30kDa	CC3, SDR44U1, TIP30
C05	Hs.37026	NM_024013	**IFNA1**	Interferon, alpha 1	IFL, IFN, IFN-ALPHA, IFN-alphaD, IFNA13, IFNA@
C06	Hs.93177	NM_002176	**IFNB1**	Interferon, beta 1, fibroblast	IFB, IFF, IFNB
C07	Hs.160562	NM_000618	**IGF1**	Insulin-like growth factor 1 (somatomedin C)	IGF-I, IGF1A, IGFI
C08	Hs.624	NM_000584	**IL8**	Interleukin 8	CXCL8, GCP-1, GCP1, LECT, LUCT, LYNAP, MDNCF, MONAP, NAF, NAP-1, NAP1
C09	Hs.644352	NM_181501	**ITGA1**	Integrin, alpha 1	CD49a, VLA1
C10	Hs.482077	NM_002203	**ITGA2**	Integrin, alpha 2 (CD49B, alpha 2 subunit of VLA-2 receptor)	BR, CD49B, GPIa, HPA-5, VLA-2, VLAA2
C11	Hs.265829	NM_002204	**ITGA3**	Integrin, alpha 3 (antigen CD49C, alpha 3 subunit of VLA-3 receptor)	CD49C, GAP-B3, GAPB3, ILNEB, MSK18, VCA-2, VL3A, VLA3a
C12	Hs.440955	NM_000885	**ITGA4**	Integrin, alpha 4 (antigen CD49D, alpha 4 subunit of VLA-4 receptor)	CD49D, IA4
D01	Hs.436873	NM_002210	**ITGAV**	Integrin, alpha V (vitronectin receptor, alpha polypeptide, antigen CD51)	CD51, MSK8, VNRA, VTNR
D02	Hs.643813	NM_002211	**ITGB1**	Integrin, beta 1 (fibronectin receptor, beta polypeptide, antigen CD29 includes MDF2, MSK12)	CD29, FNRB, GPIIA, MDF2, MSK12, VLA-BETA, VLAB
D03	Hs.218040	NM_000212	**ITGB3**	Integrin, beta 3 (platelet glycoprotein IIIa, antigen CD61)	BDPLT16, BDPLT2, CD61, GP3A, GPIIIa, GT
D04	Hs.536663	NM_002213	**ITGB5**	Integrin, beta 5	-
D05	Hs.696684	NM_002228	**JUN**	Jun proto-oncogene	AP-1, AP1, c-Jun
D06	Hs.145442	NM_002755	**MAP2K1**	Mitogen-activated protein kinase kinase 1	CFC3, MAPKK1, MEK1, MKK1, PRKMK1
D07	Hs.599039	NM_006500	**MCAM**	Melanoma cell adhesion molecule	CD146, MUC18
D08	Hs.733536	NM_002392	**MDM2**	Mdm2 p53 binding protein homolog (mouse)	ACTFS, HDMX, hdm2
D09	Hs.132966	NM_000245	**MET**	Met proto-oncogene (hepatocyte growth factor receptor)	AUTS9, HGFR, RCCP2, c-Met
D10	Hs.83169	NM_002421	**MMP1**	Matrix metallopeptidase 1 (interstitial collagenase)	CLG, CLGN
D11	Hs.513617	NM_004530	**MMP2**	Matrix metallopeptidase 2 (gelatinase A, 72kDa gelatinase, 72kDa type IV collagenase)	CLG4, CLG4A, MMP-II, MONA, TBE-1
D12	Hs.297413	NM_004994	**MMP9**	Matrix metallopeptidase 9 (gelatinase B, 92kDa gelatinase, 92kDa type IV collagenase)	CLG4B, GELB, MANDP2, MMP-9
E01	Hs.525629	NM_004689	**MTA1**	Metastasis associated 1	-
E02	Hs.173043	NM_004739	**MTA2**	Metastasis associated 1 family, member 2	MTA1L1, PID
E03	Hs.336994	NM_014751	**MTSS1**	Metastasis suppressor 1	MIM, MIMA, MIMB
E04	Hs.202453	NM_002467	**MYC**	V-myc myelocytomatosis viral oncogene homolog (avian)	MRTL, MYCC, bHLHe39, c-Myc
E05	Hs.618430	NM_003998	**NFKB1**	Nuclear factor of kappa light polypeptide gene enhancer in B-cells 1	EBP-1, KBF1, NF-kB1, NF-kappa-B, NF-kappaB, NFKB-p105, NFKB-p50, NFkappaB, p105, p50

E06	Hs.81328	NM_020529	**NFKBIA**	Nuclear factor of kappa light polypeptide gene enhancer in B-cells inhibitor, alpha	IKBA, MAD-3, NFKBI
E07	Hs.463456	NM_000269	**NME1**	Non-metastatic cells 1, protein (NM23A) expressed in	AWD, GAAD, NB, NBS, NDKA, NDPK-A, NDPKA, NM23, NM23-H1
E08	Hs.9235	NM_005009	**NME4**	Non-metastatic cells 4, protein expressed in	NDPK-D, NM23H4, nm23-H4
E09	Hs.535898	NM_002607	**PDGFA**	Platelet-derived growth factor alpha polypeptide	PDGF-A, PDGF1
E10	Hs.1976	NM_002608	**PDGFB**	Platelet-derived growth factor beta polypeptide	IBGC5, PDGF-2, PDGF2, SIS, SSV, c-sis
E11	Hs.604502	NM_181504	**PIK3R1**	Phosphoinositide-3-kinase, regulatory subunit 1 (alpha)	AGM7, GRB1, p85, p85-ALPHA
E12	Hs.77274	NM_002658	**PLAU**	Plasminogen activator, urokinase	ATF, BDPLT5, QPD, UPA, URK, u-PA
F01	Hs.466871	NM_002659	**PLAUR**	Plasminogen activator, urokinase receptor	CD87, U-PAR, UPAR, URKR
F02	Hs.409965	NM_002687	**PNN**	Pinin, desmosome associated protein	DRS, DRSP, SDK3, memA
F03	Hs.159130	NM_002880	**RAF1**	V-raf-1 murine leukemia viral oncogene homolog 1	CRAF, NS5, Raf-1, c-Raf
F04	Hs.408528	NM_000321	**RB1**	Retinoblastoma 1	OSRC, RB, p105-Rb, pRb, pp110
F05	Hs.654444	NM_002961	**S100A4**	S100 calcium binding protein A4	18A2, 42A, CAPL, FSP1, MTS1, P9KA, PEL98
F06	Hs.55279	NM_002639	**SERPINB5**	Serpin peptidase inhibitor, clade B (ovalbumin), member 5	PI5, maspin
F07	Hs.713079	NM_000602	**SERPINE1**	Serpin peptidase inhibitor, clade E (nexin, plasminogen activator inhibitor type 1), member 1	PAI, PAI-1, PAI1, PLANH1
F08	Hs.349470	NM_003087	**SNCG**	Synuclein, gamma (breast cancer-specific protein 1)	BCSG1, SR
F09	Hs.371720	NM_003177	**SYK**	Spleen tyrosine kinase	p72-Syk
F10	Hs.89640	NM_000459	**TEK**	TEK tyrosine kinase, endothelial	CD202B, TIE-2, TIE2, VMCM, VMCM1
F11	Hs.492203	NM_198253	**TERT**	Telomerase reverse transcriptase	CMM9, DKCA2, DKCB4, EST2, PFBMFT1, TCS1, TP2, TRT, hEST2, hTRT
F12	Hs.645227	NM_000660	**TGFB1**	Transforming growth factor, beta 1	CED, DPD1, LAP, TGFB, TGFbeta
G01	Hs.494622	NM_004612	**TGFBR1**	Transforming growth factor, beta receptor 1	AAT5, ACVRLK4, ALK-5, ALK5, LDS1A, LDS2A, MSSE, SKR4, TGFR-1
G02	Hs.164226	NM_003246	**THBS1**	Thrombospondin 1	THBS, THBS-1, TSP, TSP-1, TSP1
G03	Hs.522632	NM_003254	**TIMP1**	TIMP metallopeptidase inhibitor 1	CLGI, EPA, EPO, HCI, TIMP
G04	Hs.644633	NM_000362	**TIMP3**	TIMP metallopeptidase inhibitor 3	HSMRK222, K222, K222TA2, SFD
G05	Hs.241570	NM_000594	**TNF**	Tumour necrosis factor	DIF, TNF-alpha, TNFA, TNFSF2
G06	Hs.521456	NM_003842	**TNFRSF10B**	Tumour necrosis factor receptor superfamily, member 10b	CD262, DR5, KILLER, KILLER, DR5, TRAIL-R2, TRAILR2, TRICK2, TRICK2A, TRICK2B, TRICKB, ZTNFR9
G07	Hs.279594	NM_001065	**TNFRSF1A**	Tumour necrosis factor receptor superfamily, member 1A	CD120a, FPF, MS5, TBP1, TNF-R, TNF-R-I, TNF-R55, TNFAR, TNFR1, TNFR1-d2, TNFR55, TNFR60, p55, p55-R, p60
G08	Hs.462529	NM_003790	**TNFRSF25**	Tumour necrosis factor receptor superfamily, member 25	APO-3, DDR3, DR3, LARD, TNFRSF12, TR3, TRAMP, WSL-1, WSL-LR
G09	Hs.740601	NM_000546	**TP53**	Tumour protein p53	BCC7, LFS1, P53, TRP53
G10	Hs.644998	NM_000474	**TWIST1**	Twist homolog 1 (Drosophila)	ACS3, BPES2, BPES3, CRS1, SCS, TWIST, bHLHa38
G11	Hs.563491	NM_017549	**EPDR1**	Ependymin related protein 1 (zebrafish)	EPDR, MERP-1, MERP1, UCC1
G12	Hs.73793	NM_003376	**VEGFA**	Vascular endothelial growth factor A	MVCD1, VEGF, VPF
H01	Hs.534255	NM_004048	**B2M**	Beta-2-microglobulin	-
H02	Hs.412707	NM_000194	**HPRT1**	Hypoxanthine phosphoribosyltransferase 1	HGPRT, HPRT
H03	Hs.523185	NM_012423	**RPL13A**	Ribosomal protein L13a	L13A, TSTA1
H04	Hs.544577	NM_002046	**GAPDH**	Glyceraldehyde-3-phosphate dehydrogenase	G3PD, GAPD
H05	Hs.520640	NM_001101	**ACTB**	Actin, beta	BRWS1, PS1TP5BP1
H06	N/A	SA_00105	**HGDC**	Human Genomic DNA Contamination	HIGX1A
H07	N/A	SA_00104	**RTC**	Reverse Transcription Control	RTC
H08	N/A	SA_00104	**RTC**	Reverse Transcription Control	RTC
H09	N/A	SA_00104	**RTC**	Reverse Transcription Control	RTC
H10	N/A	SA_00103	**PPC**	Positive PCR Control	PPC
H11	N/A	SA_00103	**PPC**	Positive PCR Control	PPC
H12	N/A	SA_00103	**PPC**	Positive PCR Control	PPC

The PCR component mixture was prepared in a 15 ml conical tube consisting of 1350 µl 2 x RT^2 SYBR Green Mastermix and 102 µl synthesized cDNA. The contents were transferred to a clean reservoir. The RT^2 Profiler Array was carefully opened and 25 µl of the mixture was transferred into each well. The plate was sealed with optically thin 8-cap strips and covered in aluminium foil. These plates were kept in the freezer until the next day. On the day of analysis, the plates were removed and allowed to thaw for a few minutes at room temperature followed by centrifugation for 1 min at 1000 x*g* with a Heraeus Biofuge Promo R centrifuge. Real-time PCR analysis was then performed using a Biorad CFX96™ Connect Real-Time system with the following conditions; initial denaturing and activation of HotStart DNA *Taq* Polymerase (1 cycle for 10 min), further denaturation at 95 °C (40 cycles for 15 sec) followed by annealing and extension at 60 °C (for 1 min). The ramp rate of 1 °C/sec was used between the 95 °C and 60 °C steps. Melting curve analyses were performed after each run to determine PCR specificity using increments of 1 °C. The threshold cycle (C_T) value for the PCR products was calculated with the BioRad CFX Connect manager 3.0 software.

3.2.13 Data analysis for arrays

Data analysis was done either with the RT^2 Profiler Array Data Analysis version 3.5 software (available from SABiosciences) or the Profiler Array Excel template using the $\Delta\Delta C_T$ method. All C_T values were collected and those equal to or above 35 cycles were regarded as not detected. Data was not normalised against the housekeeping genes provided because the average values across the vehicle control and treated samples were more than 1. Therefore, zero was used in the $\Delta\Delta C_T$ equations and data was normalised based on the consistency input of RNA quantity and quality (Quellhorst *et al*., 2006). The fold change of each gene is determined by the vehicle control and treated sample as $2^{(-\Delta\Delta CT)}$. When the fold-change is higher than 1 it can be regarded as the fold up-regulation and when below 1 (the negative inverse) the fold down-regulation of the gene. Changes in gene expression were regarded as significant with a *P*-value of 0.05 or less.

3.3 Results

3.3.1 Structure of silver(I) phosphine complex

A silver(I) phosphine complex was synthesized (section 3.2.1) and characterized in-house by using a variety of techniques at the Department of Chemistry. The techniques included melting point analysis, IR, ^{1}H NMR, ^{13}C NMR, ^{31}P NMR and elemental analysis. The characterization was routinely done for this batch to ensure that a pure complex was used for biochemical studies. The silver(I) phosphine complex in this chapter, has a general formula of AgXLn (X = silver salt in its oxidized state, L = tertiary phosphine, n = ligand ratio of 1:3) (Meijboom *et al*., 2009). Complex **7** was synthesized by adding an AgCl salt to tris(4-chlorophenyl)phosphine (**L3**) in a ratio of 1:3 (Figure 3.1).

Complex **7** orientates in a tetrahedral geometry (similar to complexes **3**-**6** in section 2). The AgCl core is surrounded by three phosphine ligands. The complex is lipophilic in nature due to its low solubility in hydrophilic solutions.

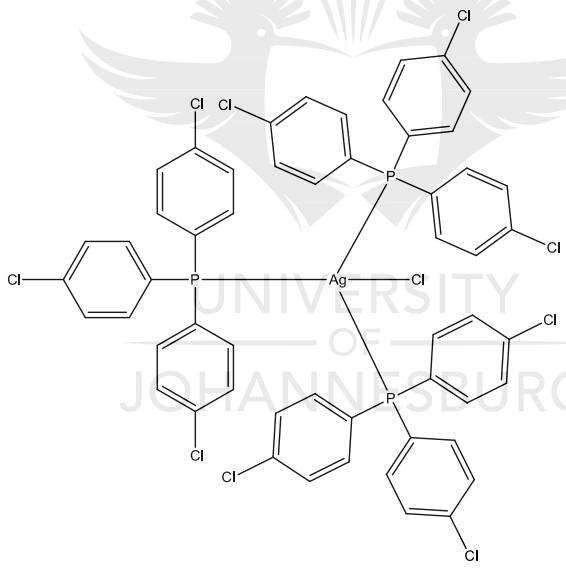

Figure 3.1: Chemical structure of complex **7**

3.3.2 Expression levels of various cancer-related genes

It was previously shown that complex **7** induced apoptotic cell death in SNO cells (Appendix 1; Figure A1.1). RT^{2} Profiler PCR arrays were done to gain further insight into the mechanism and possibly the drug target/s of the silver(I) complex. A human Cancer Pathway Finder array, which contains 84 cancer-related genes were used. The expression of each of these genes was measured based on their biological activity. Some genes included in this array has shown to be involved in the increased metastasis in oesophageal cancer. The SNO cells were either treated with 1% DMSO (vehicle) or 14 µM of complex **7** for 12 hrs. This treatment period was selected rather than 24 hrs to ensure that

earlier gene events are detected based on a previous similar experiment completed in-house (data not shown). The total RNA was isolated, cDNA synthesized and samples run on the array. Both the RNA and cDNA integrity gels (Figure A1.2 and A1.3), melting curves (Figure A1.4 and A1.5), PCR quality controls (Figure A1.6) and raw data of the array (Table A1.1) can be found in Appendix 1. The gene expression levels of the treated SNO cells are either represented as a heat map (Figure 3.2A) or a scatterplot (Figure 3.2B). The heat map represents a graphical representation of the fold regulation of expressed genes. The treated and vehicle control groups are overlaid to obtain the magnitude fold change. In Figure 3.2A, it is clear that the majority of the genes that were expressed were 2-fold down-regulated (green shades) and not up-regulated (red shades). The scatterplot is used to compare the normalised expression profiles of each gene located on the array by plotting the treated group against the control group. This aids to visualize large gene expression changes in the data set. The middle line indicates genes that were not expressed, while the top and bottom lines represent fold up- or down-regulation of 1.5-fold respectively (Figure 3.2B).

Of the 84 genes, a total of 33 were expressed 1.5-fold or more. Of these only 4 were up-regulated and included: *TNF*, *E2F1*, *TIMP1* and *FOS*. A total of 29 were down-regulated and included: *CDC25A*, *NME4*, *CDK2*, *CDK4*, *MET*, *ANGPT1*, *PLAUR*, *PDGFB*, *CXCL8*, *COL18A1*, *CDKN1A*, *MCAM*, *APAF1*, *MTA1*, *MTA2*, *NME1*, *SNCG*, *ERBB2*, *BCL-2*, *TGFB1*, *TWIST1*, *HTATIP2*, *PNN*, *MDM2*, *ITGA1*, *ITGA3*, *BAX*, *S100A4* and *ITGB1*. A total of 17 were deemed significant ($P < 0.05$) and are listed in Table 3.2.

Most the genes that were significantly altered belonged to the invasion and metastasis group (*MTA1*, *MTA2*, *PLAUR*, *S100A4* and *TWIST1*). This was followed by genes involved in cellular adhesion (*ITGA1*, *ITGA3*, *ITGAB1* and *PNN*), apoptosis (*BAX*, *BCL-2* and *HTATP2*), angiogenesis (*TNF* and *TGFB1*), signal transduction (*ERBB2* and *FOS*) and lastly cell cycle and control (*MDM2*). Overall, the top 6 most significant genes that were consequently down-regulated were *BAX* (7.15-fold), *ERBB2* (27.67-fold), *ITGB1* (5.16-fold), *MDM2* (4.99-fold), *MTA1* (4.75-fold) and *MTA2* (8.16-fold).

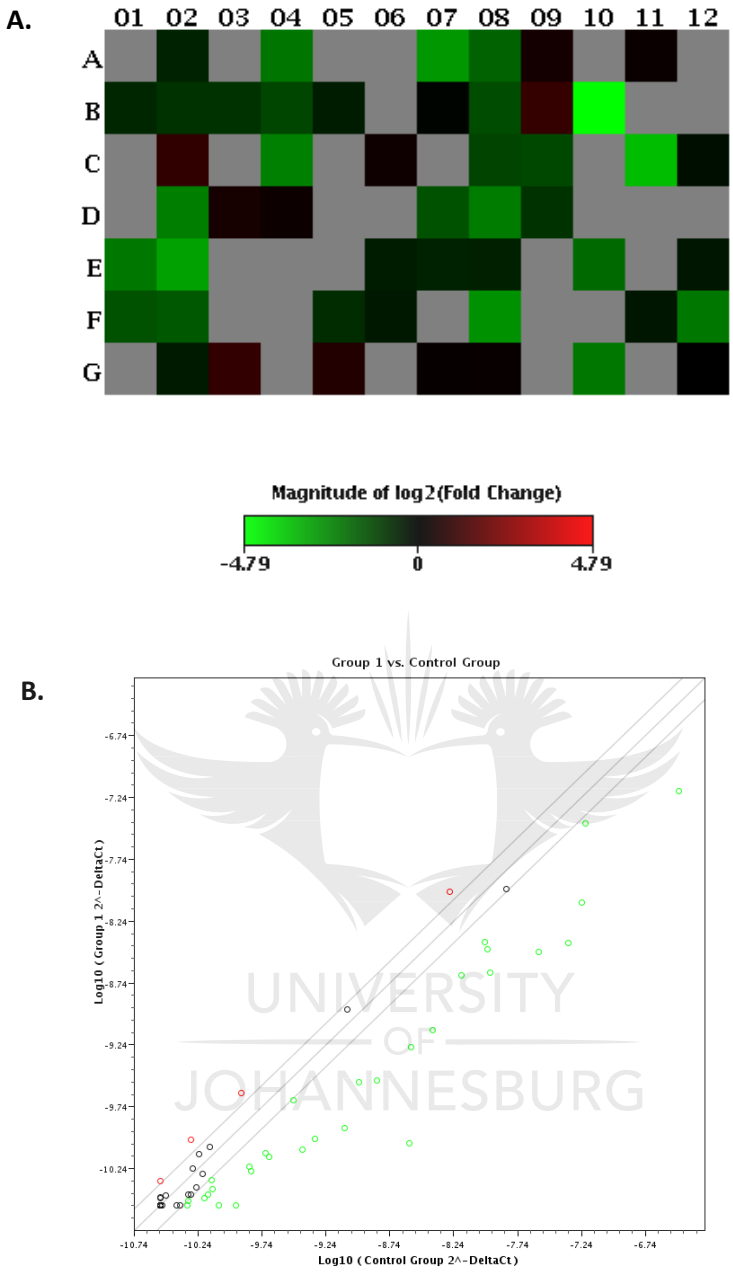

Figure 3.2: Differential expression of cancer-related genes in **SNO** oesophageal cells that were treated for 12 hrs with either 1% DMSO (control) or 14 µM of complex **7** (group 1). (A) Heat map of RT^2 Profiler PCR array (*n* = 3 per group) where each of the 84 genes is expressed in fold change with respect to control group. Red areas represent fold up-regulation while green areas represent fold down-regulation. Grey areas represent genes that were expressed at either 35 cycles or higher and were excluded. (B) Scatter plot of each of the genes where a 1.5-fold change in expression was used as the arbitrary cut off. Genes that were either up- or down-regulated 1.5-fold or more are represented red and green respectively. Genes with low expression values are represented in black.

Table 3.2: Fold regulation of significantly ($P < 0.05$) expressed genes in **SNO** cells. The cells were treated for 12 hrs with 14 µM of complex **7**. A Human Cancer PathwayFinder RT^2 Profiler PCR array was used and data is represented with respect to the vehicle control (1% DMSO). The *P*-value was calculated using the two-tailed Students *t*-test. The fold change in gene expression was calculated using the $\Delta\Delta C_T$ method. The arrows indicate either up (↑) or down-regulation (↓).

Gene symbol	Fold regulation	*P*-value	Cellular function
BAX	↓7.15	0.000004	*Apoptosis and Cell Senescence:* Protein forms a heterodimer with BCL2 protein to activate apoptosis. After interacting with mitochondria the membrane depolarizes leading to the release of cytochrome *c*.
BCL2	↓3.60	0.048212	*Apoptosis and Cell Senescence:* Encodes an outer membrane protein responsible to prevent apoptosis *via* the caspases.
ERBB2	↓27.67	0.000111	*Signal Transduction Molecules and Transcription Factors:* Encodes a family of receptor tyrosine kinases which form a heterodimer, stabilizing ligand binding and enhances downstream kinase mediated activity.
FOS	↑1.87	0.044566	*Signal Transduction Molecules and Transcription Factors:* Proteins encoded have been implicated as regulators of cell proliferation, differentiation and transformation. *FOS* gene expression has also been associated with apoptosis.
HTATIP2	↓5.23	0.003956	*Apoptosis and Cell Senescence:* Co-activator of transcription. Codes for an oxidoreductase needed for tumour suppression. Two isoforms exist where isoform-1 is pro-apoptotic and isoform-2 is anti-apoptotic.
ITGA1	↓2.57	0.035849	*Adhesion:* Encodes an integrin alpha-1 subunit of integrin receptors. Along with beta-1 subunit it forms a heterodimer creating a cell-surface receptor which plays a role in cell-cell adhesion.
ITGA3	↓11.89	0.001030	*Adhesion:* Encoded protein generates light and heavy chains that make up the integrin alpha-3 subunit. Along with the beta-1 subunit a integrin protein is formed acting as cell surface adhesion molecules.
ITGB1	↓5.16	0.000122	*Adhesion:* Gene encodes a beta-1 subunit. When combined with alpha subunits it plays a role in cell surface adhesion. Integrins also play a role in embryogenesis, homeostasis, tissue repair, immune response and metastatic diffusion of tumour cells.
MDM2	↓4.99	0.000884	*Cell Cycle Control and DNA Damage Repair:* The gene is transcriptionally regulated by p53. Encodes a nuclear-localized E3 ubiquitin ligase. This enzyme promotes tumour formation by targeting tumour suppressor genes (*e.g. p53*) to be degraded by the proteasome.
MTA1	↓4.75	0.000883	*Invasion and Metastasis:* The protein was thought to be the 70 kD unit of the NuRD complex. Even though the role in metastasis is not clear it may be involved in transcriptional regulation and chromatin remodelling.
MTA2	↓8.16	0.000020	*Invasion and Metastasis:* Encodes a protein that forms part of the NuRD complex and is found in the nucleus of human cells. Directly and indirectly (chromatin remodelling) regulates transcription through a member of a small gene family that encodes different proteins that are related with each other.
PLAUR	↓2.89	0.043418	*Invasion and Metastasis:* Encodes a receptor for urokinase plasminogen activator promoting the formation of plasmin.
PNN	↓3.17	0.014671	*Adhesion:* Gene encodes a protein pinin that is a phosphoprotein that plays a role in cell-cell adhesion.
S100A4	↓1.75	0.002317	*Invasion, Metastasis, Cell Cycle Control and DNA Damage Repair*: The S100 protein encoded by the gene is found in either the cytoplasm or the nucleus of cells. Regulates cell cycle progression, differentiation, motility, invasion and tubulin polymerization.
TGFB1	↓4.79	0.001591	*Angiogenesis:* Gene encodes a member of the TGFB cytokine family. Regulates cellular proliferation, differentiation, adhesion and migration.
TNF	↑1.56	0.011893	*Angiogenesis:* Encodes a multifunctional pro-inflammatory cytokine which forms part of the TNF superfamily. Regulates cell proliferation, differentiation, apoptosis, lipid metabolism and coagulation.
TWIST1	↓4.83	0.013564	*Invasion and Metastasis*: Gene encodes a transcription factor implicated in cellular lineage determination and differentiation.

3.4. Discussion

Gene expression microarrays have become one of the main approaches to evaluate the genetic changes in the genome after being exposed to certain conditions like anticancer agents. These arrays are a reliable approach that monitors the expression of various genes in a biochemical system. In this study, an RT^2 Profiler array was used that can analyse a total 84 genes, in this case, cancer-related genes. These arrays amplify all these genes including the controls simultaneously and aids in the identification of drug targets by comparing the expression profiles of the untreated and treated samples. In order to identify the genetic effect of complex **7** on the malignant SNO cells, the cells were treated for a 12 h period followed by analysis. Only a total of 17 genes associated with cell cycle control and DNA damage repair, apoptosis and cell senescence, signal transduction molecules and transcription factors, cellular adhesion, angiogenesis, and invasion and metastasis was significantly up- or down-regulated in the malignant SNO oesophageal cells (Table 3.2). The STRING analysis in Figure 3.3 displays the possible protein-protein interactions of all the non-significant and significant genes studied. Only the genes that show a significant change of 2.5-fold or higher will be discussed in each group.

Cell cycle control and DNA damage repair

Complex **7** significantly down-regulated the expression of *MDM2* by a 4.99-fold (Figure 3.3A). *MDM2* plays a central role in cell cycle and control by regulating the activity of p53. In addition, it interacts with other proteins (*e.g.* pRb and E2F1) which are involved in cell cycle control and growth arrest (Martin *et al*., 1995b; Lei *et al*., 2015). MDM2 was discovered to be an oncogenic product where it was amplified more than 50-fold in a transformed 3T3DM mice cell line (Fakharzadeh *et al*., 1991). The amplification of the *MDM2* gene, that resulted in overexpression of the MDM2 protein, was first discovered by Oliner *et al*. (1992) in sarcoma cancer cells. This study also revealed that the MDM2 protein interacts with p53. Overexpression of MDM2 is also observed in other cancers which include that of the oesophagus (Momand *et al*., 1998; Takahashi *et al*., 2009). In the Takahashi *et al*. (2009) study, Akt1 and MDM2 mRNA expression were significantly increased in oesophageal squamous carcinoma and was consequently involved in its carcinogenesis. When *Akt1* activity was silenced, the MDM2 protein expression was reduced that implies *MDM2* expression is regulated by *Akt1*. MDM2 inhibits p53 activity and is controlled by an autoregulatory feedback loop on a transcriptional level. For example, when the MDM2 was expressed in cells that contain active p53 functionality, the p53 function was prevented (Wu *et al*., 1993). When p53 is activated, it transcribes the *MDM2* gene of which the MDM2 protein, in turn, inhibits p53 activity. Thereafter, the inactive p53 is transported out of the nucleus and is degraded *via* E3 ubiquitin ligase by means of the proteasome (Haupt *et al*.,

1997; Freedman *et al*., 1998; Shangary and Wang, 2008). CDDP inhibited the activity of MDM2 in cancer cells that were regulated by the mitogen activated protein kinase (MAPK) signalling pathway resulting in apoptotic cell death (Zhu *et al*., 2013). Complex **7** could act in a similar manner than CDDP, by inhibiting the MDM2 production thus favouring p53-dependent cell death.

Apoptosis and cell senescence

The expression of *BAX*, *BCL-2* and *HTATIP2* were significantly down-regulated 7.15, 6.60 and 5.23-fold respectively (Figure 3.3B). Previous studies that were completed for complex **7** indicated that apoptosis *via* the intrinsic/mitochondrial-mediated pathway was activated in SNO oesophageal cancer cells (Appendix 1). This was attributed to the increased levels of caspase-9 that is characteristic of this pathway.

Bcl-2 family members play a key role in either promoting or inhibiting apoptosis *via* the mitochondrial-mediated pathway (Reed, 2008). Bax activates the cell death mechanism by permeabilizing the mitochondrial membrane resulting in the release of proteins (Suzuki *et al*., 2001; Soriano and Scorrano, 2010). In contrast, Bcl-2 inhibits cell death by targeting Bax. Bcl-2 and Bax play an important role in tumour progression and prognosis. The up-regulation of *Bax* and down-regulation of *Bcl-2* have been associated with improved malignant cell survival (Tsamandas *et al*., 2007; Zeestraten *et al*., 2016; Khodapasand *et al*., 2015). Based on the findings from complex **7**, the gene expression of *Bax* and *Bcl-2* should have increased and decreased respectively favouring apoptosis. This was not the case for the expression of *Bax* that was down-regulated 7.15-fold. It should be noted that apoptotic studies were done after 24 hrs of treatment compared to 12 hrs for the PCR arrays indicating that the specific time point might have been missed for the activity. Both increased Bax and decreased Bcl-2 activity was detected in human oesophageal carcinoma cells after 24 hrs of treatment with resveratrol (Zhou *et al*., 2003).

HTATIP2, also known as *TIP30*, is an evolutionarily conserved gene that is expressed in most normal tissue and in some malignant tissue. It is a tumour suppressor protein and has been proven to interact with the transcriptional activation of the HIV-1 TAT and therefore functions as a cofactor to enhance TAT-activated transcription (Xiao *et al*., 1998; Kumtepe *et al*., 2013). HTATIP2 is involved in the control of apoptosis, metastasis, angiogenesis, DNA repair and cancer cell metabolism (Yu *et al*., 2015). In non-small cell lung carcinoma, HTATIP2 acts as a metastasis suppressor by retarding the growth mainly due to its ability to activate apoptosis (Baker *et al*., 2000). In contrast, serum levels of HTATIP2, as determined by ELISA, was found to be significantly higher in patients with ovarian

cancer than those without the malignancy (Kumtepe *et al*., 2013). However, down-regulation of *HTATIP2/TIP30* in oesophageal cancer was associated with increased metastasis (Dong *et al*., 2014). Therefore, the role that complex **7** plays on the expression of this gene is unclear.

Signal transduction molecules and transcription factors

In the signal transduction and transcription gene group, *ERBB2* was the only gene significantly up-regulated more than 2.5-fold (Figure 3.3C). In fact, complex **7** had the greatest effect on this gene, when compared to the other studied genes, causing a 27.67-fold down-regulation.

ERBB2, also known as *HER2*, is the most studied gene in cancer and forms part of a family of transmembrane receptor tyrosine kinases (Akiyama *et al*., 1986; Stern *et al*., 1986). These receptor tyrosine kinases regulate cell growth, survival, differentiation and migration (Spector and Blackwell, 2009). In addition, ERBB2/HER2 is involved in the development and progression of some cancers (Slamon *et al*., 1989; Spigel and Burstein, 2002; Gravalos and Jimeno, 2008; Hynes and MacDonald, 2009) and is minimally expressed in normal tissue (Pressl *et al*., 1990) which makes it an attractive target for anticancer drugs. In a study reported by Safran *et al*. (2007), overexpression of HER2 was observed in the majority of patients with advanced oesophageal adenocarcinoma. Current therapeutic approaches include the use of targeted antibodies directed to *ERBB2* or the extracellular domain as well as small molecule tyrosine kinase inhibitors (Hynes and MacDonald, 2009). Trastuzumab is one example of antibody-based treatment especially used for the treatment of metastatic breast carcinoma (Baselga *et al*., 1996). This drug not only down-regulates the expression of HER2 but induces G1-phase cell cycle arrest, activates antibody-dependent and compliment-dependent toxicity, including apoptosis (Nahta *et al*., 2003). The problem is that when HER2 is highly overexpressed in cancer, tolerance against trastuzumab treatment develops and combinational therapy should be considered (Cobleigh *et al*. 1999; Tew *et al*., 2005). Thus, complex **7** could be a better alternative to target *ERBB2/HER2*.

Cellular adhesion

The expression of cell adhesion integrin receptor coding genes *ITGA3*, *ITGA1, ITGB1 and PNN* were significantly down-regulated 11.89, 2.57, 5.16, 3.17-fold respectively (Figure 3.3D).

Integrins, along with cadherins, play a role in cell-to-cell and cell-to-extracellular matrix anchoring by maintaining tissue structure of the cell, cell signalling, tissue repair and wound healing (Makrilia *et al*., 2009; Farahani *et al*., 2014). Integrins are glycoproteins that form heterodimeric receptors

comprising of α- and β-subunits on the surface of the extracellular matrix (Hynes, 2002; Danen, 2013). They regulate intracellular pathways, especially the MAPK pathway, that elicits various responses based on changes in the cellular environmental conditions, hormonal exposure and other stimuli (Giancotti and Ruoslahti, 1999; Dreesen and Brivanlou, 2007; Farahani *et al*., 2014). Integrins are involved in malignant progression and differentiation. When tumours develop from epithelial cells, integrins like α6β4, α6β1, αvβ5, α2β1 and α3β1 are retained within the tumour, but at different levels of expression (Desgrosellier and Cheresh, 2010). Overexpression of integrin receptor, ITGA3, has been associated with more aggressive phenotypes of colorectal (Linhares *et al*., 2015) and breast tumours (Shirakihara *et al*., 2013). In addition, ITGB1 is overexpressed in non-small cell lung carcinoma (Zheng *et al*., 2016). Similar to the integrins, the desmosome associated protein, PNN, stabilizes the desmosome association and reinforces the adhesion of epithelial cells (Ouyang and Sugrue, 1996). When PNN is down-regulated it suppresses the members of the cadherin subfamily resulting in the loss of corneal epithelial cell adhesion (Joo *et al*., 2005). Overexpression of PNN is linked to proliferation, invasion and metastasis in colorectal cancer (Wei *et al*., 2016).

Thus, complex **7** shows potential in disrupting the integrin-ligand interactions, including that of PNN, that are the key survival and proliferation signals supporting malignant growth.

Angiogenesis

Of all the genes involved in the angiogenesis pathway only, *TGFB1* was significantly down-regulated more than 2.5-fold (Figure 3.3E).

TGFB1, alternatively known as *TGFβ*, forms part of a multifunctional *TGFβ* gene superfamily that regulates cell growth, differentiation, invasion and metastasis, production of extracellular matrix, angiogenesis, immune response and apoptosis (Wakefield and Hill, 2013). Five isoforms of TGFβ exist, but only three forms, TGFB1, TGFB2 and TGFB3, exists in mammalian cells of which TGFB1 is the most characterized (Cheifetz *et al*., 1987; Verona *et al*., 2008). In cancer, *TGFβ* can either act as a tumour suppressor or promoter depending on the tumour type. In cancers that are detected in the early stages, *TGFβ* functions as a tumour suppressor by inhibiting cell proliferation and apoptosis. In contrast, *TGFβ* activity as a tumour promoter is observed in more aggressive and invasive tumours where it enhances the induction of epithelial-mesenchymal transition, cell adhesion, metastasis and invasion (Thiery, 2002; Dumont and Arteaga, 2003; Siegel and Massagué, 2003; Yingling *et al*., 2004; Xu *et al*., 2009; Reviewed by Lebrun, 2012). *TGFβ* activity can either be SMAD-dependant or -independent and is reviewed elsewhere (Kubiczkova *et al*., 2012). *TGFβ* is overexpressed in different

malignancies and is linked to poor prognosis (Teicher, 2001; Kubiczkova *et al*., 2012) which makes it a promising target in cancer therapy.

Invasion and metastasis

MTA2, *MTA1*, *TWIST1*, *PLAUR* and *S100A4* gene expression was significantly down-regulated 8.16, 4.75, 4.83, 2.89 and 1.75-fold respectively by complex **7** (Figure 3.3F).

Of all these genes mentioned the decreased gene expression of *MTA2* was of interest. MTA proteins are involved in the transcriptional regulation of the nucleosome remodelling deacetylase (NuRD) complex which is one of five ATP-dependent complexes responsible for chromatin remodelling (Clapier and Cairns, 2009). To date, only three MTA proteins exist that are encoded by the different *MTA1*, *MTA2* and *MTA3* genes (Manavathi *et al*., 2007). The NuRD complex is made up of histone deacetylase-1 and -2 (HDAC-1 and -2), histone binding proteins RbAp46/48, dermatomyositis-specific autoantigen Mi-2 and the MTA proteins. It exerts its effect on the tumour suppressor p53 protein. The p53 protein is inactivated by both MTA1 and MTA2 when an acetyl group is removed. This is then followed by the down-regulation of p53 dependent transcription contributing to a decrease in cell cycle arrest and apoptosis (Toh and Nicolson, 2009). MTA activity is highly up-regulated in various malignancies including that of the oesophagus (Kumar *et al*., 2003; Liu *et al*., 2012). Liu *et al*. (2012) studied the role of MTA2 expression in 162 patients with oesophageal squamous cell carcinoma. These patients were grouped based on cancer progression and metastasis. With the use of immunohistochemistry, only 65 of the 162 patients overexpressed the MTA2 protein. In fact, these MTA2-positive patients were the ones with the lowest prognosis. In oesophageal cancer patients usually have a 5-year survival rate independent of the therapeutic approach (Pickens and Orringer, 2003). In the prior study, MTA2-postive patients significantly overexpressed this protein and contributed to a low 5-year survival rate of 18.4%. In contrast, patients that under expressed the MTA2 protein had a higher 5-year survival rate of 46% (Liu *et al*., 2012). MTA2 overexpression was also associated with significant lymph node metastasis, tumour differentiation, lymphatic and blood vessel invasion.

TWIST, also known as *TWIST1*, is a transcription factor that is involved in embryonic development, metastasis and tissue reorganization (Yang *et al*., 2004; Yang *et al*., 2006). TWIST1 is highly expressed in malignancies like that of the breast, gastric, liver, prostate and bladder mainly due to its metastatic properties (Qin *et al*., 2012). The expression of TWIST1 is higher in the malignant phenotype of the oesophagus than the non-malignant phenotype, like MTA, that increases the

invasive and metastatic properties (Lee *et al*., 2012b). This protein enhances the expression of AKT2 (Cheng *et al*., 2007), inhibits the activity of p53 and apoptosis (Maestro *et al*., 1999). Although the mechanism of TWIST overexpression is unknown, it is believed to be involved in the NuRD complex. Fu *et al*. (2011) discovered that both the N- and C- terminus of TWIST interacts with MTA2 when protein-protein interaction assays were completed. Further interaction at the N- and C- terminus of components, Mi2β and RbAp46, that form part of the NuRD complex was also observed. Furthermore, when TWIST was depleted from cancer cells, cell migration and invasion was suppressed.

PLAUR, also known as urokinase-type PAR, forms part of the plasminogen activator system that is involved in various cellular processes that include membrane remodelling, regeneration of tissue, angiogenesis, cancer progression and metastasis (Baldini *et al*., 2012; Mekkawy *et al*., 2014). Plasminogen can be activated by either tissue-type (tPA) or urokinase-type plasminogen activator (uPA) of which the former is of interest in cancer models (Mekkawy *et al*., 2014). The uPA system promotes the metastasis of prostate (Sheng, 2001), breast (Han *et al*., 2005), thyroid (Baldini *et al*., 2012) and oesophageal cancer (Morrissey *et al*., 1999). Various models have been proposed of how uPA and uPAR are involved in tumour metastasis and growth. In the first, upon interaction with uPAR, plasminogen is activated to plasmin which either activates matrix metalloproteinases or degrades extracellular matrix components. The uPAR receptor ensures the activation of uPA, cell adhesion processes, migration and signal transduction (Reviewed by Mekkawy *et al*., 2014). Alternatively, uPAR interacts and activates additional growth factor receptors (integrins, EGBR and platelet-derived growth factor b-receptor) therefore stimulating mobility and growth (Wei *et al*., 1996; Herbert *et al*., 1997; Liu *et al*., 2002; Hu *et al*., 2008). Overexpression of uPAR is also linked to drug resistance in small-lung cell carcinoma when anticancer agents such as 5-fluorouracil, CDDP and etoposide are used (Gutova *et al*., 2007).

The silver(I) complex herein could reverse the inhibitory action of both the *MTA2* and *TWIST* genes that can result in the activation of cell cycle arrest and apoptosis. Furthermore, by targeting uPAR, invasion and metastasis could be decreased which will ensure improved prognosis in patients.

Taking all the above findings in consideration, complex **7** targeted multiple genes that are mostly associated with cancer metastasis, proliferation and poor prognosis. These observations were only made after 12 hrs of exposure. These gene targets can, therefore, be used as biochemical markers

when oesophageal cancer is treated specifically with complex **7**. This is especially valuable in predicting the outcome and guiding the treatments of oesophageal cancer.

A.

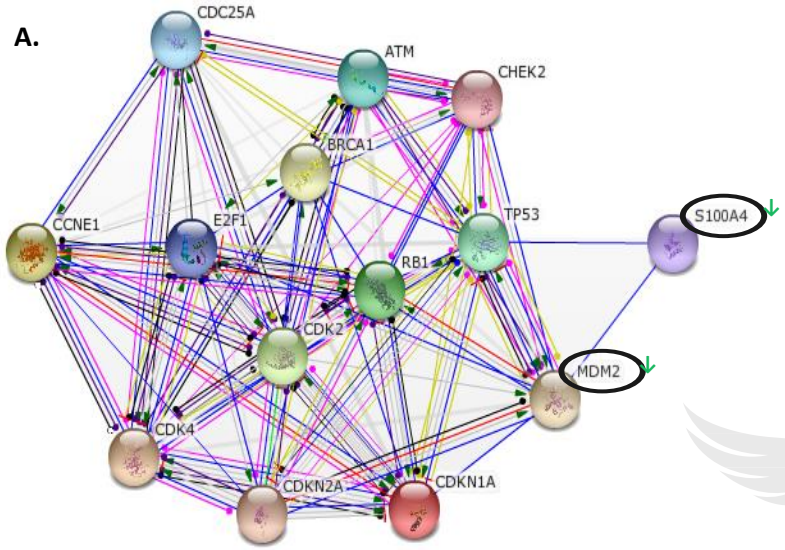

Cell cycle control and DNA damage repair

C.

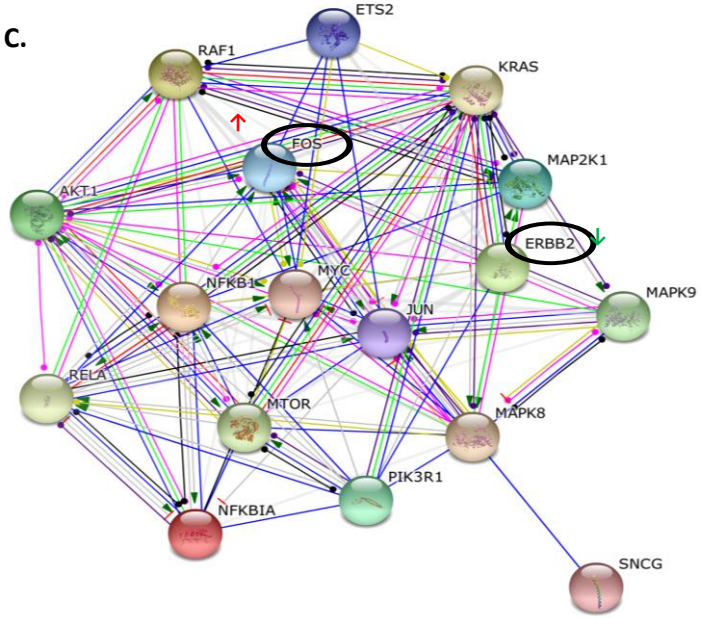

Signal transduction molecules and transcription factors

B.

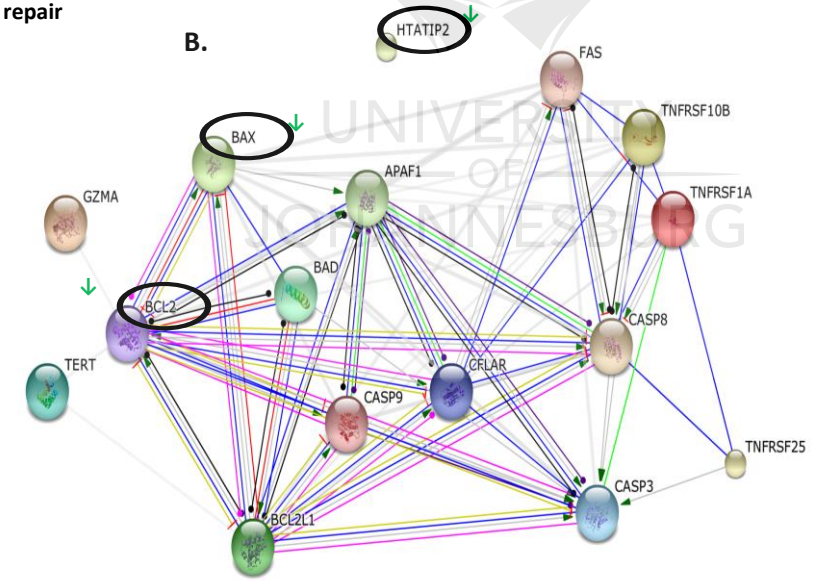

Apoptosis and cell senescence

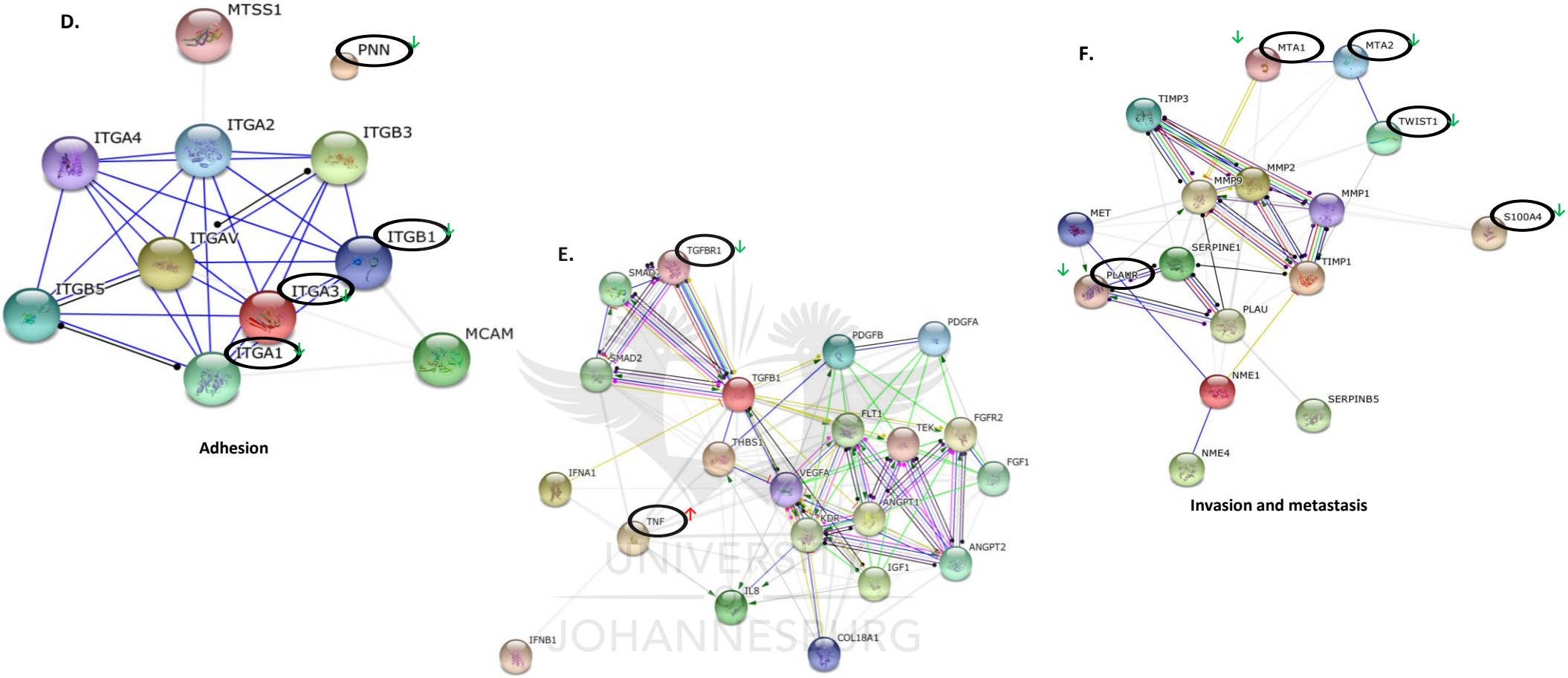

Figure 3.3: Protein-protein interaction networks of various proteins encoded by genes found on the Human Cancer Pathway Finder RT^2 Profiler PCR Array constructed by STRING. Interactions involving (A) cell cycle control and DNA damage repair, (B) apoptosis and cell senescence, (C) signal transduction molecules and transcription factors, (D) adhesion, (E) angiogenesis and (F) invasion and metastasis are shown. Proteins that are significantly expressed are encircled by black followed by either up- (↑) or down-regulation (↓).

CHAPTER 4: Conclusion

The first part of this study evaluated the anticancer activity of six silver(I) phosphine complexes in malignant oesophageal and breast cell lines. These novel silver(I) complexes inhibited cell growth in a dose-dependent manner, although the MCF-7 cells appeared to be more resistant to treatment. Cell death was associated with the caspase-dependent activation of apoptosis. In addition, cell cycle arrest was observed in either/or the G2/M-phase and S-phases. When the relative dosages are compared, the silver(I) phosphine complexes were more effective than the widely used platinum-based drug, CDDP. Most importantly, most the complexes displayed selectivity towards the malignant cell lines. One complex, complex **2**, was cytotoxic to non-malignant HDF-a and HEK293 cells which arguably limits its use as an anticancer agent per se, but its non-selective apoptotic inducing ability makes it a highly effective and appropriate positive control for evaluating Ag-phosphines as potential anticancer drugs. Multiple studies revealed that the selected complexes targeted the mitochondria thus activating the intrinsic or mitochondrial-mediated cell death pathway of apoptosis. The silver(I) phosphine complexes inhibited the antioxidant enzyme, TrxR, further implicating the mitochondria. Overall, the cytotoxicity of complex **1** was not limited, as for complex **3** and **5**, to a specific cell line and was active in the majority of the cell lines. In the second part of the study, complex **7** tend to target genes associated with specific malignant features that contribute to the growth of oesophageal cancer.

Although the different aspects of how silver(I) phosphine complexes induce malignant cell death have been addressed here, the exact mechanism is far from being understood. DNA binding studies will confirm whether these complexes do in fact target the DNA, similar to that observed in CDDP. Further studies are required to determine the potential role of the extrinsic cell death pathway, p53 and Bcl-2 family members, *e.g.* bcl-2, Bax, Smac/DIABLO and XIAP, in the apoptosis. Moreover, the inhibitory activity of the complexes on additional antioxidant enzymes, that include glutathione reductase and lipoxygenase, should be investigated. Molecular docking studies will further confirm at which site these complexes bind on/in the enzyme. It will be interesting to see whether caspase-3, Hsp70 and possibly glutathione reductase are the main cause of MCF-7 resistance in this study. This can be clarified by testing these features in an MDA-MB-231 malignant breast cancer cell line that expresses caspase-3. The changes in the expression of cellular receptors (*e.g.* ER-α and ER-β) fall beyond the scope of this study, but based on the prediction (section 2.4.8), their role should also be investigated possibly identifying an alternative drug target. Once this has been completed, ADMET software can further be used. The ADMET software involves predictive modelling of phenomena

associated with the absorption, distribution, metabolism, elimination and chemical toxicity of drugs in the human body. It uses the chemical structure of a drug and links it with possible targets, building predictive models.

The major concern is that the anticancer activity of silver(I) phosphine complexes are focussed on *in vitro* rather than *in vivo* systems. This is especially important to determine the oral toxicity, biological stability and the antitumour activity of the silver(I) complexes in animal models. Oral toxicity studies, done recently, revealed that complex **1** and **7** had a maximum lethal dose (MLD) of 2000 g/kg and 300 g/kg respectively when rats were used. These studies were completed to ensure that the drug itself does not harm the animal. Interestingly, rats treated with the MLD of complex **1** were healthy but appeared stressed when exposed to complex **7**. The low MLD observed for the latter was due to its low solubility in non-toxic solvents, therefore it would be excluded from further analysis. Because of complex **1** low toxicity, xenograft mice models will reveal whether this treatment targets tumours *in vivo*. Moreover, blood will be isolated from the mice using the dried blood spotting (DBS) technique as described by Burnett (2011). The metabolic stability and half-life of the complex in the blood will further be analysed using LC-MS/MS. Complexes **3** and **5** are also in the process of being tested for their oral toxicity.

Overall, the silver(I) complexes mentioned seem to fit the criteria proposed by Zaki *et al*. (2016) and show great promise as effective and alternative metal-based chemotherapeutic agents. These treatments could improve patient response during therapy and most importantly prevent the recurrent development of tumours.

CHAPTER 5: References

Abdel-Wahab, M., Bourque, J.M., Pynda, Y., Iżewska, J., Van der Merwe, D., Zubizarreta, E. and Rosenblatt, E. (2013). Status of radiotherapy resources in Africa: an International Atomic Energy Agency analysis. *The Lancet Oncology*, *14*(4), pp.e168-e175.

Abdulkareem, I.H. and Zurmi, I.B. (2012). Review of hormonal treatment of breast cancer. *Nigerian Journal of Clinical Practice*, *15*(1), pp.9-14.

Acehan, D., Jiang, X., Morgan, D.G., Heuser, J.E., Wang, X. and Akey, C.W. (2002). Three-dimensional structure of the apoptosome: implications for assembly, procaspase-9 binding, and activation. *Molecular Cell*, *9*(2), pp.423-432.

Acilan, C., Adiguzel, Z., Cevatemre, B., Karakas, D., Ulukaya, E., Ribeiro, N., Correia, I. and Pessoa, J.C. (2016). Synthesis, biological characterization and evaluation of molecular mechanisms of novel copper complexes as anticancer agents. *Biochimica et Biophysica Acta (BBA)-General Subjects*, *1861*(2), pp.218-234.

Adams, J.M. and Cory, S. (2007). The Bcl-2 apoptotic switch in cancer development and therapy. *Oncogene*, *26*(9), pp.1324-1337.

Águas, F., Martins, A., Gomes, T.P., de Sousa, M. and Silva, D.P. (2005). Prophylaxis approach to a-symptomatic post-menopausal women: Breast cancer. *Maturitas*, *52*, pp.23-31.

Aït-Aïssa, S., Porcher, J.M., Arrigo, A.P. and Lambre, C. (2000). Activation of the hsp70 promoter by environmental inorganic and organic chemicals: relationships with cytotoxicity and lipophilicity. *Toxicology*, *145*(2), pp.147-157.

Akiyama, T., Sudo, C., Ogawara, H., Toyoshima, K. and Yamamoto, T. (1986). The product of the human c-erbB-2 gene: a 185-kilodalton glycoprotein with tyrosine kinase activity. *Science*, *232*(4758), pp.1644-1646.

Allardyce, C.S. and Dyson, P.J. (2001). Ruthenium in medicine: current clinical uses and future prospects. *Platinum Metals Review*, *45*(2), pp.62-69.

Alnemri, E.S., Livingston, D.J., Nicholson, D.W., Salvesen, G., Thornberry, N.A., Wong, W.W. and Yuan, J. (1996). Human ICE/CED-3 protease nomenclature. *Cell*, *87*(2), pp.171.

American Cancer Society. (2010). Cancer Facts & Figures 2010. Atlanta: American Cancer Society.

American Cancer Society. (2011a). Cancer Facts & Figures 2011. Atlanta: American Cancer Society.

American Cancer Society. (2011b). Cancer in Africa. Atlanta: American Cancer Society.

American Cancer Society. (2012). Cancer Facts & Figures 2012. Atlanta: American Cancer Society.

American Cancer Society. (2013). Cancer Facts & Figures 2013. Atlanta: American Cancer Society.

American Cancer Society. (2016). Cancer Facts & Figures 2016. Atlanta: American Cancer Society.

Antonarakis, E.S. and Emadi, A. (2010). Ruthenium-based chemotherapeutics: are they ready for prime time?. *Cancer Chemotherapy and Pharmacology*, *66*(1), pp.1-9.

Arai, N., Ström, A., Rafter, J.J. and Gustafsson, J.Å. (2000). Estrogen receptor β mRNA in colon cancer cells: growth effects of estrogen and genistein. *Biochemical and Biophysical Research Communications*, *270*(2), pp.425-431.

Argyrou, A. and Blanchard, J.S. (2004). Flavoprotein disulfide reductases: advances in chemistry and function. *Progress in Nucleic Acid Research and Molecular Biology*, *78*, pp.89-142.

Arnér, E.S. (2009). Focus on mammalian thioredoxin reductases—important selenoproteins with versatile functions. *Biochimica et Biophysica Acta (BBA)-General Subjects*, *1790*(6), pp.495-526.

Arnér, E.S. and Holmgren, A. (2000). Physiological functions of thioredoxin and thioredoxin reductase. *European Journal of Biochemistry*, *267*(20), pp.6102-6109.

Arstila, A.U. and Trump, B.F. (1968). Studies on cellular autophagocytosis. The formation of autophagic vacuoles in the liver after glucagon administration. *The American Journal of Pathology*, *53*(5), pp.687-733.

Ashkenazi, A. (2002). Targeting death and decoy receptors of the tumour-necrosis factor superfamily. *Nature Reviews Cancer*, *2*(6), pp.420-430.

Ashkenazi, A. and Dixit, V.M. (1998). Death receptors: signaling and modulation. *Science*, *281*(5381), pp.1305-1308.

Baker, M.E., Yan, L. and Pear, M.R. (2000). Three-dimensional model of human TIP30, a coactivator for HIV-1 Tat-activated transcription, and CC3, a protein associated with metastasis suppression. *Cellular and Molecular Life Sciences CMLS*, *57*(5), pp.851-858.

Baldini, E., Sorrenti, S., D'Armiento, E., Di Matteo, F.M., Catania, A. and Ulisse, S. (2012). The urokinase plasminogen activating system in thyroid cancer: clinical implications. *Giornale di Chirurgia*, *33*(10), pp.305-310.

Banti, C.N., Giannoulis, A.D., Kourkoumelis, N., Owczarzak, A.M., Kubicki, M. and Hadjikakou, S.K. (2015). Silver (I) compounds of the anti-inflammatory agents salicylic acid and p-hydroxyl-benzoic acid which modulate cell function. *Journal of Inorganic Biochemistry*, *142*, pp.132-144.

Banti, C.N., Kyros, L., Geromichalos, G.D., Kourkoumelis, N., Kubicki, M. and Hadjikakou, S.K. (2014). A novel silver iodide metalo-drug: Experimental and computational modelling assessment of its interaction with intracellular DNA, lipoxygenase and glutathione. *European Journal of Medicinal Chemistry*, *77*, pp.388-399.

Banti, C.N., Papatriantafyllopoulou, C., Manoli, M., Tasiopoulos, A.J. and Hadjikakou, S.K. (2016). Nimesulide Silver Metallodrugs, Containing the Mitochondriotropic, Triaryl Derivatives of Pnictogen; Anticancer Activity against Human Breast Cancer Cells. *Inorganic Chemistry*, *55*(17), pp.8681-8696.

Barrett-Connor, E. (1998). Fortnightly review: Hormone replacement therapy. *British Medical Journal*, *317*(7156), pp.457-461.

Bartek, J. and Lukas, J. (2007). DNA damage checkpoints: from initiation to recovery or adaptation. *Current Opinion in Cell Biology*, *19*(2), pp.238-245.

Baselga, J., Cortés, J., Kim, S.B., Im, S.A., Hegg, R., Im, Y.H., Roman, L., Pedrini, J.L., Pienkowski, T., Knott, A. and Clark, E. (2012). Pertuzumab plus trastuzumab plus docetaxel for metastatic breast cancer. *New England Journal of Medicine*, *366*(2), pp.109-119.

Baselga, J., Tripathy, D., Mendelsohn, J., Baughman, S., Benz, C.C., Dantis, L., Sklarin, N.T., Seidman, A.D., Hudis, C.A., Moore, J. and Rosen, P.P. (1996). Phase II study of weekly intravenous recombinant humanized anti-p185HER2 monoclonal antibody in patients with HER2/neu-overexpressing metastatic breast cancer. *Journal of Clinical Oncology*, *14*(3), pp.737-744.

Baudino, A.T. (2015). Targeted cancer therapy: The next generation of cancer treatment. *Current Drug Discovery Technologies*, *12*(1), pp.3-20.

Bayir, H. and Kagan, V.E. (2008). Bench-to-bedside review: Mitochondrial injury, oxidative stress and apoptosis–there is nothing more practical than a good theory. *Critical Care*, *12*(1), doi: 10.1186/cc6779.

Berger, N.A. (1985). Poly (ADP-ribose) in the cellular response to DNA damage. *Radiation Research*, *101*(1), pp.4-15.

Berger, N.A. and Petzold, S.J. (1985). Identification of minimal size requirements of DNA for activation of poly (ADP-ribose) polymerase. *Biochemistry*, *24*(16), pp.4352-4355.

Berners-Price, S.J., Bowen, R.J., Fernandes, M.A., Layh, M., Lesueur, W.J., Mahepal, S., Mtotywa, M.M., Sue, R.E. and van Rensburg, C.E. (2005). Gold (I) and silver (I) complexes of 2, 3-bis (diphenylphosphino) maleic acid: Structural studies and antitumour activity. *Inorganica Chimica Acta*, *358*(14), pp.4237-4246.

Berners-Price, S.J., Bowen, R.J., Galettis, P., Healy, P.C. and McKeage, M.J. (1999). Structural and solution chemistry of gold (I) and silver (I) complexes of bidentate pyridyl phosphines: selective antitumour agents. *Coordination Chemistry Reviews*, *185*, pp.823-836.

Berners-Price, S.J., Collier, D.C., Mazid, M.A., Sadler, P.J., Sue, R.E. and Wilkie, D. (1995). [Ag (I)($Et_2PCH_2CH_2PPh_2$) $_2$] NO_3: An Antimitochondrial Silver Complex. *Metal-Based Drugs*, *2*(2), pp.111-122.

Berners-Price, S.J., Johnson, R.K., Mirabelli, C.K., Faucette, L.F., McCabe, F.L. and Sadler, P.J. (1987). Copper (I) complexes with bidentate tertiary phosphine ligands: solution chemistry and antitumor activity. *Inorganic Chemistry*, *26*(20), pp.3383-3387.

Berners-Price, S.J., Mirabelli, C.K., Johnson, R.K., Mattern, M.R., McCabe, F.L., Faucette, L.F., Sung, C.M., Mong, S.M., Sadler, P.J. and Crooke, S.T. (1986). *In vivo* antitumor activity and in vitro cytotoxic properties of bis [1, 2-bis (diphenylphosphino) ethane] gold (I) chloride. *Cancer Research*, *46*(11), pp.5486-5493.

Berners-Price, S.J. and Sadler, P.J. (1988). Phosphines and metal phosphine complexes: relationship of chemistry to anticancer and other biological activity. *Bioinorganic Chemistry*, pp.27-102.

Blanc, C., Deveraux, Q.L., Krajewski, S., Jänicke, R.U., Porter, A.G., Reed, J.C., Jaggi, R. and Marti, A. (2000). Caspase-3 is essential for procaspase-9 processing and cisplatin-induced apoptosis of MCF-7 breast cancer cells. *Cancer Research*, *60*(16), pp.4386-4390.

Blot, W.J., Devesa, S.S., Kneller, R.W. and Fraumeni, J.F. (1991). Rising incidence of adenocarcinoma of the esophagus and ngastric cardia. *Jama*, *265*(10), pp.1287-1289.

Bold, R.J., Termuhlen, P.M. and McConkey, D.J. (1997). Apoptosis, cancer and cancer therapy. *Surgical Oncology*, *6*(3), pp.133-142.

Bombardier, C., Ware, J., Russell, I.J., Larson, M., Chalmers, A., Read, J.L., Arnold, W., Bennett, R., Caldwell, J., Hench, P.K. and Lages, W. (1986). Auranofin therapy and quality of life in patients with rheumatoid arthritis. Results of a multicenter trial. *The American Journal of Medicine*, *81*(4), pp.565-578.

Borner, C. (2003). The Bcl-2 protein family: sensors and checkpoints for life-or-death decisions. *Molecular Immunology*, *39*(11), pp.615-647.

Borst, P., Rottenberg, S. and Jonkers, J. (2008). How do real tumors become resistant to cisplatin?. *Cell Cycle*, *7*(10), pp.1353-1359.

Boulares, A.H., Yakovlev, A.G., Ivanova, V., Stoica, B.A., Wang, G., Iyer, S. and Smulson, M. (1999). Role of poly (ADP-ribose) polymerase (PARP) cleavage in apoptosis Caspase 3-resistant PARP mutant increases rates of apoptosis in transfected cells. *Journal of Biological Chemistry*, *274*(33), pp.22932-22940.

Brabec, V. and Nováková, O. (2006). DNA binding mode of ruthenium complexes and relationship to tumor cell toxicity. *Drug Resistance Updates*, *9*(3), pp.111-122.

Bray, F., Jemal, A., Torre, L.A., Forman, D. and Vineis, P. (2015). Long-term realism and cost-effectiveness: primary prevention in combatting cancer and associated inequalities worldwide. *Journal of the National Cancer Institute*, *107*(12), doi: 10.1093/jnci/djv273.

Brinton, L.A., Figueroa, J.D., Awuah, B., Yarney, J., Wiafe, S., Wood, S.N., Ansong, D., Nyarko, K., Wiafe-Addai, B. and Clegg-Lamptey, J.N. (2014). Breast cancer in Sub-Saharan Africa: opportunities for prevention. *Breast Cancer Research and Treatment*, *144*(3), pp.467-478.

Budihardjo, I., Oliver, H., Lutter, M., Luo, X. and Wang, X. (1999). Biochemical pathways of caspase activation during apoptosis. *Annual Review of Cell and Developmental Biology*, *15*(1), pp.269-290.

Burnett, J.E. (2011). Dried blood spot sampling: practical considerations and recommendation for use with preclinical studies. *Bioanalysis*, *3*(10), pp.1099-1107.

Bursch, W. (2001). The autophagosomal–lysosomal compartment in programmed cell death. *Cell Death & Differentiation*, *8*(6), pp.569-581.

Bursch, W., Hochegger, K., Torok, L., Marian, B., Ellinger, A. and Hermann, R.S. (2000). Autophagic and apoptotic types of programmed cell death exhibit different fates of cytoskeletal filaments. *Journal of Cell Science*, *113*(7), pp.1189-1198.

Cadenas, C., Franckenstein, D., Schmidt, M., Gehrmann, M., Hermes, M., Geppert, B., Schormann, W., Maccoux, L.J., Schug, M., Schumann, A. and Wilhelm, C. (2010). Role of thioredoxin reductase 1 and thioredoxin interacting protein in prognosis of breast cancer. *Breast Cancer Research*, *12*(3), pp.1-15.

Cai, J., Yang, J. and Jones, D. (1998). Mitochondrial control of apoptosis: the role of cytochrome c. *Biochimica et Biophysica Acta (BBA)-Bioenergetics*, *1366*(1), pp.139-149.

Cain, K., Bratton, S.B. and Cohen, G.M. (2002). The Apaf-1 apoptosome: a large caspase-activating complex. *Biochimie*, *84*(2), pp.203-214.

Campbell-Thompson, M., Lynch, I.J. and Bhardwaj, B. (2001). Expression of estrogen receptor (ER) subtypes and ERbeta isoforms in colon cancer. *Cancer Research*, *61*(2), pp.632-640.

Cande, C., Vahsen, N., Kouranti, I., Schmitt, E., Daugas, E., Spahr, C., Luban, J., Kroemer, R.T., Giordanetto, F., Garrido, C. and Penninger, J.M. (2004). AIF and cyclophilin A cooperate in apoptosis-associated chromatinolysis. *Oncogene*, *23*(8), pp.1514-1521.

Carswell, E.A., Old, L.J., Kassel, R.L., Green, S., Fiore, N. and Williamson, B. (1975). An endotoxin-induced serum factor that causes necrosis of tumors. *Proceedings of the National Academy of Sciences*, *72*(9), pp.3666-3670.

Caruso, F., Villa, R., Rossi, M., Pettinari, C., Paduano, F., Pennati, M., Daidone, M.G. and Zaffaroni, N. (2007). Mitochondria are primary targets in apoptosis induced by the mixed phosphine gold species chlorotriphenylphosphine-1, 3-bis (diphenylphosphino) propanegold (I) in melanoma cell lines. *Biochemical Pharmacology*, *73*(6), pp.773-781.

Cauci, S., Alessio, E., Mestroni, G. and Quadrifoglio, F. (1987). Reaction of cis-Ru II (DMSO) 4 Cl 2 with DNA and with some of its bases in aqueous solution. *Inorganica Chimica Acta*, *137*(1), pp.19-24.

Chaabane, W., User, S.D., El-Gazzah, M., Jaksik, R., Sajjadi, E., Rzeszowska-Wolny, J. and Łos, M.J. (2013). Autophagy, apoptosis, mitoptosis and necrosis: interdependence between those pathways and effects on cancer. *Archivum Immunologiae et Therapiae Experimentalis*, *61*(1), pp.43-58.

Chan, F.K.M., Shisler, J., Bixby, J.G., Felices, M., Zheng, L., Appel, M., Orenstein, J., Moss, B. and Lenardo, M.J. (2003). A role for tumor necrosis factor receptor-2 and receptor-interacting protein in programmed necrosis and antiviral responses. *Journal of Biological Chemistry*, *278*(51), pp.51613-51621.

Chan, L.L., Zhong, X., Qiu, J., Li, P.Y. and Lin, B. (2011). Cellometer vision as an alternative to flow cytometry for cell cycle analysis, mitochondrial potential, and immunophenotyping. *Cytometry Part A*, *79*(7), pp.507-517.

Chang, D.W., Xing, Z., Pan Y., Algeciras-Schimnich A., Barnhart B.C., Yaish-Ohad S., Peter M.E., Yang X. (2002). c-FLIP(L) is a dual function regulator for caspase-8 activation and CD95-mediated apoptosis. *The EMBO Journal, 21*, pp.3704–3714.

Cheifetz, S., Weatherbee, J.A., Tsang, M.L.S., Anderson, J.K., Mole, J.E., Lucas, R. and Massagué, J. (1987). The transforming growth factor-β system, a complex pattern of cross-reactive ligands and receptors. *Cell*, *48*(3), pp.409-415.

Chen, D., Cui, Q.C., Yang, H., Barrea, R.A., Sarkar, F.H., Sheng, S., Yan, B., Reddy, G.P.V. and Dou, Q.P. (2007). Clioquinol, a Therapeutic Agent for Alzheimer's Disease, Has Proteasome-Inhibitory, Androgen Receptor–Suppressing, Apoptosis-Inducing, and Antitumor Activities in Human Prostate Cancer Cells and Xenografts. *Cancer Research*, *67*(4), pp.1636-1644.

Chen, G.G., Zeng, Q. and Tse, G.M. (2008). Estrogen and its receptors in cancer. *Medicinal Research Reviews*, *28*(6), pp.954-974.

Chen, L.B. (1988). Mitochondrial membrane potential in living cells. *Annual Review of Cell Biology*, *4*(1), pp.155-181.

Cheng, G.Z., Chan, J., Wang, Q., Zhang, W., Sun, C.D. and Wang, L.H. (2007). Twist transcriptionally up-regulates AKT2 in breast cancer cells leading to increased migration, invasion, and resistance to paclitaxel. *Cancer Research*, *67*(5), pp.1979-1987.

Chicheportiche, Y., Bourdon, P.R., Xu, H., Hsu, Y.M., Scott, H., Hession, C., Garcia, I. and Browning, J.L. (1997). TWEAK, a new secreted ligand in the tumor necrosis factor family that weakly induces apoptosis. *Journal of Biological Chemistry*, *272*(51), pp.32401-32410.

Chinnaiyan, A.M. (1999). The apoptosome: heart and soul of the cell death machine. *Neoplasia*, *1*(1), pp.5-15.

Chipuk, J.E., Kuwana, T., Bouchier-Hayes, L., Droin, N.M., Newmeyer, D.D., Schuler, M. and Green, D.R. (2004). Direct activation of Bax by p53 mediates mitochondrial membrane permeabilization and apoptosis. *Science*, *303*(5660), pp.1010-1014.

Cho, Y., Challa, S., Moquin, D., Genga, R., Ray, T.D., Guildford, M. and Chan, F.K.M. (2009). Phosphorylation-driven assembly of the RIP1-RIP3 complex regulates programmed necrosis and virus-induced inflammation. *Cell*, *137*(6), pp.1112-1123.

Christofferson, D.E. and Yuan, J. (2010). Necroptosis as an alternative form of programmed cell death. *Current Opinion in Cell Biology*, *22*(2), pp.263-268.

Ciftci, O., Beytur, A., Cakir, O., Gurbuz, N. and Vardi, N. (2011). Comparison of Reproductive Toxicity Caused by Cisplatin and Novel Platinum-N-Heterocyclic Carbene Complex in Male Rats. *Basic & Clinical Pharmacology & Toxicology*, *109*(5), pp.328-333.

Clapier, C.R. and Cairns, B.R. (2009). The biology of chromatin remodeling complexes. *Annual Review of Biochemistry*, *78*, pp.273-304.

Clarke, P.G. (1990). Developmental cell death: morphological diversity and multiple mechanisms. *Anatomy and Embryology*, *181*(3), pp.195-213.

Cobleigh, M.A., Vogel, C.L., Tripathy, D., Robert, N.J., Scholl, S., Fehrenbacher, L., Wolter, J.M., Paton, V., Shak, S., Lieberman, G. and Slamon, D.J. (1999). Multinational study of the efficacy and safety of humanized anti-HER2 monoclonal antibody in women who have HER2-overexpressing metastatic breast cancer that has progressed after chemotherapy for metastatic disease. *Journal of Clinical Oncology*, *17*(9), pp.2639-2639.

Crighton, D., Wilkinson, S., O'Prey, J., Syed, N., Smith, P., Harrison, P.R., Gasco, M., Garrone, O., Crook, T. and Ryan, K.M. (2006). DRAM, a p53-induced modulator of autophagy, is critical for apoptosis. *Cell*, *126*(1), pp.121-134.

Cuervo, A.M., Bergamini, E., Brunk, U.T., Dröge, W., Ffrench, M. and Terman, A. (2005). Autophagy and aging: the importance of maintaining" clean" cells. *Autophagy*, *1*(3), pp.131-140.

Cuervo, A.M. and Dice, J.F. (1998). Lysosomes, a meeting point of proteins, chaperones, and proteases. *Journal of Molecular Medicine*, *76*(1), pp.6-12.

Cunningham, D. and You, Z. (2015). In vitro and in vivo model systems used in prostate cancer research. *Journal of Biological Methods*, *2*(1), doi: 10.14440/jbm.2015.63.

Dai, Y. and Grant, S. (2010). New insights into checkpoint kinase 1 in the DNA damage response signaling network. *Clinical Cancer Research*, *16*(2), pp.376-383.

Danen, E.H. (2013). Integrin signaling as a cancer drug target. *ISRN Cell Biology*, *2013*, doi: 10.1155/2013/135164.

Danial, N.N. and Korsmeyer, S.J. (2004). Cell death: critical control points. *Cell*, *116*(2), pp.205-219.

de Almagro, M.C. and Vucic, D. (2012). The inhibitor of apoptosis (IAP) proteins are critical regulators of signaling pathways and targets for anti-cancer therapy. *Experimental Oncology*, *34*(3), pp.200-211.

Declercq, W., Berghe, T.V. and Vandenabeele, P. (2009). RIP kinases at the crossroads of cell death and survival. *Cell*, *138*(2), pp.229-232.Pattingre, S., Espert, L., Biard-Piechaczyk, M. and Codogno, P., 2008. Regulation of macroautophagy by mTOR and Beclin 1 complexes. *Biochimie*, *90*(2), pp.313-323.

DeFranco, D.B., Ramakrishnan, C. and Tang, Y. (1998). Molecular chaperones and subcellular trafficking of steroid receptors. *The Journal of Steroid Biochemistry and Molecular Biology*, *65*(1), pp.51-58.

Degterev, A., Hitomi, J., Germscheid, M., Ch'en, I.L., Korkina, O., Teng, X., Abbott, D., Cuny, G.D., Yuan, C., Wagner, G. and Hedrick, S.M. (2008). Identification of RIP1 kinase as a specific cellular target of necrostatins. *Nature Chemical Biology*, *4*(5), pp.313-321.

Demir, S.B., Keleş, T. and Serindağ, O. (2014). Antioxidant enzyme inhibitor role of phosphine metal complexes in lung and leukemia cell lines. *Bioinorganic Chemistry and Applications*, doi: 10.1155/2014/717421.

Denault, J.B. and Salvesen, G.S. (2002). Caspases: keys in the ignition of cell death. *Chemical Reviews*, *102*(12), pp.4489-4500.

De Pas, T., de Braud, F., Mandalà, M., Curigliano, G., Catania, C., Ferretti, G., Sozzi, P., Solli, P. and Goldhirsch, A. (2001). Cisplatin and vinorelbine as second-line chemotherapy in patients with advanced non-small cell lung cancer (NSCLC) resistant to taxol plus gemcitabine. *Lung Cancer*, *31*(2), pp.267-270.

Desgrosellier, J.S. and Cheresh, D.A. (2010). Integrins in cancer: biological implications and therapeutic opportunities. *Nature Reviews Cancer*, *10*(1), pp.9-22.

Desoize, B. and Madoulet, C. (2002). Particular aspects of platinum compounds used at present in cancer treatment. *Critical Reviews in Oncology/Hematology*, *42*(3), pp.317-325.

Deveraux, Q.L. and Reed, J.C. (1999). IAP family proteins—suppressors of apoptosis. *Genes & Development*, *13*(3), pp.239-252.

Disis, M.L. (2014). Mechanism of action of immunotherapy. *Seminars in Oncology*, *41*, pp.S3-S13.

Dlamini, Z. and Bhoola, K. (2005). Esophageal cancer in African blacks of Kwazulu Natal, South Africa: an epidemiological brief. *Ethnicity & Disease*, *15*(4), pp.786-789.

Dong, W., Shen, R. and Cheng, S. (2014). Reduction of TIP30 in esophageal squamous cell carcinoma cells involves promoter methylation and microRNA-10b. *Biochemical and Biophysical Research Communications*, *453*(4), pp.772-777.

Drake, C.G., Lipson, E.J. and Brahmer, J.R. (2014). Breathing new life into immunotherapy: review of melanoma, lung and kidney cancer. *Nature Reviews Clinical Oncology*, *11*(1), pp.24-37.

Dreesen, O. and Brivanlou, A.H. (2007). Signaling pathways in cancer and embryonic stem cells. *Stem Cell Reviews*, *3*(1), pp.7-17.

Du, C., Fang, M., Li, Y., Li, L. and Wang, X. (2000). Smac, a mitochondrial protein that promotes cytochrome c–dependent caspase activation by eliminating IAP inhibition. *Cell*, *102*(1), pp.33-42.

Dubrez-Daloz, L., Dupoux, A. and Cartier, J. (2008). IAPs: more than just inhibitors of apoptosis proteins. *Cell Cycle*, *7*(8), pp.1036-1046.

Dumont, N. and Arteaga, C.L. (2003). Targeting the TGFβ signaling network in human neoplasia. *Cancer Cell*, *3*(6), pp.531-536.

Dunn, G.P., Koebel, C.M. and Schreiber, R.D. (2006). Interferons, immunity and cancer immunoediting. *Nature Reviews Immunology*, *6*(11), pp.836-848.

Dunn, W.A. (1994). Autophagy and related mechanisms of lysosome-mediated protein degradation. *Trends in Cell Biology*, *4*(4), pp.139-143.

Dutton, M.F. (1996). Fumonisins, mycotoxins of increasing importance: their nature and their effects. *Pharmacology & Therapeutics*, *70*(2), pp.137-161.

Echeverria, P.C. and Picard, D. (2010). Molecular chaperones, essential partners of steroid hormone receptors for activity and mobility. *Biochimica et Biophysica Acta (BBA)-Molecular Cell Research*, *1803*(6), pp.641-649.

Eckstein, N. (2011). Platinum resistance in breast and ovarian cancer cell lines. *Journal of Experimental & Clinical Cancer Research*, *30*(1), pp.91.

Ekert, P.G., Silke, J., Hawkins, C.J., Verhagen, A.M. and Vaux, D.L. (2001). DIABLO promotes apoptosis by removing MIHA/XIAP from processed caspase 9. *The Journal of Cell Biology*, *152*(3), pp.483-490.

Ellis, H.M. and Horvitz, H.R. (1986). Genetic control of programmed cell death in the nematode C. elegans. *Cell*, *44*(6), pp.817-829.

Elmore, S. (2007). Apoptosis: a review of programmed cell death. *Toxicologic Pathology*, *35*(4), pp.495-516.

Enari, M., Sakahira, H., Yokoyama, H., Okawa, K., Iwamatsu, A. and Nagata, S. (1998). A caspase-activated DNase that degrades DNA during apoptosis, and its inhibitor ICAD. *Nature*, *391*(6662), pp.43-50.

Enzinger, P.C. and Mayer, R.J. (2003). Esophageal cancer. *New England Journal of Medicine*, *349*(23), pp.2241-2252.

Fadok, V.A., de Cathelineau, A., Daleke, D.L., Henson, P.M. and Bratton, D.L. (2001). Loss of phospholipid asymmetry and surface exposure of phosphatidylserine is required for phagocytosis of apoptotic cells by macrophages and fibroblasts. *Journal of Biological Chemistry*, *276*(2), pp.1071-1077.

Fadok, V.A., Bratton, D.L., Rose, D.M., Pearson, A., Ezekewitz, R.A.B. and Henson, P.M. (2000). A receptor for phosphatidylserine-specific clearance of apoptotic cells. *Nature*, *405*(6782), pp.85-90.

Fadok, V.A., Voelker, D.R., Campbell, P.A., Cohen, J.J., Bratton, D.L. and Henson, P.M. (1992). Exposure of phosphatidylserine on the surface of apoptotic lymphocytes triggers specific recognition and removal by macrophages. *The Journal of Immunology*, *148*(7), pp.2207-2216.

Fakharzadeh, S.S., Trusko, S.P. and George, D.L. (1991). Tumorigenic potential associated with enhanced expression of a gene that is amplified in a mouse tumor cell line. *The EMBO Journal*, *10*(6), pp.1565-1569.

Fani, S., Dehghan, F., Karimian, H., Lo, K.M., Nigjeh, S.E., Keong, Y.S., Soori, R., Chow, K.M., Kamalidehghan, B., Ali, H.M. and Hashim, N.M. (2016). Monobenzyltin Complex C1 Induces Apoptosis in MCF-7 Breast Cancer Cells through the Intrinsic Signaling Pathway and through the Targeting of MCF-7-Derived Breast Cancer Stem Cells via the Wnt/β-Catenin Signaling Pathway. *PloS One*, *11*(8), doi: 10.1371/journal.pone.0160836.

Farahani, E., Patra, H.K., Jangamreddy, J.R., Rashedi, I., Kawalec, M., Pariti, R.K.R., Batakis, P. and Wiechec, E. (2014). Cell adhesion molecules and their relation to (cancer) cell stemness. *Carcinogenesis*, *35*(4), pp.747-759.

Farrell, N. (1999). Uses of inorganic chemistry in medicine. Royal Society of Chemistry: Cambridge. pp.1-10.

Farrell, N., Kelland, L.R., Roberts, J.D. and Van Beusichem, M. (1992). Activation of the trans geometry in platinum antitumor complexes: a survey of the cytotoxicity of trans complexes

containing planar ligands in murine L1210 and human tumor panels and studies on their mechanism of action. *Cancer Research*, *52*(18), pp.5065-5072.

Featherstone, J., Dykes, P.J. and Marks, R. (1991). The effect of platinum complexes on human skin cells in vivo and in vitro. *Skin Pharmacology and Physiology*, *4*(3), pp.169-174.

Ferlay, J., Shin, H.R., Bray, F., Forman, D., Mathers, C. and Parkin, D.M. (2010). Estimates of worldwide burden of cancer in 2008: GLOBOCAN 2008. *International Journal of Cancer*, *127*(12), pp.2893-2917.

Ferlay, J., Soerjomataram, I. and Ervik, M. (2012). GLOBOCAN, cancer incidence and mortality worldwide: IARC cancer base no. 11 [24/11/2016]. Lyon, France: International Agency for Research on Cancer; 2013.

Ferreira, D., Adega, F. and Chaves, R. (2013). The importance of cancer cell lines as in vitro models in cancer methylome analysis and anticancer drugs testing. INTECH Open Access Publisher.

Ferreira, E. (2015). Silver(I) phosphine compounds selectively induce apoptosis in MCF-7 breast cancer cells. Ph.D. Thesis. University of Johannesburg. South Africa.

Ferreira, E., Munyaneza, A., Omondi, B., Meijboom, R. and Cronjé, M.J. (2015). The effect of 1: 2 Ag (I) thiocyanate complexes in MCF-7 breast cancer cells. *BioMetals*, *28*(4), pp.765-781.

Festjens, N., Berghe, T.V. and Vandenabeele, P. (2006). Necrosis, a well-orchestrated form of cell demise: signalling cascades, important mediators and concomitant immune response. *Biochimica et Biophysica Acta (BBA)-Bioenergetics*, *1757*(9), pp.1371-1387.

Fischer, S.J., Benson, L.M., Fauq, A., Naylor, S. and Windebank, A.J. (2008). Cisplatin and dimethyl sulfoxide react to form an adducted compound with reduced cytotoxicity and neurotoxicity. *Neurotoxicology*, *29*(3), pp.444-452.

Florea, A.M. and Büsselberg, D. (2011). Cisplatin as an anti-tumor drug: cellular mechanisms of activity, drug resistance and induced side effects. *Cancers*, *3*(1), pp.1351-1371.

Fogh, J. and Trempe, G. (1975). New human tumor cell lines. *Human Tumor Cells in Vitro*. pp.115-159.

Fonteh, P.N., Keter, F.K. and Meyer, D. (2010). HIV therapeutic possibilities of gold compounds. *BioMetals*, *23*(2), pp.185-196.

Forastiere, A.A., Heitmiller, R.F. and Kleinberg, L. (1997). Multimodality therapy for esophageal cancer. *CHEST Journal*, *112*(4_Supplement), pp.195S-200S.

Frantz, M.C. and Wipf, P. (2010). Mitochondria as a target in treatment. *Environmental and Molecular Mutagenesis*, *51*(5), pp.462-475.

Freedman, D.A. and Levine, A.J. (1998). Nuclear export is required for degradation of endogenous p53 by MDM2 and human papillomavirus E6. *Molecular and Cellular Biology*, *18*(12), pp.7288-7293.

Frezza, M., Hindo, S., Chen, D., Davenport, A., Schmitt, S., Tomco, D. and Ping Dou, Q. (2010). Novel metals and metal complexes as platforms for cancer therapy. *Current Pharmaceutical Design*, *16*(16), pp.1813-1825.

Fu, J., Qin, L., He, T., Qin, J., Hong, J., Wong, J., Liao, L. and Xu, J. (2011). The TWIST/Mi2/NuRD protein complex and its essential role in cancer metastasis. *Cell Research*, *21*(2), pp.275-289.

Fulda, S. and Vucic, D. (2012). Targeting IAP proteins for therapeutic intervention in cancer. *Nature reviews Drug Discovery*, *11*(2), pp.109-124.

Gajjar, K., Martin-Hirsch, P.L. and Martin, F.L. (2012). CYP1B1 and hormone-induced cancer. *Cancer Letters*, *324*(1), pp.13-30.

Gakunga, R. and Parkin, D.M. (2015). Cancer registries in Africa 2014: A survey of operational features and uses in cancer control planning. *International Journal of Cancer*, *137*(9), pp.2045-2052.

Galluzzi, L., Vitale, I., Abrams, J.M., Alnemri, E.S., Baehrecke, E.H., Blagosklonny, M.V., Dawson, T.M., Dawson, V.L., El-Deiry, W.S., Fulda, S. and Gottlieb, (2012). Molecular definitions of cell death

subroutines: recommendations of the Nomenclature Committee on Cell Death 2012. *Cell Death & Differentiation*, *19*(1), pp.107-120.

Gandin, V. and Fernandes, A.P. (2015). Metal-and Semimetal-Containing Inhibitors of Thioredoxin Reductase as Anticancer Agents. *Molecules*, *20*(7), pp.12732-12756.

Gandin, V., Fernandes, A.P., Rigobello, M.P., Dani, B., Sorrentino, F., Tisato, F., Björnstedt, M., Bindoli, A., Sturaro, A., Rella, R. and Marzano, C. (2010). Cancer cell death induced by phosphine gold (I) compounds targeting thioredoxin reductase. *Biochemical Pharmacology*, *79*(2), pp.90-101.

Gandin, V. and Marzano, C. (2011). In vitro antitumour activity of water soluble Cu (I), Ag (I) and Au (I) complexes supported by hydrophilic alkyl phosphine ligands. *Journal of Inorganic Biochemistry*, *105*(2), pp.232-240.

Garcia, M., Jemal, A., Ward, E.M., Center, M.M., Hao, Y., Siegel, R.L. and Thun, M.J. (2007). Global Cancer Facts & Figures 2007. Atlanta: American Cancer Society.

Garrido, C., Brunet, M., Didelot, C., Zermati, Y., Schmitt, E. and Kroemer, G. (2006b). Heat shock proteins 27 and 70: anti-apoptotic proteins with tumorigenic properties. *Cell Cycle*, *5*(22), pp.2592-2601.

Garrido, C., Galluzzi, L., Brunet, M., Puig, P.E., Didelot, C. and Kroemer, G. (2006a). Mechanisms of cytochrome c release from mitochondria. *Cell Death & Differentiation*, *13*(9), pp.1423-1433.

Gęgotek, A., Cyunczyk, M., Łuczaj, W., Bielawska, A., Bielawski, K. and Skrzydlewska, E. (2014). The redox status of human breast cancer cell lines (MCF-7 and MDA-MB231) treated with novel dinuclear berenil-platinum (II) complexes. *Die Pharmazie-An International Journal of Pharmaceutical Sciences*, *69*(12), pp.923-928.

Gerber, D.E. (2008). Targeted therapies: a new generation of cancer treatments. *American Family Physician*, *77*(3), pp.311-319.

Germain, C.S., Niknejad, N., Ma, L., Garbuio, K., Hai, T. and Dimitroulakos, J. (2010). Cisplatin Induces Cytotoxicity through the Mitogen-Activated Protein Kinase Pathways ana Activating Transcription Factor 3. *Neoplasia*, *12*(7), pp.527-538.

Ghavami, S., Mutawe, M.M., Sharma, P., Yeganeh, B., McNeill, K.D., Klonisch, T., Unruh, H., Kashani, H.H., Schaafsma, D., Los, M. and Halayko, A.J. (2011). Mevalonate cascade regulation of airway mesenchymal cell autophagy and apoptosis: a dual role for p53. *PloS one*, *6*(1), doi: 10.1371/journal.pone.0016523.

Giancotti, F.G. and Ruoslahti, E. (1999). Integrin signaling. *Science*, *285*(5430), pp.1028-1033.

Goldenberg, D.M. (2002). Targeted therapy of cancer with radiolabeled antibodies. *Journal of Nuclear Medicine*, *43*(5), pp.693-713.

Gomez-Ruiz, S., Maksimović-Ivanić, D., Mijatović, S. and Kaluđerović, G.N. (2012). On the discovery, biological effects, and use of cisplatin and metallocenes in anticancer chemotherapy. *Bioinorganic Chemistry and Applications*, doi: 10.1155/2012/140284.

Gottfried, Y., Rotem, A., Lotan, R., Steller, H. and Larisch, S. (2004). The mitochondrial ARTS protein promotes apoptosis through targeting XIAP. *The EMBO Journal*, *23*(7), pp.1627-1635.

Gravalos, C. and Jimeno, A. (2008). HER2 in gastric cancer: a new prognostic factor and a novel therapeutic target. *Annals of Oncology*, *19*(9), pp.1523-1529.

Greene, L.A. and Tischler, A.S. (1976). Establishment of a noradrenergic clonal line of rat adrenal pheochromocytoma cells which respond to nerve growth factor. *Proceedings of the National Academy of Sciences*, *73*(7), pp.2424-2428.

Gutova, M., Najbauer, J., Gevorgyan, A., Metz, M.Z., Weng, Y., Shih, C.C. and Aboody, K.S. (2007). Identification of uPAR-positive chemoresistant cells in small cell lung cancer. *PLoS One*, *2*(2), doi: 10.1371/journal.pone.0000243.

Gyrd-Hansen, M. and Meier, P. (2010). IAPs: from caspase inhibitors to modulators of NF-κB, inflammation and cancer. *Nature Reviews Cancer*, *10*(8), pp.561-574.

Haas, K.L. and Franz, K.J. (2009). Application of metal coordination chemistry to explore and manipulate cell biology. *Chemical Reviews*, *109*(10), pp.4921-4960.

Hadjikakou, S.K., Ozturk, I.I., Xanthopoulou, M.N., Zachariadis, P.C., Zartilas, S., Karkabounas, S. and Hadjiliadis, N. (2008). Synthesis, structural characterization and biological study of new organotin (IV), silver (I) and antimony (III) complexes with thioamides. *Journal of Inorganic Biochemistry*, *102*(5), pp.1007-1015.

Hambley, T.W. (2007). Developing new metal-based therapeutics: challenges and opportunities. *Dalton Transactions*, (43), pp.4929-4937.

Hamilton, S.R. (2008). Targeted therapy of cancer: new roles for pathologists in colorectal cancer. *Modern Pathology*, *21*, pp.S23-S30.

Han, B., Nakamura, M., Mori, I., Nakamura, Y. and Kakudo, K. (2005). Urokinase-type plasminogen activator system and breast cancer (Review). *Oncology Reports*, *14*(1), pp.105-112.

Hanahan, D. and Weinberg, R.A. (2000). The hallmarks of cancer. *Cell*, *100*(1), pp.57-70.

Hanahan, D. and Weinberg, R.A. (2011). Hallmarks of cancer: the next generation. *Cell*, *144*(5), pp.646-674.

Hannon, M.J. (2007). Metal-based anticancer drugs: from a past anchored in platinum chemistry to a post-genomic future of diverse chemistry and biology. *Pure and Applied Chemistry*, *79*(12), pp.2243-2261.

Harris, C.C. (1996). Structure and function of the p53 tumor suppressor gene: clues for rational cancer therapeutic strategies. *Journal of the National Cancer Institute*, *88*(20), pp.1442-1455.

Hartinger, C.G., Zorbas-Seifried, S., Jakupec, M.A., Kynast, B., Zorbas, H. and Keppler, B.K. (2006). From bench to bedside–preclinical and early clinical development of the anticancer agent indazolium trans-[tetrachlorobis (1H-indazole) ruthenate (III)](KP1019 or FFC14A). *Journal of Inorganic Biochemistry*, *100*(5), pp.891-904.

Hassa, P.O. (2009). The molecular "Jekyll and Hyde" duality of PARP1 in cell death and cell survival. *Frontiers Bioscience, 14*, pp.72-111.

Haupt, Y., Maya, R., Kazaz, A. and Oren, M. (1997). Mdm2 promotes therapid degradation of p53. *Nature*, *387*(6630), pp.296-299.

Heffeter, P., Böck, K., Atil, B., Hoda, M.A.R., Körner, W., Bartel, C., Jungwirth, U., Keppler, B.K., Micksche, M., Berger, W. and Koellensperger, G. (2010). Intracellular protein binding patterns of the anticancer ruthenium drugs KP1019 and KP1339. *JBIC Journal of Biological Inorganic Chemistry*, *15*(5), pp.737-748.

Herbert, J.M., Lamarche, I. and Carmeliet, P. (1997). Urokinase and tissue-type plasminogen activator are required for the mitogenic and chemotactic effects of bovine fibroblast growth factor and platelet-derived growth factor-BB for vascular smooth muscle cells. *Journal of Biological Chemistry*, *272*(38), pp.23585-23591.

Hightower, L.E. (1991). Heat shock, stress proteins, chaperones, and proteotoxicity. *Cell*, *66*(2), pp.191-197.

Hill, M.M., Adrain, C., Duriez, P.J., Creagh, E.M. and Martin, S.J. (2004). Analysis of the composition, assembly kinetics and activity of native Apaf-1 apoptosomes. *The EMBO Journal*, *23*(10), pp.2134-2145.

Hoke, G.D., Rush, G.F., Bossard, G.F., McArdle, J.V., Jensen, B.D. and Mirabelli, C.K. (1988). Mechanism of alterations in isolated rat liver mitochondrial function induced by gold complexes of bidentate phosphines. *Journal of Biological Chemistry*, *263*(23), pp.11203-11210.

Holler, N., Zaru, R., Micheau, O., Thome, M., Attinger, A., Valitutti, S., Bodmer, J.L., Schneider, P., Seed, B. and Tschopp, J. (2000). Fas triggers an alternative, caspase-8–independent cell death pathway using the kinase RIP as effector molecule. *Nature Immunology*, *1*(6), pp.489-495.

Hollstein, M., Sidransky, D., Vogelstein, B. and Harris, C.C. (1991). p53 mutations in human cancers. *Science*, *253*(5015), pp.49-54.

Holmgren, A. (1985). Thioredoxin. *Annual Review of Biochemistry*, *54*(1), pp.237-271.

Housman, G., Byler, S., Heerboth, S., Lapinska, K., Longacre, M., Snyder, N. and Sarkar, S. (2014). Drug resistance in cancer: an overview. *Cancers*, *6*(3), pp.1769-1792.

Hsu, H., Xiong, J. and Goeddel, D.V. (1995). The TNF receptor 1-associated protein TRADD signals cell death and NF-κB activation. *Cell*, *81*(4), pp.495-504.

Hu, N. (1990). Genetic epidemiology of esophageal cancer: 10-year follow-up of 622 positive families in Yangcheng County. *Zhonghua yi Xue Za Zhi*, *70*(12), pp.679-81.

Hu, X.W., Duan, H.F., Duan, H.F., Pan, S.Y., Li, Y.M., Xi, Y., Zhao, S.R., Yin, L., Li, J.F., Chen, H.P. and Wu, C.T. (2008). Inhibition of tumor growth and metastasis by ATF-Fc, an engineered antibody targeting urokinase receptor. *Cancer Biology & Therapy*, *7*(5), pp.651-659.

Huang, R. and Liu, W. (2015). Identifying an essential role of nuclear LC3 for autophagy. *Autophagy*, *11*(5), pp.852-853.

Huang, R., Wallqvist, A. and Covell, D.G. (2005). Anticancer metal compounds in NCI's tumor-screening database: putative mode of action. *Biochemical Pharmacology*, *69*(7), pp.1009-1039.

Human, Z. (2013). Silver(I) phosphine compounds selectively induced apoptosis in SNO-oesophageal cancer cells and displayed antibacterial activity. M.Sc. Dissertation. University of Johannesburg. South Africa.

Human, Z., Munyaneza, A., Omondi, B., Sanabria, N.M., Meijboom, R. and Cronjé, M.J. (2015). The induction of cell death by phosphine silver (I) thiocyanate complexes in SNO-esophageal cancer cells. *BioMetals*, *28*(1), pp.219-228.

Humphreys, A.S., Filipovska, A., Berners-Price, S.J., Koutsantonis, G.A., Skelton, B.W. and White, A.H. (2007). Gold (I) chloride adducts of 1, 3-bis (di-2-pyridylphosphino) propane: synthesis, structural studies and antitumour activity. *Dalton Transactions*, (43), pp.4943-4950.

Hurd, A.M., Schiff, R., Parra, I., Friedrichs, W.E., Osborne, C.K., Morimoto, R.I., Hopp, T. and Fuqua, S.A.W. (2000). Heat shock protein 70 can modulate estrogen receptor activity in breast cancer cells. *Proceedings of the American Association for Cancer Research*, *41*, pp.73.

Husbeck, B. and Powis, G. (2002). The redox protein thioredoxin-1 regulates the constitutive and inducible expression of the estrogen metabolizing cytochromes P450 1B1 and 1A1 in MCF-7 human breast cancer cells. *Carcinogenesis*, *23*(10), pp.1625-1630.

Hynes, N.E. and MacDonald, G. (2009). ErbB receptors and signaling pathways in cancer. *Current Opinion in Cell Biology*, *21*(2), pp.177-184.

Hynes, R.O. (2002). Integrins: bidirectional, allosteric signaling machines. *Cell*, *110*(6), pp.673-687.

Ilson, D.H., Saltz, L., Enzinger, P., Huang, Y., Kornblith, A., Gollub, M., O'Reilly, E., Schwartz, G., DeGroff, J., Gonzalez, G. and Kelsen, D.P. (1999). Phase II trial of weekly irinotecan plus cisplatin in advanced esophageal cancer. *Journal of Clinical Oncology*, *17*(10), pp.3270-3275.

Jäättelä, M. (1999). Heat shock proteins as cellular lifeguards. *Annals of medicine*, *31*(4), pp.261-271.

Jackson, A., Davis, J., Pither, R.J., Rodger, A. and Hannon, M.J. (2001). Estrogen-derived steroidal metal complexes: agents for cellular delivery of metal centers to estrogen receptor-positive cells. *Inorganic Chemistry*, *40*(16), pp.3964-3973.

Jackson, J.G., Post, S.M. and Lozano, G. (2011). Regulation of tissue-and stimulus-specific cell fate decisions by p53 in vivo. *The Journal of Pathology*, *223*(2), pp.127-137.

Jagadish, N., Agarwal, S., Gupta, N., Fatima, R., Devi, S., Kumar, V., Suri, V., Kumar, R., Suri, V., Sadasukhi, T.C. and Gupta, A. (2016). Heat shock protein 70-2 (HSP70-2) overexpression in breast cancer. *Journal of Experimental & Clinical Cancer Research*, *35*(1), doi: 10.1186/s13046-016-0425-9.

Jänicke, R.U., Sprengart, M.L., Wati, M.R. and Porter, A.G. (1998). Caspase-3 is required for DNA fragmentation and morphological changes associated with apoptosis. *Journal of Biological Chemistry*, *273*(16), pp.9357-9360.

Jaskiewicz, F.E. (1987). Oesophageal and other main cancer patterns in four districts of Transkei, 1981-1984. *South African Medical Journal*, *72*(1), pp.27-30.

Javle, M. and Curtin, N.J. (2011). The role of PARP in DNA repair and its therapeutic exploitation. *British Journal of Cancer*, *105*(8), pp.1114-1122.

Jemal, A., Center, M.M., DeSantis, C. and Ward, E.M. (2010). Global patterns of cancer incidence and mortality rates and trends. *Cancer Epidemiology and Prevention Biomarkers*, *19*(8), pp.1893-1907.

Johnstone, T.C., Suntharalingam, K. and Lippard, S.J. (2015). Third row transition metals for the treatment of cancer. *Philosophical Transactions of the Royal Society of London A: Mathematical, Physical and Engineering Sciences*, *373*(2037), doi: 10.1098/rsta.2014.0185.

Joo, J.H., Alpatov, R., Munguba, G.C., Jackson, M.R., Hunt, M.E. and Sugrue, S.P. (2005). Reduction of Pnn by RNAi induces loss of cell-cell adhesion between human corneal epithelial cells. *Molecular Vision*, *11*(1), pp.133-142.

Jordan, V.C. (2003). Antiestrogens and selective estrogen receptor modulators as multifunctional medicines. 1. Receptor interactions. *Journal of Medicinal Chemistry*, *46*(6), pp.883-908.

Joza, N., Susin, S.A., Daugas, E., Stanford, W.L., Cho, S.K., Li, C.Y., Sasaki, T., Elia, A.J., Cheng, H.Y.M., Ravagnan, L. and Ferri, K.F. (2001). Essential role of the mitochondrial apoptosis-inducing factor in programmed cell death. *Nature*, *410*(6828), pp.549-554.

Jungwirth, U., Kowol, C.R., Keppler, B.K., Hartinger, C.G., Berger, W. and Heffeter, P. (2011). Anticancer activity of metal complexes: involvement of redox processes. *Antioxidants & Redox Signaling*, *15*(4), pp.1085-1127.

Kabeya, Y., Mizushima, N., Ueno, T., Yamamoto, A., Kirisako, T., Noda, T., Kominami, E., Ohsumi, Y. and Yoshimori, T. (2000). LC3, a mammalian homologue of yeast Apg8p, is localized in autophagosome membranes after processing. *The EMBO Journal*, *19*(21), pp.5720-5728.

Kang, M.H. and Reynolds, C.P. (2009). Bcl-2 inhibitors: targeting mitochondrial apoptotic pathways in cancer therapy. *Clinical Cancer Research*, *15*(4), pp.1126-1132.

Kang, R., Zeh, H.J., Lotze, M.T. and Tang, D. (2011). The Beclin 1 network regulates autophagy and apoptosis. *Cell Death & Differentiation*, *18*(4), pp.571-580.

Kapitza, S., Jakupec, M.A., Uhl, M., Keppler, B.K. and Marian, B. (2005). The heterocyclic ruthenium (III) complex KP1019 (FFC14A) causes DNA damage and oxidative stress in colorectal tumor cells. *Cancer Letters*, *226*(2), pp.115-121.

Kaplan, A., Ciftci, G.A. and Kutlu, H.M. (2015). Cytotoxic, anti-proliferative and apoptotic effects of silver nitrate against H-ras transformed 5RP7. *Cytotechnology*, pp.1-9.

Kathiresan, S., Dhivya, R., Vigneshwar, M., Rajasekaran, M., Ranjani, J., Rajendhran, J., Srinivasan, S., Mugesh, S., Murugan, M., Athappan, P. and Annaraj, J. (2016). Biological evaluation of redox stable cisplatin/Cu (II)-DNA adducts as potential anticancer agents. *Journal of Coordination Chemistry*, *69*(2), pp.238-252.

Katzenellenbogen, B.S. and Katzenellenbogen, J.A. (2002). Defining the" S" in SERMs. *Science*, *295*(5564), pp.2380-2381.

Kaufmann, S.H., Desnoyers, S., Ottaviano, Y., Davidson, N.E. and Poirier, G.G. (1993). Specific proteolytic cleavage of poly (ADP-ribose) polymerase: an early marker of chemotherapy-induced apoptosis. *Cancer Research*, *53*(17), pp.3976-3985.

Kaufmann, S.H. and Earnshaw, W.C. (2000). Induction of apoptosis by cancer chemotherapy. *Experimental Cell Research*, *256*(1), pp.42-49.

Kawanishi, K., Shiozaki, H., Doki, Y., Sakita, I., Inoue, M., Yano, M., Tsujinaka, T., Shamma, A. and Monden, M. (1999). Prognostic significance of heat shock proteins 27 and 70 in patients with squamous cell carcinoma of the esophagus. *Cancer*, *85*(8), pp.1649-1657.

Kelland, L.R., Mistry, P., Abel, G., Loh, S.Y., O'Neill, C.F., Murrer, B.A. and Harrap, K.R. (1992). Mechanism-related circumvention of acquired cis-diamminedichloroplatinum (II) resistance using two pairs of human ovarian carcinoma cell lines by ammine/amine platinum (IV) dicarboxylates. *Cancer Research*, *52*(14), pp.3857-3864.

Kelly, J.M., Feeney, M.M., Tossi, A.B., Lecomte, J.P. and Kirsch-De Mesmaeker, A. (1990). Interaction of tetra-azaphenanthrene ruthenium complexes with DNA and oligonucleotides. A photophysical and photochemical investigation. *Anti-cancer Drug Design*, *5*(1), pp.69-75.

Kelly, L.A., Seidlova-Wuttke, D., Wuttke, W., O'Leary, J.J. and Norris, L.A. (2014). Estrogen receptor alpha augments changes in hemostatic gene expression in HepG2 cells treated with estradiol and phytoestrogens. *Phytomedicine*, *21*(2), pp.155-158.

Kelsen, D.P., Ginsberg, R., Pajak, T.F., Sheahan, D.G., Gunderson, L., Mortimer, J., Estes, N., Haller, D.G., Ajani, J., Kocha, W. and Minsky, B.D. (1998). Chemotherapy followed by surgery compared with surgery alone for localized esophageal cancer. *New England Journal of Medicine*, *339*(27), pp.1979-1984.

Kerr, J.F., Winterford, C.M. and Harmon, B.V. (1994). Apoptosis. Its significance in cancer and cancer therapy. *Cancer*, *73*(8), pp.2013-2026.

Kerr, J.F., Wyllie, A.H. and Currie, A.R. (1972). Apoptosis: a basic biological phenomenon with wide-ranging implications in tissue kinetics. *British Journal of Cancer*, *26*(4), pp.239-257.

Khodapasand, E., Jafarzadeh, N., Farrokhi, F., Kamalidehghan, B. and Houshmand, M. (2015). Is Bax/Bcl-2 ratio considered as a prognostic marker with age and tumor location in colorectal cancer?. *Iranian Biomedical Journal*, *19*(2), pp.69-75.

Kiang, J.G. and Tsokos, G.C. (1998). Heat shock protein 70 kDa: molecular biology, biochemistry, and physiology. *Pharmacology & Therapeutics*, *80*(2), pp.183-201.

Kim, J. and Klionsky, D.J., 2000. Autophagy, cytoplasm-to-vacuole targeting pathway, and pexophagy in yeast and mammalian cells. *Annual Review of Biochemistry*, *69*(1), pp.303-342.

Kischkel, F.C., Hellbardt, S., Behrmann, I., Germer, M., Pawlita, M., Krammer, P.H. and Peter, M.E. (1995). Cytotoxicity-dependent APO-1 (Fas/CD95)-associated proteins form a death-inducing signaling complex (DISC) with the receptor. *The EMBO Journal*, *14*(22), p.5579.

Klionsky, D.J. and Emr, S.D. (2000). Autophagy as a regulated pathway of cellular degradation. *Science*, *290*(5497), pp.1717-1721.

Knowlton, A.A. and Salfity, M. (1996). Nuclear localization and the heat shock proteins. *Journal of Biosciences*, *21*(2), pp.123-132.

Kochanek, K.D., Xu, J., Murphy, S.L., Miniño, A.M. and Kung, H.C. (2011). Deaths: final data for 2009. *National vital statistics reports: from the Centers for Disease Control and Prevention, National Center for Health Statistics, National Vital Statistics System*, *60*(3), pp.1-116.

Krajewski, S., Krajewska, M., Ellerby, L.M., Welsh, K., Xie, Z., Deveraux, Q.L., Salvesen, G.S., Bredesen, D.E., Rosenthal, R.E., Fiskum, G. and Reed, J.C. (1999). Release of caspase-9 from mitochondria during neuronal apoptosis and cerebral ischemia. *Proceedings of the National Academy of Sciences*, *96*(10), pp.5752-5757.

Kriel, F.H. and Coates, J. (2012). Synthesis and antitumour activity of gold (I) and silver (I) complexes of hydrazine-bridged diphosphine ligands. *South African Journal of Chemistry*, *65*, pp.271-279.

Kroemer, G., Galluzzi, L. and Brenner, C. (2007). Mitochondrial membrane permeabilization in cell death. *Physiological Reviews*, *87*(1), pp.99-163.

Kroemer, G., Galluzzi, L., Vandenabeele, P., Abrams, J., Alnemri, E.S., Baehrecke, E.H., Blagosklonny, M.V., El-Deiry, W.S., Golstein, P., Green, D.R. and Hengartner, M. (2009). Classification of cell death: recommendations of the Nomenclature Committee on Cell Death 2009. *Cell Death & Differentiation*, *16*(1), pp.3-11.

Kroemer, G., Zamzami, N. and Susin, S.A. (1997). Mitochondrial control of apoptosis. *Immunology Today*, *18*(1), pp.44-51.

Kubiczkova, L., Sedlarikova, L., Hajek, R. and Sevcikova, S. (2012). TGF-β–an excellent servant but a bad master. *Journal of Translational Medicine*, *10*(1), doi**:** 10.1186/1479-5876-10-183.

Kumar, R., Wang, R.A. and Bagheri-Yarmand, R. (2003), October. Emerging roles of MTA family members in human cancers. *Seminars in Oncology*, *30*, pp.30-37.

Kumtepe, Y., Halici, Z., Sengul, O., Kunak, C.S., Bayir, Y., Kilic, N., Cadirci, E., Pulur, A. and Bayraktutan, Z. (2013). High serum HTATIP2/TIP30 level in serous ovarian cancer as prognostic or diagnostic marker. *European Journal of Medical Research*, *18*(1), doi: 10.1186/2047-783X-18-18.

Kuwahara, D., Tsutsumi, K., Kobayashi, T., Hasunuma, T. and Nishioka, K. (2000). Caspase-9 regulates cisplatin-induced apoptosis in human head and neck squamous cell carcinoma cells. *Cancer Letters*, *148*(1), pp.65-71.

Kuwano, H., Kato, H., Miyazaki, T., Fukuchi, M., Masuda, N., Nakajima, M., Fukai, Y., Sohda, M., Kimura, H. and Faried, A. (2005). Genetic alterations in esophageal cancer. *Surgery Today*, *35*(1), pp.7-18.

Kyros, L., Banti, C.N., Kourkoumelis, N., Kubicki, M., Sainis, I. and Hadjikakou, S.K. (2014). Synthesis, characterization, and binding properties towards CT-DNA and lipoxygenase of mixed-ligand silver(I) complexes with 2-mercaptothiazole and its derivatives and triphenylphosphine. *Journal of Biological Inorganic Chemistry*, *19*, pp.449-464, doi:10.1007/s00775-014-1089-6.

Kyros, L., Kourkoumelis, N., Kubicki, M., Male, L., Hursthouse, M.B., Verginadis, I.I., Gouma, E., Karkabounas, S., Charalabopoulos, K. and Hadjikakou, S.K. (2010). Structural properties, cytotoxicity, and anti-inflammatory activity of silver (I) complexes with tris (p-tolyl) phosphine and 5-chloro-2-mercaptobenzothiazole. *Bioinorganic Chemistry and Applications*, doi: 10.1155/2010/386860.

Larisch, S., Yi, Y., Lotan, R., Kerner, H., Eimerl, S., Parks, W.T., Gottfried, Y., Reffey, S.B., De Caestecker, M.P., Danielpour, D. and Book-Melamed, N. (2000). A novel mitochondrial septin-like protein, ARTS, mediates apoptosis dependent on its P-loop motif. *Nature Cell Biology*, *2*(12), pp.915-921.

Lavrik, I.N. (2011). Regulation of death receptor-induced apoptosis induced via CD95/FAS and other death receptors. *Molecular Biology*, *45*(1), pp.150-155.

Lebrun, J.J. (2012). The dual role of TGF in human cancer: from tumor suppression to cancer metastasis. *ISRN Molecular Biology*, doi: 10.5402/2012/381428.

Lee, E., Mun, G.H., Oh, C.S., Chung, Y.H., Lee, Y.S. and Shin, D.H. (2004). A subcellular distribution of estrogen receptor-alpha is changed during artificially induced senescence of PC12 pheochromocytoma cells. *Neuroscience Letters*, *372*(1), pp.80-84.

Lee, H.R., Kim, T.H. and Choi, K.C. (2012a). Functions and physiological roles of two types of estrogen receptors, ERα and ERβ, identified by estrogen receptor knockout mouse. *Laboratory Animal Research*, *28*(2), pp.71-76.

Lee, K.B., Wang, D., Lippard, S.J. and Sharp, P.A. (2002). Transcription-coupled and DNA damage-dependent ubiquitination of RNA polymerase II in vitro. *Proceedings of the National Academy of Sciences*, *99*(7), pp.4239-4244.

Lee, K.W., Kim, J.H., Han, S., Sung, C.O., Do, I.G., Ko, Y.H., Um, S.H. and Kim, S.H. (2012b). Twist1 is an independent prognostic factor of esophageal squamous cell carcinoma and associated with its epithelial–mesenchymal transition. *Annals of Surgical Oncology*, *19*(1), pp.326-335.

Lei, C., Zhang, W., Fan, J., Qiao, B., Chen, Q., Liu, Q. and Zhao, C. (2015). MDM2 T309G polymorphism and esophageal cancer risk: a meta-analysis. *International Journal of Clinical and Experimental Medicine*, *8*(8), pp.13413-13416.

Letai, A., Bassik, M.C., Walensky, L.D., Sorcinelli, M.D., Weiler, S. and Korsmeyer, S.J. (2002). Distinct BH3 domains either sensitize or activate mitochondrial apoptosis, serving as prototype cancer therapeutics. *Cancer Cell*, *2*(3), pp.183-192.

Li, B., Li, Y.Y., Tsao, S.W. and Cheung, A.L. (2009). Targeting NF-κB signaling pathway suppresses tumor growth, angiogenesis, and metastasis of human esophageal cancer. *Molecular Cancer Therapeutics*, *8*(9), pp.2635-2644.

Li, L.Y., Luo, X. and Wang, X. (2001). Endonuclease G is an apoptotic DNase when released from mitochondria. *Nature*, *412*(6842), pp.95-99.

Li, P., Nijhawan, D., Budihardjo, I., Srinivasula, S.M., Ahmad, M., Alnemri, E.S. and Wang, X. (1997). Cytochrome c and dATP-dependent formation of Apaf-1/caspase-9 complex initiates an apoptotic protease cascade. *Cell*, *91*(4), pp.479-489.

Li, Y.L., Qin, Q.P., An, Y.F., Liu, Y.C., Huang, G.B., Luo, X.J. and Zhang, G.H. (2014). Study on potential antitumor mechanism of quinoline-based silver (I) complexes: Synthesis, structural characterization, cytotoxicity, cell cycle and caspase-initiated apoptosis. *Inorganic Chemistry Communications*, *40*, pp.73-77.

Liang, Y., Yan, C. and Schor, N.F. (2001). Apoptosis in the absence of caspase 3. *Oncogene*, *20*(45), pp.6570-6578.

Liberti, M.V. and Locasale, J.W. (2016). The Warburg effect: how does it benefit cancer cells?. *Trends in Biochemical Sciences*, *41*(3), pp.211-218.

Liehr, J.G., Wan-Fen, F., Sirbasku, D.A. and Ari-Ulubelen, A. (1986). Carcinogenicity of catechol estrogens in Syrian hamsters. *Journal of Steroid Biochemistry*, *24*(1), pp.353-356.

Linhares, M.M., Affonso Jr, R.J., de Souza Viana, L., Silva, S.R.M., Denadai, M.V.A., de Toledo, S.R.C. and Matos, D. (2015). Genetic and Immunohistochemical Expression of Integrins ITGAV, ITGA6, and ITGA3 As Prognostic Factor for Colorectal Cancer: Models for Global and Disease-Free Survival. *PloS One*, *10*(12), doi: 10.1371/journal.pone.0144333.

Lippert, B. (1999). *Cisplatin: chemistry and biochemistry of a leading anticancer drug*. John Wiley & Sons.

Liu, D., Ghiso, J.A.A., Estrada, Y. and Ossowski, L. (2002). EGFR is a transducer of the urokinase receptor initiated signal that is required for in vivo growth of a human carcinoma. *Cancer Cell*, *1*(5), pp.445-457.

Liu, J.J., Galettis, P., Farr, A., Maharaj, L., Samarasinha, H., McGechan, A.C., Baguley, B.C., Bowen, R.J., Berners-Price, S.J. and McKeage, M.J. (2008). *In vitro* antitumour and hepatotoxicity profiles of Au (I) and Ag (I) bidentate pyridyl phosphine complexes and relationships to cellular uptake. *Journal of Inorganic Biochemistry*, *102*(2), pp.303-310.

Liu, Y.P., Shan, B.E., Wang, X.L. and Ma, L. (2012). Correlation between MTA2 overexpression and tumour progression in esophageal squamous cell carcinoma. *Experimental and Therapeutic Medicine*, *3*(4), pp.745-749.

Lockshin, R.A. and Williams, C.M. (1964). Programmed cell death—II. Endocrine potentiation of the breakdown of the intersegmental muscles of silkmoths. *Journal of Insect Physiology*, *10*(4), pp.643-649.

Locksley, R.M., Killeen, N. and Lenardo, M.J. (2001). The TNF and TNF receptor superfamilies: integrating mammalian biology. *Cell*, *104*(4), pp.487-501.

Loeffler, M. and Kroemer, G. (2000). The mitochondrion in cell death control: certainties and incognita. *Experimental Cell Research*, *256*(1), pp.19-26.

Loman, N., Johannsson, O., Bendahl, P.O., Borg, Å., Fernö, M. and Olsson, H. (1998). Steroid receptors in hereditary breast carcinomas associated with BRCA1 or BRCA2 mutations or unknown susceptibility genes. *Cancer*, *83*(2), pp.310-319.

Lopez, J., John, S.W., Tenev, T., Rautureau, G.J., Hinds, M.G., Francalanci, F., Wilson, R., Broemer, M., Santoro, M.M., Day, C.L. and Meier, P. (2011). CARD-mediated autoinhibition of cIAP1's E3 ligase activity suppresses cell proliferation and migration. *Molecular Cell*, *42*(5), pp.569-583.

Los, M., Mozoluk, M., Ferrari, D., Stepczynska, A., Stroh, C., Renz, A., Herceg, Z., Wang, Z.Q. and Schulze-Osthoff, K. (2002). Activation and caspase-mediated inhibition of PARP: a molecular switch between fibroblast necrosis and apoptosis in death receptor signaling. *Molecular Biology of the Cell*, *13*(3), pp.978-988.

Lu, J. and Holmgren, A. (2009). Selenoproteins. *Journal of Biological Chemistry*, *284*(2), pp.723-727.

Lu, J. and Holmgren, A. (2014). The thioredoxin antioxidant system. *Free Radical Biology and Medicine*, *66*, pp.75-87.

Luo, X., Budihardjo, I., Zou, H., Slaughter, C. and Wang, X. (1998). Bid, a Bcl2 interacting protein, mediates cytochrome c release from mitochondria in response to activation of cell surface death receptors. *Cell*, *94*(4), pp.481-490.

Ma, C.X., Janetka, J.W. and Piwnica-Worms, H. (2011). Death by releasing the breaks: CHK1 inhibitors as cancer therapeutics. *Trends in Molecular Medicine*, *17*(2), pp.88-96.

Maestro, R., Dei Tos, A.P., Hamamori, Y., Krasnokutsky, S., Sartorelli, V., Kedes, L., Doglioni, C., Beach, D.H. and Hannon, G.J. (1999). Twist is a potential oncogene that inhibits apoptosis. *Genes & Development*, *13*(17), pp.2207-2217.

Makrilia, N., Kollias, A., Manolopoulos, L. and Syrigos, K. (2009). Cell adhesion molecules: role and clinical significance in cancer. *Cancer Investigation*, *27*(10), pp.1023-1037.

Manavathi, B., Singh, K. and Kumar, R. (2007). MTA family of coregulators in nuclear receptor biology and pathology. *Nuclear Receptor Signaling*, *5*(10), pp.1621-1629.

Marcsek, Z., Kocsis, Z., Jakab, M., Szende, B. and Tompa, A. (2004). The efficacy of tamoxifen in estrogen receptor-positive breast cancer cells is enhanced by a medical nutriment. *Cancer Biotherapy & Radiopharmaceuticals*, *19*(6), pp.746-753.

Martin, K., Trouche, D., Hagemeier, C., Sørensen, T.S., La Thangue, N.B. and Kouzarides, T. (1995b). Stimulation of E2F1/DP1 transcriptional activity by MDM2 oncoprotein. *Nature*, *375*(6533), pp.691-694.

Martin, M.B., Reiter, R., Pham, T., Avellanet, Y.R., Camara, J., Lahm, M., Pentecost, E., Pratap, K., Gilmore, B.A., Divekar, S. and Dagata, R.S. (2003). Estrogen-like activity of metals in MCF-7 breast cancer cells. *Endocrinology*, *144*(6), pp.2425-2436.

Martin, S., Reutelingsperger, C.P., McGahon, A.J., Rader, J.A., Van Schie, R.C., LaFace, D.M. and Green, D.R. (1995a). Early redistribution of plasma membrane phosphatidylserine is a general feature of apoptosis regardless of the initiating stimulus: inhibition by overexpression of Bcl-2 and Abl. *The Journal of Experimental Medicine*, *182*(5), pp.1545-1556.

Martin, S.J. and Green, D.R. (1995). Protease activation during apoptosis: death by a thousand cuts?. *Cell*, *82*(3), pp.349-352.

Martinez, V.G., O'connor, R., Liang, Y. and Clynes, M. (2008). CYP1B1 expression is induced by docetaxel: effect on cell viability and drug resistance. *British Journal of Cancer*, *98*(3), pp.564-570.

Martins, L.M., Iaccarino, I., Tenev, T., Gschmeissner, S., Totty, N.F., Lemoine, N.R., Savopoulos, J., Gray, C.W., Creasy, C.L., Dingwall, C. and Downward, J. (2002). The serine protease Omi/HtrA2 regulates apoptosis by binding XIAP through a reaper-like motif. *Journal of Biological Chemistry*, *277*(1), pp.439-444.

Marzagalli, M., Casati, L., Moretti, R.M., Marelli, M.M. and Limonta, P. (2015). Estrogen Receptor β Agonists Differentially Affect the Growth of Human Melanoma Cell Lines. *PloS One*, *10*(7), doi: 10.1371/journal.pone.0134396.

Marzano, C., Gandin, V., Folda, A., Scutari, G., Bindoli, A. and Rigobello, M.P. (2007). Inhibition of thioredoxin reductase by auranofin induces apoptosis in cisplatin-resistant human ovarian cancer cells. *Free Radical Biology and Medicine*, *42*(6), pp.872-881.

Marzano, C., Gandin, V., Pellei, M., Colavito, D., Papini, G., Lobbia, G.G., Del Giudice, E., Porchia, M., Tisato, F. and Santini, C. (2008). In vitro antitumor activity of the water soluble copper (I) complexes bearing the tris (hydroxymethyl) phosphine ligand. *Journal of Medicinal Chemistry*, *51*(4), pp.798-808.

Marzban, H., Del Bigio, M.R., Alizadeh, J., Ghavami, S., Zachariah, R.M. and Rastegar, M. (2015). Cellular commitment in the developing cerebellum. *Frontiers in Cellular Neuroscience*, doi: 10.3389/fncel.2014.00450.

McFadyen, M.C., McLeod, H.L., Jackson, F.C., Melvin, W.T., Doehmer, J. and Murray, G.I. (2001). Cytochrome P450 CYP1B1 protein expression: A novel mechanism of anticancer drug resistance11Abbreviations: CYP, cytochrome P450; ANF, alpha-naphthoflavone; MTT, 3-[4, 5-dimethylthiazol-2yl]-2, 5-diphenyltetrazolium bromide; and 5-FU, 5-fluorouracil. *Biochemical Pharmacology*, *62*(2), pp.207-212.

Mc Gee, M.M., Hyland, E., Campiani, G., Ramunno, A., Nacci, V. and Zisterer, D.M. (2002). Caspase-3 is not essential for DNA fragmentation in MCF-7 cells during apoptosis induced by the pyrrolo-1, 5-benzoxazepine, PBOX-6. *FEBS Letters*, *515*(1-3), pp.66-70.

McKeage, M.J., Berners-Price, S.J., Galettis, P., Bowen, R.J., Brouwer, W., Ding, L., Zhuang, L. and Baguley, B.C. (2000). Role of lipophilicity in determining cellular uptake and antitumour activity of gold phosphine complexes. *Cancer Chemotherapy and Pharmacology*, *46*(5), pp.343-350.

McKeage, M.J., Papathanasiou, P., Salem, G., Sjaarda, A., Swiegers, G.F., Waring, P. and Wild, S.B. (1998). Antitumor activity of gold (I), silver (I) and copper (I) complexes containing chiral tertiary phosphines. *Metal-Based Drugs*, *5*, pp.217-224.

Medema, R.H. and Macůrek, L. (2012). Checkpoint control and cancer. *Oncogene*, *31*(21), pp.2601-2613.

Medici, S., Peana, M., Crisponi, G., Nurchi, V.M., Lachowicz, J.I., Remelli, M. and Zoroddu, M.A. (2016). Silver coordination compounds: a new horizon in medicine. *Coordination Chemistry Reviews, 327-328*, pp.349-359.

Meggers, E. (2009). Targeting proteins with metal complexes. *Chemical Communications*, (9), pp.1001-1010.

Meijboom, R., Bowen, R.J. and Berners-Price, S.J. (2009). Coordination complexes of silver (I) with tertiary phosphine and related ligands. *Coordination Chemistry Reviews*, *253*(3), pp.325-342.

Mekkawy, A.H., Pourgholami, M.H. and Morris, D.L. (2014). Involvement of Urokinase-Type Plasminogen Activator System in Cancer: An Overview. *Medicinal Research Reviews*, *34*(5), pp.918-956.

Micheau, O. and Tschopp, J. (2003). Induction of TNF receptor I-mediated apoptosis via two sequential signaling complexes. *Cell*, *114*(2), pp.181-190.

Michels, J., Obrist, F., Castedo, M., Vitale, I. and Kroemer, G. (2014). PARP and other prospective targets for poisoning cancer cell metabolism. *Biochemical Pharmacology*, *92*(1), pp.164-171.

Milacic, V. and Dou, Q.P. (2009). The tumor proteasome as a novel target for gold (III) complexes: implications for breast cancer therapy. *Coordination Chemistry Reviews*, *253*(11), pp.1649-1660.

Mirabelli, C.K., Johnson, R.K., Sung, C.M., Faucette, L., Muirhead, K. and Crooke, S.T. (1985). Evaluation of the in vivo antitumor activity and in vitro cytotoxic properties of auranofin, a coordinated gold compound, in murine tumor models. *Cancer Research*, *45*(1), pp.32-39.

Mishra, N.K., Agarwal, S. and Raghava, G.P. (2010). Prediction of cytochrome P450 isoform responsible for metabolizing a drug molecule. *BMC Pharmacology*, *10*(1), doi: 10.1186/1471-2210-10-8.

Mizushima, N. (2004). Methods for monitoring autophagy. *The International Journal of Biochemistry & Cell Biology*, *36*(12), pp.2491-2502.

Mizushima, N. (2007). Autophagy: process and function. *Genes & Development*, *21*(22), pp.2861-2873.

Momand, J., Jung, D., Wilczynski, S. and Niland, J. (1998). The MDM2 gene amplification database. *Nucleic Acids Research*, *26*(15), pp.3453-3459.

Monti, E., Gariboldi, M., Maiocchi, A., Marengo, E., Cassino, C., Gabano, E. and Osella, D. (2005). Cytotoxicity of cis-platinum (II) conjugate models. The effect of chelating arms and leaving groups on cytotoxicity: a quantitative structure− activity relationship approach. *Journal of Medicinal Chemistry*, *48*(3), pp.857-866.

Morimoto, R.I. (1998). Regulation of the heat shock transcriptional response: cross talk between a family of heat shock factors, molecular chaperones, and negative regulators. *Genes & Development*, *12*(24), pp.3788-3796.

Morrissey, D., O'Connell, J., Lynch, D., O'Sullivan, G.C., Shanahan, F. and Collins, J.K. (1999). Invasion by esophageal cancer cells: functional contribution of the urokinase plasminogen activation system, and inhibition by antisense oligonucleotides to urokinase or urokinase receptor. *Clinical & Experimental Metastasis*, *17*(1), pp.87-95.

Mosser, D.D., Caron, A.W., Bourget, L., Meriin, A.B., Sherman, M.Y., Morimoto, R.I. and Massie, B. (2000). The chaperone function of hsp70 is required for protection against stress-induced apoptosis. *Molecular and Cellular Biology*, *20*(19), pp.7146-7159.

Moubarak, R.S., Yuste, V.J., Artus, C., Bouharrour, A., Greer, P.A., Menissier-de Murcia, J. and Susin, S.A. (2007). Sequential activation of poly (ADP-ribose) polymerase 1, calpains, and Bax is essential in apoptosis-inducing factor-mediated programmed necrosis. *Molecular and Cellular Biology*, *27*(13), pp.4844-4862.

Muller, P.A. and Vousden, K.H. (2013). p53 mutations in cancer. *Nature Cell Biology*, *15*(1), pp.2-8.

Murata, M., Gong, P., Suzuki, K. and Koizumi, S. (1999). Differential metal response and regulation of human heavy metal-inducible genes. *Journal of Cellular Physiology*, *180*(1), pp.105-113.

Murphy, M.P. (2009). How mitochondria produce reactive oxygen species. *Biochemical Journal*, *417*(1), pp.1-13.

Murray, G.I., Taylor, M.C., McFadyen, M.C., McKay, J.A., Greenlee, W.F., Burke, M.D. and Melvin, W.T. (1997). Tumor-specific expression of cytochrome P450 CYP1B1. *Cancer Research*, *57*(14), pp.3026-3031.

Nahta, R., Hortobagyi, G.N. and Esteva, F.J. (2003). Growth factor receptors in breast cancer: potential for therapeutic intervention. *The Oncologist*, *8*(1), pp.5-17.

Naismith, J.H. and Sprang, S.R. (1998). Modularity in the TNF-receptor family. *Trends in Biochemical Sciences*, *23*(2), pp.74-79.

Nasrollahzadeh, D., Kamangar, F., Aghcheli, K., Sotoudeh, M., Islami, F., Abnet, C.C., Shakeri, R., Pourshams, A., Marjani, H.A., Nouraie, M. and Khatibian, M. (2008). Opium, tobacco, and alcohol use in relation to oesophageal squamous cell carcinoma in a high-risk area of Iran. *British Journal of Cancer*, *98*(11), pp.1857-1863.

Nath, N.S., Bhattacharya, I., Tuck, A.G., Schlipalius, D.I. and Ebert, P.R. (2011). Mechanisms of phosphine toxicity. *Journal of Toxicology*, *2011*.

Neuner, G., Patel, A. and Suntharalingam, M. (2009). Chemoradiotherapy for esophageal cancer. *Gastrointestinal Cancer Research*, *3*(2), pp.57-65.

Niu, P., Liu, L., Gong, Z., Tan, H., Wang, F., Yuan, J., Feng, Y., Wei, Q., Tanguay, R.M. and Wu, T. (2006). Overexpressed heat shock protein 70 protects cells against DNA damage caused by ultraviolet C in a dose-dependent manner. *Cell stress & Chaperones*, *11*(2), pp.162-169.

Noda, T. and Ohsumi, Y. (1998). Tor, a phosphatidylinositol kinase homologue, controls autophagy in yeast. *Journal of Biological Chemistry*, *273*(7), pp.3963-3966.

Norbury, C.J. and Hickson, I.D. (2001). Cellular responses to DNA damage. *Annual Review of Pharmacology and Toxicology*, *41*(1), pp.367-401.

Ogier-Denis, E., Houri, J.J., Bauvy, C. and Codogno, P. (1996). Guanine nucleotide exchange on heterotrimeric Gi3 protein controls autophagic sequestration in HT-29 cells. *Journal of Biological Chemistry*, *271*(45), pp.28593-28600.

Oliner, J.D., Kinzler, K.W., Meltzer, P.S., George, D.L. and Vogelstein, B. (1992). Amplification of a gene encoding a p53-associated protein in human sarcomas. *Nature*, *358*(6381), pp.80-83.

Oliver, F.J., Menissier-de Murcia, J. and de Murcia, G. (1999). Poly (ADP-ribose) polymerase in the cellular response to DNA damage, apoptosis, and disease. *The American Journal of Human Genetics*, *64*(5), pp.1282-1288.

Orvig, C. and Abrams, M.J. (1999). Medicinal inorganic chemistry: introduction. *Chemical Reviews*, *99*(9), pp.2201-2204.

Osbild, S., Brault, L., Battaglia, E. and Bagrel, D. (2006). Resistance to cisplatin and adriamycin is associated with the inhibition of glutathione efflux in MCF-7-derived cells. *Anticancer Research*, *26*(5A), pp.3595-3600.

Ott, I. (2009). On the medicinal chemistry of gold complexes as anticancer drugs. *Coordination Chemistry Reviews*, *253*(11), pp.1670-1681.

Ott, M., Robertson, J.D., Gogvadze, V., Zhivotovsky, B. and Orrenius, S. (2002). Cytochrome *c* release from mitochondria proceeds by a two-step process. *Proceedings of the National Academy of Sciences*, *99*(3), pp.1259-1263.

Ouyang, L., Shi, Z., Zhao, S., Wang, F.T., Zhou, T.T., Liu, B. and Bao, J.K. (2012). Programmed cell death pathways in cancer: a review of apoptosis, autophagy and programmed necrosis. *Cell Proliferation*, *45*(6), pp.487-498.

Ouyang, P. and Sugrue, S.P. (1996). Characterization of pinin, a novel protein associated with the desmosome-intermediate filament complex. *The Journal of Cell Biology*, *135*(4), pp.1027-1042.

Packham, G. and Stevenson, F.K. (2005). Bodyguards and assassins: Bcl-2 family proteins and apoptosis control in chronic lymphocytic leukaemia. *Immunology*, *114*(4), pp.441-449.

Pacor, S., Zorzet, S., Cocchietto, M., Bacac, M., Vadori, M., Turrin, C., Gava, B., Castellarin, A. and Sava, G. (2004). Intratumoral NAMI-A treatment triggers metastasis reduction, which correlates to CD44 regulation and tumor infiltrating lymphocyte recruitment. *Journal of Pharmacology and Experimental Therapeutics*, *310*(2), pp.737-744.

Papp, L.V., Lu, J., Holmgren, A. and Khanna, K.K. (2007). From selenium to selenoproteins: synthesis, identity, and their role in human health. *Antioxidants & Redox Signaling*, *9*(7), pp.775-806.

Pattingre, S., Espert, L., Biard-Piechaczyk, M. and Codogno, P. (2008). Regulation of macroautophagy by mTOR and Beclin 1 complexes. *Biochimie*, *90*(2), pp.313-323.

Pearce, S.T. and Jordan, V.C. (2004). The biological role of estrogen receptors α and β in cancer. *Critical Reviews in Oncology/Hematology*, *50*(1), pp.3-22.

Pelgrift, R.Y. and Friedman, A.J. (2013). Nanotechnology as a therapeutic tool to combat microbial resistance. *Advanced Drug Delivery Reviews*, *65*(13), pp.1803-1815.

Peter, M.E. and Krammer, P.H. (1998). Mechanisms of CD95 (APO-1/Fas)-mediated apoptosis. *Current Opinion in Immunology*, *10*(5), pp.545-551.

Peters, W.H. and Roelofs, H.M. (1992). Biochemical characterization of resistance to mitoxantrone and adriamycin in Caco-2 human colon adenocarcinoma cells: a possible role for glutathione S-transferases. *Cancer Research*, *52*(7), pp.1886-1890.

Petiot, A., Ogier-Denis, E., Blommaart, E.F., Meijer, A.J. and Codogno, P. (2000). Distinct classes of phosphatidylinositol 3'-kinases are involved in signaling pathways that control macroautophagy in HT-29 cells. *Journal of Biological Chemistry*, *275*(2), pp.992-998.

Pettinari, C., Marchetti, F., Lupidi, G., Quassinti, L., Bramucci, M., Petrelli, D., Vitali, L.A., Guedes da Silva, M.F.C., Martins, L.M., Smolenski, P. and Pombeiro, A.J. (2011). Synthesis, antimicrobial and antiproliferative activity of novel silver (I) tris (pyrazolyl) methanesulfonate and 1, 3, 5-triaza-7-phosphadamantane complexes. *Inorganic Chemistry*, *50*(21), pp.11173-11183.

Pickens, A. and Orringer, M.B. (2003). Geographical distribution and racial disparity in esophageal cancer. *The Annals of Thoracic Surgery*, *76*(4), pp.S1367-S1369.

Pisani, P., Parkin, D.M. and Ferlay, J. (1993). Estimates of the worldwide mortality from eighteen major cancers in 1985. Implications for prevention and projections of future burden. *International Journal of Cancer*, *55*(6), pp.891-903.

Plimack, E.R., Dunbrack, R.L., Brennan, T.A., Andrake, M.D., Zhou, Y., Serebriiskii, I.G., Slifker, M., Alpaugh, K., Dulaimi, E., Palma, N. and Hoffman-Censits, J. (2015). Defects in DNA repair genes predict response to neoadjuvant cisplatin-based chemotherapy in muscle-invasive bladder cancer. *European Urology*, *68*(6), pp.959-967.

Pluim, D., van Waardenburg, R.C., Beijnen, J.H. and Schellens, J.H. (2004). Cytotoxicity of the organic ruthenium anticancer drug Nami-A is correlated with DNA binding in four different human tumor cell lines. *Cancer Chemotherapy and Pharmacology*, *54*(1), pp.71-78.

Porchia, M., Dolmella, A., Gandin, V., Marzano, C., Pellei, M., Peruzzo, V., Refosco, F., Santini, C. and Tisato, F. (2013). Neutral and charged phosphine/scorpionate copper (I) complexes: Effects of ligand assembly on their antiproliferative activity. *European Journal of Medicinal Chemistry*, *59*, pp.218-226.

Potgieter, K., Cronjé, M.J. and Meijboom, R. (2015). Synthesis and characterisation of silver (I) benzyldiphenylphosphine complexes: Towards the biological evaluation on SNO cells. *Inorganica Chimica Acta*, *437*, pp.195-200.

Potgieter, K., Cronjé, M.J. and Meijboom, R. (2016). Synthesis of silver (I) p-substituted phenyl diphenyl phosphine complexes with the evaluation of the toxicity on a SNO cancer cell line. *Inorganica Chimica Acta*, *453*, pp.443-451.

Poyraz, M., Banti, C.N., Kourkoumelis, N., Dokorou, V., Manos, M.J., Simčič, M., Golič-Grdadolnik, S., Mavromoustakos, T., Giannoulis, A.D., Verginadis, I.I. and Charalabopoulos, K. (2011). Synthesis, structural characterization and biological studies of novel mixed ligand Ag (I) complexes with triphenylphosphine and aspirin or salicylic acid. *Inorganica Chimica Acta*, *375*(1), pp.114-121.

Pressl, M.F., Cordon-Cardo, C. and Slamon, D.J. (1990). Expression of the HER-Z/neu proto-oncogene in normal human adult and fetal tissues. *Liver*, *7*, pp.7.

Proskuryakov, S.Y., Konoplyannikov, A.G. and Gabai, V.L. (2003). Necrosis: a specific form of programmed cell death?. *Experimental Cell Research*, *283*(1), pp.1-16.

Puddephatt, R.J. (1978). The chemistry of gold. Elsevier Scientific Pub. Co.; distributors for the US and Canada Elsevier/North-Holland.

Puig, S. and Thiele, D.J. (2002). Molecular mechanisms of copper uptake and distribution. *Current Opinion in Chemical Biology*, *6*(2), pp.171-180.

Qin, Q., Xu, Y., He, T., Qin, C. and Xu, J. (2012). Normal and disease-related biological functions of Twist1 and underlying molecular mechanisms. *Cell Research*, *22*(1), pp.90-106.

Quellhorst, G., Prabhakar, S., Han, Y. and Yang, J. (2006). PCR Array: A simple and quantitative method for gene expression profiling. *Frederick, MD: SuperArray Bioscience Corp*.

Rackham, O., Nichols, S.J., Leedman, P.J., Berners-Price, S.J. and Filipovska, A. (2007). A gold (I) phosphine complex selectively induces apoptosis in breast cancer cells: implications for anticancer therapeutics targeted to mitochondria. *Biochemical Pharmacology*, *74*(7), pp.992-1002.

Rademaker-Lakhai, J.M., van den Bongard, D., Pluim, D., Beijnen, J.H. and Schellens, J.H. (2004). A phase I and pharmacological study with imidazolium-trans-DMSO-imidazole-tetrachlororuthenate, a novel ruthenium anticancer agent. *Clinical Cancer Research*, *10*(11), pp.3717-3727.

Rafique, S., Idrees, M., Nasim, A., Akbar, H. and Athar, A. (2010). Transition metal complexes as potential therapeutic agents. *Biotechnology and Molecular Biology Reviews*, *5*(2), pp.38-45.

Rau, K.M., Kang, H.Y., Cha, T.L., Miller, S.A. and Hung, M.C. (2005). The mechanisms and managements of hormone-therapy resistance in breast and prostate cancers. *Endocrine-related Cancer*, *12*(3), pp.511-532.

Reed, J.C. (1999). Dysregulation of apoptosis in cancer. *Journal of Clinical Oncology*, *17*(9), pp.2941-2941.

Reed, J.C. (2000). Mechanisms of apoptosis (Warner-Lambert/Parke-Davis Award Lecture). *The American Journal of Pathology*, *157*, pp.1415-1430.

Reed, J.C. (2008). Bcl-2–family proteins and hematologic malignancies: history and future prospects. *Blood*, *111*(7), pp.3322-3330.

Reed, E., Dabholkar, M., Chabner, BA. (1996). Platinum analogues. In: Chabner BA, Longo DL, editors. Cancer chemotherapy and biotherapy: principles and practice 2nd ed. Philadelphia: Lippincott–Raven Publishers, pp.357-378.

Rheeder, J.P., Marasas, W.F.O., Thiel, P.G., Sydenham, E.W., Shephard, G.S. and Van Schalkwyk, D.J. (1992). Fusarium moniliforme and fumonisins in corn in relation to human esophageal cancer in Transkei. *Phytopathology*, *82*(3), pp.353-357.

Riedl, S.J. and Shi, Y. (2004). Molecular mechanisms of caspase regulation during apoptosis. *Nature Reviews Molecular Cell Biology*, *5*(11), pp.897-907.

Rigobello, M.P., Folda, A., Dani, B., Menabò, R., Scutari, G. and Bindoli, A. (2008). Gold (I) complexes determine apoptosis with limited oxidative stress in Jurkat-T cells. *European Journal of Pharmacology*, *582*(1), pp.26-34.

Rigobello, M.P., Messori, L., Marcon, G., Cinellu, M.A., Bragadin, M., Folda, A., Scutari, G. and Bindoli, A. (2004). Gold complexes inhibit mitochondrial thioredoxin reductase: consequences on mitochondrial functions. *Journal of Inorganic Biochemistry*, *98*(10), pp.1634-1641.

Rodriguez, J. and Lazebnik, Y. (1999). Caspase-9 and APAF-1 form an active holoenzyme. *Genes & Development*, *13*(24), pp.3179-3184.

Rolon, P.A., Castellsague, X., Benz, M. and Munoz, N. (1995). Hot and cold mate drinking and esophageal cancer in Paraguay. *Cancer Epidemiology and Prevention Biomarkers*, *4*(6), pp.595-605.

Rosenberg, B. and Vancamp, L. (1969). Platinum compounds: a new class of potent antitumour agents. *Nature*, *222*, pp.385-386.

Ross, M.F., Kelso, G.F., Blaikie, F.H., James, A.M., Cocheme, H.M., Filipovska, A., Da Ros, T., Hurd, T.R., Smith, R.A.J. and Murphy, M.P. (2005). Lipophilic triphenylphosphonium cations as tools in mitochondrial bioenergetics and free radical biology. *Biochemistry (Moscow)*, *70*(2), pp.222-230.

Rousset, M. (1986). The human colon carcinoma cell lines HT-29 and Caco-2: two *in vitro* models for the study of intestinal differentiation. *Biochimie*, *68*(9), pp.1035-1040.

Rubio-Moscardo, F., Blesa, D., Mestre, C., Siebert, R., Balasas, T., Benito, A., Rosenwald, A., Climent, J., Martinez, J.I., Schilhabel, M. and Karran, E.L. (2005). Characterization of 8p21. 3 chromosomal deletions in B-cell lymphoma: TRAIL-R1 and TRAIL-R2 as candidate dosage-dependent tumor suppressor genes. *Blood*, *106*(9), pp.3214-3222.

Rush, G.F., Alberts, D.W., Meunier, P., Leffler, K. and Smith, P.F. (1987). *In vivo* and *in vitro* hepatotoxicity of a novel antineoplastic agent, SK&F 101772, in male beagle dogs. *Toxicologist*, *7*(59), pp.1-584.

Sabolová, D., Kožurková, M., Plichta, T., Ondrušová, Z., Hudecová, D., Šimkovič, M., Paulíková, H. and Valent, A. (2011). Interaction of a copper (II)–Schiff base complexes with calf thymus DNA and their antimicrobial activity. *International Journal of Biological Macromolecules*, *48*(2), pp.319-325.

Saelens, X., Festjens, N., Walle, L.V., Van Gurp, M., van Loo, G. and Vandenabeele, P. (2004). Toxic proteins released from mitochondria in cell death. *Oncogene*, *23*(16), pp.2861-2874.

Safran, H., DiPetrillo, T., Akerman, P., Ng, T., Evans, D., Steinhoff, M., Benton, D., Purviance, J., Goldstein, L., Tantravahi, U. and Kennedy, T. (2007). Phase I/II study of trastuzumab, paclitaxel,

cisplatin and radiation for locally advanced, HER2 overexpressing, esophageal adenocarcinoma. *International Journal of Radiation Oncology* Biology* Physics*, *67*(2), pp.405-409.

Saggioro, D., Rigobello, M.P., Paloschi, L., Folda, A., Moggach, S.A., Parsons, S., Ronconi, L., Fregona, D. and Bindoli, A. (2007). Gold (III)-dithiocarbamato complexes induce cancer cell death triggered by thioredoxin redox system inhibition and activation of ERK pathway. *Chemistry & Biology*, *14*(10), pp.1128-1139.

Saini, S., Hirata, H., Majid, S. and Dahiya, R. (2009). Functional significance of cytochrome P450 1B1 in endometrial carcinogenesis. *Cancer Research*, *69*(17), pp.7038-7045.

Saitoh, M., Nishitoh, H., Fujii, M., Takeda, K., Tobiume, K., Sawada, Y., Kawabata, M., Miyazono, K. and Ichijo, H. (1998). Mammalian thioredoxin is a direct inhibitor of apoptosis signal-regulating kinase (ASK) 1. *The EMBO Journal*, *17*(9), pp.2596-2606.

Sakahira, H., Enari, M. and Nagata, S. (1998). Cleavage of CAD inhibitor in CAD activation and DNA degradation during apoptosis. *Nature*, *391*(6662), pp.96-99.

Salvesen, G.S. and Duckett, C.S. (2002). IAP proteins: blocking the road to death's door. *Nature Reviews Molecular Cell Biology*, *3*(6), pp.401-410.

Sannella, A.R., Casini, A., Gabbiani, C., Messori, L., Bilia, A.R., Vincieri, F.F., Majori, G. and Severini, C. (2008). New uses for old drugs. Auranofin, a clinically established antiarthritic metallodrug, exhibits potent antimalarial effects *in vitro*: Mechanistic and pharmacological implications. *FEBS Letters*, *582*(6), pp.844-847.

Santini, C., Pellei, M., Papini, G., Morresi, B., Galassi, R., Ricci, S., Tisato, F., Porchia, M., Rigobello, M.P., Gandin, V. and Marzano, C. (2011). *In vitro* antitumour activity of water soluble Cu (I), Ag (I) and Au (I) complexes supported by hydrophilic alkyl phosphine ligands. *Journal of Inorganic Biochemistry*, *105*(2), pp.232-240.

Sava, G., Zorzet, S., Giraldi, T., Mestroni, G. and Zassinovich, G. (1984). Antineoplastic activity and toxicity of an organometallic complex of ruthenium (II) in comparison with cis-PDD in mice bearing solid malignant neoplasms. *European Journal of Cancer and Clinical Oncology*, *20*(6), pp.841-847.

Savill, J. and Fadok, V. (2000). Corpse clearance defines the meaning of cell death. *Nature*, *407*(6805), pp.784-788.

Sbeity, H. and Younes, R. (2015). Review of optimization methods for cancer chemotherapy treatment planning. *Journal of Computer Science & Systems Biology*, doi: 10.4172/jcsb.1000173.

Scaffidi, C., Fulda, S., Srinivasan, A., Friesen, C., Li, F., Tomaselli, K.J., Debatin, K.M., Krammer, P.H. and Peter, M.E. (1998). Two CD95 (APO-1/Fas) signaling pathways. *The EMBO Journal*, *17*(6), pp.1675-1687.

Schwartz, L.M., Smith, S.W., Jones, M.E. and Osborne, B.A. (1993). Do all programmed cell deaths occur via apoptosis?. *Proceedings of the National Academy of Sciences*, *90*(3), pp.980-984.

Schweichel, J.U. and Merker, H.J. (1973). The morphology of various types of cell death in prenatal tissues. *Teratology*, *7*(3), pp.253-266.

Seelig, M.H., Berger, M.R. and Keppler, B.K. (1992). Antineoplastic activity of three ruthenium derivatives against chemically induced colorectal carcinoma in rats. *Journal of Cancer Research and Clinical Oncology*, *118*(3), pp.195-200.

Segapelo, T.V., Guzei, I.A., Spencer, L.C., Van Zyl, W.E. and Darkwa, J. (2009). (Pyrazolylmethyl) pyridine platinum (II) and gold (III) complexes: Synthesis, structures and evaluation as anticancer agents. *Inorganica Chimica Acta*, *362*(9), pp.3314-3324.

Shabani, S., Nourizadeh, N. and Soltankhah, M. (2014). The over expression of thioredoxin during malignancies. *Reviews in Clinical Medicine*, *1*(4), pp.218-224.

Shah, N. and Dizon, D.S. (2009). New-generation platinum agents for solid tumors. *Future Oncology*, 5(1), pp.33-42.

Shangary, S. and Wang, S. (2008). Targeting the MDM2-p53 interaction for cancer therapy. *Clinical Cancer Research*, *14*(17), pp.5318-5324.

Sharkey, R.M. and Goldenberg, D.M. (2006). Targeted therapy of cancer: new prospects for antibodies and immunoconjugates. *CA: A Cancer Journal for Clinicians*, *56*(4), pp.226-243.

Sheikh, A., Hussain, S.A., Ghori, Q., Naeem, N., Fazil, A., Giri, S., Sathian, B., Mainali, P. and Al Tamimi, D.M. (2015). The spectrum of genetic mutations in breast cancer. *Asian Pacific Journal of Cancer Prevention*, *16*(6), pp.2177-2185.

Sheng, S. (2001). The urokinase-type plasminogen activator system in prostate cancer metastasis. *Cancer and Metastasis Reviews*, *20*(3-4), pp.287-296.

Sherman, M.Y. and Gabai, V.L. (2015). Hsp70 in cancer: back to the future. *Oncogene*, *34*(32), pp.4153-4161.

Shimada, T., Gillam, E.M., Sutter, T.R., Strickland, P.T., Guengerich, F.P. and Yamazaki, H. (1997). Oxidation of xenobiotics by recombinant human cytochrome P450 1B1. *Drug Metabolism and Disposition*, *25*(5), pp.617-622.

Shirakihara, T., Kawasaki, T., Fukagawa, A., Semba, K., Sakai, R., Miyazono, K., Miyazawa, K. and Saitoh, M. (2013). Identification of integrin α3 as a molecular marker of cells undergoing epithelial–mesenchymal transition and of cancer cells with aggressive phenotypes. *Cancer Science*, *104*(9), pp.1189-1197.

Siddik, Z.H. (2003). Cisplatin: mode of cytotoxic action and molecular basis of resistance. *Oncogene*, *22*(47), pp.7265-7279.

Siegel, P.M. and Massagué, J. (2003). Cytostatic and apoptotic actions of TGF-β in homeostasis and cancer. *Nature Reviews Cancer*, *3*(11), pp.807-820.

Siegel, R.L., Miller, K.D. and Jemal, A. (2016). Cancer statistics, 2016. *CA: A Cancer Journal for Clinicians*, *66*(1), pp.7-30.

Silver, S., Phung, L.T. and Silver, G. (2006). Silver as biocides in burn and wound dressings and bacterial resistance to silver compounds. *Journal of Industrial Microbiology and Biotechnology*, *33*(7), pp.627-634.

Simon, T.M., Kunishima, D.H., Vibert, G.J. and Lorber, A. (1981). Screening trial with the coordinated gold compound auranofin using mouse lymphocytic leukemia P388. *Cancer Research*, *41*(1), pp.94-97.

Slamon, D.J., Godolphin, W., Jones, L.A., Holt, J.A., Wong, S.G., Keith, D.E., Levin, W.J., Stuart, S.G., Udove, J., Ullrich, A. and Press, M.F. (1989). Studies of the HER-2/neu proto-oncogene in human breast and ovarian cancer. *Science*, *244*(4905), pp.707-712.

Snelders, D.J., Casini, A., Edafe, F., van Koten, G., Gebbink, R.J.K. and Dyson, P.J. (2011). Ruthenium (II) arene complexes with oligocationic triarylphosphine ligands: Synthesis, DNA interactions and in vitro properties. *Journal of Organometallic Chemistry*, *696*(5), pp.1108-1116.

Somdyala, N.I., Parkin, D.M., Sithole, N. and Bradshaw, D. (2015). Trends in cancer incidence in rural Eastern Cape Province; South Africa, 1998–2012. *International Journal of Cancer*, *136*(5), pp.E470-E474.

Soriano, M.E. and Scorrano, L. (2010). The interplay between BCL-2 family proteins and mitochondrial morphology in the regulation of apoptosis. *BCL-2 Protein Family*, pp.97-114.

Spector, N.L. and Blackwell, K.L. (2009). Understanding the mechanisms behind trastuzumab therapy for human epidermal growth factor receptor 2–positive breast cancer. *Journal of Clinical Oncology*, *27*(34), pp.5838-5847.

Spigel, D.R. and Burstein, H.J. (2002). HER2 overexpressing metastatic breast cancer. *Current Treatment Options in Oncology*, *3*(2), pp.163-174.

Stennicke, H.R., Deveraux, Q.L., Humke, E.W., Reed, J.C., Dixit, V.M. and Salvesen, G.S. (1999). Caspase-9 can be activated without proteolytic processing. *Journal of Biological Chemistry*, *274*(13), pp.8359-8362.

Stern, D.F., Heffernan, P.A. and Weinberg, R.A. (1986). p185, a product of the neu proto-oncogene, is a receptorlike protein associated with tyrosine kinase activity. *Molecular and Cellular Biology*, *6*(5), pp.1729-1740.

Soini, Y., Kahlos, K., Näpänkangas, U., Kaarteenaho-Wiik, R., Säily, M., Koistinen, P., Pääakkö, P., Holmgren, A. and Kinnula, V.L. (2001). Widespread expression of thioredoxin and thioredoxin reductase in non-small cell lung carcinoma. *Clinical Cancer Research*, *7*(6), pp.1750-1757.

Suliman, A., Lam, A., Datta, R. and Srivastava, R.K. (2001). Intracellular mechanisms of TRAIL: apoptosis through mitochondrial-dependent and-independent pathways. *Oncogene*, *20*(17), p.2122-2133.

Sullivan, L.B. and Chandel, N.S. (2014). Mitochondrial reactive oxygen species and cancer. *Cancer & Metabolism*, *2*(1), doi: 10.1186/2049-3002-2-17.

Sumeruk, R., Segal, I., Te Winkel, W. and Van Der Merwe, C.F. (1992). Oesophageal cancer in three regions of South Africa. *South African Medical Journal*, *81*(2), pp.91-93.

Sun, X., Yin, J., Starovasnik, M.A., Fairbrother, W.J. and Dixit, V.M. (2002). Identification of a novel homotypic interaction motif required for the phosphorylation of receptor-interacting protein (RIP) by RIP3. *Journal of Biological Chemistry*, *277*(11), pp.9505-9511.

Susin, S.A., Lorenzo, H.K., Zamzami, N., Marzo, I., Brenner, C., Larochette, N., Prévost, M.C., Alzari, P.M. and Kroemer, G. (1999). Mitochondrial release of caspase-2 and-9 during the apoptotic process. *The Journal of Experimental Medicine*, *189*(2), pp.381-394.

Suwalsky, M., Zambenedetti, P., Carpené, E., IbnLkayat, M., Wittkowski, W., Messori, L. and Zatta, P. (2004). Effects of chronic treatment with sodium tetrachloroaurate (III) in mice and membrane models. *Journal of Inorganic Biochemistry*, *98*(12), pp.2080-2086.

Suzuki, Y., Imai, Y., Nakayama, H., Takahashi, K., Takio, K. and Takahashi, R. (2001). A serine protease, HtrA2, is released from the mitochondria and interacts with XIAP, inducing cell death. *Molecular Cell*, *8*(3), pp.613-621.

Sylla, B.S. and Wild, C.P. (2012). A million africans a year dying from cancer by 2030: what can cancer research and control offer to the continent?. *International Journal of Cancer*, *130*(2), pp.245-250.

Szefler, S.J. (1992). Anti-inflammatory drugs in the treatment of allergic disease. *The Medical Clinics of North America*, *76*(4), p.953.

Takahashi, K., Miyashita, M., Makino, H., Akagi, I., Orita, H., Hagiwara, N., Nomura, T., Gabrielson, E.W. and Tajiri, T. (2009). Expression of Akt and Mdm2 in human esophageal squamous cell carcinoma. *Experimental and Molecular Pathology*, *87*(1), pp.42-47.

Takahashi, R., Deveraux, Q., Tamm, I., Welsh, K., Assa-Munt, N., Salvesen, G.S. and Reed, J.C. (1998). A single BIR domain of XIAP sufficient for inhibiting caspases. *Journal of Biological Chemistry*, *273*(14), pp.7787-7790.

Tan, J., Wang, B. and Zhu, L. (2009). DNA binding and oxidative DNA damage induced by a quercetin copper (II) complex: potential mechanism of its antitumor properties. *JBIC Journal of Biological Inorganic Chemistry*, *14*(5), pp.727-739.

Tanida, I., Minematsu-Ikeguchi, N., Ueno, T. and Kominami, E. (2005). Lysosomal turnover, but not a cellular level, of endogenous LC3 is a marker for autophagy. *Autophagy*, *1*(2), pp.84-91.

Tanida, I., Tanida-Miyake, E., Komatsu, M., Ueno, T. and Kominami, E. (2002). Human Apg3p/Aut1p homologue is an authentic E2 enzyme for multiple substrates, GATE-16, GABARAP, and MAP-LC3, and facilitates the conjugation of hApg12p to hApg5p. *Journal of Biological Chemistry*, *277*(16), pp.13739-13744.

Tasdemir, E., Maiuri, M.C., Orhon, I., Kepp, O., Morselli, E., Criollo, A. and Kroemer, G. (2008). p53 represses autophagy in a cell cycle-dependent fashion. *Cell Cycle*, *7*(19), pp.3006-3011.

Teicher, B.A. (2001). Malignant cells, directors of the malignant process: role of transforming growth factor-beta. *Cancer and Metastasis Reviews*, *20*(1-2), pp.133-143.

Tepper, J., Krasna, M.J., Niedzwiecki, D., Hollis, D., Reed, C.E., Goldberg, R., Kiel, K., Willett, C., Sugarbaker, D. and Mayer, R. (2008). Phase III trial of trimodality therapy with cisplatin, fluorouracil, radiotherapy, and surgery compared with surgery alone for esophageal cancer: CALGB 9781. *Journal of Clinical Oncology*, *26*(7), pp.1086-1092.

Tew, W.P., Kelsen, D.P. and Ilson, D.H. (2005). Targeted therapies for esophageal cancer. *The Oncologist*, *10*(8), pp.590-601.

Thati, B., Noble, A., Creaven, B.S., Walsh, M., McCann, M., Devereux, M., Kavanagh, K. and Egan, D.A. (2009). Role of cell cycle events and apoptosis in mediating the anti-cancer activity of a silver (I) complex of 4-hydroxy-3-nitro-coumarin-bis (phenanthroline) in human malignant cancer cells. *European Journal of Pharmacology*, *602*(2), pp.203-214.

Thiery, J.P. (2002). Epithelial–mesenchymal transitions in tumour progression. *Nature Reviews Cancer*, *2*(6), pp.442-454.

Thornberry, N.A. and Lazebnik, Y. (1998). Caspases: enemies within. *Science*, *281*(5381), pp.1312-1316.

Thornberry, N.A., Rano, T.A., Peterson, E.P., Rasper, D.M., Timkey, T., Garcia-Calvo, M., Houtzager, V.M., Nordstrom, P.A., Roy, S., Vaillancourt, J.P. and Chapman, K.T. (1997). A combinatorial approach defines specificities of members of the caspase family and granzyme B Functional relationships established for key mediators of apoptosis. *Journal of Biological Chemistry*, *272*(29), pp.17907-17911.

Toh, Y. and Nicolson, G.L. (2009). The role of the MTA family and their encoded proteins in human cancers: molecular functions and clinical implications. *Clinical & Experimental Metastasis*, *26*(3), pp.215-227.

Tsamandas, A.C., Kardamakis, D., Petsas, T., Zolota, V., Vassiliou, V., Matatsoris, T., Kalofonos, H., Vagianos, C.E. and Scopa, C.D. (2007). Bcl-2, bax and p53 expression in rectal adenocarcinoma. Correlation with classic pathologic prognostic factors and patients' outcome. *In Vivo*, *21*(1), pp.113-118.

Tsang, R.Y., Al-Fayea, T. and Au, H.J. (2009). Cisplatin overdose. *Drug Safety*, *32*(12), pp.1109-1122.

Urani, C., Melchioretto, P., Morazzoni, F., Canevali, C. and Camatini, M. (2001). Copper and zinc uptake and hsp70 expression in HepG2 cells. *Toxicology in Vitro*, *15*(4), pp.497-502.

Urruticoechea, A., Alemany, R., Balart, J., Villanueva, A., Vinals, F. and Capella, G. (2010). Recent advances in cancer therapy: an overview. *Current Pharmaceutical Design*, *16*(1), pp.3-10.

Vandenabeele, P., Declercq, W., Van Herreweghe, F. and Vanden Berghe, T. (2010). The role of the kinases RIP1 and RIP3 in TNF-induced necrosis. *Science Signaling*, *3*(115), doi: 10.1126/scisignal.3115re4.

van der Groep, P., van der Wall, E. and van Diest, P.J. (2011). Pathology of hereditary breast cancer. *Cellular Oncology*, *34*(2), pp.71-88.

Van Herreweghe, F., Festjens, N., Declercq, W. and Vandenabeele, P. (2010). Tumor necrosis factor-mediated cell death: to break or to burst, that's the question. *Cellular and Molecular Life Sciences*, *67*(10), pp.1567-1579.

van Loo, G., Van Gurp, M., Depuydt, B., Srinivasula, S.M., Rodriguez, I., Alnemri, E.S., Gevaert, K., Vandekerckhove, J., Declercq, W. and Vandenabeele, P. (2002). The serine protease Omi/HtrA2 is released from mitochondria during apoptosis. Omi interacts with caspase-inhibitor XIAP and induces enhanced caspase activity. *Cell Death and Differentiation*, *9*(1), pp.20-26.

Vanneman, M. and Dranoff, G. (2012). Combining immunotherapy and targeted therapies in cancer treatment. *Nature Reviews Cancer*, *12*(4), pp.237-251.

Varfolomeev, E., Blankenship, J.W., Wayson, S.M., Fedorova, A.V., Kayagaki, N., Garg, P., Zobel, K., Dynek, J.N., Elliott, L.O., Wallweber, H.J. and Flygare, J.A. (2007). IAP antagonists induce autoubiquitination of c-IAPs, NF-κB activation, and TNFα-dependent apoptosis. *Cell*, *131*(4), pp.669-681.

Vaughan, T.L., Davis, S., Kristal, A. and Thomas, D.B. (1995). Obesity, alcohol, and tobacco as risk factors for cancers of the esophagus and gastric cardia: adenocarcinoma versus squamous cell carcinoma. *Cancer Epidemiology and Prevention Biomarkers*, *4*(2), pp.85-92.

Vaughn, D.J. and Malkowicz, S.B. (2001). Recent developments in chemotherapy for bladder cancer. *Oncology*, *15*(6), pp.763-771.

Vaux, D.L. and Silke, J. (2003). Mammalian mitochondrial IAP binding proteins. *Biochemical and Biophysical Research Communications*, *304*(3), pp.499-504.

Verhagen, A.M., Ekert, P.G., Pakusch, M., Silke, J., Connolly, L.M., Reid, G.E., Moritz, R.L., Simpson, R.J. and Vaux, D.L. (2000). Identification of DIABLO, a mammalian protein that promotes apoptosis by binding to and antagonizing IAP proteins. *Cell*, *102*(1), pp.43-53.

Verona, E.V., Tang, Y., Millstead, T.K., Hinck, A.P., Agyin, J.K. and Sun, L.Z. (2008). Expression, purification and characterization of BGERII: a novel pan-TGFβ inhibitor. *Protein Engineering Design and Selection*, *21*(7), pp.463-473.

Vineis, P. and Wild, C.P. (2014). Global cancer patterns: causes and prevention. *The Lancet*, *383*(9916), pp.549-557.

Voellmy, R. (1996). Sensing stress and responding to stress. *Stress-inducible Cellular Responses*, pp. 121-137.

Vorobiof, D.A., Sitas, F. and Vorobiof, G. (2001). Breast cancer incidence in South Africa. *Journal of Clinical Oncology*, *19*, pp.125s-127s.

Vousden, K.H. and Lu, X. (2002). Live or let die: the cell's response to p53. *Nature Reviews Cancer*, *2*(8), pp.594-604.

Vucic, D., Dixit, V.M. and Wertz, I.E. (2011). Ubiquitylation in apoptosis: a post-translational modification at the edge of life and death. *Nature Reviews Molecular Cell Biology*, *12*(7), pp.439-452.

Wang, X. (2001). The expanding role of mitochondria in apoptosis. *Genes & Development*, *15*(22), pp.2922-2933.

Wang, K., Yin, X.M., Chao, D.T., Milliman, C.L. and Korsmeyer, S.J. (1996). BID: a novel BH3 domain-only death agonist. *Genes & Development*, *10*(22), pp.2859-2869.

Wang, S.Y., Yu, Q.J., Zhang, R.D. and Liu, B. (2011). Core signaling pathways of survival/death in autophagy-related cancer networks. *The International Journal of Biochemistry & Cell Biology*, *43*(9), pp.1263-1266.

Wajant, H. (2002). The Fas signaling pathway: more than a paradigm. *Science*, *296*(5573), pp.1635-1636.

Wakefield, L.M. and Hill, C.S. (2013). Beyond TGFβ: roles of other TGFβ superfamily members in cancer. *Nature Reviews Cancer*, *13*(5), pp.328-341.

Walsh, J.G., Cullen, S.P., Sheridan, C., Lüthi, A.U., Gerner, C. and Martin, S.J. (2008). Executioner caspase-3 and caspase-7 are functionally distinct proteases. *Proceedings of the National Academy of Sciences*, *105*(35), pp.12815-12819.

Walsh, T.N., Noonan, N., Hollywood, D., Kelly, A., Keeling, N. and Hennessy, T.P. (1996). A comparison of multimodal therapy and surgery for esophageal adenocarcinoma. *New England Journal of Medicine*, *335*(7), pp.462-467.

Warburg, O. (1925). The metabolism of carcinoma cells. *The Journal of Cancer Research*, *9*(1), pp.148-163.

Warburg, O., Wind, F. and Negelein, E. (1927). The metabolism of tumors in the body. *The Journal of General Physiology*, *8*(6), pp.519-530.

Wei, Y., Lukashev, M., Simon, D.I. and Bodary, S.C. (1996). Regulation of integrin function by the urokinase receptor. *Science*, *273*(5281), pp.1551.

Wei, Z., Ma, W., Qi, X., Zhu, X., Wang, Y., Xu, Z., Luo, J., Wang, D., Guo, W., Li, X. and Xin, S. (2016). Pinin facilitated proliferation and metastasis of colorectal cancer through activating EGFR/ERK signaling pathway. *Oncotarget*, 7(20), pp. 29429-29439.

Weinberg, O.K., Marquez-Garban, D.C. and Pietras, R.J. (2005). New approaches to reverse resistance to hormonal therapy in human breast cancer. *Drug Resistance Updates*, *8*(4), pp.219-233.

Willis, S.N., Fletcher, J.I., Kaufmann, T., van Delft, M.F., Chen, L., Czabotar, P.E., Ierino, H., Lee, E.F., Fairlie, W.D., Bouillet, P. and Strasser, A. (2007). Apoptosis initiated when BH3 ligands engage multiple Bcl-2 homologs, not Bax or Bak. *Science*, *315*(5813), pp.856-859.

Wolchok, J.D., Hoos, A., O'Day, S., Weber, J.S., Hamid, O., Lebbé, C., Maio, M., Binder, M., Bohnsack, O., Nichol, G. and Humphrey, R. (2009). Guidelines for the evaluation of immune therapy activity in solid tumors: immune-related response criteria. *Clinical Cancer Research*, *15*(23), pp.7412-7420.

Wu, X., Bayle, J.H., Olson, D. and Levine, A.J. (1993). The p53-mdm-2 autoregulatory feedback loop. *Genes & Development*, *7*(7a), pp.1126-1132.

Wu, X. and Deng, Y. (2002). Bax and BH3-domain-only proteins in p53-mediated apoptosis. *Frontiers in Biosciences*, *7*(1), pp.151-156.

Xiao, H., Tao, Y., Greenblatt, J. and Roeder, R.G. (1998). A cofactor, TIP30, specifically enhances HIV-1 Tatactivated transcription. *Proceedings of the National Academy of Sciences*, *95*(5), pp.2146-2151.

Xu, J., Lamouille, S. and Derynck, R. (2009). TGF-β-induced epithelial to mesenchymal transition. *Cell Research*, *19*(2), pp.156-172.

Xu, Y., Huang, S., Liu, Z.G. and Han, J. (2006). Poly (ADP-ribose) polymerase-1 signaling to mitochondria in necrotic cell death requires RIP1/TRAF2-mediated JNK1 activation. *Journal of Biological Chemistry*, *281*(13), pp.8788-8795.

Yager, J.D. and Leihr, J.G. (1996). Molecular mechanisms of estrogen carcinogenesis. *Annual Review of Pharmacology and Toxicology*, *36*(1), pp.203-232.

Yang, J., Mani, S.A., Donaher, J.L., Ramaswamy, S., Itzykson, R.A., Come, C., Savagner, P., Gitelman, I., Richardson, A. and Weinberg, R.A. (2004). Twist, a master regulator of morphogenesis, plays an essential role in tumor metastasis. *Cell*, *117*(7), pp.927-939.

Yang, J., Mani, S.A. and Weinberg, R.A. (2006). Exploring a new twist on tumor metastasis. *Cancer Research*, *66*(9), pp.4549-4552.

Yang, Y., Fang, S., Jensen, J.P., Weissman, A.M. and Ashwell, J.D. (2000). Ubiquitin protein ligase activity of IAPs and their degradation in proteasomes in response to apoptotic stimuli. *Science*, *288*(5467), pp.874-877.

Yang, X.H., Sladek, T.L., Liu, X., Butler, B.R., Froelich, C.J. and Thor, A.D. (2001). Reconstitution of caspase 3 sensitizes MCF-7 breast cancer cells to doxorubicin-and etoposide-induced apoptosis. *Cancer Research*, *61*(1), pp.348-354.

Yang, Z., Schumaker, L.M., Egorin, M.J., Zuhowski, E.G., Guo, Z. and Cullen, K.J. (2006). Cisplatin preferentially binds mitochondrial DNA and voltage-dependent anion channel protein in the mitochondrial membrane of head and neck squamous cell carcinoma: possible role in apoptosis. *Clinical Cancer Research*, *12*(19), pp.5817-5825.

Yang, Z., Wang, X., Diao, H., Zhang, J., Li, H., Sun, H. and Guo, Z. (2007). Encapsulation of platinum anticancer drugs by apoferritin. *Chemical Communications*, (33), pp.3453-3455.

Yde, C.W. and Issinger, O. (2006). Enhancing cisplatin sensitivity in MCF-7 human breast cancer cells by down-regulation of Bcl-2 and cyclin D1. *International Journal of Oncology*, *29*(6), pp.1397-1404.

Yilmaz, V.T., Gocmen, E., Icsel, C., Cengiz, M., Susluer, S.Y. and Buyukgungor, O. (2014). Synthesis, crystal structures, in vitro DNA binding, antibacterial and cytotoxic activities of new di-and polynuclear silver (I) saccharinate complexes with tertiary monophosphanes. *Journal of Photochemistry and Photobiology B: Biology*, *131*, pp.31-42.

Yingling, J.M., Blanchard, K.L. and Sawyer, J.S. (2004). Development of TGF-β signalling inhibitors for cancer therapy. *Nature Reviews Drug Discovery*, *3*(12), pp.1011-1022.

Yoo, M.H., Xu, X.M., Carlson, B.A., Gladyshev, V.N. and Hatfield, D.L. (2006). Thioredoxin reductase 1 deficiency reverses tumor phenotype and tumorigenicity of lung carcinoma cells. *Journal of Biological Chemistry*, *281*(19), pp.13005-13008.

Yoshimori, T. (2004). Autophagy: a regulated bulk degradation process inside cells. *Biochemical and Biophysical Research Communications*, *313*(2), pp.453-458.

Yu, X., Li, Z. and Wu, W.K. (2015). TIP30: A Novel Tumor-Suppressor Gene. *Oncology Research Featuring Preclinical and Clinical Cancer Therapeutics*, *22*(5-6), pp.339-348.

Yuan, J., Shaham, S., Ledoux, S., Ellis, H.M. and Horvitz, H.R. (1993). The C. elegans cell death gene ced-3 encodes a protein similar to mammalian interleukin-1β-converting enzyme. *Cell*, *75*(4), pp.641-652.

Zachariadis, P.C., Hadjikakou, S.K., Hadjiliadis, N., Skoulika, S., Michaelides, A., Balzarini, J. and De Clercq, E. (2004). Synthesis, Characterization and in Vitro Study of the Cytostatic and Antiviral Activity of New Polymeric Silver (I) Complexes with Ribbon Structures Derived from the Conjugated Heterocyclic Thioamide 2-Mercapto-3, 4, 5, 6-tetra-hydropyrimidine. *European Journal of Inorganic Chemistry*, *2004*(7), pp.1420-1426.

Zaki, M., Arjmand, F. and Tabassum, S. (2016). Current and future potential of metallo drugs: Revisiting DNA-binding of metal containing molecules and their diverse mechanism of action. *Inorganica Chimica Acta*, *444*, pp.1-22.

Zartilas, S., Hadjikakou, S.K., Hadjiliadis, N., Kourkoumelis, N., Kyros, L., Kubicki, M., Baril, M., Butler, I.S., Karkabounas, S. and Balzarini, J. (2009). Tetrameric 1: 1 and monomeric 1: 3 complexes of silver (I) halides with tri (p-tolyl)-phosphine: a structural and biological study. *Inorganica Chimica Acta*, *362*(3), pp.1003-1010.

Zeestraten, E.C., Benard, A., Reimers, M.S., Schouten, P.C., Liefers, G.J., van de Velde, J.H. and Kuppen, P.J. (2013). The prognostic value of the apoptosis pathway in colorectal cancer: a review of the literature on biomarkers identified by immunohistochemistry. *Biomarkers in Cancer*, *5*, pp.13-29.

Zeiss, C.J. (2003). The apoptosis-necrosis continuum: insights from genetically altered mice. *Veterinary Pathology*, *40*(5), pp.481-495.

Zhang, C.X. and Lippard, S.J. (2003). New metal complexes as potential therapeutics. *Current Opinion in Chemical Biology*, *7*(4), pp.481-489.

Zhang, D.W., Shao, J., Lin, J., Zhang, N., Lu, B.J., Lin, S.C., Dong, M.Q. and Han, J. (2009). RIP3, an energy metabolism regulator that switches TNF-induced cell death from apoptosis to necrosis. *Science*, *325*(5938), pp.332-336.

Zhang, J., Wang, L., Xing, Z., Liu, D., Sun, J., Li, X. and Zhang, Y. (2010). Status of bi-and multi-nuclear platinum anticancer drug development. *Anti-Cancer Agents in Medicinal Chemistry*, *10*(4), pp.272-282.

Zhang, L., Cheng, Q., Zhang, L., Wang, Y., Merrill, G.F., Ilani, T., Fass, D., Arnér, E.S. and Zhang, J. (2016). Serum thioredoxin reductase is highly increased in mice with hepatocellular carcinoma and its activity is restrained by several mechanisms. *Free Radical Biology and Medicine*, *99*, pp.426-435.

Zhao, M. and Ramaswamy, B. (2014). Mechanisms and therapeutic advances in the management of endocrine-resistant breast cancer. *World Journal of Clinical Oncology*, *5*(3), pp.248-262.

Zheng, W., Jiang, C. and Li, R. (2016). integrin and gene network analysis reveals that iTga5 and iTgB1 are prognostic in non-small-cell lung cancer. *OncoTargets and Therapy*, *9*, pp.2317-2327.

Zhou, H.B., Yan, Y., Sun, Y.N. and Zhu, J.R. (2003). Resveratrol induces apoptosis in human esophageal carcinoma cells. *World Journal of Gastroenterology*, *9*(3), pp.408-411.

Zhu, B.T. and Conney, A.H. (1998). Functional role of estrogen metabolism in target cells: review and perspectives. *Carcinogenesis*, *19*(1), pp.1-27.

Zhu, X., Zhang, K., Wang, Q., Chen, S., Gou, Y., Cui, Y. and Li, Q. (2015). Cisplatin-mediated c-myc overexpression and cytochrome c (cyt c) release result in the up-regulation of the death receptors DR4 and DR5 and the activation of caspase 3 and caspase 9, likely responsible for the TRAIL-sensitizing effect of cisplatin. *Medical Oncology*, *32*(4), pp.1-15

Zhu, Y., Regunath, K., Jacq, X. and Prives, C. (2013). Cisplatin causes cell death via TAB1 regulation of p53/MDM2/MDMX circuitry. *Genes & Development*, *27*(16), pp.1739-1751.

Zimmermann, K.C., Bonzon, C. and Green, D.R. (2001). The machinery of programmed cell death. *Pharmacology & Therapeutics*, *92*(1), pp.57-70.

Zou, H., Li, Y., Liu, X. and Wang, X. (1999). An APAF-1· cytochrome c multimeric complex is a functional apoptosome that activates procaspase-9. *Journal of Biological Chemistry*, *274*(17), pp.11549-11556.

APPENDIX 1

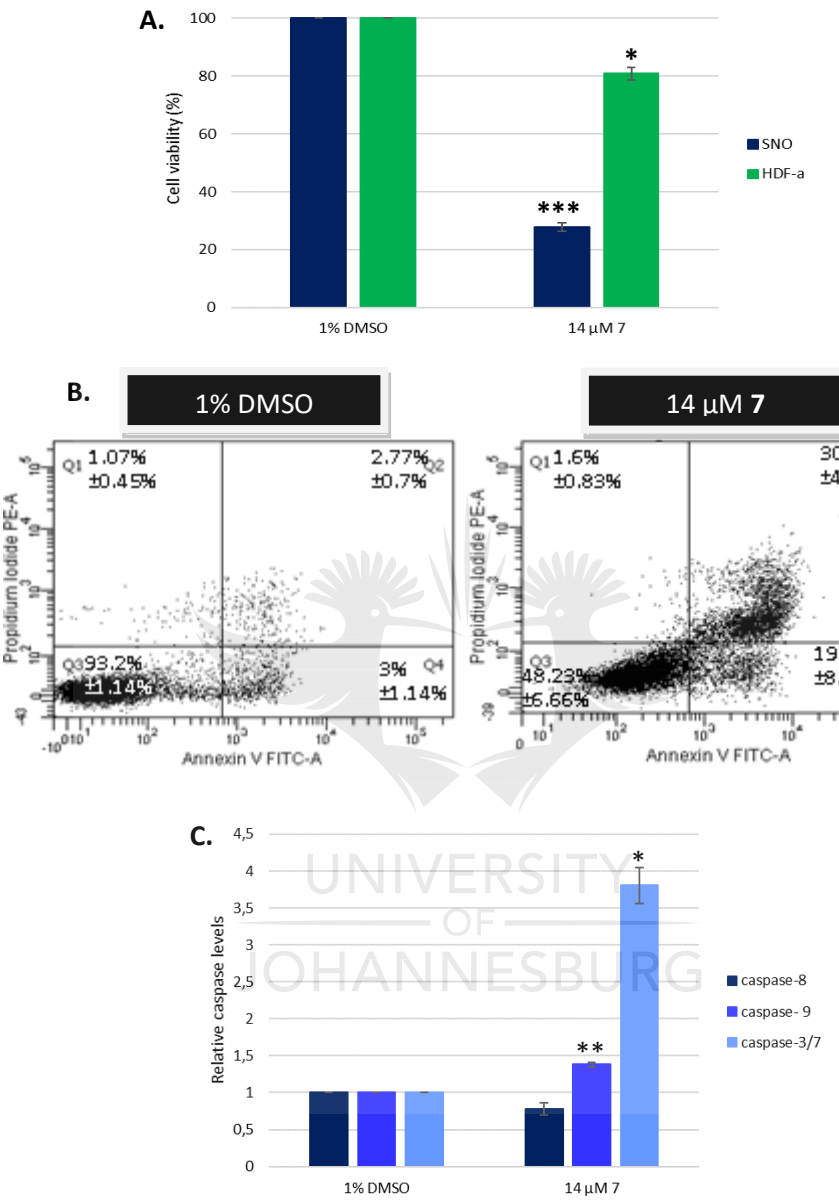

Figure A1.1: The cellular viability of malignant **SNO** and non-malignant **HDF-a** cells (A), the mode of cell death induced (B) and caspase activity in the **SNO** cells (C) after 24 hrs of treatment. The cells were treated with either 1% DMSO (vehicle) or 14 µM of complex **7**. Both the viability and relative caspase levels are expressed with respect to DMSO. Error bars were constructed based on the ±SEM (n = 9 for viability and n = 6 for caspases). The P-value was calculated using the two-tailed Students t-Test. The treatments with a P-value *P < 0.05 and ** P < 0.01 were deemed significant with respect to DMSO. The average percentage was calculated for all four quadrants, followed by the SEM (n = 3) (Human, 2013).

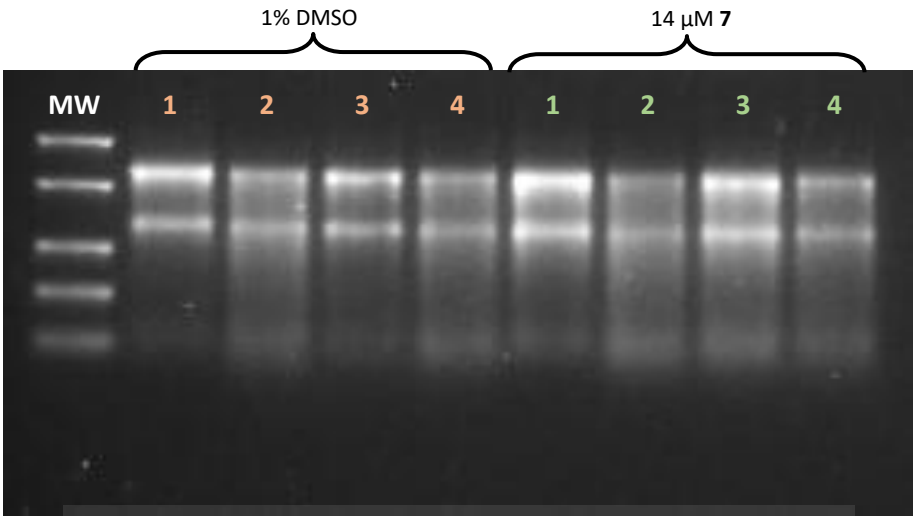

Figure A1.2: Agarose gel indicating the purity and integrity the total RNA isolated from malignant **SNO** cells after being treated for 12 hrs with 1% DMSO (vehicle) and 14 µM of complex **7**. The gel represents four biological repeats per treatment group.

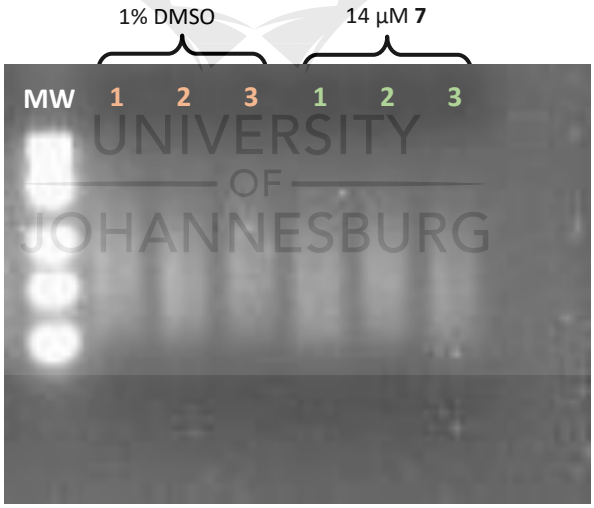

Figure A1.3: Agarose integrity gel of cDNA synthesized from total RNA that was isolated from malignant **SNO** cell treated for 12 hrs with 1% DMSO (vehicle) and 14 µM of complex **7**. The gel represents three biological repeats per treatment group.

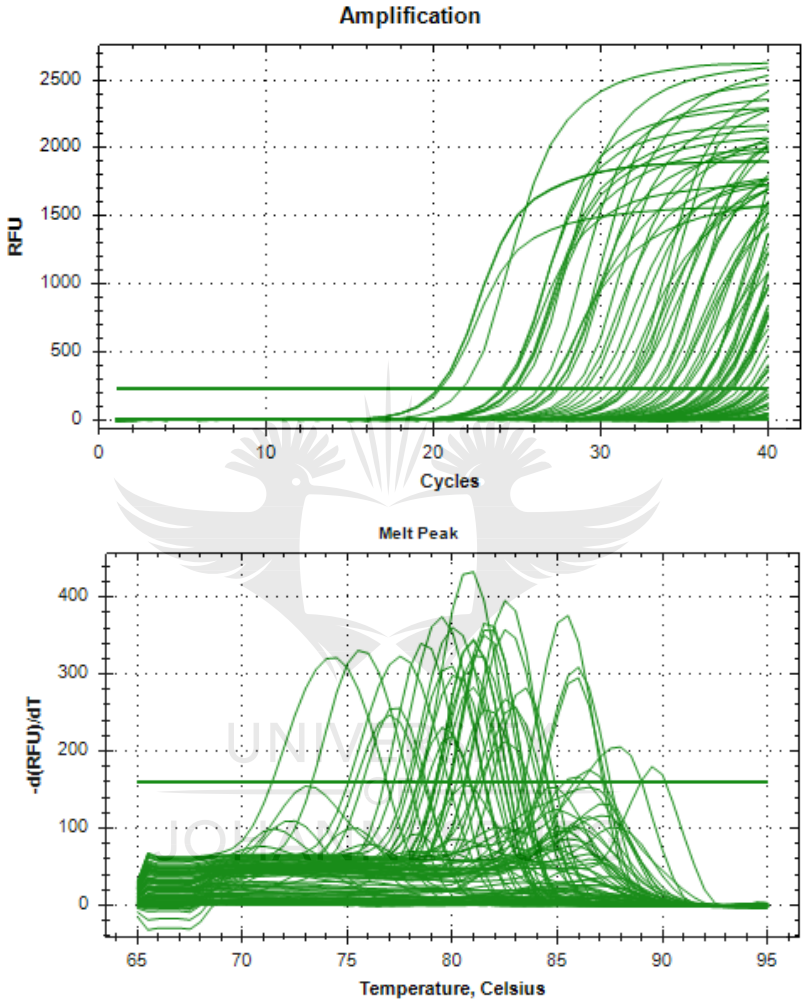

Figure A1.4: A representative image of the amplification (A) and melting point curve (B) of malignant **SNO** cells after being treated with 1% DMSO for 12 hrs.

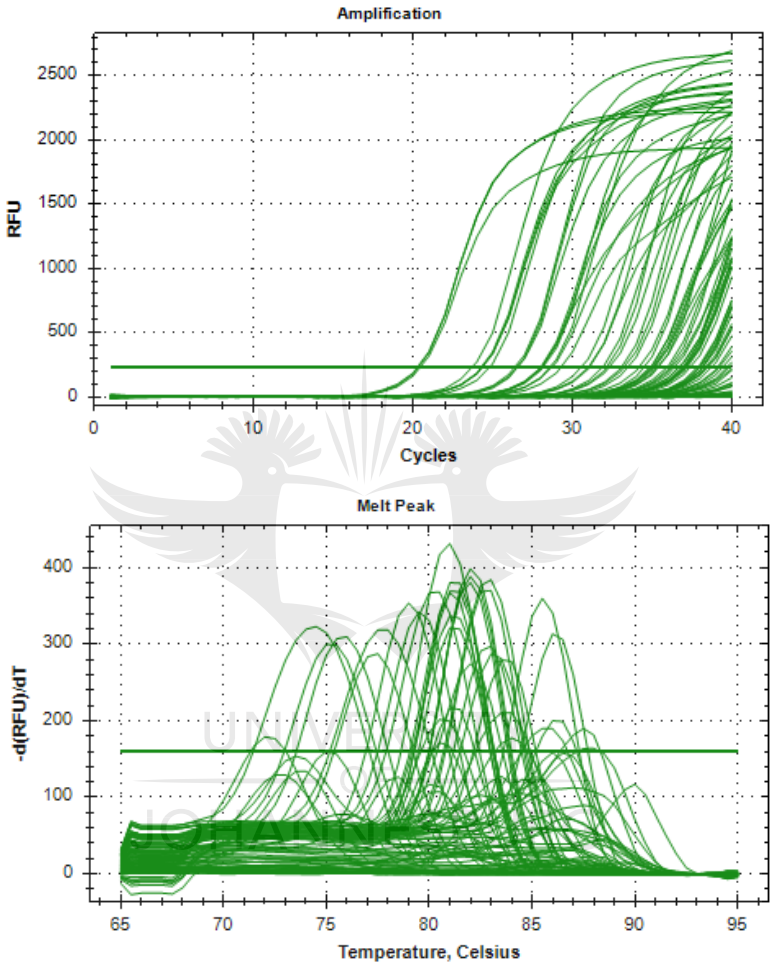

Figure A1.5: A representative image of the amplification (A) and melting point curve (B) of malignant **SNO** cells after being treated with 14 µM of complex **7** for 12 hrs.

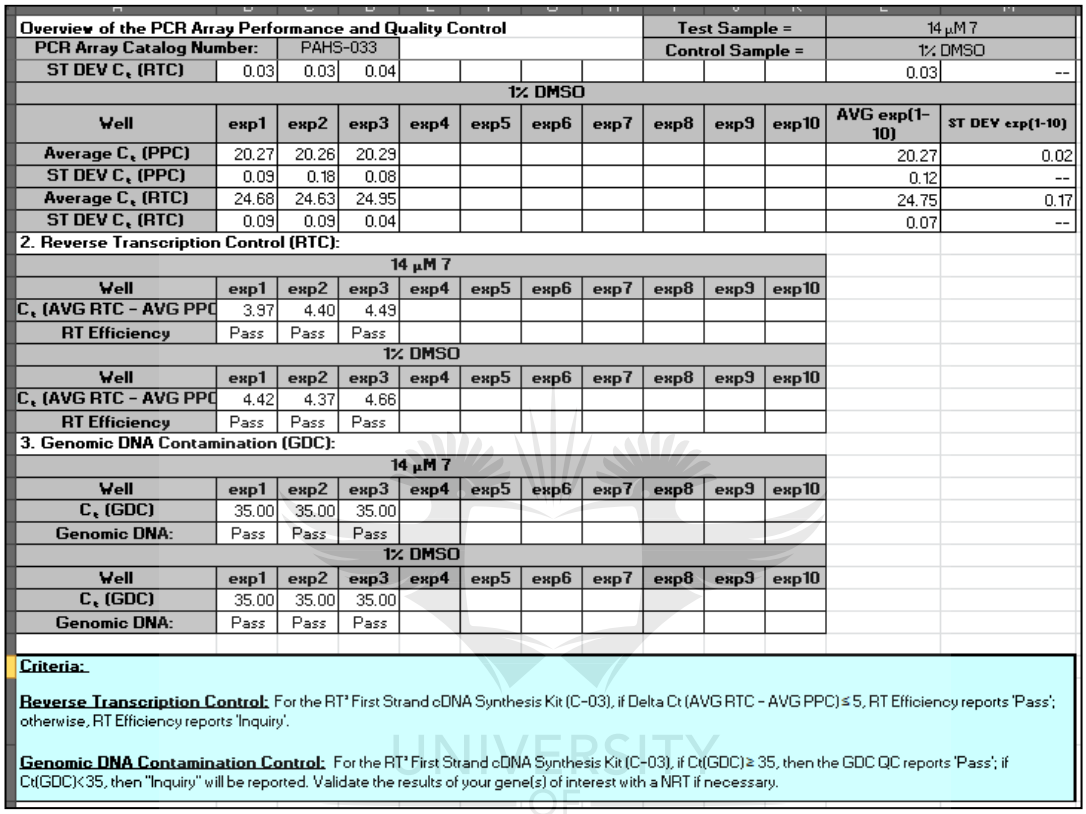

Overview of the PCR Array Performance and Quality Control								Test Sample =			14 µM 7	
PCR Array Catalog Number:	PAHS-033							Control Sample =			1% DMSO	
ST DEV C_t (RTC)	0.03	0.03	0.04								0.03	--
1% DMSO												
Well	exp1	exp2	exp3	exp4	exp5	exp6	exp7	exp8	exp9	exp10	AVG exp(1-10)	ST DEV exp(1-10)
Average C_t (PPC)	20.27	20.26	20.29								20.27	0.02
ST DEV C_t (PPC)	0.09	0.18	0.08								0.12	--
Average C_t (RTC)	24.68	24.63	24.95								24.75	0.17
ST DEV C_t (RTC)	0.09	0.09	0.04								0.07	--
2. Reverse Transcription Control (RTC):												
14 µM 7												
Well	exp1	exp2	exp3	exp4	exp5	exp6	exp7	exp8	exp9	exp10		
C_t (AVG RTC - AVG PPC	3.97	4.40	4.49									
RT Efficiency	Pass	Pass	Pass									
1% DMSO												
Well	exp1	exp2	exp3	exp4	exp5	exp6	exp7	exp8	exp9	exp10		
C_t (AVG RTC - AVG PPC	4.42	4.37	4.66									
RT Efficiency	Pass	Pass	Pass									
3. Genomic DNA Contamination (GDC):												
14 µM 7												
Well	exp1	exp2	exp3	exp4	exp5	exp6	exp7	exp8	exp9	exp10		
C_t (GDC)	35.00	35.00	35.00									
Genomic DNA:	Pass	Pass	Pass									
1% DMSO												
Well	exp1	exp2	exp3	exp4	exp5	exp6	exp7	exp8	exp9	exp10		
C_t (GDC)	35.00	35.00	35.00									
Genomic DNA:	Pass	Pass	Pass									

Criteria:

Reverse Transcription Control: For the RT² First Strand cDNA Synthesis Kit (C-03), if Delta Ct (AVG RTC - AVG PPC) ≤ 5, RT Efficiency reports 'Pass'; otherwise, RT Efficiency reports 'Inquiry'.

Genomic DNA Contamination Control: For the RT² First Strand cDNA Synthesis Kit (C-03), if Ct(GDC) ≥ 35, then the GDC QC reports 'Pass'; if Ct(GDC) < 35, then "Inquiry" will be reported. Validate the results of your gene(s) of interest with a NRT if necessary.

Figure A1.6: The overview of the PCR performance and quality control which includes three biological repeats of either 1% DMSO (vehicle) or 14 µM of complex **7** treatments.

Table A1.1: The raw data of the malignat **SNO** cells from Human Cancer Pathway Finder RT^2 Profiler PCR array after being treated with 1% DMSO (vehicle) and 14 µM of complex **7** for 12 hrs. Blue indicates the fold down-regulation.

Symbol	Well	AVG ΔC_t (Ct(GOI) - Ave Ct (HKG))		2^-ΔC_t		Fold Change	T-TEST	Fold Up- or Down-Regulation
		14 µM 7	1% DMSO	14 µM 7	1% DMSO	14 µM 7 /1% DMSO	*P*-value	14 µM 7 /1% DMSO
AKT1	A01	35.00	35.00	2.9E-11	2.9E-11	1.00	N/A	-1.00
ANGPT1	A02	34.32	33.67	4.7E-11	7.3E-11	0.64	0.242419	-1.56
ANGPT2	A03	35.00	35.00	2.9E-11	2.9E-11	1.00	N/A	-1.00
APAF1	A04	33.51	31.31	8.2E-11	3.7E-10	**0.22**	0.142723	**-4.59**
ATM	A05	35.00	35.00	2.9E-11	2.9E-11	1.00	N/A	-1.00
BAD	A06	35.00	35.00	2.9E-11	2.9E-11	1.00	N/A	-1.00
BAX	A07	26.87	24.03	8.2E-09	5.8E-08	**0.14**	**0.000004**	**-7.15**
BCL2	A08	31.69	29.84	2.9E-10	1.0E-09	**0.28**	**0.048212**	**-3.60**
BCL2L1	A09	33.63	34.00	7.5E-11	5.8E-11	1.30	0.795946	1.30
BRCA1	A10	35.00	35.00	2.9E-11	2.9E-11	1.00	N/A	-1.00
CASP8	A11	34.80	35.00	3.4E-11	2.9E-11	1.15	0.373901	1.15
CCNE1	A12	35.00	35.00	2.9E-11	2.9E-11	1.00	N/A	-1.00
CDC25A	B01	35.00	34.29	2.9E-11	4.8E-11	0.61	0.279294	-1.64
CDK2	B02	34.80	33.86	3.3E-11	6.4E-11	0.52	0.161487	-1.92
CDK4	B03	34.56	33.63	3.9E-11	7.5E-11	0.52	0.281822	-1.91
CDKN1A	B04	33.59	32.26	7.7E-11	1.9E-10	0.40	0.372292	-2.52
CDKN2A	B05	34.72	34.19	3.5E-11	5.1E-11	0.70	0.467320	-1.44
CFLAR	B06	35.00	35.00	2.9E-11	2.9E-11	1.00	N/A	-1.00
CHEK2	B07	35.00	34.94	2.9E-11	3.0E-11	0.96	0.373901	-1.04
COL18A1	B08	34.07	32.63	5.5E-11	1.5E-10	0.37	0.311253	-2.71
E2F1	B09	33.24	34.21	9.9E-11	5.0E-11	1.96	0.399250	1.96
ERBB2	B10	33.33	28.54	9.3E-11	2.6E-09	**0.04**	**0.000111**	**-27.67**
ETS2	B11	35.00	35.00	2.9E-11	2.9E-11	1.00	N/A	-1.00
FAS	B12	35.00	35.00	2.9E-11	2.9E-11	1.00	N/A	-1.00
FGFR2	C01	35.00	35.00	2.9E-11	2.9E-11	1.00	N/A	-1.00
FOS	C02	26.58	27.48	1.0E-08	5.3E-09	1.87	**0.044566**	1.87
GZMA	C03	35.00	35.00	2.9E-11	2.9E-11	1.00	N/A	-1.00
HTATIP2	C04	30.29	27.91	7.6E-10	4.0E-09	**0.19**	**0.003956**	**-5.23**
IFNA1	C05	35.00	35.00	2.9E-11	2.9E-11	1.00	N/A	-1.00
IFNB1	C06	33.44	33.71	8.6E-11	7.1E-11	1.21	0.811627	1.21
IGF1	C07	35.00	35.00	2.9E-11	2.9E-11	1.00	N/A	-1.00
IL8	C08	33.97	32.69	6.0E-11	1.4E-10	0.41	0.428698	-2.42
ITGA1	C09	27.93	26.57	3.9E-09	1.0E-08	0.39	**0.035849**	-2.57
ITGA2	C10	35.00	35.00	2.9E-11	2.9E-11	1.00	N/A	-1.00
ITGA3	C11	27.96	24.38	3.8E-09	4.6E-08	**0.08**	**0.001030**	**-11.89**

ITGA4	C12	34.16	33.89	5.2E-11	6.3E-11	0.83	0.610212	-1.20
ITGAV	D01	35.00	35.00	2.9E-11	2.9E-11	1.00	N/A	-1.00
ITGB1	D02	23.88	21.51	6.5E-08	3.3E-07	**0.19**	**0.000122**	**-5.16**
ITGB3	D03	29.74	30.14	1.1E-09	8.5E-10	1.32	0.827817	1.32
ITGB5	D04	34.78	35.00	3.4E-11	2.9E-11	1.17	0.373901	1.17
JUN	D05	35.00	35.00	2.9E-11	2.9E-11	1.00	N/A	-1.00
MAP2K1	D06	35.00	35.00	2.9E-11	2.9E-11	1.00	N/A	-1.00
MCAM	D07	33.70	32.16	7.2E-11	2.1E-10	0.35	0.373062	-2.90
MDM2	D08	28.74	26.42	2.2E-09	1.1E-08	**0.20**	**0.000884**	**-4.99**
MET	D09	34.70	33.76	3.6E-11	6.9E-11	0.52	0.386830	-1.92
MMP1	D10	35.00	35.00	2.9E-11	2.9E-11	1.00	N/A	-1.00
MMP2	D11	35.00	35.00	2.9E-11	2.9E-11	1.00	N/A	-1.00
MMP9	D12	35.00	35.00	2.9E-11	2.9E-11	1.00	N/A	-1.00
MTA1	E01	33.22	30.97	1.0E-10	4.7E-10	**0.21**	**0.000883**	**-4.75**
MTA2	E02	28.20	25.17	3.3E-09	2.7E-08	**0.12**	**0.000020**	**-8.16**
MTSS1	E03	35.00	35.00	2.9E-11	2.9E-11	1.00	N/A	-1.00
MYC	E04	35.00	35.00	2.9E-11	2.9E-11	1.00	N/A	-1.00
NFKB1	E05	35.00	35.00	2.9E-11	2.9E-11	1.00	N/A	-1.00
NFKBIA	E06	35.00	34.49	2.9E-11	4.1E-11	0.70	0.373901	-1.42
NME1	E07	32.18	31.54	2.1E-10	3.2E-10	0.64	0.208298	-1.56
NME4	E08	34.88	34.27	3.2E-11	4.8E-11	0.65	0.411498	-1.53
PDGFA	E09	35.00	35.00	2.9E-11	2.9E-11	1.00	N/A	-1.00
PDGFB	E10	35.00	33.02	2.9E-11	1.1E-10	**0.25**	0.169974	**-3.93**
PIK3R1	E11	35.00	35.00	2.9E-11	2.9E-11	1.00	N/A	-1.00
PLAU	E12	35.00	34.58	2.9E-11	3.9E-11	0.75	0.373901	-1.34
PLAUR	F01	35.00	33.47	2.9E-11	8.4E-11	0.35	**0.043418**	-2.89
PNN	F02	28.83	27.17	2.1E-09	6.6E-09	**0.32**	**0.014671**	**-3.17**
RAF1	F03	35.00	35.00	2.9E-11	2.9E-11	1.00	N/A	-1.00
RB1	F04	35.00	35.00	2.9E-11	2.9E-11	1.00	N/A	-1.00
S100A4	F05	24.76	23.95	3.5E-08	6.2E-08	0.57	**0.002317**	-1.75
SERPINB5	F06	34.53	34.07	4.0E-11	5.6E-11	0.73	0.526458	-1.38
SERPINE1	F07	35.00	35.00	2.9E-11	2.9E-11	1.00	N/A	-1.00
SNCG	F08	32.93	30.21	1.2E-10	8.1E-10	**0.15**	0.404691	**-6.61**
SYK	F09	35.00	35.00	2.9E-11	2.9E-11	1.00	N/A	-1.00
TEK	F10	35.00	35.00	2.9E-11	2.9E-11	1.00	N/A	-1.00
TERT	F11	34.70	34.28	3.6E-11	4.8E-11	0.75	0.506332	-1.34
TGFB1	F12	31.64	29.38	3.0E-10	1.4E-09	**0.21**	**0.001591**	**-4.79**
TGFBR1	G01	35.00	35.00	2.9E-11	2.9E-11	1.00	N/A	-1.00
THBS1	G02	26.50	25.99	1.1E-08	1.5E-08	0.71	0.255633	-1.42
TIMP1	G03	31.97	32.90	2.4E-10	1.2E-10	1.91	0.455801	1.91
TIMP3	G04	35.00	35.00	2.9E-11	2.9E-11	1.00	N/A	-1.00
TNF	G05	34.36	35.00	4.6E-11	2.9E-11	1.56	**0.011893**	1.56
TNFRSF10B	G06	35.00	35.00	2.9E-11	2.9E-11	1.00	N/A	-1.00

TNFRSF1A	G07	34.74	34.87	3.5E-11	3.2E-11	1.09	0.641966	1.09
TNFRSF25	G08	34.01	34.15	5.8E-11	5.2E-11	1.11	0.948208	1.11
TP53	G09	35.00	35.00	2.9E-11	2.9E-11	1.00	N/A	-1.00
TWIST1	G10	30.76	28.49	5.5E-10	2.7E-09	**0.21**	**0.013564**	**-4.83**
EPDR1	G11	35.00	35.00	2.9E-11	2.9E-11	1.00	N/A	-1.00
VEGFA	G12	35.00	34.99	2.9E-11	2.9E-11	0.99	0.373901	-1.01
B2M	H01	35.00	35.00	2.9E-11	2.9E-11	1.00	N/A	-1.00
HPRT1	H02	28.14	26.49	3.4E-09	1.1E-08	**0.32**	**0.004062**	**-3.12**
RPL13A	H03	30.66	31.92	5.9E-10	2.5E-10	2.40	0.539884	2.40
GAPDH	H04	35.00	35.00	2.9E-11	2.9E-11	1.00	N/A	-1.00
ACTB	H05	34.11	32.92	5.4E-11	1.2E-10	0.44	0.395286	-2.27

APPENDIX 2

List of manufacturers of reagents, materials, apparatus and software used for this study

Reagents

Acetonitrile (*Sigma, St. Louis, MO*)

Acrylamide (*Sigma, St. Louis, MO)*

Agarose (*FMC BioProducts, Philadelphia, PA*)

alamarBlue® (*Serotec, UK*)

Alexa-Fluor® 488 labelled anti-cytochrome *c* antibody (*Abcam, Cambridge, UK*)

2X Amido black staining solution (*Sigma, St. Louis, MO*)

Ammonium persulphate (APS) (*Sigma, St. Louis, MO*)

Annexin-V FITC Assay Kit (*Serotec, UK*)

Apo-ONE® homogenous caspase-3/7 Assay Kit (*Promega, Madison, USA*)

β-mercaptoethanol (*Sigma, St. Louis, MO)*

Boric acid (*Associated Chemical Enterprises, Southdale, RSA*)

Bovine serum albumin (BSA) (*Sigma, St Louis, MO)*

Bisacrylamide (*Sigma, St. Louis, MO)*

CellTiter-Glo® Luminescent Cell Viability Assay (*Promega, Madison, USA)*

Cisplatin (CDDP) (*Molekula, Dorset, UK*)

Clarity™ Western ECL substrate (*Bio-Rad, Hercules, CA*)

Cytochrome P450-Glo™ Assay kit specific for CYP1B1 (*Promega, Madison, USA)*

Dulbecco's modified Eagle's medium (DMEM) (*Highveld Biological, Kelvin, RSA)*

Dimethyl sulfoxide (DMSO) (*AppliChem, Darmstadt, Germany*)

Ethanol (*Merck, Wadeville, RSA*)

Ethylenediaminetetraacetic acid (EDTA) (*Sigma, St Louis, MO*)

Fetal bovine serum (FBS) (*Biowest, Kansas City, MO*)

Fibroblast growth supplements (FGS) (*ScienCell™, Carlsbad, USA)*

Fibroblast Medium (FM) (*ScienCell™, Carlsbad, USA*)

Formaldehyde (*Sigma, St. Louis, MO)*

Gentamicin sulphate (*Lonza, New Jersey, USA*)

Glycerol *(Rochelle Chemicals, Johannesburg, RSA)*

Glycine (*Merck, Wadeville, RSA*)

Goat anti-mouse IgG secondary antibody with horse radish conjugate (*Bio-Rad, Hercules, CA*)

Goat anti-rabbit IgG secondary antibody with horse radish conjugate (*Sigma, St. Louis, MO*)

Gelstar® nucleic acid gel stain (*Lonza, Rockland, ME*)

Hanks balanced salt solution (HBSS) (*Highveld Biologicals, Kelvin, RSA*)

Hoechst-33258 (*Invitrogen, Eugene, OR*)

Human Cancer PathwayFinder RT^2 Profiler PCR array (PAHS-033A) (*Qiagen, Hilden, Germany*)

Hydrogen peroxide (H_2O_2) *(Minema, Gauteng, RSA)*

2X Laemmli sample buffer (*Bio-Rad, Hercules, CA*)

Methanol (*Sigma, St. Louis, MO*)

MitoProbe™ JC-1 Assay Kit (*Thermofisher, Rochester, NY*)

MitoTracker Orange CMTMRos (*Invitrogen, Molecular Probes, Eugene, OR*)

Mouse primary antibody directed against human β-actin (*Sigma, St. Louis, MO)*

Mouse primary antibody directed against human inducible Hsp70, 5A5 (*Abcam, Cambridge, UK*)

Muse® Oxidative Stress Kit (*Merck, Wadeville, RSA*)

6X Orange loading dye (*Fermentas Life Sciences, Glen Burnie, MD*)

Penicillin/Streptomycin/Fungizone (*Lonza, New Jersey, USA*)

Phosphate Buffered Saline tablets (PBS) (*Sigma, St. Louis, MO)*

Precision Plus Protein™ Standard (*Bio-Rad, Hercules, CA*)

Propidium iodide (PI) (*Sigma, St. Louis, MO*)

Protease inhibitor cocktail tablets (*Sigma, St. Louis, MO*)

Quick-RNA™ MiniPrep kit (*Zymo Research Corporation, Irvine, CA*)

Rabbit monoclonal antibody directed against human PARP, E102 (*Abcam, Cambridge, UK*)

Rabbit primary antibody directed against human caspase 9, #9502 (*Cell Signalling Technology, Beverley, MA*)

RNase A (*Macherey-Nagel, Düren, Germany*)

RT^2 First Strand kit (*Qiagen, Hilden, Germany*)

RT^2 SYBR Green Mastermix (*Qiagen, Hilden, Germany*)

Silverchloride (AgCl) (*Sigma, St. Louis, MO*)

Silverbromide (AgBr) (*Sigma, St. Louis, MO*)

Silvercyanide (AgCN) (*Sigma, St. Louis, MO*)

Silvernitrate ($AgNO_3$) (*Sigma, St. Louis, MO*)

Silverthiocyanate (AgSCN) (*Sigma, St. Louis, MO*)

Sodium chloride (NaCl) (*Promark Chemicals, South dale, RSA)*

Sodium bicarbonate ($NaHCO_3$) (*Merck, Wadeville, RSA)*

Sodium dodecyl sulphate (SDS) (*Merck, Wadeville, RSA)*

Sodium hydroxide (NaOH) (*Associated Chemical Enterprises, Southdale, RSA*)

N,N,N',N'-Tetramethylethylenediamine (TEMED) (*Sigma, St. Louis, MO*)

Tri(*p*-tolyl)phosphine ($P(CH_3C_6H_4)_3$) (*Sigma, St. Louis, MO*)

Triphenylphosphine (PPh_3) (*Sigma, St. Louis, MO*)

Tris(4-chlorophenyl)phosphine ($P(ClC_6H_4)_3$) (*Sigma, St. Louis, MO*)

Tris(4-methoxyphenyl)phosphine ($P(4\text{-}CH_3OC_6H_4)_3$) (*Sigma, St. Louis, MO*)

Tris(hydroxymethyl)aminomethane (Tris) (*Merck, Wadeville, RSA*)

Triton X-100 (*BDH, Midrand, RSA*)

Trypan blue (*Bio-Rad, Hercules, USA*)

Trypsin (*Lonza, New Jersey, USA*)

TrxR Assay kit (*Abcam, Cambridge, UK*)

Tween-20 (*BDH, Midrand, RSA*)

Ultra-low range DNA ladder (*Fermentas Life Sciences, Glen Burnie, MD*)

Materials

50 ml centrifuge tubes (*Corning incorporated, New York, USA*)

Corning® CellBIND® 96-well plates (*Corning Incorporated, New York, USA*)

Corning® 75 cm^2 CellBIND® surface cell culture flasks (*Corning Incorporated, New York, USA*)

Corning® 150 cm^2 CellBIND® surface cell culture flasks (*Corning Incorporated, New York, USA*)

1.8 ml cryogenic vials (*Corning Incorporated, New York, USA*)

75 cm^2 culture flasks (*NEST, New Jersey, USA*)

1.2 x 7.5 cm flow cytometry tubes (*Becton Dickinson, Franklin Lakes, NJ*)

Polyvinylidene Fluoride (PVDF) membrane Hybond-P (*GE Healthcare, Buckinghamshire, England*)

3.5 x 1 cm treated cell culture dishes, Biolite (*Thermofisher, Rochester, NY*)

2 ml microfuge tubes (*Eppendorf AG, Hamburg, Germany*)

Nitrocellulose membrane, 45 µm (*Bio-Rad, Hercules, CA*)

TC10™ System Counting Slides Dual-Chamber (*Bio-Rad, Hercules, CA*)

24-well plate (*Nunc™, Roskilde, Denmark*)

96-well plates, Biolite (*Thermofisher, Rochester, NY*)

96-well plates, black (*SPL Life Sciences, Korea*)

Apparatus

Agarose gel electrophoresis system, BioRad Mini-Sub® GT gel system (*Bio-Rad, Hercules, CA*)

Axio Cam camera (*Carl Zeiss, Göttingen, Germany*)

Axioplan 2 inverted fluorescence microscope (*Carl Zeiss, Göttingen, Germany*)

Axiovert 25 inverted light microscope (*Carl Zeiss, Göttingen, Germany)*

Bandelin Sonopuls HD 2070 sonicator (*Bandelin Electronic, Berlin, Germany*)

Bio-Rad CFX96™ Connect Real-Time system (*Bio-Rad, Hercules, CA*)

Bio-Rad Chemidoc™ Image analyser (*Bio-Rad, Hercules, CA*)

Bio-Rad Mini-PROTEAN® Tetra electrophoresis transfer system (*Bio-Rad, Hercules, CA*)

Bruker Tensor 27 FT-IR spectrometer (*Bruker, Cramerview, RSA*)

Bruker Ultrashield Avance III 400 MHz spectrometer (*Bruker, Cramerview, RSA*)

Eppendorf® 5415R Centrifuge bench top centrifuge (*Merck, Wadeville, RSA*)

FACSAria™ flow cytometer (*BD Biosciences, San Jose, CA*)

HERAcell 150i CO_2 incubator (*Thermo scientific, New York, USA*)

Heraeus Biofuge Promo R centrifuge (*Thermo scientific, New York, USA*)

Image analyser, Bio-Rad Universal Hood II (*Bio-Rad, Hercules, CA)*

Muse® Cell Analyser (*Merck, Wadeville, RSA*)

NanoDrop ND-1000 Spectrophotometer (*NanoDrop Technologies Wilmington, DE*)

Stuart Scientific Melting Point apparatus SMP10 (*Bibby Scientific Limited, Staffordshire, ST15 OSA, UK*)

Synergy HT Multi-Detection Microplate reader (*BioTek, Winooski, Vermont*)

TC10™ Automated Cell Counter (*Bio-Rad, Hercules, CA)*

Thermo Flash 2000 series CHNS/O, Organic Elemental Analyser (*Thermo Scientific, Waltham, MA*)

Software

Axio Version 3.1 software (*Carl Zeiss, Göttingen, Germany*)

Bio-Rad CFX Connect manager 3.0 software (*Bio-Rad, Hercules, CA*)

FACSDiva™ software (*BD Biosciences, San Jose, CA*)

FCS Express Plus 5 Software (*De Novo, Glendale, CA*)

Image Lab™ Version 4.1 image acquisition and analysis software (*Bio-Rad, Hercules, CA*)

Microsoft® Excel 2007

Quantity One® Software Version 4.6.1 (*Bio-Rad, Hercules, CA*)